Universiteit Antwerpen

Faculteit Wetenschappen

Departement Chemie (Applied NMR) - Departement Biologie (SPHERE) -
Departement Wiskunde-Informatica

^{1}H-NMR based Metabolomics to explore the anoxia/hypoxia tolerance strategies in fresh water and marine fish

^{1}H-NMR Metabolomics in de zoektocht naar verschillende strategieën voor anoxie/hypoxie resistentie bij zoetwater- en mariene vissen

Interdisciplinair Proefschrift voorgelegd tot het behalen van de graad van Doctor in de Wetenschappen aan de Universiteit Antwerpen

Te verdedigen door Isabelle Lardon

Promotoren: Prof. dr. Gudrun de Boeck & Prof. dr. Roger Dommisse

Antwerpen 2012

CONTENTS

List of abbreviations

Acetyl CoA	Acetyl Coenzyme A
ADH	Alcohol dehydrogenase
ADP	Adenosine diphosphate
ALDH	Aldehyde dehydrogenase
AMIX	Analysis of Mixtures
AMP	Adenosine monophosphate
ATP	Adenosine-5'-triphosphate
BCAA's	Branched Chain Amino Acids (valine, isoleucine and leucine)
BW-ratio	Between-group and Within-group sum of squares
CluPa	Cluster-based Peak Alignment algorithm
CTH	Cystathionase
CWT	Continuous Wavelet Transform
GABA	Gamma (γ)-Amino Butyric Acid, = 4-aminobutanoate
GDH	Glutamate dehydrogenase
GS	Glutamine synthetase
Hb	Hemoglobin
kPa	kiloPascal (partial pressure unit of gases)
NAA	N-Acetylaspartate
M/C/W	Methanol/Chloroform/Water extraction
NMDA	N-Methyl-D-Aspartate
NMR	Nuclear Magnetic Resonance
NO	Nitric oxide

mM	millimolar
M_{O2}	Oxygen consumption rate
P_{crit}	Critical O_2 tension
P_{O2}	Partial pressure of O_2
PCA	Principal Component Analysis OR
	Perchloric acid extraction (Chapter 3)
PCr	Phosphocreatine or Creatine Phosphate
PLS-DA	Partial Least Squares for linear Discriminant Analysis
RBC	Red blood cells
ROS	Reactive Oxygen Species
Speaq	Spectrum alignment and quantitation
TMAO	Trimethylamine oxide
µM	micromolar

Chapter 1

Problem statement - Research goals

1.1 Problem statement

At present, our atmosphere is mainly composed of 21 % of oxygen and 79 % of nitrogen gases [Hochachka and Somero 2002]. Oxygen is a vital gas, necessary for many life forms on Earth. It is a unique molecule since an acute deficiency can lead to immediate and permanent effects at multiple levels of individual organisms to complete ecosystems.

In general, four different oxygen conditions can be distinguished: hyperoxia, normoxia, hypoxia and anoxia. Hyperoxia and hypoxia indicate higher and lower levels of oxygen, respectively in comparison to normoxia (normal oxygen levels). Anoxia can be defined as the complete absence of oxygen. Figure 1.1 illustrates the different oxygen levels, expressed in partial pressure units (kPa). Simple and somewhat arbitrary thresholds are generally accepted but do not take into account natural variation in hypoxia tolerance among fish species [Richards 2011]. Commonly, dissolved oxygen concentrations below 5-6 mg O_2 l^{-1} in freshwater and below 2-3 mg O_2 l^{-1} in marine/estuarine environments are defined as 'hypoxic'. Normal is considered 9-10 and 7-8 mg O_2 l^{-1} for freshwater and marine zones respectively, depending on the ambient temperature [Diaz and Breitburg 2009].

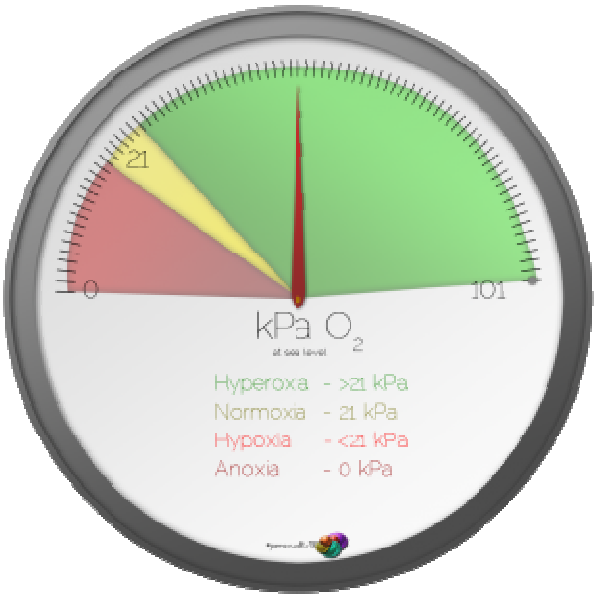

Figure 1.1 – Distinctive oxygen levels illustrated by their partial pressures (kPa): Hyperoxia (> 21 kPa), Normoxia (21 kPa), Hypoxia (< 21 kPa) and Anoxia (0 kPa).

Fluctuating levels of dissolved oxygen can be the result of a natural phenomenon due to daily fluctuations in oxygen concentrations. Particularly stagnant, stratified or poorly mixed waters frequently encounter naturally-induced hypoxia. Anthropogenic activities, however, and their resulting eutrophication and pollution enhance bacterial/algal growth which often lead to chronic hypoxic conditions worldwide (so called 'dead zones'), frequently resulting in mass mortality and a reduced biodiversity [Mustafa *et al.* 2011].

Living without oxygen is, for the majority of vertebrates (including humans) impossible and often results in catastrophic consequences. This oxygen is needed to provide metabolic energy in the form of ATP, by oxidative phosphorylation in the inner mitochondrial membranes. In the animal kingdom, it is known that certain vertebrate species have developed strategies to cope with anoxia and/or hypoxia. It is perhaps not surprising that within the group of vertebrates, particularly fish are likely to encounter hypoxia or anoxia more frequently. Clearly, fluctuating oxygen levels have been a potent evolutionary force in fishes, resulting in a natural selection of species with many unique adaptive traits. Water can hold less oxygen than can air (< 10 ml l^{-1} compared with 210 ml l^{-1}) and the oxygen diffusion rate in water is only about 1/10000 of that in air. Therefore, it is not surprising that fishes exhibit the largest number of hypoxia-tolerant species [Richards 2011].

Among the water breathing teleost fish, the Cyprinidae group includes some fish species that are extremely hypoxia- and/or anoxia-tolerant such as the goldfish (*Carassius auratus*) and several carp species (*Cyprinus carpio*, *Carassius carassius*). Within the reptiles, aquatic turtles (e.g. Trachemys) can survive prolonged periods of hypoxia and even anoxia.

By means of a phylogenetic point of view, the next two paragraphs describe briefly the conservative and/or adaptable features in the evolution of hypoxia-response physiology of turtles and fishes.

Evolution of hypoxia tolerance physiology in turtles

Although information about the evolution of hypoxia tolerance in turtles is rather scarce, more is known about their phylogeny. Comparative data, resulting from a study conducted by Ultsch e.g. demonstrated that even terrestrial turtles exhibited hypoxia- and anoxia tolerance [Ultsch 1989]. Furthermore, Bellamy and co-workers then suggested that this tolerance was present in the entire lineage, a so called 'once in a lineage' event [Bellamy and Petersen 1968]. However, this speculation was subsequently contradicted by Hochachka and Lutz

[Hochachka and Lutz 2001] who illustrated their theory with the phylogenetic tree in Figure 1.2.

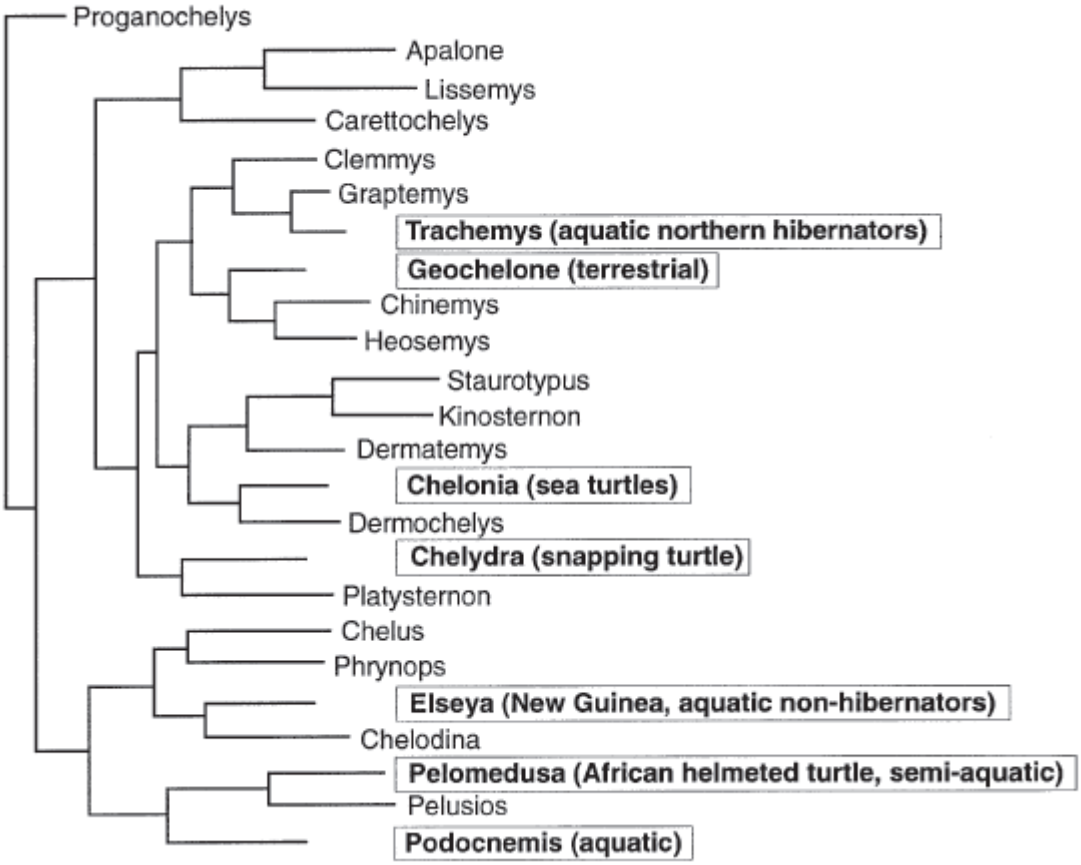

Figure 1.2 - A simplified phylogenetic hypothesis for turtles obtained and modified from Shaffer [Shaffer *et al.* 1997]. The boxes indicate groups that include one or more hypoxia-tolerant species. Researchers in this field suggest that hypoxia tolerance is partly ancestral to turtles as a group and partly adaptable through evolution due to the observed differences in the expression of hypoxia defense mechanisms in various turtle groups. Additionally, the wide-spread distribution of hypoxia tolerance in the phylogenetic tree is consistent with multiple, independent origins of hypoxia tolerance in turtles.

First, the phylogenetic tree in Figure 1.2 indicates that hypoxia tolerance of turtles as a group might be higher than that of sister taxa. This is indicated by data suggesting that even terrestrial turtles are more hypoxia-tolerant then other reptiles. Secondly, it also reveals that extreme hypoxia-tolerance might have evolved more than once within this lineage, possibly several times. For example, in the aquatic Trachemys; in the aquatic tropical Podocnemis; in snapping turtles and in sea turtles. Other studies also pointed out that tropical (non-

hibernating) and northern (hibernating) turtles shared similar physiological hypoxia/anoxia mechanisms (i.e. conservative traits) although quantitative differences were present [Crocker *et al.* 1999]. Compared to the tropical species, the northern turtles tolerated hypoxia more effectively i.e. displayed more effective or upregulated hypoxia defense mechanisms. Remarkably, even subspecies of highly hypoxia-tolerant turtles differ in the effectiveness of physiological and metabolic defense mechanisms [Ultsch *et al.* 1999].

To date, we consider turtles as being the most anoxia-tolerant group of all reptiles, with substantial different degrees of tolerance. For example, North American freshwater turtles from the genera Trachemys and Chrysemys are extremely anoxia-tolerant and can survive anoxia for months at low temperatures whereas soft-shelled turtles (Apalone) are relatively hypoxia to anoxia-intolerant, with mortality rates of 50 % following 2 weeks of anoxia at 3 °C. More moderately anoxia-tolerant turtles include the group of snapping turtles (Chelydra serpentine) that tolerate 100 days of anoxia [Bickler and Buck 2007].

In conclusion, multiple features of molecular hypoxia defense in turtles must be adaptable. Unfortunately, there is no further information available about the evolution of hypoxia tolerance, nor about the balance between conservative and adaptable features.

Evolution of hypoxia tolerance physiology in fishes

In fishes, a larger amount of empirical information is provided on the hypoxia tolerance of different fish groups and fortunately, their phylogeny is also well known. Figure 1.3 demonstrates the phylogenetic relationships of teleost lineages, including some extremely hypoxia-tolerant fish species (e.g. goldfish, carp).

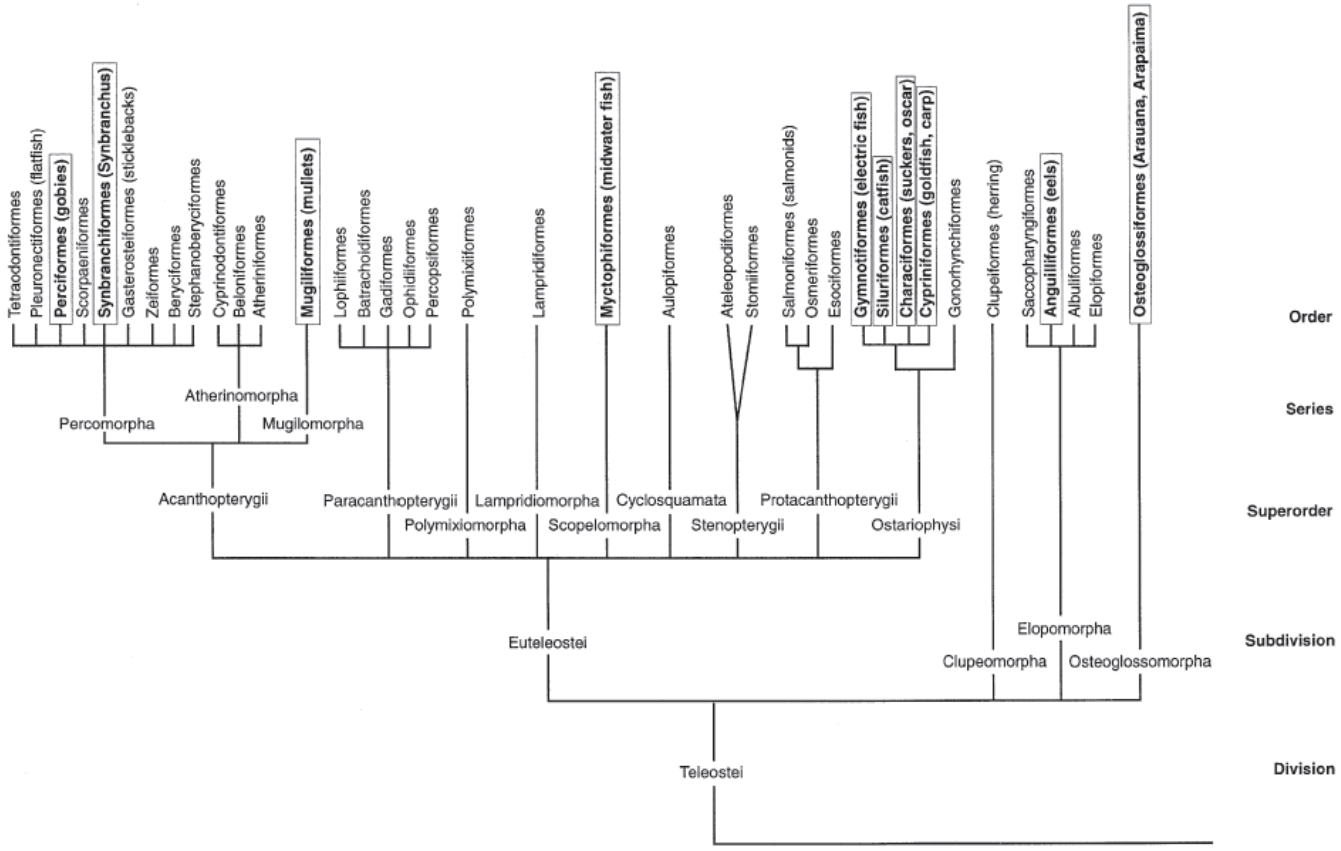

Figure 1.3 - A simplified phylogenetic tree of fishes obtained and modified from Nelson [Nelson 1994]. The boxes indicate groups that contain one or more hypoxia-tolerant species. The tree shows that hypoxia tolerance is very widely distributed within fishes. Researchers think that in some cases, hypoxia tolerance is a highly conserved ancestral characteristic but they also suggest that it arose independently in different lineages and in different geographical regions at several times.

A first glance at Figure 1.3 reveals the sporadic distribution of hypoxia tolerance in fishes. This finding appears to be consistent with multiple, independent origins of hypoxia tolerance mechanisms in teleostei. Examples include the exceptional anoxia tolerance in the crucian carp or the air-breathing fish where air breathing can be considered as a hypoxia defense adaptation on its own. This feature of air breathing as a hypoxia defense adaptation and a hypoxia tolerance mechanism has evolved several times within the group of fishes.

In conclusion, due to the large amount of hypoxia-tolerant fish species, hypoxia tolerance can and has evolved independently many times within this group [Val *et al.* 1996; Graham 1997].

1.2 Research goals

The previously described problem of environmental hypoxia/anoxia and the evolutionary adaptive responses in fish, provide the background for this thesis.

The principal aim of this project was to investigate the dynamic metabolic responses (Metabolomics) of various tissues of the anoxia-resistant crucian carp (*Carassius carassius*), exposed to acute and chronic anoxia (Chapter 5). Subsequently, we also studied the metabolic adjustments in the tissues of the related, hypoxia-tolerant but anoxia-intolerant common carp (*Cyprinus carpio*) (Chapter 6). To explore the metabolomics of these fish, we opted for proton nuclear magnetic resonance or ^{1}H-NMR. The observed metabolic responses of both fish species will be compared and evaluated in order to elucidate the underlying mechanisms of hypoxia/anoxia tolerance in fish (Chapter 8). Furthermore, besides the study of the metabolomic responses of freshwater fish (carp) to anoxia and hypoxia, this work also includes the ^{1}H-NMR analysis of the metabolome of one of the most primitive marine fishes, the dogfish shark (*Squalus acanthias*). The biochemical adaptations of sharks to fluctuating oxygen concentrations can provide additional useful information on their hypoxic survival strategies as well as interesting comparative insights towards the anoxia mechanisms of bony fish (Chapter 7).

In order to answer the upper biological questions in this project, we opted for proton nuclear magnetic resonance or ^{1}H-NMR to study the metabolomics of fish. For a detailed description of NMR spectroscopy and Metabolomics, the reader is kindly referred to Chapter 2.
We focussed on brain and heart tissues, two vital and metabolically active organs for which anoxia/hypoxia has adverse consequences. In addition, liver and white muscle tissues were investigated due to their metabolically important roles.
Next to the biological questions that need to be answered, this project also aimed at analyzing and subsequently improving the applied methodologies. This includes the optimization of tissue extraction protocols in fish and optimizing the set-up of NMR measurements for the different tissues in this study. Subsequently, various chemometric/biostatistical tools were tested and evaluated to extract relevant biochemical information from the complex spectroscopic datasets.

By studying the metabolic adaptations of fish to anoxia/hypoxic events, much can be learned from the physiology of animals and their approaches to survive such detrimental conditions. As such, the identification and the better understanding of their evolutionary conserved strategies can positively contribute to a better diagnosis and therapy of hypoxia-related diseases in humans such as stroke, myocardial infarction, pulmonary hypertension and surgery-induced ischemia/reperfusion, etc. [Krivoruchko and Storey 2010].

Therefore, by clarifying the anoxia/hypoxia tolerance mechanisms of fish, we hope to attain new insights that will positively contribute to a better understanding of the impact of limited oxygen levels in humans and other anoxia/hypoxia sensitive vertebrates.

Chapter 2

General introduction

2.1 Experimental animals

In order to provide a comprehensive overview of the physiological hypoxia tolerance mechanisms of the studied animals in this work, we subsequently describe what is already known about their responses to anoxia and/or hypoxia. Specifically, the anoxia strategies of the crucian carp (subchapter 2.1.1) and the anoxia/hypoxia responses of the related common carp (subchapter 2.1.2) are discussed, as well as the hypoxia tolerance of marine sharks (subchapter 2.1.3).

2.1.1 The crucian carp (Carassius carassius)

The crucian carp (Figure 2.1) is a sedentary freshwater fish from the family of Cyprinidae that inhabits lakes, rivers and reservoirs in various countries of Asia and Europe. They normally dwell in the bottom layer of the water column and feed on organic detritus, algae, small benthic animals and aquatic weeds. Furthermore, they are able to withstand a broad range of environmental conditions. For example, crucian carp have a strong disease resistance and are extremely anoxia-tolerant. They can survive prolonged periods of complete anoxia, depending on the ambient temperature and evolved different physiological strategies to cope with the adverse consequences of anoxic/hypoxic load.

Figure 2.1 - The crucian carp (*Carassius carassius*) [From: eo.wikipedia.org].

General physiological adaptations of crucian carp to anoxia

The crucian carp is commonly found in shallow North European ponds and lakes. During wintertime, these ponds can become anoxic due to the thick ice layer coverage, blocking photosynthesis from plants and preventing oxygen diffusion from the air. No fish is able to survive such extreme environmental conditions, except for the crucian carp. It is an expert in surviving anoxic waters but also in extracting the little oxygen that is present in hypoxic water columns. Its haemoglobin exhibits an extreme affinity for oxygen, allowing it to maintain its routine oxygen consumption rate down to a water oxygen level of 5-10 % of air saturation [Sollid *et al.* 2003].

An additional and remarkable adaptation of crucian carp is the absence of protruding gill lamellae in normoxic (aerated) water and secondly, their ability to change their gill morphology in response to fluctuating oxygen availabilities such as anoxia/hypoxia. A study by Sollid and co-workers [Sollid *et al.* 2003] illustrated the adaptive morphological changes of crucian carp gills following hypoxia and normoxia by means of scanning and transmission electron microscopy. Concretely, no protruding lamellae were observed in crucian carp gills under normoxic water conditions - in contrast to the majority of other fish gills - and this unusual trait results in a very small respiratory surface area, apparently large enough to extract O_2 sufficiently from the water and efficient in minimizing a potential loss of ions through the gills surface. These unique, adaptive morphological changes in the gills structure are reversible and thus enable crucian carp to respond to restricted O_2 availabilities in a very flexible and efficient way. Figure 2.2 demonstrates the morphological changes in gills of normoxic, hypoxic and reoxygenated crucian carp.

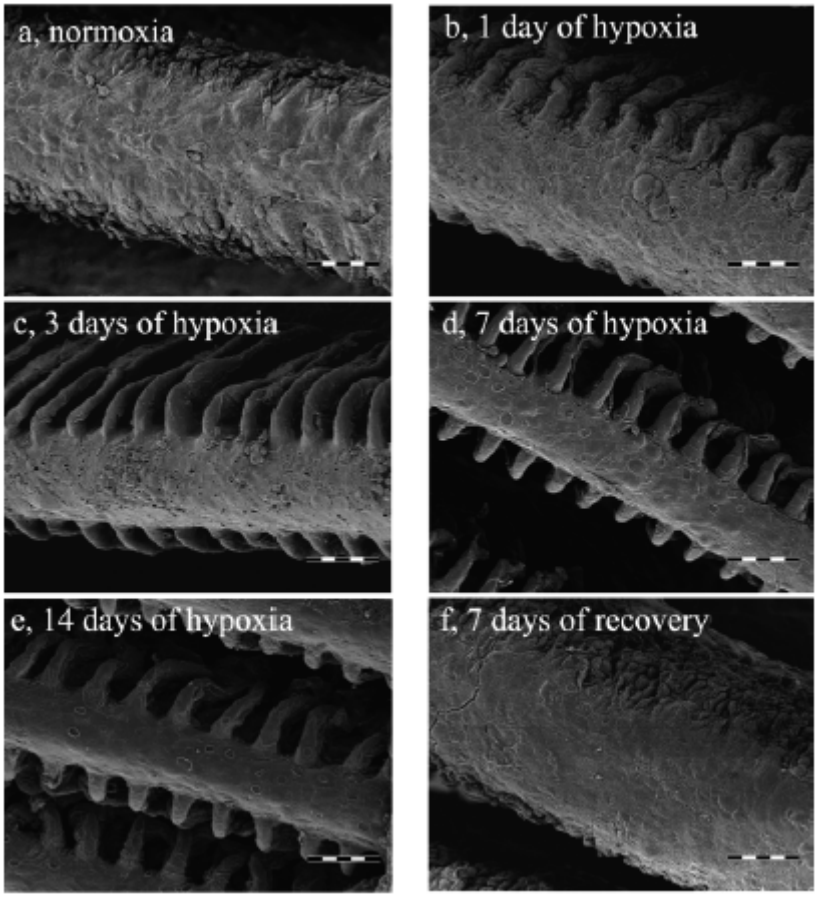

Figure 2.2 - Scanning electron micrographs (scale bar: 50 mm) of the 2nd gill arch of crucian carp kept in normoxia or hypoxia (0.75 mg O_2 l^{-1}): (a) no protruding gill lamellae visible during normoxia, (b) progressive changes in the gill morphology following 1 day of hypoxia up to 7 days of hypoxia (c), (d). No further changes in the gill morphology at 14 days of hypoxia (e) and reversal of the changes within 7 days of normoxic reoxygenation (f) [Sollid *et al.* 2003].

If we compare the physical activities of crucian carp and the tolerant turtle during anoxia, we clearly can see the differences in their anoxia survival strategies. While turtles become practically comatose, crucian carp continue to swim around, although at a reduced level [Nilsson 1993]. This enables fish to seek out for oxygen in the spring. However, some sensory functions as vision and hearing are suppressed in periods of anoxia. On the other hand, if winter time induces the anoxic state in lakes by covering them with a thick layer of ice, light invasion is blocked anyway so that vision is temporarily not of primary importance [Lutz, Nilsson & Prentice 2003].

Known glycolytic and metabolic adaptations to anoxia

Furthermore, an organism can only survive anoxic conditions when it is able to cope with the adverse consequences of anaerobic respiration and capable of avoiding tissue acidification and the subsequent cellular damage. The crucian carp manages to withstand all these potential obstacles by applying different physiological adaptive strategies.

First of all, crucian carp livers contain the largest glycogen store amongst all vertebrates (30 % of the total liver mass). Other tissues that store glycogen to a lesser extent include muscle, heart and brain. In brain, the glycogen reserves are situated almost exclusively in glia cells (astrocytes) and can be considered as nutritional support for neurons. Glycogen is a vital energy storage and substrate for anaerobic organisms because it can be metabolized to produce ATP in periods of anoxia or hypoxia. The critical role of brain glycogen stores in *Carassius* during the onset of anoxia is illustrated by the remarkable finding that the ATP level in goldfish brain is kept constant for 30 min after decapitation [McDougal *et al.* 1968]. Possibly, brain glycogen reserves are used as glucose supplies during the initial phase of anoxia whereas the massive liver glycogen store takes over this task after depleting brain glycogen reserves. Of course, these glycogen stores are not inexhaustible and decrease rapidly after long-term anoxia. In fact, the size of the body stores of glycogen can be considered as one of the factors limiting the anoxia tolerance of crucian carp [Vornanen *et al.* 2011]. Consistent with this, the size of glycogen stores in crucian carp varies according to the seasons: the build-up starts in August-October before the anoxic winter beginning, followed by a maintained high level in November-January and depletion in February-April. In order to allow a maximum build-up of glycogen, crucian carp use lipids for energy during the warmer summer months, instead of carbohydrates (i.e. glucose/glycogen) [Vornanen *et al.* 2011].
Although the size of glycogen stores can lengthen the period of anoxia endurance, there is another important factor contributing to the anoxia survival mechanism in crucian carp. Metabolic depression or the downregulation of energetic fluxes is an important strategy to reduce the ATP consumption rate of all biological processes in a certain organism. Basically, it is the combination of decreased energy (ATP) requirements with larger glycogen stores that provide the ultimate key adaptations towards a maximum survival time in anoxia.
Also, crucian carp try to swim to cooler waters when anoxic conditions arise (= behavioural temperature regulation). This is highly beneficial since the lower temperatures decrease the metabolic rate.

During anoxia, glucose is the only cellular substrate and the enhanced anaerobic glycolysis results in the production of anaerobic end products such as lactate. Hence, an accumulation of lactate decreases the cellular pH and thus, causes a tissue acidification. This acidic cellular environment undoubtedly would have detrimental consequences for the whole organism but crucian carp solved this problem cleverly. Instead of producing lactate, crucian carp have adapted to produce ethanol as end product.

The unique ethanol pathway of *Carassius* starts with pyruvate, which is either produced from the normal equilibrium reaction from lactate (catalyzed by lactate dehydrogenase) or directly resulting from the glycolysis. In the mitochondria, pyruvate is metabolized into acetaldehyde by pyruvate dehydrogenase. Normally, acetaldehyde is never allowed to leave the pyruvate dehydrogenase complex but in *Carassius*, the pyruvate dehydrogenase complex starts to 'leak' in muscle tissue during anoxia. As a consequence, acetaldehyde diffuses out of the mitochondria and in the cytosol, it is converted rapidly into ethanol by alcohol dehydrogenase (ADH). The latter enzyme is present solely in high concentrations in skeletal muscle (red as well as white) but absent in other tissues such as the brain. So, lactate is still the major anaerobic end product in brain. Possibly, crucian carp brain does not produce ethanol due to the relatively high activities of aldehyde dehydrogenase (ALDH), which catalyzes an important step in the degradation of monoamine neurotransmitters. Concretely, ALDH has a stronger affinity for acetaldehyde then ADH. In other words, if ALDH were present in an ethanol producing tissue, both ADH and ALDH would compete for acetaldehyde and the majority of acetaldehyde would be converted into acetic acid by ALDH rather than to ethanol [Lutz, Nilsson & Prentice 2003]. This means that any produced lactate from all glycolytic processes in the brain must be transported via the blood stream to the muscles to be converted into ethanol and CO_2 and to subsequently excrete it across the gills. Therefore, maintaining activity in anoxia demands an active circulatory system for shuttling glycolytic substrates and end products. Ethanol production to avoid lactate self-poisoning is beneficial in a number of ways. Primarily, ethanol is not acidic and thus will not decrease the cellular pH nor will it induce acidification-related cell damage. Secondly, ethanol is eventually excreted across the gills of crucian carp, avoiding its accumulation in the body.

Figure 2.3 displays the metabolic adaptations to prolonged anoxia in crucian carp: lactate resulting from glycolysis is converted to ethanol in muscle tissue. Due to its volatility, ethanol diffuses rapidly across the gills, preventing lactate self-poisoning.

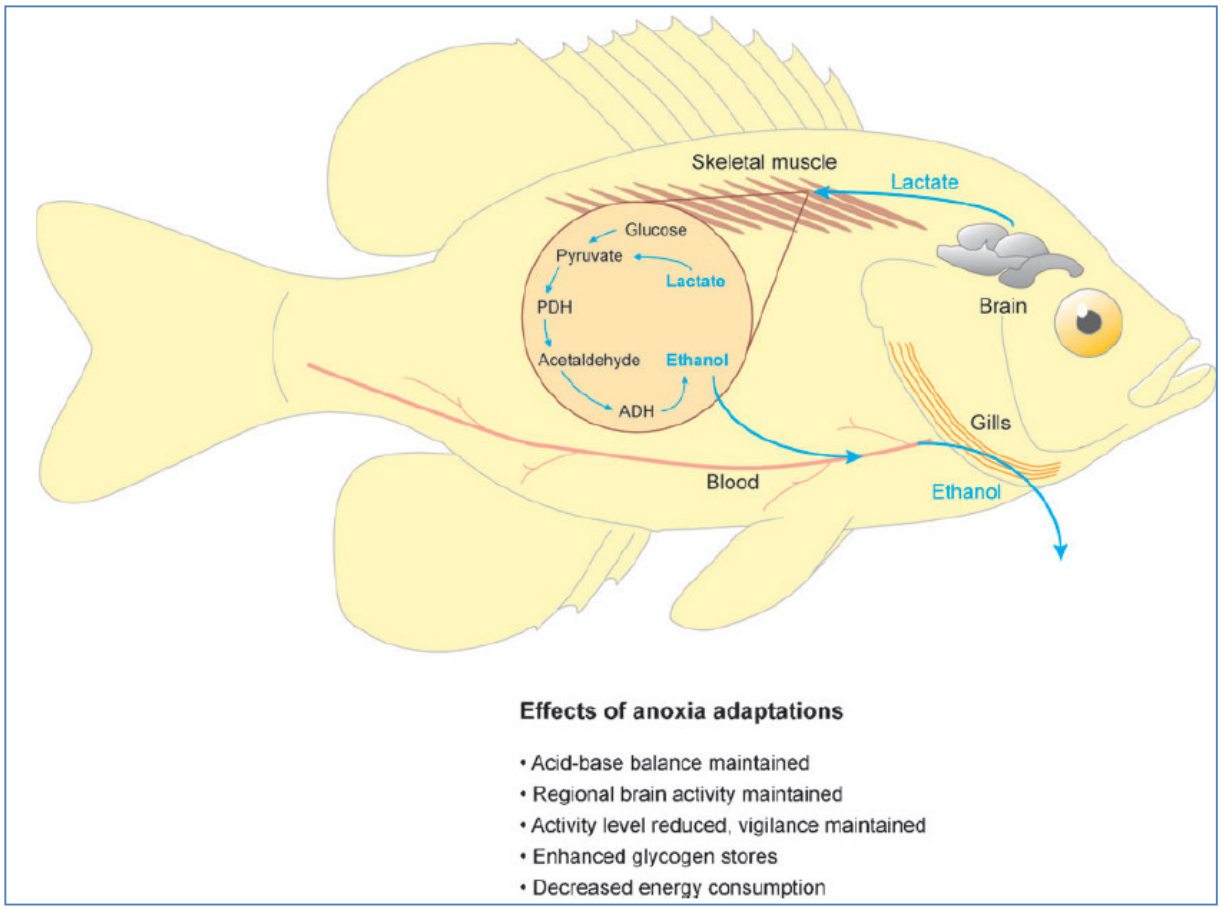

Figure 2.3 – Overview of the metabolic adaptations in anoxic crucian carp [Bickler & Buck 2007].

Neurotransmitters and neuromodulators

As mentioned before, crucian carp maintain their activity level during anoxia and this also implies that brain and heart continue to work properly. Indeed, previous literature indicates that crucian carp brain and heart performances remain fully functional during anoxia [Stecyk *et al.* 2011].

Certain molecules such as neurotransmitters and neuromodulators play a major role in the initiation and coordination of the processes that result in anoxia tolerance. An increased release of inhibitory neurotransmitters can induce a depression of synaptic transmission in the brain whereas (detrimental) excitatory neurotransmitters are commonly decreased during anoxia. Thus, inhibitory neurotransmitters may be considered as 'a first line of defence', protecting the anoxia-tolerant brain from energy failure [Nilsson 1990].

Firstly, adenosine release is associated with low levels of oxygen whenever the blood oxygen levels are low and hence, when ATP levels start to fall. The immediate result is an increase in

cerebral blood flow, through cerebral vasodilatation. In crucian carp and the turtle, adenosine mediates an increase in brain blood flow in response to anoxia. This increased brain blood flow is probably contributing to an increased glycolytic energy supply (glucose) and to an enhanced removal of waste products such as lactate and protons. In the anoxic turtle, this increased brain blood flow is only temporary [Hylland *et al.* 1994] whereas the 'active' crucian carp brain preserves this state during anoxia [Nilsson 1994]. Furthermore, previous studies have hypothesized an additional protective role of adenosine in anoxia-tolerant fish. In the related goldfish, for example, adenosine suppresses K^+ stimulated Ca^{2+}-dependent glutamate release in cerebellar slices [Rosati *et al.* 1995]. Blocking the adenosine receptors with aminophylline in crucian carp brain resulted in a 3-folded increase in the rate of ethanol removal which could indicate a significant inhibition of the metabolic depression [Nilsson 1991]. To conclude, adenosine release in response to anoxia induces a drastically reduced energy demand combined with an increased glycolytic supply and this eventually results in a recovery of cellular energy.

Other neurotransmitters playing a role during anoxia, in order to suppress the brain energy needs include the inhibitory γ-amino butyric acid (GABA) and glycine; and excitatory neurotransmitters such as glutamate.

GABA is the major inhibitory neurotransmitter in the adult vertebrate central nervous system. The release of brain GABA, both in tissue [Nilsson 1990] and extracellularly [Hylland and Nilsson 1999] is commonly observed in anoxic crucian carp. When the energy stores of the brain (or parts of the brain) become depleted during anoxia, a major GABA release is initiated. As a consequence of the activation of inhibitory GABA receptors, the synaptic and electrical activities in the brain decrease and hence, the overall energy consumption is reduced (neuronal depression) to restore the ATP levels. Hence, the rise in brain GABA in response to anoxia is a defense mechanism to decrease the metabolic rate. The most likely reason why GABA increases following hypoxia or anoxia is the conversion of glutamate into GABA. The synthesis of GABA from glutamate is anaerobic and proceeds during anoxia whereas the breakdown of GABA is aerobic. Logically, an increase of the inhibitory GABA is accompanied by a decrease of the excitatory glutamate. Additionally, the decrease in glutamate may be due to its aerobic synthesis since neuronal glutamate is typically derived from glutamine and α-ketoglutarate [Lutz, Nilsson & Prentice 2003]. The continued production of GABA at the expense of glutamate during anoxia could provide further depression of brain activity, since glutamate is the major excitatory neurotransmitter in vertebrates. The possible regulatory effects of GABA and glutamate on the reduction of the

metabolism during anoxia or hypoxia can be considered as a very ancient mechanism in the evolution [Nilsson 1993]. However, the release of glutamate following anoxia is delayed and relatively modest in contrast to the rapid and firm increase in brain GABA. Possibly, this can be explained by the fact that glutamate, as being the major cerebral excitatory neurotransmitter, can become a deadly neurotransmitter in the brain of anoxia-intolerant organisms.

Glycine is an inhibitory neurotransmitter in lower brain areas and in the spinal cord, and the activation of glycine receptors opens Cl^- channels. Anoxia induces an increase in glycine concentrations in both the turtle and the crucian carp brain [Nilsson 1990]. In mammals, however, no increase in tissue levels of glycine was observed during anoxia or ischemia. This can highlight an important difference between anoxia-tolerant organisms and mammals.

To summarize, the sustained release of inhibitory neurotransmitters/neuromodulators plays an active role in stabilizing the anoxic brain by preserving the hypometabolic brain status [Lutz, Nilsson & Prentice 2003].

2.1.2 The common carp (Cyprinus carpio)

Figure 2.4 - The common carp (*Cyprinus carpio*) [From: mueritzeum.de].

The common carp (Figure 2.4) is a freshwater fish, a member of the Cyprinidae family and found throughout the world in still or slowly flowing waters, lakes and permanent wetlands, commonly with silt bottoms and abundant aquatic vegetation. Adult common carp feed on sediments by sucking up mud from the bottom and selectively consuming items, which results in an increased siltation and bioturbidity. They prey on aquatic plants, macroinvertebrates and there is evidence that common carp also prey on eggs of other fish species [ISSG database *Cyprinus carpio*]. They can also be found in brackish lower reaches of some rivers and

coastal lakes. They are able to adjust to seasonal variations in temperature from < 4 °C up to > 38 °C and water oxygen saturations down to just a few % of saturation [Tota *et al.* 2011]. Presently, common carp are important in aquaculture to provide an important source of proteins in third world countries, in hobby fishing and for ornamental purposes.
Their remarkable tolerance to endure low oxygen levels possesses a great advantage to other, hypoxia-intolerant fish species. That way, common carp became successful widespread freshwater invaders, exploiting a range of available habitats [Jones and Stuart 2009]. Also, they are fairly resistant to pollutants and turbidity, enabling them to survive in degraded habitats or streams with sewage and substantial runoff from agricultural land.

General physiological adaptations of common carp to anoxia/hypoxia

In paragraph 2.1.1, the different strategies of the extremely anoxia-tolerant crucian carp were discussed. Both common– and crucian carp are members of the Cyprinidae family and are thus highly related but they display a different response to anoxia and hypoxia. In contrast to the well documented anoxia tolerance in crucian carp, less is known about the strategies of the hypoxic common carp.

Van Ginneken and co-workers [Van Ginneken *et al.* 1998] described the subsequent responses of Cyprinids to lowered oxygen concentrations: (a) an increased respiration frequency and volume of gill ventilation combined with bradycardia, (b) depletion of the phosphocreatine pool to stabilize the ATP pool in white muscle tissue, (c) depletion of the glycogen pool and hence, a lactate build-up, (d) the strategy of metabolic depression, (e) a decrease of the free fatty acid pool in plasma of hypoxic carp, indicative for a role as substrate, (f) production of anaerobic endproducts such as succinate and alanine. These endproducts result from the use of amino acids as substrates via the coupling of carbohydrate and amino acid catabolism, although the mechanisms may possibly not be quantitatively significant.
Common carp are moderately hypoxia- and anoxia intolerant. They survive severe hypoxia only for hours (at 15 °C) to 1 day (at 5 °C) [Stecyk and Farrell 2006] and survive 1-2 h of anoxia at room temperature during which time a continuous fall in brain ATP levels is seen [Van der Linden *et al.* 2001]. Other studies illustrated the survival of common carp, exposed for 5 days to anoxia at 25-31 °C [Jeng *et al.* 2008] or subjected to 5 h of anoxia at 15 °C [Lushchak *et al.* 2005].

When encountering hypoxia (0.8 mg O_2 l^{-1} at 23 °C), the common carp doubles its cerebral blood flow [Yoshikawa *et al.* 1995], which is a shared adaptive strategy with the anoxic crucian carp. The increased blood flow is an excellent way of increasing glucose and other supplies to the brain, thereby facilitating the upregulated glycolytic ATP production and removing the waste products. When faced with 12.5 h of severe hypoxia (0.3 mg O_2 l^{-1}), the common carp survives but greatly depresses its cardiac activity by adenosinergic cardiovascular control [Stecyk *et al.* 2007]. This is in sharp contrast to the crucian carp, which maintains normal cardiac performance and autonomic cardiovascular control for 5 days at 8 °C [Tota *et al.* 2011].

During hypoxia exposure, common carp typically suppress ATP turnover due to the inhibition of mitochondrial functions and they rely on an increased substrate-level phosphorylation or an increased anaerobic glycolysis to maintain energy balance [Bickler and Buck 2007]. Unlike crucian carp, common carp are unable to produce ATP through ethanol producing glycolysis [Van Ginneken *et al.* 1996].

A study by Van der Linden and colleagues investigated the effects of anoxia on brain swelling in common carp and crucian carp [Van der Linden *et al.* 2001]. The paper demonstrated that anoxic crucian carp showed no signs of brain swelling or changes in brain water homeostasis after 24 h of anoxia. In contrast, the entire common carp brain suffered from cellular oedema and a volume increase by 6.5 %, which proceeded during the first stages of the normoxic recovery phase. Eventually, common carp recovered completely, indicating that the observed changes were reversible and suggesting that the oversized brain cavity in many ectotherms allows brain swelling during energy deficiency without increasing intracranial pressure and global ischemia.

2.1.3 The spiny dogfish (Squalus acanthias)

Elasmobranchs are a subclass of Chondrichthyes or cartilaginous fish and include sharks, rays and skates. The spiny dogfish (Figure 2.5) is one of the most abundant shark species in the world and is used frequently as an experimental model species to study comparative and evolutionary biology, genomics, physiology, pharmacology, toxicology and immunology research topics. Spiny dogfish are highly migratory and swim in large schools with individuals of the same size or sexe. Populations can be found in the western Atlantic Ocean from Greenland to Argentina and in the eastern Atlantic from Iceland and Murmanski Coast (Russia) to South Africa including the Mediterranean Sea and Black Sea. In the western

Pacific Ocean, the spiny dogfish occurs from the Bering Sea to New Zealand while in the eastern Pacific, this species is found from the Bering Sea to Chile. They are detected mainly in shallow waters and further offshore in temperate waters (< 15 °C).

They usually prey on a variety of small fish and invertebrates. Although several names are commonly used for this species, *Squalus acanthias* can be distinguished by the presence of two dorsal spines (anterior to the dorsal fins) and the lack of an anal fin. The spines are used as a defensive tool and glands at the base of the spines secrete a mild poison, which is moderately irritating or strongly allergic to sensitive individuals.

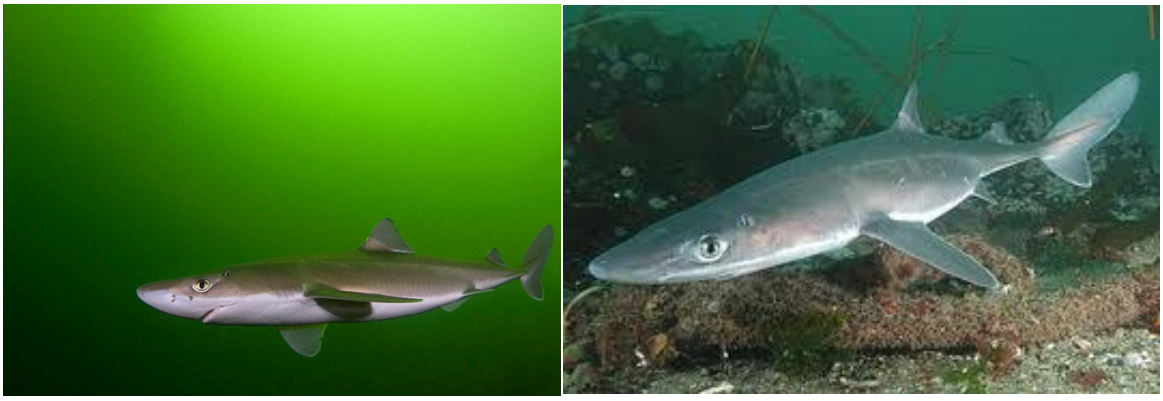

Figure 2.5 – The spiny dogfish shark (*Squalus acanthias*) [From: fish-journal.com].

Due to their migratory behaviour, spiny dogfish likely encounter hypoxia, although environmental hypoxia is less common to occur in marine ecosystems in comparison to fresh water habitats. Hypoxic areas are generally observed in shallow and open ocean areas and thus, due to this variable marine environment, spiny dogfish probably developed strategies to cope with the adverse effects of oxygen deprivation.

Since elasmobranchs fish are the oldest extant group of jawed vertebrates, they offer a number of advantages in experimental design and interpretation [Rytkönen *et al.* 2010]. Concretely, they exhibit the major functions of all subsequently appearing animals but in a more simple organized way [Barnes 2012]. To date, studies are available that investigated responses to oxygen limitation in the subsequent shark species: the dogfish [Metcalf and Butler 1984], the grey carpet shark (*Chiloscyllium punctatum*) [Renshaw and Chapman 2009], the bonnethead shark (*Sphyrna tiburo*) [Carlson 1998; Parsons and Carlson 1998], the blacknose shark (*Carcharhinus acronotus*) [Carlson 1998], the Florida smoothound shark (*Mustelus norrisi*) [Carlson 1998] and the epaulette shark (*Hemiscyllium ocellatum*) [Speers-Roesch *et al.* 2012b; Nilsson and Renshaw 2004; Renshaw *et al.* 2002].

Especially the Australasian epaulette shark is of particular interest due to its extreme hypoxia as well as anoxia tolerance at tropical temperatures (close to 30 °C) since epaulette sharks are found in shallow reef platforms to the southern end of the Great Barrier Reef in Australia.
At nocturnal low tides, the water of these reef platforms becomes cut off from the surrounding ocean and the dissolved oxygen level may fall to hypoxic levels below 18% of air saturation as a consequence of the absent photosynthesis and the continued oxygen consumption by coral organisms and algae [Nilsson and Renshaw 2004].
The unique habitat of the epaulette shark and its repeated, episodic exposure to diminished oxygen levels appears to be a natural equivalent to 'hypoxic preconditioning', a term applied in biomedical science. 'Preconditioning' refers to a common phenomenom in which exposure to an initial stress elicits physiological and biochemical responses that protect against a subsequent, often more severe stress. Eventually, this aims at reducing tissue/molecular damage and/or increased survivorship [Dowd *et al.* 2010]. Although clear evidence of hypoxic preconditioning is lacking in the epaulette shark, this species likely represents a 'constitutively preconditioned' model of hypoxia/anoxia tolerance. As an example, a study carried out by Renshaw and Chapman demonstrated that epaulette sharks raised in captivity (thus naïve to oxygen limitation) are indeed tolerant to cyclic anoxia [Renshaw and Chapman 2009].
The molecular mechanisms that protect epaulette sharks to episodic hypoxia or anoxia are multi-phase and complex. On the respiratory level, sharks alter the pattern of gill blood flow and increase their ventilator frequency to facilitate oxygen uptake from the hypoxic environment. Additionally, metabolic strategies are needed and applied to conserve the precious energy stores during periods of progressive or extended hypoxia. First of all, brain energy is preserved throughout the strategy of metabolic depression (e.g. a reduced protein turnover), probably initiated by the increased levels of neuromodulatory metabolites such as adenosine. The latter metabolite is also responsible for an increased arterio-venous circulation in gills during hypoxia and enhances the blood supply to the heart and gills [Mulvey and Renshaw 2009]. Furthermore, a change in the balance of excitatory (e.g. glutamate) and inhibitory neurotransmitters (e.g. GABA) takes place to prevent any excitotoxicity in the epaulette shark's brain. Previous studies have shown that proteins, related to glutamate production and release, were downregulated in the shark's cerebellum following hypoxia and anoxia [Dowd *et al.* 2010]. In contrast to other, more temperate hypoxia and anoxia tolerant vertebrates such as the crucian carp, which enter metabolic depression through homogeneous increases in their brain GABA levels, the epaulette shark's brain displays a different response.

A study by Mulvey and Renshaw reported that epaulette sharks do not increase overall brain concentrations of GABA in response to diminished O_2 (in contrast to crucian carp). Instead, an elevated GABA immunoreactivity was only found in specific regions of the brain, such as in key motor and sensory nuclei, which correspond to areas of previously reported neuronal hypometabolism [Mulvey and Renshaw 2009]. This overall lack of global increase in GABA following anoxia/hypoxia warrants further research since other, new key modulators of neuroprotection may occur in the phyllogenetically older epaulette shark.

Apparently, during sequential hypoxic exposures, epaulette sharks exhibit physiological responses to maintain the O_2 delivery to the tissues, rather than depressing the aerobic metabolism. For example, the hemoglobin of epaulette sharks possesses a high affinity for oxygen and the critical oxygen tension further decreases after preexposure to hypoxia [Dowd *et al.* 2010]. Additionally, increased lactate levels following hypoxia treatment indicate that anaerobic pathways must be invoked to supplement the aerobic ATP production, enabling sharks to maintain their metabolic activity and to avoid hypoxic damage. Upon reoxygenation, this lactate can be used as oxidative fuel and as gluconeogenic substrate in elasmobranchs tissues.

To further support a continued metabolic activity during hypoxia, epaulette sharks also use different substrates to ensure a sustained ATP production in brain and rectal gland. Specifically, a decreased reliance on glucose and branced-chain amino acids catabolism occurs when brains are faced with hypoxia, combined with a compensatory increased reliance on ketone bodies (β-hydroxybutyrate). An opposite response is reported in rectal gland tissue, however, that decreases its reliance on ketones and relies heavily on glucose as substrate during hypoxia. Interestingly, both tissues rely markedly on fatty acid metabolism, suggesting that fatty acids may supplement ATP production at critical times [Dowd *et al.* 2010].

Another metabolic strategy of epaulette sharks exposed to diminished oxygen levels is the modulation of cellular prosurvival signaling pathways. For instance, Dowd and co-workers observed an upregulation of cystathionase (CTH) production in hypoxic rectal glands. The CTH's production of the signalling gas hydrogen sulphide (H_2S) is inversely related to oxygen levels in fish and H_2S formation has recently shown to rescue cells from ischemia/reperfusion injury and apoptosis in several tissues [Dowd *et al.* 2010].

Furthermore, a potential beneficial role of nitric oxide (NO) in response to a hypoxic challenge is discussed in the paper of Dowd *et al.* [Dowd *et al.* 2010]. Interestingly, an increase in NO synthetase was noticed in the vasculature and neurons of epaulette sharks following hypoxia. It was then hypothesized that the increased NO-dependent cerebral

vasodilatation is neuroprotective when oxygen is lacking [Swenson *et al.* 2005]. Similarily in spiny dogfish, hypoxia induced a large NO-production of vascular origin and resulted in hypotension and hypoxic vasodilatation [Swenson *et al.* 2005]. Although the functional significance of this NOS upregulation upon hypoxia is currently unknown and literature about NO-regulation in elasmobranchs is limited and contradictory (class, species, type of organ, etc.), future studies in fish will undoubdelty reveal interesting perspectives in the role of this metabolite. In case of mammals, for instance, NO exerted different intra- and extracellular roles in heart tissue that served to diminish the extent of hypoxia-reperfusion injury [Nilsson and Renshaw 2004].

Finally, epaulette sharks are capable of avoiding the potential adverse effects of enhanced metabolism such as the accumulation of toxic metabolic byproducts and the formation of reactive oxygen species (ROS). As an example, an elevated biosynthesis of ubiquinone was observed in rectal gland tissue when sharks were exposed to hypoxia. Ubiquinone is known to exert antioxidant properties and acts as a cofactor to mitochondrial uncoupling proteins that reduce the generation of ROS at the electron transport chain. A second example is the enhanced cellular sequestration of Fe^{2+} ions to prevent O_2 radical formation in these shark species. To conclude, epaulette sharks exposed to hypoxia will upregulate anaerobic metabolism while conserving the consumption of ATP via adaptive mechanisms (ventilatory and metabolic depression), bradycardia and neuronal hypometabolism [Chapman and Renshaw 2009].

Besides the epaulette shark, additional papers are available which describe the metabolic strategies that are applied by other shark species such as the bonnethead shark (*Sphyrna tiburo*), the blacknose (*Carcharhinus acronotus*) and the Florida smoothhound sharks (*Mustelus norrisi*). From these studies, it was obvious that the responses to hypoxia clearly differ among the various shark species. This possibly reflects the different tolerance levels to limited oxygen levels or the alternate regulatory mechanisms (behavioural responses, metabolic strategies, etc.). The bonnethead and the blacknose sharks are obligate ram-ventilating species and displayed different responses to hypoxia in comparison to the smoothhound shark, which is a buccal-ventilating shark. For *S. Tiburo* and *C. Acronotus*, hypoxic exposure resulted in an increased swimming speed and mouth gape as well as enhanced oxygen consumption. Likely, the increased swimming speed of ram-ventilating sharks is a mechanism to maintain oxygen delivery to the organism or to stabilize the blood O_2 levels [Carlson and Parsons 2001]. In contrast, *M. Norrisi*, decreased its swimming speed

and activity level when facing hypoxic stress and therefore, followed the generalized hypothesis for teleosts (i.e. a reduced activity in periods of oxygen lack). Probably, this behavioural mechanism is aimed at reducing the energy demand for activity and that way, the saved energy may the dedicated to additional respiratory needs (e.g. an increased gillbeat frequency).

Finally, literature is available on the grey carpet shark (*Chiloscyllium punctatum*), which is a close relative of the epaulette shark and capable to tolerate both anoxia and hypoxia. Following anoxia, grey carpet sharks displayed an increased hematocrit and haemoglobin concentration and an elevated red blood cell (RBC) concentration, suggesting a release of erythrocytes into the circulation. This could result from the actions of one or more compensatory mechanisms: (a) an accelerated division and maturation of blood cells in the circulation, (b) an increase in oxygenated [RBC], released from a storage organ such as the spleen, hemopoetic organs as the epigonal organ and Leydig organ, (c) an increase in oxygenated [RBC] due to a diversion of blood from muscles and/or the gastrointestinal tract [Chapman and Renshaw 2009]. Furthermore, plasma glucose concentrations were maintained during anoxia but increased markedly after 2h of normoxic reoxygenation. Additionally, plasma lactate levels elevated significantly upon anoxic stress (indicating the upregulated anaerobic metabolism) and similar to glucose, the highest peak of plasma lactate was found after 2h of normoxic reoxygenation. Likely, the hyperglycaemia during normoxic reoxygenation reflects the upregulation of aerobic metabolism, to rapidly replenish the ATP levels [Chapman and Renshaw 2009]. Although closely related to the carpet shark, the epaulette shark displays both convergent as divergent responses to anoxia and hypoxia. Anoxia, for instance, induces a higher hematocrit as well as an elevated RBC volume (RBC swelling) in epaulette sharks to increase the O_2 unloading from RBC whereas carpet sharks mainly increase the number of RBC as a result of the redirection of O_2 stores (spleen, etc.). Similarily, plasma glucose levels were maintained in anoxic epaulette sharks and peaked after 2h of normoxic reoxygenation, combined with a peak in plasma lactate levels. Interestingly, these elevated lactate levels are the highest ever to be reported in elasmobranchs [Chapman and Renshaw 2009] and indicate the high anaerobic capacity of epaulette sharks as well as the high tolerance to accumulate metabolic end products (lactate), associated with acidosis.

2.2 Metabolomics and its relation to the other ‘omics’ technologies

Metabolomics was first defined in 1998 by Oliver and co-workers as "the quantitative complement of all of the low molecular weight molecules present in cells in a particular physiological or developmental state" [Oliver 1998]. In 1999, Nicholson’s research team formally defined metabolomics as "the quantitative measurement of the dynamic multiparametric metabolic response of living systems to pathophysiological stimuli or genetic modifications" [Nicholson *et al.* 1999]. Later on, in 2001, the term "metabolomics" was further refined by Olivier Fiehn as "a comprehensive and quantitative analysis of all metabolites in a system"[Fiehn 2001].

The primary aim of all ‘omics’ technologies is the non-targeted detection of all gene products (transcripts, proteins and metabolites) for a given biological system [Weckwerth 2003]. As one of the newest and rapidly developing ‘omics’ sciences, metabolomics joins up with genomics, transcriptomics and proteomics as a tool to understand the global systems biology (Figure 2.6). Although metabolomics is certainly complementary to the other ‘omics’, studying the metabolome provides unique advantages.

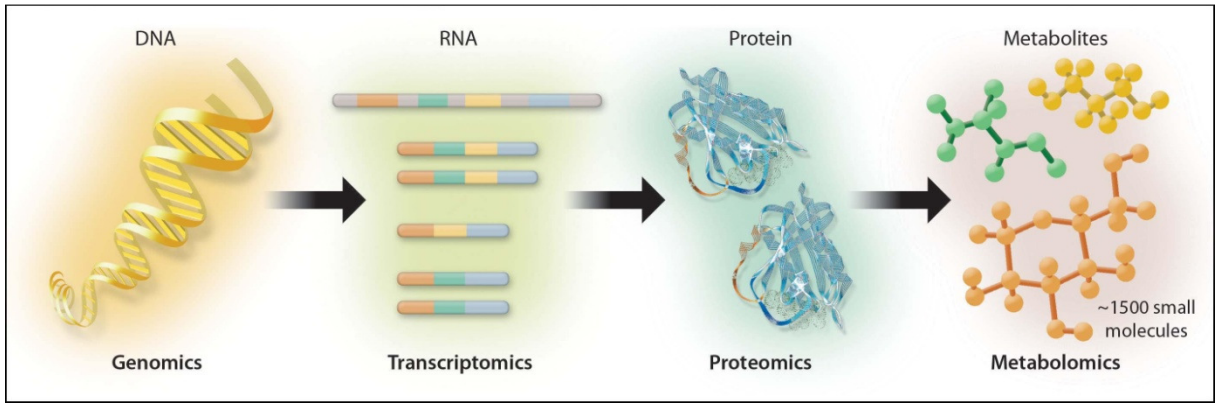

Figure 2.6 – Different ‘omics’ technologies [From: http://genomicscience.energy.gov].

In comparison to the proteome or transcriptome, the metabolome is more diverse and dynamic in terms of chemical and physical properties [Dunn *et al.* 2005]. The overall size of the metabolome is large and ranges from a few thousand to tens of thousands of small molecules [Kaddurah *et al.* 2008]. As an example, the Human Metabolome Project has estimated the number of endogenous metabolites in the human body at approximately 3000 [Blow 2008]. Metabolic studies include rapid and tractable analytical measurements and hereby require no ‘a priori’ knowledge of the genome sequence of an organism. Moreover, the measurement of genes, mRNA and protein levels cannot be used to directly determine cellular functions [Lin

et al. 2006]. One gene can direct the production of various proteins and various post-translational modifications can lead proteins to different locations and functions [Choi *et al.* 2006]. The chemical environment such as the pH and the redox status may also influence protein functions. The metabolome is further down the line from gene to function and therefore, it provides an instantaneous 'snapshot' of the physiology of cells or tissues under investigation [Ludwig and Viant 2010]. Moreover, changes in the metabolome are expected to be amplified relative to the transcriptomic and proteomic changes [Urbanczyk *et al.* 2003] but contrarily, metabolic fluxes (fluxomics) are not regulated by gene expression alone. This provides another argument for researchers to study metabolomics when functional information about the cell status is preferred. One of the most exciting advances is situated in the area of metabolic networks and the possibility to integrate metabolic data together with the corresponding transcriptomic and proteomic data [Bundy *et al.* 2007; Fan *et al.* 2006, Tian *et al.* 2007). In fact, metabolomics bridges the gentotype-to-phenotype gap by linking metabolic (dys) functions to altered gene expression profiles [Fiehn and Weckwerth 2002]. Together with the other more established omics technologies, metabolomics can strengthen its claim to contribute to the detailed understanding of the in vivo function of gene products, biochemical analysis, regulatory networks, etc. [Gomase *et al.* 2008]. However, knowledge of the complete set of metabolites is not always sufficient to predict the phenotype, especially in higher cells in which the complex metabolic processes are finely regulated and interconnected. In this case, quantitative knowledge of intracellular fluxes could be useful to understand the biological responses [Cascante *et al.* 2002; Cascante and Marin 2008]. A final advantage of metabolomics is the significantly lower cost on a per-sample basis in comparison to other ‘omic’ techniques [Ekman *et al.* 2008].

The broad area of metabolite analysis involves many different strategies and definitions, which have been developed to answer different questions and include metabolomics, metabonomics, metabolite target analysis, metabolic profiling, metabolic fingerprinting and metabolic footprinting [Fiehn 2001; Goodacre *et al.* 2004; Dunn *et al.* 2005; Xia *et al.* 2009].

Firstly, **Metabolomics** is defined as “the comprehensive and non-biased identification and quantification of all metabolites in an organic system under a given set of conditions” [Fiehn 2001; Goodacre *et al.* 2004; Xia *et al.* 2009]. Secondly, **Metabonomics** measures “the fingerprint of biochemical perturbations caused by disease, drugs and toxins” [Goodacre *et al.* 2004]. Thirdly, **Metabolite target analysis** aims at “the qualitative and quantitative analysis of one or a few metabolites, related to a specific metabolic pathway after extensive sample

preparation, employing a chromatographic separation and a sensitive detection" [Dunn *et al.* 2005; Xia 2009]. It is mainly used for screening purposes and for analyses that demand an extreme sensitivity [Fiehn 2001]. Fourthly, **Metabolic profiling** includes "the identification and quantification of a selected number of predefined metabolites, generally related through similar chemistries or metabolic pathways" [Dunn *et al.* 2005; Xia *et al.* 2009]. In normal circumstances, chromatographic separations are performed before detection. Fifthly, **Metabolic fingerprinting** is defined as "the global, rapid and high-throughput analysis of samples to provide a sample classification according to their origin or their biological relevance" [Xia *et al.* 2009]. This approach requires minimal sample preparation and the identification and quantification is not executed. Lastly, **Metabolic footprinting** is "the global measurement of metabolites secreted from the intracellular spent growth medium" [Dunn *et al.* 2005].

Throughout this doctoral thesis, the term 'metabolomics' is applied to refer to the study of the metabolome of fish tissue extracts.

Metabolic studies commonly investigate biochemical responses of biofluids or cell or tissue extracts. Biofluids of interest can include plasma, cerebrospinal fluid, urine, seminal fluid, dialysis fluids, cyst fluids, lung aspirates, synovial fluid, etc. [Lindon *et al.* 2007]. The approach is also used to characterize in vitro cell systems e.g. Caco-2 cells that are commonly used in cell uptake studies [Lamers *et al.* 2003]. Tissue extracts can be generated by applying different extraction techniques to the sample of interest. Unfortunately, there is no universal method to allow the detection of the complete metabolome and there is a payoff between technologies and objectives [Dunn *et al.* 2005]. However, the extraction method should be selected with great care and should seek to satisfy various relevant criteria, depending on the examined sample matrix. In this work, a thorough selection of the appropriate extraction technique to study the metabolomics of tissue extracts from fish was executed and is outlined in chapter 3.

A metabolomics experiment is divided into different stages: experimental design, sampling, sample preparation, instrumental analysis, data pre-processing and data processing/interpretation [Dunn *et al*. 2005]. All stages should be carefully designed and executed to ensure valid datasets, a subsequent correct interpretation and conclusions.

The next chapter will describe the analytical instruments that can be applied to explore the metabolome.

2.3 Analytical tools to explore the metabolome

Mass spectroscopy (MS) and nuclear magnetic resonance (NMR) are the main techniques commonly applied in metabolomic studies. Both are able to detect non-selectively a large number of endogenous metabolites in a single analysis with high reproducibility. Logically, it should be noted that neither approach is able to detect all present metabolites in the metabolome [Lin *et al.* 2006].

MS provides a sensitive, rapid and selective qualitative and (potentially) quantitative analysis with the possibility to identify the metabolites. In metabolomic MS-experiments, generally pre-separation of the metabolic components is required using chromatographic methods. For example, MS coupled to high-performance liquid chromatography (HPLC), gas chromatography (GC) or capillary electrophoresis (CE) [Lin *et al.* 2006] are often applied. Currently, the newest method of ultra high-pressure LC (UPLC), which employs ultrahigh pressure LC systems with small diameter particle (< 2 µm) columns are used increasingly [Lindon and Nicholson 2008]. Anyhow, MS provides both a highly sensitive detection (typically in pg/ml concentrations) which allows for more compounds to be screened [Serkova *et al.* 2008] and the possibility to identify the various metabolites. However, in contrary to NMR, it is a destructive technique. A comprehensive overview of all the MS-applications in metabolomic experiments can be found in [Lin *et al.* 2006].

Although high-resolution NMR is less sensitive than MS (i.e. identifying fewer metabolites in the same sample), it proved to be one of the most powerful technologies to study metabolic changes. NMR can be considered as a specific and yet a non-selective detector which provides rapid, unbiased, robust, reproducible and quantitative profiles of the metabolome. Another advantage is the non-destructive nature of the technique and its ability to investigate intact tissues by magic angle spinning (MAS)-NMR [Wilson and Lenz 2007]. Furthermore, NMR produces a comprehensive metabolic profile without the separation, derivatization and preselected measurement parameters [Nicholson and Wilson 1989]. Variable detection responses such as those occurring in MS as a consequence of differential volatilization or ionization are uncommon in NMR.

Since this project only employs high-resolution NMR to study fish metabolomics, the subsequent paragraph describes into detail the theory and practical considerations necessary for NMR-based metabolomics.

2.4 Nuclear magnetic resonance spectroscopy (NMR)

2.4.1 Theoretical principles

Spectroscopy involves the study of the interaction of electromagnetic radiation with matter. Subatomic particles such as electrons, neutrons and protons can be considered to be spinning around their own axes. Spinning charged nuclei generate a small magnetic field and the resulting spin-magnet is characterized by a magnetic moment, μ, proportional to the spin *I* (Figure 2.7).

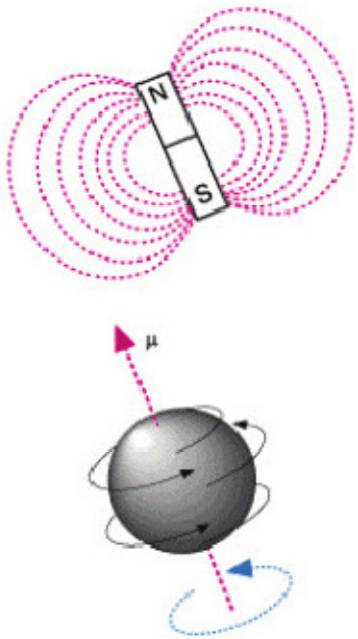

Figure 2.7 – A spinning and charged nucleus with I # 0 behaves like a small magnet, displaying a magnetic moment, μ [From: http://fs512.fshn.uiuc.edu/3D-NMR-chazin.gif].

The magnetic moment μ of a spinning and charged nucleus can also be described by the subsequent equation:

$$\mu = \frac{\gamma I h}{2\pi}$$

The constant, γ, is the gyromagnetic ratio which is different for every nucleus and h is Plank's constant (6.626×10^{-34} J s). For instance, the γ value of a ^{1}H nucleus is 2.675×10^{8} T^{-1} s^{-1}.

Nuclei with an even number of protons and neutrons have no overall spin (e.g. ^{12}C). However, other atoms (e.g. ^{1}H, ^{15}N, ^{19}F, ^{31}P and ^{13}C) have a nucleus with a spin. When the number of neutrons and the number of protons are odd, then the nucleus has a half-integer spin (i.e. 1/2, 3/2, 5/2). An integral spin number (i.e. 1, 2, 3) belongs to a nucleus which possesses an odd number of neutrons and protons. According to quantum mechanics, a nucleus with spin I can have 2I+1 possible orientations when placed in a magnetic field. Therefore, a nucleus with spin ½ will have 2 possible orientations. In the absence of an applied magnetic field, the nuclear spins are oriented randomly and of equal energy. However, when a sample is placed in an external magnetic field, the nuclei twist and turn to align themselves with or against the external magnetic field. This is demonstrated by Figure 2.8a and b.

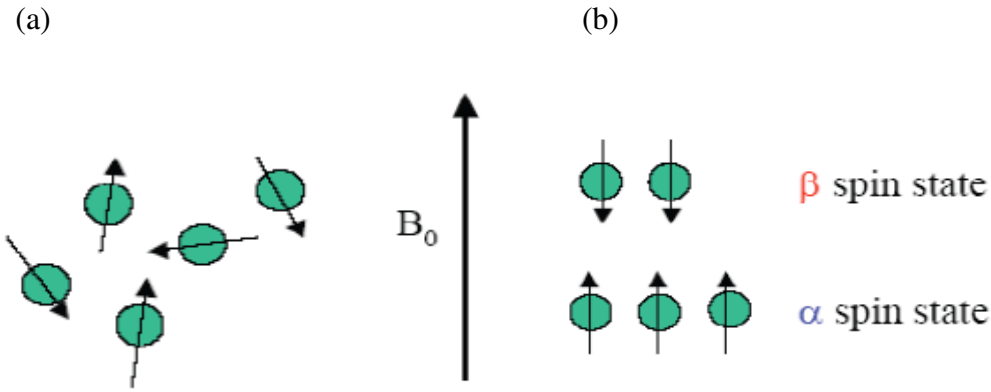

Figure 2.8 – Orientation of ^{1}H nuclei with their respective magnetic moments **(a)** in the absence of an applied magnetic field and **(b)** when a magnetic field (B_0) is applied [From: http://fs512.fshn.uiuc.edu/3D-NMR-chazin.gif].

Hence, the energy levels are then split. The initial populations of the energy levels are determined by thermodynamics, described by the Boltzmann equation.

$$N_\alpha / N_\beta = e^{-E/kT}$$

E is the energy difference between the spin states, k is the Boltzmann's constant (1.3805×10^{-23} J/Kelvin) and T is the temperature expressed in Kelvin.

The lower energy level is called the α-spin state and the higher energy level is defined as the β-spin state. Logically, more energy is needed to align against the field and thus, more nuclei are localized in the stable α-spin state than in the β-spin state.

The small energy difference (ΔE) between the α- and β-spin states of a nucleus is proportional to the strength of the external magnetic field (B_0). The ΔE is also correspondingly large when the nucleus has a relatively large gyromagnetic ratio (γ). This is demonstrated by Figure 2.9 and the subsequent equation.

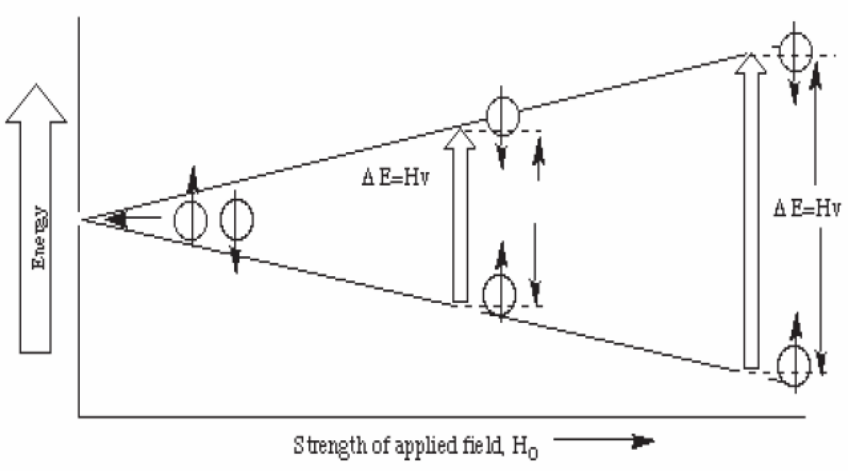

Figure 2.9 – A stronger magnetic field is associated with a greater difference in energy levels [From: http://www.uaf.edu/chem/green/Chapter13McMurry.pdf].

$$\Delta E = h\nu = h \frac{\gamma}{2\pi} B_0$$

or

$$\nu = \frac{\gamma}{2\pi} B_0$$

The upper equation also shows that the magnetic field (B_0) is proportional to the operating frequency (MHz) of the NMR. Modern NMR spectrometers use powerful magnets with fields ranging from 1 to 20 tesla (T) and operate at frequencies ranging from 60 to 900 MHz. The operating frequency of an NMR depends on the strength of the built-in magnet and the specific nucleus being studied. The higher the operating frequencies of the spectrometer, the

better are the resolution (separation capacity of the peaks) of the NMR spectrum and the sensitivity.

2.4.2 Electromagnetic radiation or radiofrequency pulse

When the energy of the radiation pulse corresponds to the energy difference (ΔE) between the α- and β-spin states, nuclei in the α-spin state 'flip' or are 'excited' to the higher β-spin state. Because the energy difference between the α- and β-spin states is so small, only a small amount of energy is necessary to flip the spin. This amount of energy is provided to the nuclei as radio frequency (rf) energy or an electromagnetic pulse and the frequency of radiation needed is determined by the difference in energy between the two spin states. After the absorption of energy, nuclei undergo 'relaxation' i.e. they return to their original state (Figure 2.10). While relaxing, nuclei emit electromagnetic signals of which the frequencies are dependent on the energy difference between the α- and β-spin states. The NMR spectrometer detects these signals and displays them as a plot of signal frequency versus intensity after Fourier transformation – an NMR spectrum. Hence, the term nuclear magnetic *resonance* refers to the nuclei being *in resonance* with the applied radiofrequency pulse.

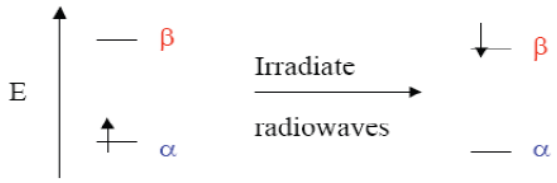

Figure 2.10 – Irradiation of nuclei with the proper frequency (corresponding to the energy difference between the α- and β-states) will cause a 'flip' from the α-state to the β spin state while absorbing energy. Subsequently, nuclei will return to their original state (*resonance*) [From: http://www.uaf.edu/chem/green/Chapter13McMurry.pdf].

2.4.3 Classical representation of the behaviour of a nucleus in a magnetic field

Imagine a nucleus with spin ½ which possesses a magnetic moment μ and therefore, acts like a small nuclear magnet. Conducting NMR experiments involves the application of an applied, second magnetic field B_1. Subsequently, when placed in a strong applied magnetic field, nuclei tend to align themselves parallel or antiparallel with that field. In fact, due to their spin, the nuclear magnets do not line up exactly but their axis *precesses* around the applied

magnetic field (Fig. 2.11) with a frequency called the Larmor precession frequency ω, given by the lower equation.

$$\omega = \gamma B_o \ (rad/s)$$
$$\upsilon = \gamma B_o/2\pi \qquad \textit{Larmor Frequency}$$

Where ω and ν correspond to the Larmor frequency, B_o is the applied magnetic field and γ is the gyromagntic ratio for the examined nucleus.

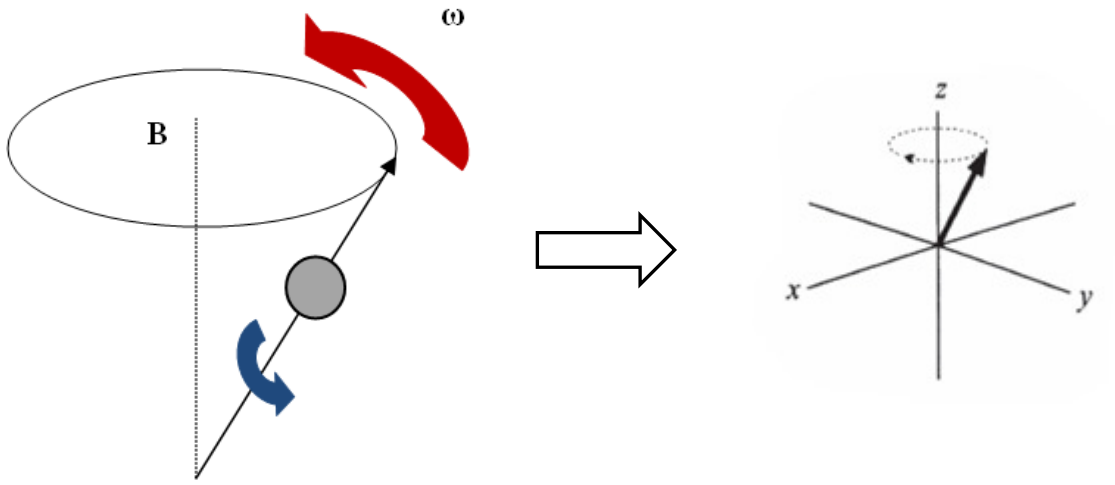

Figure 2.11 – A nuclear magnetic moment rotates around the axis of the externally applied field (*precession*). By convention, the field is applied along the z-axis of a Cartesian co-ordinate frame [From: http://www.uaf.edu/chem/green/Chapter13McMurry.pdf].

The potential energy of the precessing nucleus is given by the subsequent formula:

$$E = -\mu B \cos\theta$$

where θ is defined as the angle between the direction of the applied field and the axis of nuclear rotation (commonly 90°).

If we now consider many spins with the same Larmor frequency, we notice a random distribution of these spins around the precessional cone. Hence, a random distribution of all individual magnetic moments is apparent around that cone (Figure 2.7a). Since there is no net

magnetization in the transverse xy-plane, all single magnetic moments can be replaced by a 1 net magnetization vector, M_0 (Figure 2.12b). This vector is parallel to B_0 because the majority of nuclei are rather in the parallel than in the anti-parallel state.

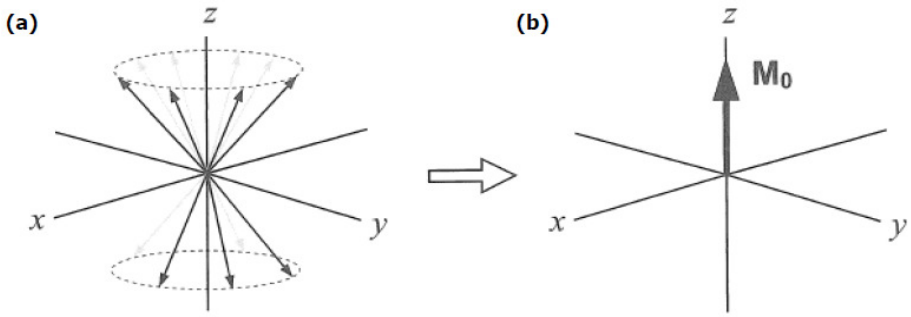

Figure 2.12 – **(a)** randomly distributed individual magnetic moments around the precessional cone and **(b)** replacement by one bulk magnetization vector, M_0.

Imagine that the radiofrequency pulse is provided along the x-axis (= B_1), orthogonal to the existing magnetic field, B_0 (along the z-axis). As a consequence, the bulk magnetization will be transferred to the y-axis. The angle θ will be dependent on the amplitude and the duration of the pulse. For instance, a 90° pulse is given when the radiofrequency pulse ends at the moment at which the bulk magnetisation reached the y-axis. Subsequently, a net magnetisation along the xy-plane is obtained (Figure 2.13).

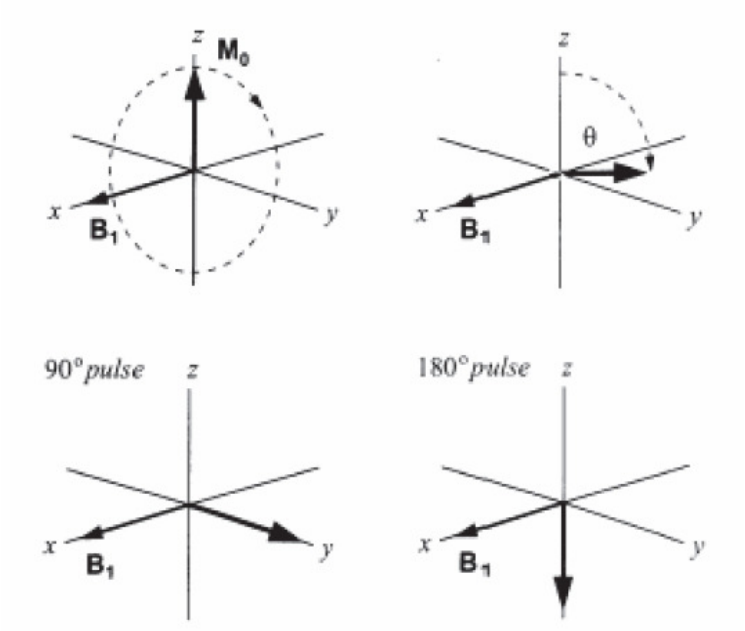

Figure 2.13 - An rf pulse (B1) applies a torque to the bulk magnetization vector, M_0, driving it to the xy-plane from equilibrium. A 90° pulse moves the net magnetization from the z-axis to the xy-plane whereas a 180° pulse moves it from α- to the β-state [From: http://www.uaf.edu/chem/green/Chapter13McMurry.pdf].

As already mentioned before, all nuclei will eventually return to their original equilibrium condition as a consequence of the relaxation process. When the nuclei flip back to their original state, they emit electromagnetic signals of which the frequency is similar to the energy difference between α- and β-spin states. This is called the Free Induction Decay or FID signal. The intensity of the signal decays as the nuclei lose the energy they absorbed from the rf pulse. Nowadays, mathematical conversions by Fourier transformation are applied to convert time domain data into a frequency domain data. This results in an NMR spectrum that plots the frequency versus the intensity of signals.

2.4.4 Chemical shift

The significance of NMR spectroscopy in chemistry is based on its ability to distinguish a particular nucleus, proton (^{1}H in this doctoral thesis) with respect to its environment in the molecule. Hence, the resonance frequency of that nucleus, also defined as *chemical shift* is influenced by the distribution of electrons in the chemical bonds of the molecule.

The value of the chemical shift resonance of a specific nucleus is therefore dependent upon molecular structure. Chemical shift positioning can be considered as a tool to estimate how far a signal is positioned from the signal of an internal reference compound (e.g. TMSP calibrated at 0 ppm). The scale for chemical shifts is generally designated by the symbol $\boldsymbol{\delta}$ as location unit. The chemical shift is determined by measuring the distance of any given signal to that from the TMSP peak (in hertz) and dividing this by the operating frequency of the instrument (in megahertz). Dividing hertz by megahertz eventually results in a unit of parts per million or ppm.

$$\delta = \text{chemical shift (ppm)} = \frac{\text{distance downfield from TMSP (Hz)}}{\text{operating frequency NMR (MHz)}}$$

The most important perturbation of the NMR frequency is the shielding effect of the surrounding shells of electrons in the surrounding molecular orbital of a particular nucleus, generally described as *nuclear shielding*. Electrons, similar to the nucleus, are also charged and rotate with a spin to produce a magnetic field opposite to the magnetic field produced by the nucleus. As a consequence of this electronic shielding, the magnetic field *at the nucleus* (which is what determines the NMR frequency) is reduced and thus, a higher external field is required to meet the resonance conditions in an experiment [Günther 1994]. This will be reflected in the spectra since the NMR frequency will be shifted *upfield* (that is, a lower chemical shift), whereas if it is less shielded by such surrounding electron density, then its NMR frequency will be shifted "downfield" (that is, a higher chemical shift).

Anyhow, the great advantage of the δ scale is that the chemical shift of a given nucleus is independent of the operating frequency of the NMR machine.

2.4.5 Proton NMR (^{1}H-NMR)

Each nucleus possesses a characteristic gyromagnetic ratio and therefore, a different RF-frequency is required to bring any of them into resonance. NMR spectrometers are equipped with RF-amplifiers which can be tuned to the desired frequencies in order to achieve NMR spectra from different nuclei such as ^{1}H, ^{13}C, ^{15}N, ^{31}P, etc.

The 1D proton experiment is one of the most commonly used high resolution NMR experiments and often the first experiment performed to verify or to investigate the structure of a (small) molecule. The ability to resolve all small-molecule metabolites at a concentration of approximately 10 µM is a unique advantage of NMR spectroscopy. This concentration limit even can be below 10 µM if cryogenic probes and high field spectrometers are used [Serkova *et al.* 2008].

^{1}H nuclei are ubiquitous in organic molecules and have a natural abundance of 99.98 %. Consequently, ^{1}H-NMR experiments can be applied to a broad range of biofluids and extracts. The signals arise from protons of aromatic, methyl and methylene groups. This way, researchers can obtain information about the chemical structure and the chemical environment but also on the dynamic interactions between molecules [Wilson and Lenz 2007].

^{1}H-NMR measurements are simple, fast and provide a wealth of information about the proton nuclei in organic materials. First of all, the proton chemical shift can be used to distinguish different functional groups. Moreover, integrating the proton signals yields information about

the number of protons that contribute to these signals. Thirdly, the multiplicity of the signals provides information about the scalar coupling revealing more structural information about the molecule [Bruice 2004].

One of the encountered problems in ^{1}H-NMR spectra is the extensive signal overlap due to the large amount of detected peaks and the narrow chemical shift range (10-12 ppm). This problem is partly solved by employing higher field spectrometers (e.g. 700 to 950 MHz).

Improved signal dispersion can then be achieved but the enhanced sensitivity unfortunately increases the spectral complexity as well [Wilson and Lenz 2007].

Nevertheless, ^{1}H-NMR spectroscopy has proven to be a useful tool to explore the rich biochemical content of biological matter.

In this project, 1D ^{1}H-NMR (and 2D NMR to a lesser extent) were employed to study the metabolomics of fresh water (common- and crucian carp) and marine (dogfish shark) fish, exposed to different oxygen conditions.

2.4.6 Used spectrometers

Two different NMR spectrometers were used in this work: a 400 MHz and a 700 MHz NMR (Figures 2.14a and b).

(a) **(b)**

Figure 2.14 – **(a)** 400 MHz NMR at the University of Antwerp, **(b)** 700 MHz NMR at the University of Ghent.

The Bruker Avance II-400 MHz (Figure 2.14a) operates at a proton frequency of 400.13 MHz and is situated at the University of Antwerp, in the research group of Applied NMR at the department of Chemistry. It is equipped with a 5 mm BBO-Z probe and a 24-SampleCase automatic sample changer. This spectrometer was mainly used during the first year of the project, to evaluate the results of different tissue extraction techniques for fish. By using the 400 MHz NMR, we achieved a first, global idea about the ^{1}H-NMR spectra of tissue extracts of fresh water and marine fish. Subsequently, the next step was to measurement of these tissue extracts with higher magnetic field spectrometers such as the 700 MHz NMR to ensure a maximal dispersion of the signals and the highest sensitivity that is required to perform metabolomics experiments.

The Bruker Avance II-700 MHz NMR (Figure 2.14b) operates at a proton frequency of 700.13 MHz and is located at the University of Ghent, in the NMRSTR group at the department of Organic Chemistry. The 700 MHz can be considered as the ‘crown jewel' of the interuniversitary NMR facility, financed by the University of Ghent, the Free University of Brussels (VUB) and the University of Antwerp to support fundamental, basic and applied

research in the chemical, material and biomolecular sciences. The spectrometer is equipped with a BACS-60 automatic sample changer and a 5 mm inverse TXI-Z probe was used to perform ^{1}H-NMR experiments.

In all cases, the 700 MHz NMR was used to explore the metabolic responses of various tissue extracts of fish to oxygen deprivation throughout this work.

2.5 Applications of Metabolomics

The capacity of Metabolomics to measure hundreds of important metabolites in a quickly, easily and inexpensively manner has obviously opened the door to many applications in a large number of areas.

The main applications of metabolomics are situated in the areas of toxicity and drug assessment, nutrition, animal model studies, drug treatment (pharmacometabolomics), disease monitoring and biomarker identification, environmental sciences and even organ transplant monitoring [Lindon *et al.* 2007; Lindon and Nicholson 2008; Martineau *et al.* 2011; Moco *et al.* 2007; Dunn *et al.* 2005].

Toxicology studies have implemented metabolomics extensively to evaluate the response of an organism to different toxins. Any toxin can induce a series of metabolic perturbations and the degree to which an organism can recover from this toxic insult depends on the mode of action and the type of toxin, the duration of exposure and the physiological status of that organism at the time of toxin exposure.

Metabolomics can also be used for the phenotyping of mutant and transgenic animals. Specifically, the consequences of the transgenesis process can be investigated and the metabolomic approach can distinguish the unintended effects of this process from the intended consequences. Metabolic information about the differences between mutant and transgenic animals can be gained as well as information about the human diseases they aim to simulate [Lindon *et al.* 2007]. As such, a more accurate evaluation of their suitability as disease models can be obtained.

Metabolomics applied to nutritional sciences (*foodomics*) offers interesting insights in food and nutrition domains. The study investigates the chemical composition (compound profiling) and authenticity of food products, the presence and identity of food contaminants and enables the detection of biomarkers related to food quality- and safety. That way, foodomics can

contribute to the improvement of consumer's well-being, health and confidence. As a representative example, a study carried out by Sobolev and co-workers applied NMR spectroscopy to determine the metabolic profiling of sea bass extracts. The ultimate goal of the paper was to evaluate whether NMR metabolic profiling could discriminate between wild and cultured sea bass samples, based on the profiles of hydrophilic and hydrophobic metabolites in muscle tissue [Sobolev *et al.* 2008]. Other studies highlighted the applicability of NMR-based metabolomics in determining the link between the origin and quality of wine products [Lee *et al.* 2008].

Metabolomics already has an important and broad impact in different areas of pharmaceutical science. It includes the validation of animal models, e.g. the evaluation of genetically-modified animals and the preclinical toxicological screening of candidate drugs. The selection process of robust candidate drugs aims at minimizing the occurrence of adverse drugs effects and is one of the most important steps in the pharmaceutical industry. Furthermore, an improved understanding of the toxicity mechanisms of marketed drugs can be achieved by investigating representative biofluids of humans or animals such as urine, blood serum, cerebrospinal fluids, etc. Any drug/toxin will undoubtedly induce a series of characteristic metabolic responses and by studying biofluids (urine, plasma,etc.) over a series of time intervals, a biochemical trajectory of response can be calculated. That way, metabolomics provides specific biochemical information at the individual level and this offers many possibilities to subsequent drug treatment.

Pharmacometabolomics is such a promising tool: it investigates the genetic make-up of organisms (their genetic polymorphisms) and their varying abilities to cope with both beneficial and adverse pharmaceuticals [Lindon *et al.* 2007]. The aim is to reach a real 'personalized healthcare' in the near future and this field is likely to expand rapidly.

In addition, metabolomics can aid to the diagnosis and prognosis of human diseases through biomarker discovery, particularly for chronic and degenerative diseases and inherent metabolic diseases [Lindon and Nicholson 2008]. Plasma can be used to study diabetes, cerebrospinal fluid for investigating Alzheimer's disease, synovial fluid for osteoarthritis and urine to study various renal diseases as a few examples [Lindon *et al.* 2007]. Of particular interest is the High Resolution Magic Angle Spinning technique (HR-MAS). Entire tissues can be examined with this technique without any extraction or other preparation. The number

of publications using this method is rapidly increasing mainly for cancer studies (e.g. prostate, brain and breast tumours).

The application of metabolomics to study environmental adaptations is of particular importance in this work since we studied the metabolic response of organisms (fish) to oxygen deprivation as environmental stress factor. Therefore, this application of the metabolomics approach is described in detail in paragraph 2.5.

The application of metabolomics in the field of organ transplant monitoring started approximately 40 years ago [Salaman 1991]. In general, metabolite measurements are performed to monitor two key aspects of organ physiology: the organ perfusion injury and its (dys) functioning. Organs that were investigated following transplantation include kidneys, liver, pancreas, lungs and heart. Both *ex vivo* (i.e. biofluids as urine, serum, etc.) as *in vivo* measurements (i.e. inorganic phosphate or phosphorylated metabolites as ATP, PCr, etc.) were applied to evaluate organ transplants. The majority of the observed metabolites are associated with universal metabolic processes such as glycolysis, gluconogenesis and lipid metabolism. These molecules provide instant information about the cellular status/function and hence, the organ viability/function [Wishart 2005]. Other metabolites are involved in inflammation, tissue damage, reperfusion injury and transplant rejection.

In summary, it is clear that metabolomics is a very promising tool which will continue to have a major impact in different application areas. The continuing challenge in metabolomics, however, is the ability to rationalize the source and cause for the observed metabolite signals, both quantitative and qualitative. For example, increased levels of certain metabolites can simply arise from intensive exercising, diet changes or other non-disease related factors. Distinguishing these inconsequential metabolite changes from the more consequential changes is still a key challenge. Additionally, in order to evaluate these metabolic changes correctly, researchers should know which levels of metabolites are considered to be ‘normal’. Normal ranges are known for standard compounds e.g. creatinine, urea, glucose, etc. but less is known about other metabolites. Detailed comparisons are therefore needed to determine these levels before any conclusion can be drawn.

Although there still are some constraints associated with NMR-based metabolomics, such as the poor sensitivity of NMR spectroscopy and the complexity of biochemical and spectroscopic data, new developments and improvements have been made to solve these problems. For example, a single compound can result in multiple peaks and the position of

one metabolite in different samples or in various tissues might differ as a consequence of pH influences and/or sample characteristics (salt concentration, etc.). Statistical analysis, on the other hand, assumes that peaks from one metabolite are found in one column of a data table (bucket table). For every error, the statistical analysis loses power and the risk of missing a potential biomarker increases [Aberg *et al.* 2009]. Therefore, statistical approaches have been developed to synchronise data sets and as such, to enable an accurate interpretation of the observations. One might expect that further developments in this field will increase rapidly.
Of course, one must realize that metabolomics is not the 'ultimate approach', capable of solving all the problems [Wishart 2005]. Metabolites only comprise a small part in the overall composition of an organism and reflect changes that occur at many different levels (organ, tissue, cells and molecules). Therefore, important future trends include the integration of transcriptomic, genomic and proteomic data. This systems biology-approach hopefully enables an improved understanding of an organism's total biology [Lindon and Nicholson 2008].

2.6 ^{1}H-NMR metabolomics in environmental sciences

2.6.1 Introduction

Nowadays, the application of metabolomics in environmental sciences is still in its infancy but it offers undoubtedly great possibilities to this area. In general, metabolomics in environmental research is used in three main domains: 1) toxicology studies and risk assessment, 2) responses to environmental stressors and 3) disease monitoring.

The environmental toxicology studies aim at the unbiased assessment of the response of an organism to toxicants and the subsequent identification of biomarkers for risk assessment. For example, Samuelsson and colleagues applied ^{1}H-NMR-based metabolomics in combination with multivariate data analysis to study the environmental effects of the estrogen ethinylestradiol on plasma and lipid extracts in rainbow trout [Samuelsson *et al.* 2006].

The second research area evaluates an organism's metabolic response to different environmental stressors such as temperature, salinity, and changes in oxygenation. As an example, Viant and co-workers investigated in 2003 the metabolic responses of steelhead trout to thermal stress [Viant *et al.* 2003]. Lastly, metabolomics can be successfully applied in disease monitoring of wild aquatic animals. This could be of particular interest to aquaculture.

Stentiford and colleagues applied metabolomics to study liver tumours in flatfish and identified relevant biomarkers to disease diagnosis [Stentiford *et al.* 2005].

By using a metabolomics approach, researchers can achieve a lot of relevant answers to complex biological questions. Since metabolites are crucial to cellular regulatory processes, they provide real-time snapshots of the biochemical status of cells. This is not the case for the measurements of genes, mRNA levels and protein levels because they cannot be used to directly determine cellular functions [Lin *et al.* 2006]. Therefore, studying genes or proteins may still require additional information on the metabolites to understand a given biological response thoroughly.

In this project, we also used metabolomics to study the responses of fish to environmental stressors. More specifically, we aim to characterize the metabolic responses of fresh water and marine fish to varying aquatic oxygen concentrations. By applying high resolution ^{1}H-NMR to tissue extracts of fish, a window is provided to study the biochemical changes that are caused by anoxia and/or hypoxia.

2.6.2 Why is it important to study the environmental oxygen tolerance of fish?

Hypoxia (depletion of dissolved oxygen) or anoxia (absence of dissolved oxygen) is a widespread phenomenon in aquatic environments, affecting a broad range of organisms. More likely, the fluctuating oxygen levels will be more severely experienced in aquatic animals than in other species. Due to their long evolutionary history and the different oxygen requirements between species, fish have experienced a wide range of aquatic oxygen variations and hence, a dramatic selection for anoxia/hypoxia tolerance occurred. In other words, the key to survive extreme environmental conditions such as anoxia or hypoxia is directly linked to the adaptive capacity of a certain species. Hypoxia can be caused by a number of factors: changes in photosynthesis and respiration, tidal and seasonal influences, specific hydrographic conditions [Claireaux and Chabot 2005] preventing the appropriate mixing of the water column and due to increased anthropogenic activities [Hassell *et al.* 2009]. For example, oceanic tide pools have a wide diurnal variation in oxygen availability, ranging from hyperoxic during daylight hours (due to high algal contents and photosynthesis) to severely hypoxic at night. The gradient of fluctuating oxygen levels as seen along the marine nearshore is well known to strongly influence species distribution. For example, sculpins (*Scorpaeniformes*) are marine fish that inhabit a broad range of environments including deeper water, subtidal and intertidal zones. A study by Richards pointed out that

hypoxia-sensitive sculpin species can be located in O_2-stable zones i.e. deeper water and subtidal zones whereas hypoxia-tolerant fish were mainly observed in O_2-variable intertidal zones [Richards 2011]. The Amazon River basin, for instance, experiences dramatic seasonal variations in oxygen concentrations and the combination of fluctuating temperatures and organic waste greatly reduces the dissolved oxygen levels [Walsh *et al.* 2007]. Northern fresh water lakes can become severely hypoxic due to a reduced light penetration and an impaired atmospheric gas exchange caused by winter ice covering and excessive organic decay [Bickler and Buck 2007]. Aquatic hypoxia/anoxia is a worldwide problem and can have serious consequences such as periodic fish kills or a reduced presence and distribution of fish. Importantly, the frequency and intensity of hypoxic events has increased during the last decades [Hassell *et al.* 2009]. In the future, global warming may even affect the aquatic environments much more. Particularly increasing temperatures can affect oxygen dynamics severely because the solubility of oxygen decreases when the temperature increases whereas the respiratory oxygen consumption increases [Hansen and Bendtsen 2009]. Therefore, it is relevant to investigate the impact of varying environmental stressors (hypoxia/anoxia, temperature, ect.) on the aquatic systems.

Furthermore, the study on anoxia/hypoxia adaptations in vertebrates can help us to identify novel targets for the therapy of human diseases following tissue hypoxia. Concretely, humans can suffer from diseases caused by acute hypoxia such as pulmonary hypertension, stroke, myocardial infarction, surgery-induced ischemia/reperfusion, etc. Chronic hypoxia diseases include cancer, foetal/newborn hypoxia, congenital heart syndrome, etc. Hypoxia is a complex phenomenon and its biochemical repercussions are not easily defined. By studying the (metabolic) adaptations of fish to hypoxia/anoxia, novel information can be gained including the discovery of new biomarkers, specific pathway information, etc. [Serkova *et al.* 2008]

Therefore, by investigating the anoxia/hypoxia tolerance mechanisms in fish, we can attain a lot of useful information that will positively contribute to a better insight towards the impact of limited oxygen levels on vertebrates.

Chapter 3

Selection of the appropriate tissue extraction technique

BASED ON:

"Methanol/Chloroform/Water extraction to be preferred over Perchloric acid extraction for the ^{1}H-NMR based metabolomics study of white muscle and liver extracts in fish"

Isabelle Lardon[*(1,2)], Gudrun De Boeck[(1)], Roger Dommisse[(2)]

Submitted to the ***Journal of Mediterranean Chemistry***

[(1)] University of Antwerp – Department of Biology – Research Group of Systemic Physiological and Ecotoxicological Research (SPHERE) - Groenenborgerlaan 171, B-2020 Antwerp, Belgium

[(2)] University of Antwerp - Department of Chemistry – Research Group for Applied NMR - Groenenborgerlaan 171, B-2020 Antwerp, Belgium

Abstract

High-resolution ^{1}H-NMR has become a key method to explore the metabolic changes in cells, tissues and intact organisms (Metabolomics). In order to generate reproducible NMR spectra with many different metabolites, it is of prime importance to apply an efficient and reliable extraction method. In this paper, an appropriate extraction technique was selected to study the ^{1}H-NMR based metabolomics of liver and muscle tissues in fish. Two commonly applied extractions were tested: perchloric acid and methanol/chloroform/water respectively. These two methods were evaluated in terms of total metabolite yield, reproducibility, ease, speed and diversity of metabolites. In conclusion, the methanol/chloroform/water method is superior to the perchloric acid approach because it enables the simultaneous extraction of both hydrophilic and hydrophobic fractions from one sample, results in more reproducible spectra and leads to a higher yield of metabolites. Therefore, the methanol/chloroform/water extraction was selected to provide unique metabolic profiles of tissue extracts in fish.

Keywords: tissue extraction, fish, perchloric acid, methanol/chloroform/water, ^{1}H-NMR

3.1 Introduction

A metabolomic study involves the sampling, the analysis, the identification and the quantification of small molecular weight compounds (metabolites) in biological tissues, bio-fluids or cells to generate unique metabolic profiles. Sample preparation is critical in metabolome analysis, it is of particular importance to immediately inactivate all enzymatic activities to prevent any metabolic turnover.

In tissue metabolomics, liquid nitrogen-cooled mortar and pestle grinding has become a standard procedure to prepare the samples tissue for extraction [Fernandez *et al.* 2010]. Indeed, the low temperature of −196 °C inhibits the activities of enzymes and the sample reflects its biological status at the time of snap-freezing. Grinding the sample thoroughly also ensures that the extraction is performed on a homogeneous sample. The next crucial step in the sample preparation process involves the tissue extraction. Although ^{1}H-NMR spectroscopy is perfectly suited to produce high-quality metabolic profiles, the extraction of metabolites from animal tissues is the most labor-intensive and rate-limiting step. Due the presence of different (quantitative) metabolites in cells with a particular chemical stability, solubility and polarity, extraction procedures can vary in the volume, proportion and the type of solvent, the number of repeated extractions and the duration of the incubation cycles or in the partition time on ice. An ideal extraction method should be able to extract all metabolites in a nonselective and reproducible way but in reality, there is no universal extraction method that can detect the entire metabolome. Therefore, the selection of an extraction method will depend on the nature of the examined samples and should be adapted to the analytical tool that analyses the extracts. For instance, the extraction methods for GC-MS and LC-MS samples cannot be applied for NMR-based metabolomic studies due to the derivatization procedures and/or the chromatography columns which results in the selective removal of some metabolites. The latter implies that, although LC-MS and GC-MS have better sensitivities and a higher detection limit than NMR, these techniques do not offer the nonselectivity of NMR [Martineau *et al.* 2011].

Recently, significant advances have been made to optimize the extraction techniques by improving the efficiency and reproducibility of extraction strategies to study the metabolomics of animal tissues [Lin *et al.* 2007], plant [Kaiser *et al.* 2009], yeast and bacterial systems [Winder *et al.* 2008; Canelas *et al.* 2009; Shin *et al.* 2010; Sekiyama *et al.* 2011]. More specifically in fish, [Lin *et al.* 2007] and [Wu *et al.* 2008] evaluated different

metabolite extraction strategies from tissue samples for NMR-based metabolomics. Generally, the optimal extraction method should fulfil the subsequent three criteria: (1) to extract the highest number of many different metabolites from the cells by preventing their exclusion due to physical or chemical properties, (2) to be reliable, reproducible and robust and (3) to be adapted to the applied analytical instrument [Martineau *et al.* 2011].

The purpose of this study was to test different extraction techniques and to select the most suited approach to study the ^{1}H-NMR based metabolomics of fish tissue extracts. Specifically, we examined the extraction of metabolites from liver and white muscle in fish by using the perchloric acid extraction and the methanol/chloroform/water (M/C/W) method. Both extraction techniques were evaluated in terms of reproducibility, ease, speed, total yield and diversity of metabolites.

3.2 Perchloric acid extraction

3.2.1 Properties

Perchloric acid ($HClO_4$) extraction is the most ubiquitous method and commonly used to precipitate proteins and to extract water-soluble metabolites in general. Similar to other analytical techniques, the perchloric acid extraction has its advantages and disadvantages. Bouchereau and coworkers, for instance, applied this technique successfully to plant tissues in order to extract amines and other unknown metabolites [Bouchereau *et al.* 2000]. Nevertheless, the pH adjustment following sample homogenization, the time dependence of extraction efficiency or yield and the potential to chemically modify metabolites are important drawbacks of this method. Even a destruction of metabolites (pyruvate, nucleotides, NAD, $NADH^{+}$) has been described in the literature [Maharjan and Ferenci 2003; Villas-Boas *et al.* 2005]. On the other hand, perchloric acid is a strong denaturant, rapidly inactivating enzymatic processes in a biological system.

3.2.2 Protocol

The perchloric acid extraction was tested by adding 6 % of ice cold perchloric acid (5 ml/g) to 100 mg of homogeneous tissue powder. Samples were vortexed for 1 min and stored on ice for 10 min. Following centrifugation (12.000 g, 10 min, 4 °C), the supernatant was removed and neutralized to a final pH of 7.2 with 2 M K_2CO_3. The resulting supernatant was then kept on ice for 30 min, pH values were checked again, followed by a second centrifugation step to

remove the precipitated salts. Prior to ^{1}H-NMR analyses, samples were lyophilized overnight to avoid the presence of a dominant water signal in the spectra.

3.3 Methanol/Chloroform/Water extraction

3.3.1 Properties

Tissues will contain both hydrophilic and lipophilic components, hence polar and non-polar solvents are needed to extract both fractions from cells. Polar organic solvents as methanol (or acetonitrile) are typically mixed with water to extract hydrophilic compounds [Le Belle *et al.* 2002; Dunn *et al.* 2005; Viant *et al.* 2008]. In addition, chloroform can be added to the sample to extract the hydrophobic metabolites. The simultaneous extraction of both lipidomic and hydrophilic compounds from one tissue sample is of particular importance in lipid-rich tissues such as brain and liver. The methanol/chloroform/water approach is less widely used as the perchloric acid extraction but it can be advantageous in disease diagnosis e.g. to detect the perturbations in the lipid and aqueous metabolites due to brain tumours [Le Belle *et al.* 2002].

3.3.2 Protocol

The methanol/chloroform/water extraction (ratio 2:1:1.8) was tested by adding ice cold methanol (4 ml/g; analaR normapur, min. 99.8 %, VWR, Pennsylvania, USA) and ice cold milliQ water (0.85 ml/g) to the powder. The homogenate was then vortexed for 1 min. Subsequently, ice cold chloroform (4 ml/g; normapur, 99.3 %, VWR, Pennsylvania, USA) and milliQ water (2 ml/g) was added to extract the hydrophobic metabolites; the mixture was vortexed for 1 min and then incubated on ice for 10 min to partition. The obtained supernatant was centrifuged at 4 °C for 10 min at 2000 g, resulting in a biphasic solution. The upper polar and lower non-polar layers were carefully separated and transferred to 15 ml sterile Falcon tubes. Finally, all samples were lyophilized overnight.

3.4 Evaluation experiment of the two extraction methods

3.4.1 Fish sampling

Three adult common carp (*Cyprinus carpio*), kept in filtered Antwerp City tap water (15–16 °C) at the laboratory of the University of Antwerp were used in this study. Fish were euthanized in an overdose of neutralised MS222 (1 g l^{-1}, pH 7.4, Sigma Chemical, St. Louis, MO, USA). Subsequently, liver and white muscle were dissected on ice and each tissue was

divided into three parts. In total, nine liver and nine muscle samples were obtained from three fish, immediately snap-frozen in liquid nitrogen and stored at -80 °C until further analysis.

3.4.2 Tissue extraction methods

Two extraction methods were selected for evaluation based on the existing literature: perchloric acid [Lin *et al.* 2007] and the M/C/W extraction [Lin *et al.* 2007; Wu *et al.* 2008]. Frozen liver and muscle samples were ground in a liquid nitrogen-cooled mortar and pestle and approximately 100 mg of homogeneous tissue powder (based on the protocol in *Nature* by Nicholson *et al.* 2007) was used for the extraction procedures.

Tissues were extracted by perchloric acid or by methanol/chloroform/water according to the protocols described in sections 3.2 and 3.3 respectively. Concerning the M/C/W extraction, only the polar fractions of liver and white muscle tissue are considered for the assessment of the two extraction methods.

Total metabolite yield, reproducibility, ease, speed and diversity of metabolites were the criteria utilized to assess the quality of the extraction techniques.

3.4.3 1D ^{1}H-NMR analysis of liver and white muscle extracts

Prior to ^{1}H-NMR measurement, all dried extracts were dissolved in 580 µl of sodium phosphate buffer prepared in D_2O to minimize variations in sample pH and allow for deuterium locking, sodium-3-trimethylsilylpropionate (TMSP) was added to the buffer as an internal standard (see following paragraph). Subsequently, samples were transferred to a 5 mm NMR tube (NE-HP5-7, Cortecnet, France) and analyzed immediately by ^{1}H-NMR.

The 50 mM sodium phosphate buffer in D_2O (99.9 atom % D) consisted of Na_2HPO_4, 33.5 mM (AnalaR Normapur); NaH_2PO_4, 16.45 mM (GPR rectapur) (all from Merck, Darmstadt, Germany); 0.1 mM TMSP (≥ 98 %, Cambridge Isotope Laboratories, MA, USA); 0.5 mM sodium azide (99 %, Acros Organics, NJ, USA). Deuterium chloride in D_2O (ClD, > 99 atom % D, 20 wt %) and sodium deuteroxide in D_2O (NaOD, > 99 atom % D, 40 wt %) (both from Acros Organics, NJ, USA) were added to achieve a pH of ~ 7.

Spectroscopy was performed at 25 °C with a Bruker Avance spectrometer operating at 399.83 MHz (Bruker Biospin, Europe), equipped with a 5 mm inverse TXI-Z probe and a BACS-60 automatic sample changer. Tuning, matching and shimming were performed automatically for each sample in order to minimize the variation due to sample manipulation.

One-dimensional ^{1}H-NMR spectra of liver and white muscle were acquired with a standard sequence using a 90° pulse, a relaxation delay of 2.0 s with water presaturation, 128 scans collected into 65 k data points, a spectral width of 8 kHz and an acquisition time of 3.98 s per sample. Data were Fourier transformed with an exponential line broadening of 0.3 Hz. Finally, all spectra were phase -and baseline corrected and chemical shifts were referenced to TMSP (0.0 ppm) using the Topspin software (version 2.1, Bruker Biospin). In total, 18 ^{1}H-NMR spectra were measured for liver extracts of which 9 were extracted by perchloric acid and 9 extracted by M/C/W extraction. The same procedure was applied for muscle extracts. Furthermore, in order to evaluate the reproducibility of an extraction technique, three replicate spectra of one homogenous liver and one muscle sample were measured by ^{1}H-NMR.

3.4.4 Data processing and statistical analysis

The 1D spectra of liver and white muscle extracts were converted to an appropriate format for statistical analysis by automatically segmenting each spectrum in 0.05 ppm integrated spectral regions (bins or buckets) between 0.5 and 10 ppm using AMIX (Analysis of Mixtures, version 3.8.5, Bruker Biospin). Buckets from 4.68 to 5.0 ppm, containing the suppressed water resonance residual signal, were excluded. All spectra were mean-centered and were normalized to total intensity to reduce the influence of concentration variability among the samples.

The generated bucket tables of the tissue extracts were exported as a spread sheet to Excel (Microsoft Office Excel 2007). Student's t-tests were performed in liver and white muscle to compare the metabolite concentrations (yields) from the two extraction techniques. More precisely, nine M/C/W spectra were compared to nine perchloric acid spectra to identify significant changes in the yield of metabolites for liver and muscle tissue. Correction for multiple testing was applied according to a Benjamini-Hochberg test [Benjamini and Hochberg 1995]. In all instances, $p < 0.05$ was used as the level of significance.

Furthermore, in order to assess the reproducibility of the two extraction methods and to identify potential outliers in the datasets, multivariate statistical analysis was performed using principal component analysis (PCA). Specifically, three replicate spectra of one homogenous tissue sample (liver and/or muscle), either extracted by M/C/W or perchloric acid, were compared in the scores plot.

3.4.5 Results and Discussion

Figure 3.1 demonstrates an overview of the liver spectra from one fish, either obtained by perchloric acid extraction (3 spectra at the top of the figure; green) or by the M/C/W method (3 spectra at the bottom of the figure; black).

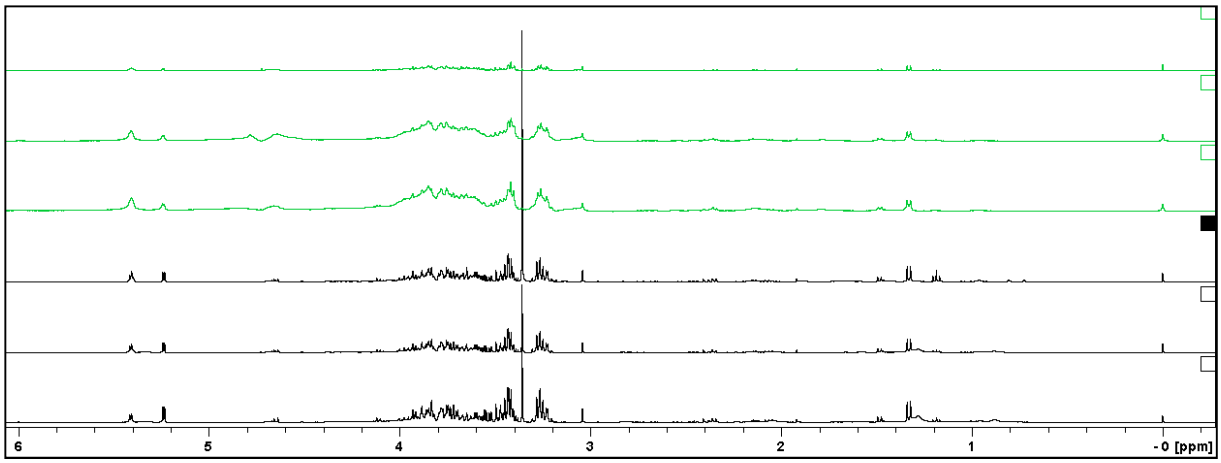

Figure 3.1 - Overview of six ^{1}H-NMR spectra of one liver sample from one fish, of which three spectra result from the perchloric acid extraction (green) and three spectra extracted by methanol/chloroform/water (black).

The reproducibility of the two extraction techniques was determined by evaluating the proximity of the replicate samples in the scores plot of the PCA analysis. Figure 3.2 demonstrates that the perchloric acid extraction is less reproducible as reflected in a larger sample-to-sample variation, and evidenced by the lack of clustering in the PCA scores plot.

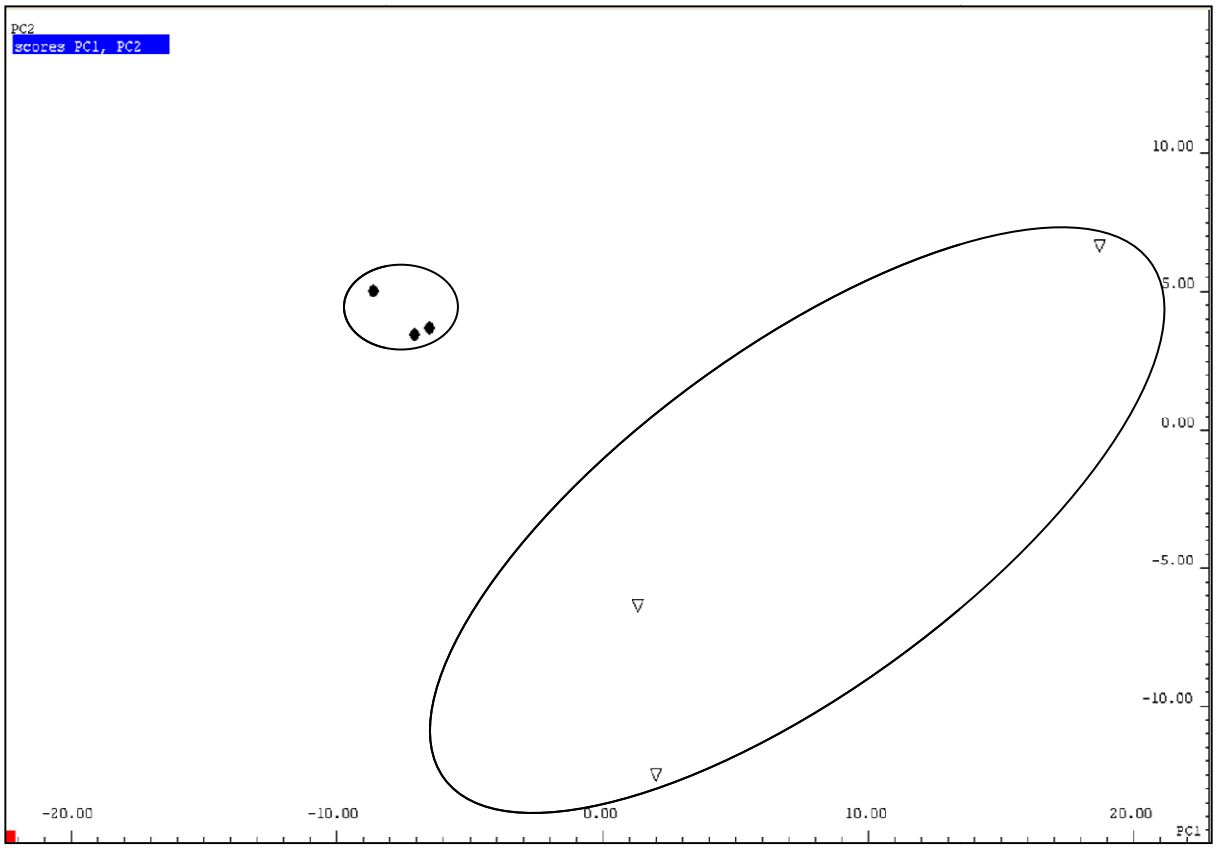

Figure 3.2 - Principal Component Analysis scores plot which compares the ^{1}H-NMR spectra of six liver replicates, either extracted by the M/C/W method (•) or by the perchloric acid method (▽).

The perchloric acid method has some drawbacks which could explain the observed lower reproducibility in the PCA scores plot. Firstly, the samples extracted by perchloric acid needed a neutralization step (K_2CO_3) to avoid further destruction of metabolites by the acidic pH. However, a possible loss of metabolites in perchloric acid can occur during the sample preparation process because metabolites may precipitate when K^+ salt is used to neutralize the perchloric acid. Even after buffering the perchloric acid extracts, the metabolites are extremely sensitive to variations in sample pH, which can result in peak shifting [Martineau *et al.* 2011]. Furthermore, table 3.1 shows that the M/C/W method resulted in higher metabolite yields, compared to the perchloric acid method. Particularly, the yields of alanine, valine, glucose, lactate, glutamate and scyllo-inositol were consistently higher using the M/C/W extraction. Concerning the diversity of metabolites, the M/C/W method is preferred due to the simultaneous extraction of a substantial part of both the hydrophilic and the hydrophobic metabolites in the supernatant. Especially in fish, it is of particular interest to investigate the lipidomic profile due to the significant nutritional health benefits. Perchloric acid extraction,

however, only allows for the extraction of non-selective water-soluble metabolites [LeBelle *et al.* 2002].

Table 3.1 - Comparison of metabolite yields from liver according to the methanol/chloroform/water (M/C/W) and the perchloric acid methods. Data were mean-centered and were normalized to total intensity in order to reduce the influence of concentration variability among the samples. Yields are expressed as area under the curve values (AUC) and represented by means ± SD.

	M/C/W	PCA	*p*-Values
Alanine	0.01 ± 0.001	0.008 ± 0.001	0.02
Creatine	0.03 ± 0.004	0.04 ± 0.005	0.0004
Glucose	0.02 ± 0.005	0.009 ± 0.002	0.002
Glutamate	0.009 ± 0.003	0.006 ± 0.002	0.01
Lactate	0.03 ± 0.008	0.01 ± 0.004	0.006
Scyllo-inositol	0.05 ± 0.03	0.02 ± 0.006	0.007
Valine	0.003 ± 0.001	0.001 ± < 0.001	< 0.001

In terms of speed and ease of the protocol, we can assume that the single perchloric acid extraction is easier and faster than the M/C/W method. Indeed, the latter method is more time consuming due to the time necessary for the biphasic separation of the two layers.

Similar to the liver results, white muscle extracts were evaluated in order to select the best suitable extraction technique. Figure 3.3 shows the comparison of the muscle spectra obtained by perchloric acid extraction (upper three spectra; green) M/C/W extraction and those resulting from the M/C/W method (lower three spectra; black).

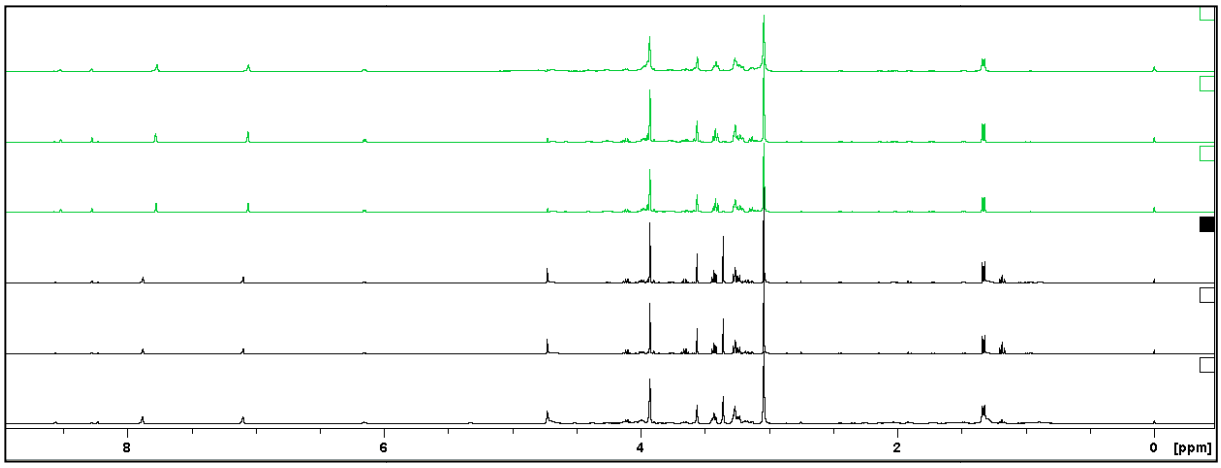

Figure 3.3 - Overview of six ^{1}H-NMR spectra of white muscle, of which three samples are extracted by the perchloric acid method (3 spectra at the top; green) and three spectra achieved by the methanol/chloroform/water extraction (spectra at the bottom; black).

Principal component analysis was conducted to assess the reproducibility of the two extraction methods in muscle tissue. Figure 3.4 shows that the three replicates extracted by the perchloric acid method are again less reproducible compared to the samples extracted using the M/C/W approach.

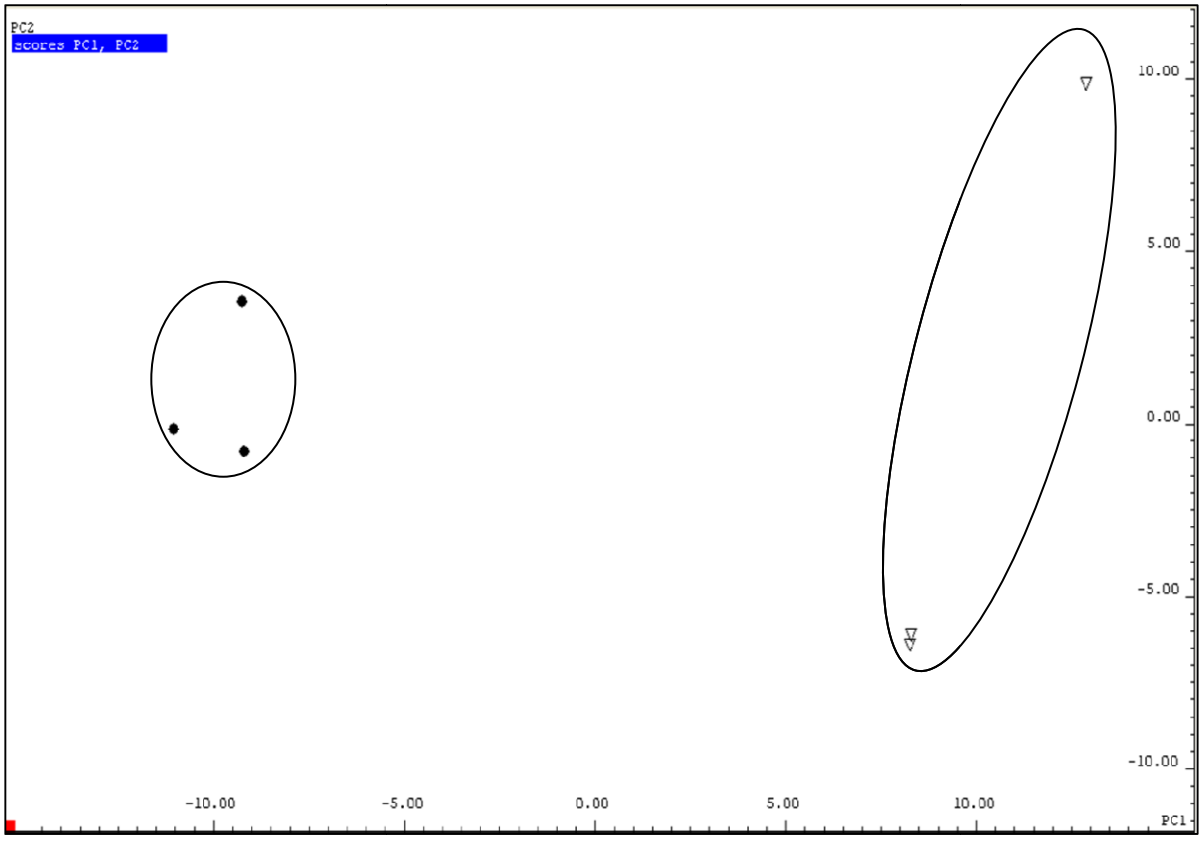

Figure 3.4 - Principal Component Analysis scores plot from the ^{1}H-NMR spectra of three replicate muscle samples, extracted using the M/C/W method (•) and the perchloric acid approach (▽).

Moreover, table 3.2 shows that the metabolite yields from the M/C/W extraction were greater than those obtained by perchloric acid extraction with significant differences in the yields of alanine, ATP, β-OH butyrate, glutamate, (iso) leucine, formate and valine.

Table 3.2 - Comparison of metabolite yields from white muscle, extracted by the methanol/chloroform/water (M/C/W) and/or the perchloric acid methods. Yields are expressed as area under the curve values (AUC) and represented by means ± SD.

	M/C/W	PCA	*p*-Values
Alanine	0.003 ± < 0.001	0.002 ± < 0.001	0.002
ATP	0.004 ± 0.001	0.002 ± 0.001	0.005
β-OH butyrate	0.002 ± 0.001	< 0.001 ± < 0.001	0.003
Glutamate	0.004 ± 0.002	0.003 ± < 0.001	0.02
(Iso)Leucine	0.005 ± 0.002	0.002 ± < 0.001	0.001
Formate	0.0005 ± < 0.001	< 0.001 ± < 0.001	0.04
Valine	0.003 ± 0.001	0.001 ± < 0.001	< 0.001

3.5 Conclusions

These results prompt us to conclude that M/C/W extraction is the best suitable technique to study the ^{1}H-NMR-based metabolomics of fish extracts. The technique is efficient, reliable and reproducible and leads to a higher yield of metabolites in liver as well as in white muscle. Moreover, a substantial amount of both the lipid and aqueous compounds can be obtained from a single sample by M/C/W extraction, making it well-suited to explore the NMR-based metabolomics of fish extracts on a large scale and automated basis.

Chapter 4

Development of an in-house metabolic database

4.1 Introduction

The automated and robust identification of metabolites in a complex biological sample remains one of the greatest challenges in metabolomics. In this project, fish extracts of liver, muscle, brain and heart were analyzed by ^{1}H-NMR and the amount of spectral information was undoubtedly substantial and complex. The typical spectrum can contain thousands of sharp lines from predominantly low molecular weight metabolites and broad bands from protein and lipoprotein signals, depending on the applied pulse sequence/program [Nicholson *et al.* 2007]. Furthermore, extensive peak overlap in certain chemical shift ranges is a frequently occurring feature in NMR based metabolomics and hinders the identification and quantification of the metabolites in complex mixtures.

Generally, signal (metabolite) identification of biological materials is generally based on the chemical shift of the resonances and their relative intensities, the pH dependency of the chemical shifts, the multiplicity of the proton signals and coupling constants. Specifically, the experimental NMR spectra will be matched with databases of standard compounds and/or signals with known chemical shifts and coupling constants [Wilson and Lenz 2007] to confirm the identity of metabolites. Alternatively, when the presence of a certain compound is expected, confirmation of the identity can be achieved by adding a standard compound to the sample and observing if the signal intensity increases or not. Additionally, two-dimensional (2D) NMR experiments can also be useful to elucidate the connectivity between signals, thereby facilitating the spectral assignment of metabolites. [Nicholson *et al.* 2007].

The great challenge facing metabolomics today is the construction of a public database for data storing and sharing information, similar to the well-established DNA sequence databases for molecular biology [Verpoorte *et al.* 2011]. At present, there are several non-commercial, free NMR databases for metabolite identification and databases for standard compounds. For instance, there are the Biological Magnetic Resonance Data Bank (BMRD, www.bmrb.wisc.edu), the Human Metabolome Database (HMDB, www.hmdb.ca), the NMR database of Linkoeping (MDL, http://www.liu.se/hu/mdl/main/), the Magnetic Resonance Metabolomics Database (http://www.metabolomics.bioc.cam.ac.uk/metabolomics), Prime [Akiyama *et al.* 2008] and the NMR Lab of Biomolecules (http://spinportal.magnet.fsu.edu). Other possible databases include the NMRShiftDB (www.ebi.ac.uk/NMRshiftdb/), the Spectral Database for Organic Compounds (SDBS, www.riodb01.ibase.aist.go.jp) and the BioMagResBank (www.bmrb.wisc.edu).

A limited number of companies started with the construction of comprehensive metabolite libraries, including Bruker (http://bruker-biospin.com) and Chenomx Inc. (http://chenomx.com). Unfortunately, these databases are very expensive and therefore, the identification of the metabolites in this work was executed throughout comparisons with public, free databases such as HMDB.

However, both literature papers and databases contain a diverse collection of spectral data, measured under different pH/temperature/etc. regimes and analyzed by spectrometers operating at different magnetic field strengths. Matrix effects such as pH, ionic strength, temperature have important consequences because it can cause peak positional deviations in the spectra. Moreover, the chemical shift of a resonance and the spectral dispersion is also dependent upon the applied field frequency of the spectrometer. Currently, most metabolite profiling studies in the literature are carried out at high magnetic field strengths (600 MHz or higher) to obtain a good spectral resolution.

In other words, an accurate identification of the metabolites in our data is only feasible if we compare the NMR spectra to corresponding literature and/or to public databases that have resembling experimental conditions (pH, temperature, magnetic field strength, etc.) as used in our studies. Due to the limited availability of both relevant literature and compatible databases, it was decided to construct a basic, individual in-house metabolic database.

4.2 Sample preparation protocol

For each standard compound, a 10 mM stock solution was calculated. The product was then dissolved in 3 ml of sodium phosphate buffer prepared in D_2O to minimize variations in sample pH and allow for deuterium locking, containing 0.1 mM DSS and 0.05 mM NaN_3 as internal standard and antibacterial reagents respectively. The 50 mM sodium phosphate buffer in D_2O (99.9 atom % D) consisted of Na_2HPO_4, 33.5 mM; NaH_2PO_4, 16.45 mM (Merck, Darmstadt, Germany); 0.1 mM TMSP (≥ 98 %, Cambridge Isotope Laboratories, MA, USA); 0.5 mM sodium azide (99 %, Acros Organics, USA). Deuterium chloride in D_2O (ClD, > 99 atom % D, 20 wt %) and sodium deuteroxide in D_2O (NaOD, > 99 atom % D, 40 wt %) (Acros Organics, USA) were added to achieve a pH of ~ 7 (± 0.2). Subsequently, buffer was added to the sample to reach a final volume of 4 ml. Finally, the prepared samples were transferred to a 5 mm NMR tube (NE-HP5-7, Cortecnet, France) and analyzed immediately by NMR.

4.3 NMR experiments

The standard components were analyzed on a Bruker Avance II-700 NMR spectrometer at the University of Ghent, operating at 700.13 MHz (Bruker Biospin, Europe), equipped with a 5 mm inverse TXI-Z probe and a BACS-60 automatic sample changer. Tuning, matching and shimming were performed automatically for each sample in order to minimize the variation due to sample manipulation. All spectra were acquired at 303K and 1D (ZGPR, 1D-NOESY and CPMG) as well as 2D experiments (j-RES, COSY, TOCSY, HSQC and HMBC) were performed for each sample and spectra were referenced to the internal standard DSS at 0.00 ppm.

1D NMR spectroscopy

The specific parameters of the various pulse programs are described below in the subsequent subparagraphs. In all 1D experiments, 32 number of scans (8 dummy scans) were collected in 32 k data points, resulting in an acquisition time of 0.78s.

Detailed graphical representations of the 1D NMR pulse programs (ZGPR, 1D NOESY, CPMG) are provided in the Supplementary Information section.

■ *ZGPR*

The ZG program is a simple one-pulse sequence consisting of the recycling delay d1 and either a 90° (p1) or a 30° pulse (p1*0.3) for faster multiscan experiments. The pulse program is called ZG or ZG30 respectively when a 90° or 30° pulse is applied.

In NMR-based metabolomic experiments, the ZG pulse sequence is often combined with presaturation of the water protons in biological samples (ZGPR). Especially tissue extracts and biofluids contain a lot of water and by applying an appropriate solvent-suppression technique such as presaturation, the large NMR water signal can be reduced. The water resonance is saturated by frequency selective irradiation meaning that a continuous irradiation of the water signal will eliminate the energy differences between the α- and β-state. As a consequence, a transition between the two energy states will not happen during the RF pulse and no water signal will be observed in the NMR spectrum. In this ZGPR experiment, a selective irradiation of the water signal was performed during 3s.

■ *1D NOESY*

The 1D NOESY program is a robust, frequently used pulse sequence of choice for NMR-based metabolomics due to several factors. Firstly, 1D NOESY offers an adequate solvent suppression which requires little optimization. Secondly, the physical requirements for the 1D NOESY pulse sequence are present in every modern NMR spectrometer. Presaturation, cycling of various pulse phases combined with the intrinsic volume selection, and T1 discrimination all contribute to make the 1D NOESY an effective pulse sequence for metabolomics [McKay 2011].

■ *CMPG*

The Carr-Purcell-Meiboom-Gill or CPMG pulse sequence is especially attractive to study blood serum or plasma samples that contain high molecular weight compounds (macromolecules) such as proteins, lipids and lipoproteins [Lindon *et al.* 2007]. The pulse sequence results in a reduction of the broad peaks resulting from the high molecular weight metabolites and enables the detection of the resonances from small metabolites, which would otherwise be obscured by these broad peaks.

2D NMR spectroscopy

■ *COSY (cosygpprqf)*

Correlation spectroscopy (COSY) is the easiest 2D NMR experiment displaying crosspeaks whenever 2 protons are directly coupled via 2 or 3 bonds (germinal and vicinal couplings). The position of the crosspeaks yields information about directly coupled protons and hence, strong signals are observed if protons are bond to adjacent carbon atoms. In this study, COSY-experiments were executed with 4 scans and 256 dummy scans for each sample.

■ *TOCSY (mlevphpr)*

Whereas a COSY correlates protons via germinal or vicinal scalar spin couplings, TOCSY (total correlation spectroscopy) experiments provide scalar couplings so that the entire spin network of molecules can be acquired [Fan 1996]. Only quaternary carbon atoms or hetero-atoms without directly bonded protons or with exchangeable protons can interrupt these spin systems. Therefore, a TOCSY can be used for the assignment of groups.

In the TOCSY pulse program we applied, 16 scans and 256 dummy scans were measured for each sample. A graphical representation of this pulse program was not displayed due to the excessive information in the scheme and hence, the invisibility of the parameters.

■ *HSQC (hsqcetgpsisp2.3)*

Heteronuclear Single Quantum Correlation or HSQC-experiments involved the use of pulse programs hsqcetgpsisp2.3 (without multiplicity editing) and hsqcedetgpsisp2.3 (with multiplicity editing). The HSQC provides information about the chemical shift of the directly bonded carbons. In total, 8 scans and 256 dummy scans per sample were performed.

■ *HMBC (hmbcgplpndqf)*

Heteronuclear Multiple Bond Correlation or HMBC spectroscopy provides information about the carbon chemical shift of carbon atoms that are approximately 2-3 bonds distanced from the proton to which they correlated. An advantage is that HMBC also can detect the quaternary carbon atoms. For each sample 16 scans and 256 dummy scans were measured.

■ *j-RES (jresgpprqf)*

This pulse program can be employed to minimize the ambiguity in spin multiplicity and coupling constants [Fan 1996]. In this pulse program, 16 scans and 256 dummy scans were performed for each compound.

4.4 List of metabolites

In total, 26 metabolites were analyzed and included in the database. They are displayed below by their molecular formula and chemical structure.

Acetic acid - CH_3COOH

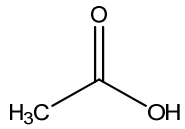

N-Acetyl-aspartate - $C_6H_9NO_5$

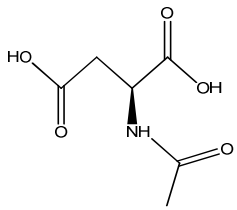

Acetylcholine bromide - $C_7H_{16}BrNO_2$

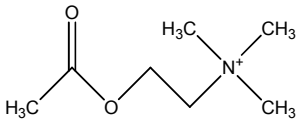

Br-

Agmatine sulphate - $C_5H_{16}N_4O_4S$

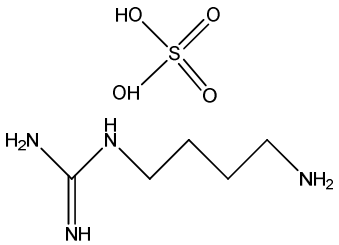

ATP disodium salt - $C_{10}H_{14}N_5Na_2O_{13}P_3$

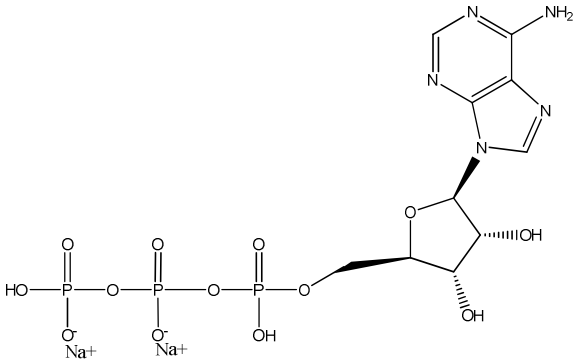

L-Alanine – $C_3H_7NO_2$

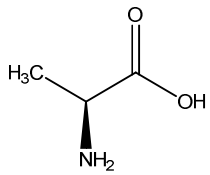

L-Ascorbic acid – $C_6H_8O_6$

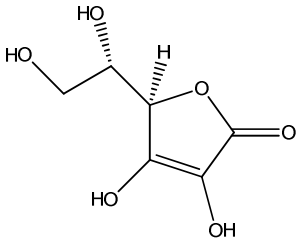

Choline chloride – $C_5H_{14}ClNO$

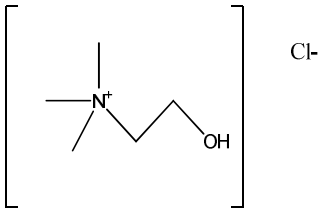

Citric acid – $C_6H_8O_7$

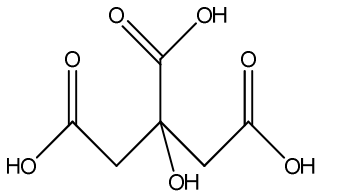

Creatine – $C_4H_9N_3O_2$

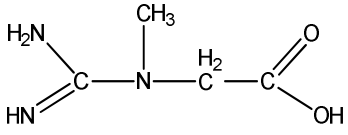

D-Fructose - $C_6H_{12}O_6$

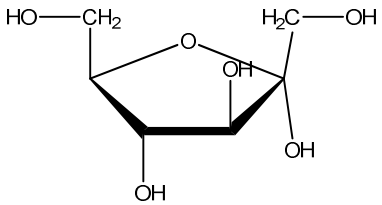

D-Galactose – $C_6H_{12}O_6$

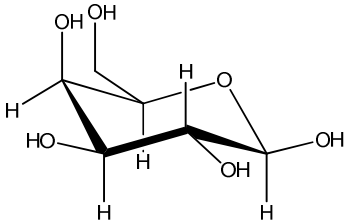

D-Glucose – $C_6H_{12}O_6$

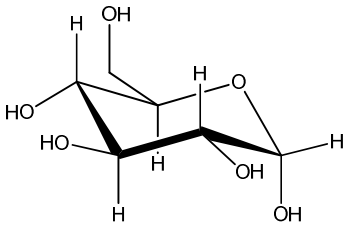

L-Glutamate – $C_5H_9NO_4$

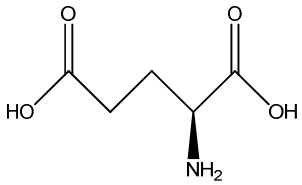

L-Glutamine – $C_5H_{10}N_2O_3$

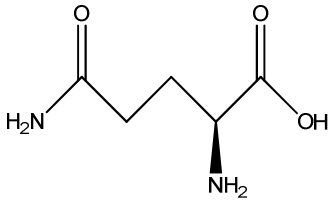

Glycine – $C_2H_5NO_2$

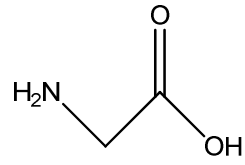

Glycogen - [$C_6H_{10}O_5$]

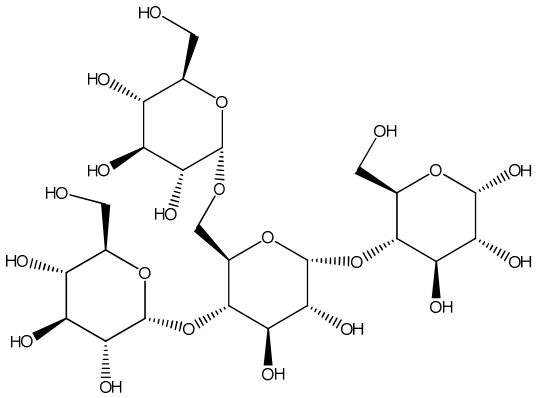

L-Histidine – $C_6H_9N_3O_2$

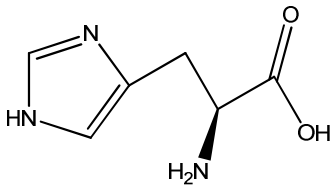

Inositol – $C_6H_{12}O_6$

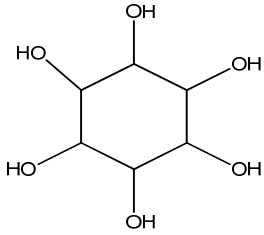

L-Leucine – $C_6H_{13}NO_2$

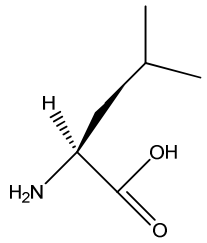

D-Mannose – $C_6H_{12}O_6$

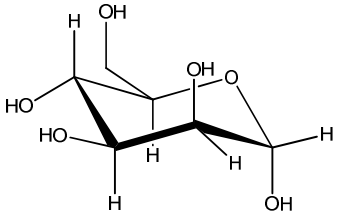

Myo-Inositol - $C_6H_{12}O_6$

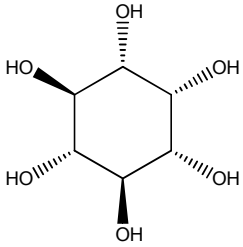

Succinic acid – $C_4H_6O_4$

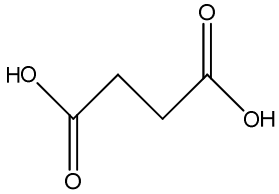

L-Tryptophan – $C_{11}H_{12}N_2O_2$

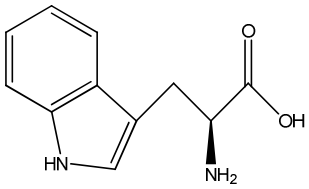

L-Tyrosine – $C_9H_{11}NO_3$

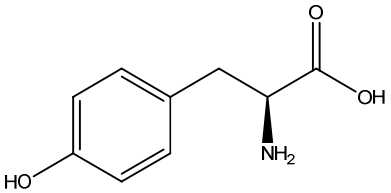

L-Valine – $C_5H_{11}NO_2$

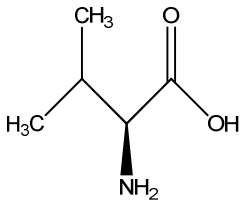

Chapter 5

The anoxic crucian carp (Carassius carassius)

BASED ON:

"^{1}H-NMR study of the metabolome of an exceptionally anoxia tolerant vertebrate, the crucian carp (*Carassius carassius*)"

Isabelle Lardon[*(1)], Göran E. Nilsson [(2)], Jonathan A.W. Stecyk [(2)], Trung Nghia Vu [(3,4)], Kris Laukens [(3,4)], Roger Dommisse [(1)], Gudrun De Boeck [(1)]

Metabolomics, DOI 10.1007/s11306-012-0448-y

[(1)] University of Antwerp - Departments of Chemistry (Research Group for Applied NMR) and Biology (SPHERE) - Groenenborgerlaan 171, B-2020 Antwerp, Belgium

[(2)] University of Oslo - Department of Molecular Biosciences - Blindernveien 31, N-0316 Oslo, Norway

[(3)] University of Antwerp - Department of Mathematics & Computer Science - Middelheimlaan 1, B-2020 Antwerp, Belgium - [(4)] Biomina - biomedical informatics research center Antwerp, Wilrijkstraat 10, 2650 Edegem (Antwerp), Belgium

Abstract

The crucian carp (*Carassius carassius*) can tolerate anoxia for days to months, depending on the temperature. In this study, we applied ^{1}H-NMR based metabolomics to polar extracts of crucian carp brain, heart, muscle and liver samples obtained from fish exposed to either control normoxic conditions, acute anoxia (24 h), chronic anoxia (1 week) or reoxygenation (for 1 week following chronic anoxia) at 5 °C. Spectra of the examined tissues revealed changes in several energy-related compounds. In particular, anoxic stress resulted in decreased concentrations of phosphocreatine and glycogen (liver) and ATP/ADP (liver, heart and muscle) and increased concentrations of lactate (brain, heart, muscle) and beta-hydroxybutyric acid (all tissues). Likewise, increased concentrations of inhibitory compounds (glycine, gamma-amino butyric acid or GABA) and decreased concentrations of excitatory metabolites (glutamate, glutamine) were confirmed in the anoxic brain extracts. Additionally, a decrease of N-acetylaspartate (NAA), an important neuronal marker, was also observed in anoxic brains. The branched-chain amino acids (BCAA) valine/isoleucine/leucine increased in all anoxic tissues. Possibly, this general tissue increase can be due to an inhibited mitochondrial function or due to protein degradation/protein synthesis inhibition. In this study, the potential and strength of the ^{1}H-NMR is highlighted by the detection of previously unrecognized changes in metabolites. Specifically, myo-inositol substantially decreased in the heart of anoxic crucian carp and anoxic muscle tissue displayed a decreased concentration of taurine, providing novel insights into the anoxia responses of the crucian carp.

Keywords: anoxia, crucian carp, metabolomics, NMR, tissue extraction

5.1 Introduction

While the vast majority of vertebrates die almost instantly following anoxia exposure due to the failure of highly energy demanding tissues as the brain and heart, some species have evolved the ability to survive prolonged periods without oxygen (anoxia). This unusual capacity reveals that evolution has solved the problems of anoxia tolerance, an achievement that has eluded biomedical science. The best-studied examples of anoxia tolerant vertebrates are some North American freshwater turtles (Genera *Trachemys* and *Chrysemys*) and a few fish including the crucian carp (*Carassius carassius*) and the congeneric goldfish (*Carassius auratus*) [Bickler and Buck 2007]. In contrast to the crucian carp, the related common carp (*Cyprinus carpio*) survives severe hypoxia only for hours (at 15 °C) to one day (at 5 °C) [Stecyk and Farrell 2002].

Crucian carp are capable of surviving one or two days of anoxia at room temperature and several months during winter [Vornanen *et al.* 2009, for review]. In order to tolerate such extreme environmental conditions, a coordinated balance between energy (ATP) demand and supply must be maintained, especially in the metabolically active brain and heart. The anoxic crucian carp utilizes a combination of two strategies to balance ATP supply and demand and thus survive prolonged anoxia: the increase of the anaerobic glycolytic ATP production (Pasteur effect) and the reduction of ATP consumption (metabolic depression) [Lutz and Nilsson 1997]. The latter involves both behavioural and cellular adjustments, and for the closely related goldfish a 70 % depression of metabolic rate has been measured during anoxia [Van Waversveld *et al.* 1989]. Still, anoxic crucian carp retain full cardiac output (Stecyk *et al.* 2004), and also brain function [Nilsson and Lutz 2004], although vision is suppressed [Johansson *et al.* 1997]. Cellular adjustments to anoxic stress include increased levels of inhibitory amino acids neurotransmitters (GABA, glycine), combined with decreased levels of the excitatory neurotransmitter glutamate in order to mediate the lowering of the brain activity and, thus, energy consumption during anoxia [Hylland and Nilsson 1999]. Simultaneously, energy demands are met by the massive liver glycogen store, the largest ever found in vertebrates [Nilsson 1990; Vornanen *et al.* 2009]. This glycogen is needed to maintain the glycolytic ATP production during prolonged periods of energy distress. Additionally, lactate/H^+ self-poisoning, due to a higher anaerobic metabolic activity, is almost absent in crucian carp due to their exotic ability to transform lactate into ethanol in the muscles [Shoubridge and Hochachka 1980; Nilsson 1988].

Metabolomics permits insights into the dynamic biochemical processes of living systems at a certain point in time. For example, nuclear magnetic resonance has proven to be a key tool to study the metabolic profiles of complex biofluids in/from humans and animals [Lindon *et al.* 1999], neuronal tissues of humans [Cheng *et al.* 1997] and tissue extracts of mammals and fish [Coen *et al.* 2003; Kullgren *et al.* 2010]. In the present paper, high resolution proton nuclear magnetic resonance (^{1}H-NMR) was applied to study the effects of anoxia exposure (24 h and 1 week) and subsequent reoxygenation (1 week) on the metabolomics of cold-acclimated (5 °C) crucian carp in order to lend insight into its anoxia survival mechanisms. We focused on the brain and the heart, the organs that normally show the highest sensitivity to oxygen deprivation, as well as on the liver and muscle due to their roles in glycogen storage and ethanol production, respectively. The NMR spectra of the different exposure groups were investigated using chemometric tools for pattern recognition, including principal component analysis (PCA) and partial least squares discriminant analysis (PLS-DA). Our results not only confirm known metabolic changes in tissues of anoxic crucian carp but also demonstrate the ability of ^{1}H-NMR to discover hitherto unrecognized metabolic adjustments.

5.2 Materials and methods

5.2.1 Fish exposure and sampling

Sampling of crucian carp (*Carassius carassius*) tissues was conducted at the Department of Molecular Biosciences, University of Oslo, Oslo, Norway. All exposure protocols were performed in adherence with the regulations of the Norwegian Animal Health Authority and approved by the animal ethics authority at the University of Oslo.

Forty crucian carp of both sexes and with a mean body mass of 26.7 ± 14.0 g (mean ± S.D.) and a mean body length of 11.5 ± 2.5 cm (mean ± S.D.) were utilized. Fish were captured from a local pond in Oslo (Tjernsrud) and acclimated to 5 °C for at least 2 months prior to experimentation in tanks continuously supplied with aerated and dechlorinated Oslo tap water. Fish were maintained under a 12 h: 12 h L: D photoperiod and fed daily with commercial carp food (Tetra Pond sticks, Tetra, Melle, Germany), but were not fed during the experimental period.

Four exposure groups of 10 fish were examined: 1 week control normoxia, 24 h anoxia, 1 week anoxia and 1 week anoxia followed by 1 week normoxic recovery. Exposures

were performed in flow-through (2-4 l/h) circular 25 l tanks (10 fish in each) submerged in a 5 °C large water bath wherein the fish were left to acclimate for 24 h in the dark prior to experimental onset. For anoxia, the tanks were sealed and the flow through water bubbled with nitrogen gas. Water oxygen levels and temperature were continuously recorded with an oxygen electrode (WTW oxi 3400i, Weilheim, Germany) connected to a computer. Water conditions considered anoxic (< 0.01 mg O_2/l) were reached within 3 h. For control normoxia and reoxygenation, the flow-through water was bubbled with air.

At the conclusion of the exposure, fish were stunned by a sharp blow to the head, the spinal cord severed and tissues sampled. During tissue-sampling, the water in the anoxic tank was continuously nitrogen-gassed to ensure anoxic conditions for the remaining fish in the container. Four tissues were collected from each fish in the following order: brain, heart, liver and white muscle. All samples were immediately snap-frozen in liquid nitrogen and stored at -80 °C until further analysis at the University of Antwerp (Departments of Chemistry and Biology), Belgium.

5.2.2 Tissue extraction procedure: methanol/chloroform/water method (ratio 2/1/1.8)

Extraction of metabolites from tissues is often the most labour-intensive and rate-limiting step in metabolomics. Therefore, a deliberate, rapid, straightforward and reproducible tissue extraction technique is critical to achieve accurate profiles of the metabolome of an organism. For this reason, we evaluated several extraction strategies for fish tissues and eventually elected the methanol/chloroform/water technique (paper submitted to the *Journal of Mediterranean Chemistry*) described by Lin and Wu [Lin *et al.* 2007; Wu *et al.* 2008]. The latter extraction method resulted in two separate fractions containing the hydrophilic (polar) and the hydrophobic (apolar) metabolites respectively.

Frozen tissues were ground in a liquid nitrogen-cooled mortar and pestle and approximately 100 mg of homogeneous tissue powder was used for the extraction procedure. Ice cold methanol (4 ml per gram of tissue; analaR normapur, min. 99.8 %, VWR, Pennsylvania, USA) and ice cold milliQ water (0.85 ml/g) were added to the powder and the homogenate was vortexed for 1 min. Polar organic solvents such as methanol are typically mixed with water to extract hydrophilic metabolites [Coen *et al.* 2003; Stentiford *et al.* 2005]. Subsequently, ice cold chloroform (4 ml/g; normapur, 99.3 %, VWR, Pennsylvania, USA) and milliQ water (2 ml/g) was added to extract the hydrophobic metabolites; the mixture was

vortexed for 1 min and then incubated on ice for 10 min to partition. The supernatant was then centrifuged at 4 °C for 10 min at 2000 g, resulting in a biphasic solution. The upper polar and lower nonpolar layers were carefully removed and transferred to 15 ml sterile Falcon tubes. Subsequently, all samples were lyophilized overnight to avoid the presence of a dominant water signal in the ^{1}H-NMR spectra. Both the polar and apolar fractions will be described in this chapter.

Prior to ^{1}H-NMR measurement, the polar tissue extracts were dissolved in 580 µl of sodium phosphate buffer prepared in D_2O to minimize variations in sample pH and allow for deuterium locking, containing sodium-3-trimethylsilylpropionate (TMSP) as an internal standard (see following paragraph). Finally, the resulting samples were transferred to a 5 mm NMR tube (NE-HP5-7, Cortecnet, France) and analyzed immediately by ^{1}H-NMR.

The 50 mM sodium phosphate buffer in D_2O (99.9 atom % D) consisted of Na_2HPO_4, 33.5 mM (AnalaR Normapur); NaH_2PO_4, 16.45 mM (GPR rectapur) (all from Merck, Darmstadt, Germany); 0.1 mM TMSP (≥ 98 %, Cambridge Isotope Laboratories, MA, USA); 0.5 mM sodium azide (99 %, Acros Organics, NJ, USA). Deuterium chloride in D_2O (ClD, > 99 atom % D, 20 wt %) and sodium deuteroxide in D_2O (NaOD, > 99 atom % D, 40 wt %) (both from Acros Organics, NJ, USA) were added to achieve a pH of ~ 7.

5.2.3 ^{1}H-NMR based metabolomics of brain, heart, liver and white muscle extracts

Tissue extracts of crucian carp were analyzed on a Bruker Avance II-700 NMR spectrometer, operating at 700.13 MHz (Bruker Biospin, Europe), equipped with a 5 mm inverse TXI-Z probe and a BACS-60 automatic sample changer. Tuning, matching and shimming were performed automatically for each sample in order to minimize the variation due to sample manipulation.

5.2.3.1 ^{1}H-NMR analysis of polar tissue extracts

One-dimensional ^{1}H-NMR spectra of brain, heart, liver and muscle extracts were acquired at 25 °C with a standard sequence using a 90° pulse (pulse sequence *zgpr*), a relaxation delay of 1.0 s with water presaturation, 64 scans collected into 16 k data points, a spectral width of 14 kHz and an acquisition time of 0.57 s per sample. Prior to Fourier transformation, all datasets were zerofilled to 32 k points and exponential line broadenings of 0.3 Hz were applied as

well. Finally, all spectra were phase and baseline corrected and chemical shifts were referenced to TMSP (0.0 ppm) using the Topspin software (version 2.1, Bruker Biospin).

In order to confirm the metabolite identities, the spectra were compared to in-house and public databases and, additionally, to the results of 2D NMR experiments. Table 5.1 provides an overview of all metabolites that were discovered by ^{1}H-NMR in the four examined tissue extracts.

Table 5.1 – Overview of all metabolites that were discovered by ^{1}H-NMR in this study, organized per tissue type.

Brain	**Heart**	**Muscle**	**Liver**
Alanine	Acetate	Acetate	Acetate
Creatine	Alanine	Alanine	Alanine
Glucose	ATP/ADP	ATP/ADP	Aspartate
Glutamate	Creatine	Creatine	ATP/ADP
Glutamine	Formate	Formate	Formate
Glycine	Glucose	Glucose	Fumarate
Lactate	Glutamate	Glutamate	Glucose
Lysine	Glycine	Glutamine	Glutamate
Myo-inositol	Lactate	Glycine	Glutamine
N-acetylaspartate (NAA)	Myo-inositol	Lactate	Glycine
Scyllo-inositol	Scyllo-inositol	Malonate	Glycogen
Succinate	Succinate	Myo-inositol	Malate
Taurine	Taurine	Scyllo-inositol	Oxypurinol
Valine/(Iso)Leu	Valine/(Iso)Leu	Taurine	(Phospho)Choline
β-Hydroxybutyric acid	β-Hydroxybutyric acid	Valine/(Iso)Leu	(Phospho)Creatine
γ-amino butyric acid (GABA)		β-Hydroxybutyric acid	Scyllo-inositol
			Succinate
			β-Hydroxybutyric acid
			Valine/(Iso)Leu

5.2.3.2 ^{1}H-NMR analysis of apolar tissue extracts

One-dimensional ^{1}H-NMR spectra of brain, heart, liver and muscle extracts were acquired at 25 °C with a standard sequence (zg) using a 90° pulse, 128 scans collected into 32 k data points, a spectral width of 21 kHz and an acquisition time of 0.78 s per sample. Prior to Fourier transformation, all datasets were zerofilled to 65 k points and exponential line broadenings of 0.3 Hz were applied as well. Finally, all spectra were phase and baseline corrected and chemical shifts were referenced to TMSP (0.0 ppm) using the Topspin software (version 2.1, Bruker Biospin).

5.2.4 Pre-processing of NMR data

The 1D spectra were converted to an appropriate format for statistical analysis by automatically segmenting each spectrum in 0.05 ppm integrated spectral regions (bins or buckets) between 0.5 and 10 ppm using AMIX (Analysis of Mixtures, version 3.8.5, Bruker Biospin). Buckets from 4.70 to 5.0 ppm, containing the residual water resonance, were excluded. All spectra were mean-centered and were normalized to total intensity in order to reduce the influence of concentration variability among the samples.

5.2.5 Statistical analyses of polar (hydrophilic) spectra

5.2.5.1 Univariate analysis

The generated bucket tables of the four tissue extracts were exported as a spread sheet to Excel (Microsoft Office Excel 2007) and a two-way analysis of variance (ANOVA), followed by a Benjamini-Hochberg test [Benjamini and Hochberg 1995] to counter the effect of multiple testing, were applied in R (version 2.9.2) to identify the buckets/metabolites that differed significantly between the control and the exposed fish. In all instances, $p < 0.05$ was used as the level of significance. Furthermore, in order to investigate whether these buckets also differed significantly between the different exposure groups, a student's t-test in excel followed by a Benjamini-Hochberg correction test in R were applied. In this case, $p < 0.05$ was applied as the level of statistical significance.

5.2.5.2 Multivariate analysis: pattern recognition techniques

The pre-processed NMR spectra were analysed by principal component analysis (PCA) using AMIX, to reduce the dimensionality of the data and to obtain an overview by showing trends, clusters and potential outliers within the data sets. Data points were considered as outliers

when they were not situated within the 95 % confidence ellipse (Hotelling T^2 multivariate profiling) [Lindon *et al.* 2007].

In addition, to cope for the unsupervised nature of PCA, partial least squares for linear discriminant analysis (PLS-DA) was employed using AMIX. This supervised classification technique attempts to separate the samples according to their class membership, based on the linear combination of the original input variables, in such a way that an optimal inter-class separation is achieved. The obtained scores plots reveal the separation between the samples based on their class membership. The retrieved loadings plots offer insights in the variables responsible for the observed separation.

The use of PLS-DA models to classify groups of samples based on their class membership creates both advantages as well as challenges for metabolomics data sets. Due to the typically presence of a relatively small number of samples compared to the large number of variables in metabolomics studies, the PLS-DA statistical model can suffer from 'overfitting'. This means that this can easily lead to 'chance' classifications of samples by statistical models i.e. models that just by chance give a good classification of e.g. two groups (often defined as case/treatment and control groups) [Westerhuis *et al.* 2008]. Therefore, a rigorous validation of the applied statistical model is extremely important and necessary to assure that new samples are classified correctly. Here, the double cross-validation (2CV) strategy and permutation tests, described by Westerhuis [Westerhuis *et al.* 2008] were applied on our data to estimate the quality of the developed PLS-DA model.

Various parameters can be used to quantify the quality of the obtained class separation and, in this study, we focussed on parameters as Q^2 values, the number of misclassifications and the area under the receiver operator characteristic (AUROC). To date, it is rather unknown which value of these parameters corresponds perfectly to a good discrimination between the groups.

The prediction error measure $\mathbf{Q^2}$, is a reflection of how well the class labels of new data are predicted. An optimal Q^2 value is 1 but this value is usually difficult to reach since this requires that the class prediction of each individual sample should be exactly equal to its class label. The latter is hard to obtain as a consequence of the inherent variation between the individuals in the same class. Furthermore, the Q^2 value both depends on the between class separation but also on the within class variability. Hence, this hinders the ability to formulate a general Q^2 value that corresponds to a sufficiently good classification. Therefore, by using permutation tests, it is possible to assess whether the obtained Q^2 values from our data sets

correlate well with a good classification since permutation tests give a sensible measure for the Q^2 value [Westerhuis *et al.* 2008]. The second and third parameters i.e. 'number of misclassifications' and 'AUROC' respectively are both classification error measures: they only make a distinction between good and wrongly classified whereas the Q^2 value is a prediction error that makes a distinction between slightly wrong and very wrong.
The **AUROC** is defined as the area under the receiver operator characteristic and represents a quality measure for which the value goes to 1 in case of a perfect separation between the classes. In fact, a ROC curve plots the sensitivity (the number of true positives as a percentage of all positives) versus the 1-specificity (the number of false positives as a percentage of all negatives) of a test. Sensitivities are between 0 and 1 and should be close to 1. The specificity should preferably be close to 1, and 1-specificity should be close to 0. The AUROC is then defined as the area under this curve and the value goes to 100 % for a perfect separation of sample groups.

The validation and classification accuracy of the employed PLS-DA model was executed as follows.

First, the optimal number of PLS-DA components was selected for the model by applying a 5-fold 2CV for 100 times. All data points were randomly divided into 5 fractions, of which one was used for testing whereas others were used for training and validating. Leave-one-out (LOOCV) according to Kohavi [Kohavi 1995] was used to select the optimal training model and uses all but one data point as the training set. The left-out data point is then used for validation. Next, training and validation data were combined and used to construct a final PLS-DA classification model in combination with the selected number of optimal PLS-DA components. Subsequently, this model is then used to predict the samples in the test set and this procedure is repeated until all samples have been in the test set once. In order to select the optimal number of PLS-DA components, different numbers are tested, ranking from 1 to the number of samples. The data were randomly ordered 100 times and the average of the area under the ROC curve (AUROC) was used as the criteria. Additionally, the number of misclassification and the Q^2 value were collected for the permutation test.

This is followed by the generation of a distribution for the H_0 hypothesis that states that there is no difference between the two classes. In the permutation test, the class labels of case and control are permutated and randomly assigned to different individuals. With 'wrong' class

labels, a classification model is calculated again. The data were permutated 1000 times, and for each permutated set, the cross validation was repeated 20 times.

We analyzed the different exposure groups in polar extracts of brain, heart, liver and white muscle (as described in Table 5.2). The average parameter values (Q^2, number of misclassifications and AUROC) were computed in R (version 2.7.2, http://www.r-project.org, packages FactoMineR version 1.14 and caret version 4.76).

Generally, the values of Q^2, the number of misclassifications and AUROC of the original classifications are plotted in combination with the permutation distributions and a typical example is shown in Figure 5.1. An obtained classification is significant (and thus not due to chance) if the values of the parameters are situated outside the random distribution (cfr. the black dot), as illustrated by Figure 5.1 which displays the results of brain extracts from 1 week anoxia-exposed fish versus 1 week normoxic recovered animals.

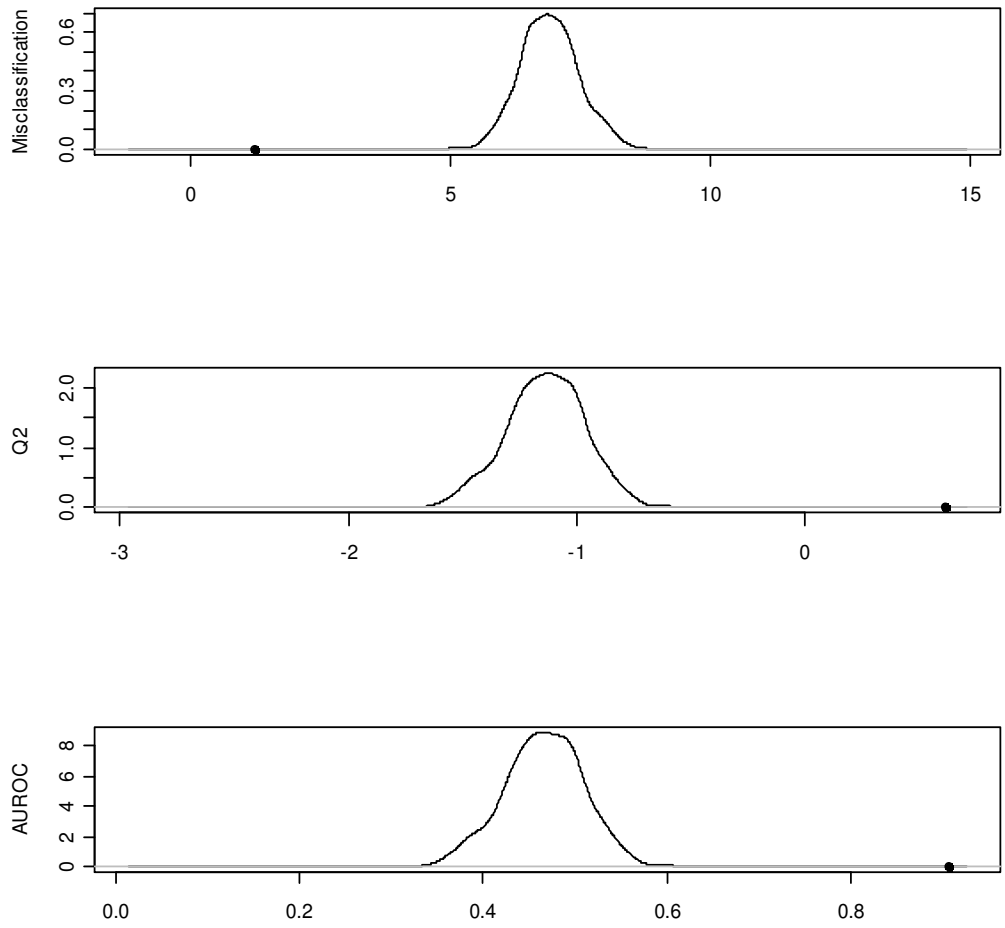

Fig. 5.1 – Assessment of the quality and classification accuracy of the PLS-DA model in brain for the comparison of 1 w anoxic and 1w recovered groups. The class separation is significant, as evidenced by the location of the original classification i.e. the black dot that is situated outside the random distribution, for all three parameters (Q^2, misclassification and AUROC).

By means of summary, the results of the PLS-DA double cross-validation strategies in all tissues are provided in Table 5.2.

Table 5.2 – Assessment of the quality of the constructed PLS-DA model by summarizing the values of Q^2, number of misclassification and AUROC for different exposure group comparisons (Co = controls) in tissue extracts of brain, heart, liver and white muscle.

BRAIN	Exposure groups	Q^2	Misclassification	AUROC
	Co – 24h anoxia	0.04	3.11	0.77
	Co – 1w anoxia	0.98	0.06	1
	24h – 1w anoxia	1	0	1
	1w anoxia – 1w recovery	0.61	1.26	0.91
	Co – 1w recovery	0.67	1.16	0.92
HEART				
	Co – 24h anoxia	0.02	3.18	0.76
	Co – 1w anoxia	1	0.01	1
	24h – 1w anoxia	1	0.01	1
	1w anoxia – 1w recovery	0.98	0.08	1
	Co – 1w recovery	0.59	1.54	0.90
LIVER				
	Co – 24h anoxia	- 0.005	4.69	0.70
	Co – 1w anoxia	0.93	0.38	0.98
	24h – 1w anoxia	0.75	1	0.94
	1w anoxia – 1w recovery	0.92	0.35	0.98
	Co – 1w recovery	0.99	0.04	0.99
WHITE MUSCLE				
	Co – 24h anoxia	- 0.15	4.6	0.66
	Co – 1w anoxia	1	0	1
	24h – 1w anoxia	0.79	0.83	0.93
	1w anoxia – 1w recovery	1	0	1
	Co – 1w recovery	0.75	1.2	0.93

5.2.5.3 Relationships between differential metabolites: metabolic network reconstruction

In order to get a rough global view on potential relationships between the differentially observed metabolites, an exploratory data analysis was carried out for the polar brain extracts, using the network manipulation software Cytoscape [Shannon *et al.* 2003] extended with the Metabolic network analysis plugin Metscape (version 2.0). That way, reactions and relationships between experimental compounds are illustrated by integrated data from known (human) pathway databases [Gao *et al.* 2010]. To this end, the list of differential compound identifiers was loaded through Metscape, and a human compound interaction network was generated. The network lay-out was adapted using the Cytoscape VizMapper.

5.2.5.4 Heat map construction of brain data

A heat map is a cluster analysis technique and a 2D graphical representation of the data to visualize a potentially correlation of the different experimental groups. In fact, the construction of heat maps was not the main goal in this work but it was used as an additional clustering tool (next to PLS-DA) just to find out whether there was a good separation of the four exposure groups in the brain data sets of crucian carp i.e. the normoxic control and recovered groups and the 1d and 1w anoxic groups.

Briefly, the created bucket table from brain data which contained 190 individual buckets of 0.05 ppm width (bins) or features was uploaded in R and hierarchal clustering was computed on the data. Subsequently, a single feature was left out of the data and the hierarchal clustering was computed again till all 190 features were tested. Hence, if there was no change in the results after leaving out one feature from the data set, then this might indicate that this feature was not significant for the clustering of the various exposure groups and therefore, the feature will be put in the eliminated feature set. Lastly, all features in the eliminated feature set are removed and a heat map is plotted from the remaining features.

5.2.6 Statistical analysis of apolar (hydrophobic) spectra

5.2.6.1 The presence of shifted NMR peaks

Next to the hydrophilic fractions, the M/C/W extraction also resulted in apolar (hydrophobic) fractions that generally consist of lipids (e.g. cholesterol, fatty acids, etc.), lipoproteins

(VLDL, LDL, IDL; HDL) and phospholipids (e.g. phosphatidylcholine, phosphatidylinositol, etc.).

Apolar ^{1}H-NMR spectra were obtained from all crucian carp tissues and examined thoroughly. When overlapping all spectra (per tissue type), a nice overlay was observed. However, some NMR peaks appeared to be shifted in the spectra and interestingly, approximately the same NMR signals appeared to be shifted in the four different tissues. In general, downfield-shifted NMR signals were situated particularly between 1.2 and 2 ppm; between 3.2 and 3.4 ppm and between 3.9 and 4.4 ppm. An example of shifted peak regions in the muscle spectra of control fishes is illustrated by Figures 5.2 A, B and C.

(A)

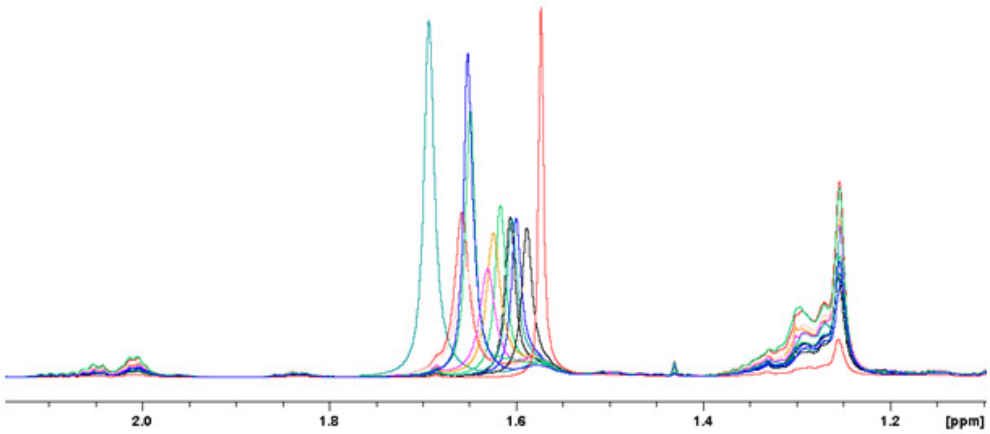

(B)

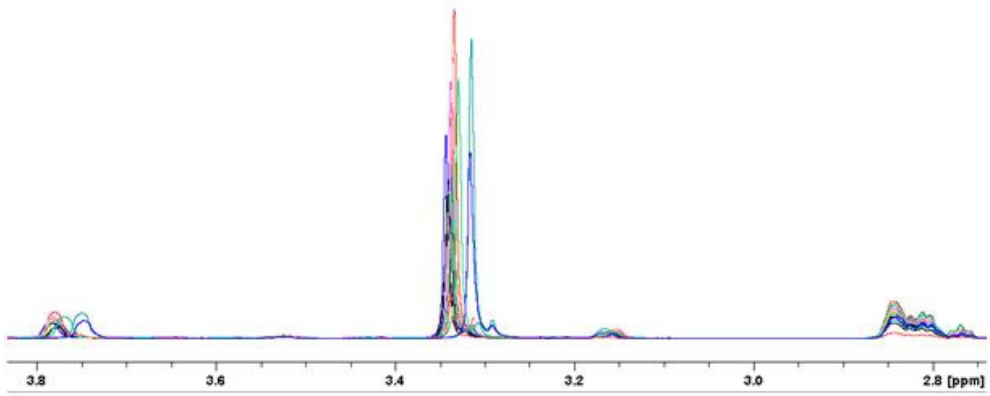

(C)

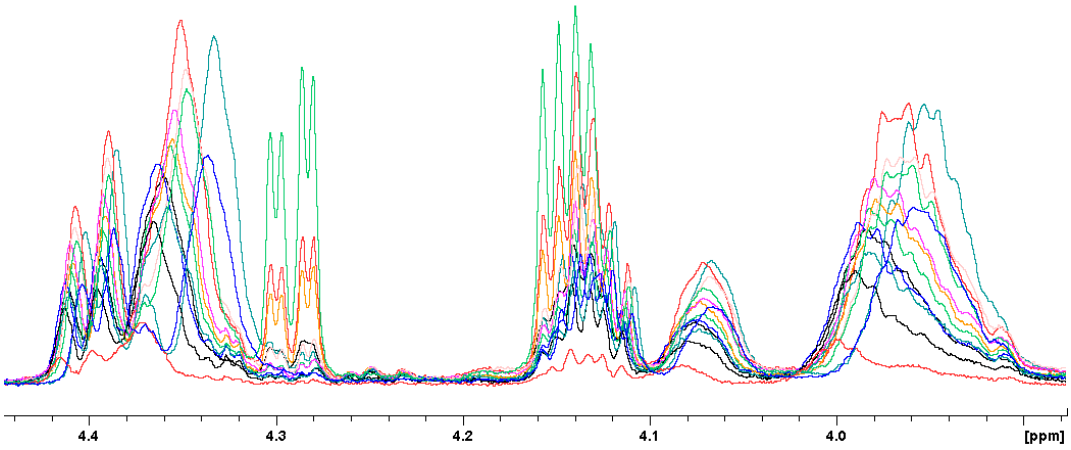

Figure 5.2 – An overlap of apolar muscle ^{1}H-NMR spectra of all control fish. **(A)** represents the spectral region from 1.2 to 2 ppm and clearly demonstrates the shifted peaks around 1.6 ppm. **(B)** highlights the shifted signals around 3.3 ppm and **(C)** displays the shifted NMR signals around 4 and 4.4 ppm. The X-axis is expressed in ppm (parts per million) units whereas the relative intensity of the NMR signals is indicated by the Y-axis.

Commonly, a frequency shift of NMR signals can be caused by three main factors. First of all, pH differences between different samples can result in pronounced pH-induced chemical shift variations in the NMR spectra. Therefore, to avoid this source of 'unwanted' variation, the sample pH is generally normalized by adding a phosphate buffer (e.g. pH 7.2) [Lindon *et al.* 2007]. Adjustment of pH in biological samples alone does not always remove the chemical shift variation of compounds as citrate, etc. Further shift effects can then be related to differences in ion strength of the samples [Stoyanova *et al.* 2004]. In samples with higher ionic contents, for example, interactions occur between the ions and certain metabolites (e.g. citrate) to finally stabilize their charge. These undesired interactions can be bypassed by adding a high NaCl concentration to the sample in order to obtain the same ion strength in all samples. Thirdly, fluctuating peak positions can also be related to isotope effects, e.g. when switching to another solvent (e.g. from H_2O to D_2O) caused by varying salt concentrations in samples.

Although the range of the spectral shifts was relatively small, it will have a direct impact on data reduction procedures and complicates further data evaluation. Therefore, the apolar

datasets were examined by Kris Laukens and Nghia Trung Vu from the Intelligent Systems Laboratory at the University of Antwerp. They developed an appropriate spectral alignment method which is based on a hierarchical Cluster-based Peak Alignment algorithm (CluPa).

5.2.6.2 Detailed description of the CluPa alignment method

- *Methods*

The CluPa alignment is embedded in a workflow called 'speaq' which stands for 'spectrum alignment and quantitation' and consists of four major steps which are integrated in one pipeline [Du *et al.* 2006, Yang *et al.* 2009, Vu *et al.* 2011]. First, instrumental noise was reduced/eliminated and peaks are collected from the NMR spectra by peak picking approaches. A typical peak detection approach consists of three steps: smoothing or denoising, baseline correction and the actual peak picking. Since the detected peaks can be considered as the input of the alignment procedure, selecting an appropriate technique is very crucial. In this implementation, the method of continuous wavelet transform (CWT) is applied to detect the peaks in NMR spectra. The second step in the workflow consists of the selection of a dominant and representative reference spectrum to be a template for the alignment of the other spectra. In principle, the method projects each high-dimensional NMR spectrum as a data-point in a one-dimensional space and selects the data-point in the middle of the data cloud as the reference. Ideally, the perfect reference candidate has enough peaks corresponding to chemical resonance areas, i.e. frequencies and the peaks of the reference stay at the centre of the distribution of peaks of other spectra in order to minimize the distance. Thirdly, the CluPa or hierarchical cluster-based peak algorithm is applied to align a target spectrum to the reference spectrum. This is accomplished in a top-down fashion by building a hierarchial cluster tree from peak lists of reference and target spectra and then dividing the spectra into smaller segments based on the most distant clusters of the tree. Briefly, CluPa first performs the alignment on the whole spectrum and subsequently, CluPa splits the segment(s) of previous steps into smaller segments and apllies an individual alignment shift to each of these. The last step includes the quantitative analysis. The spectra aligned by the CluPA approach are well aligned and are represented as a matrix in which the rows denote the spectra and the columns indicate the resonance frequency instances. In our approach, an analysis of the data, based on the ratio of the between-group to within-group sums of squares (BW ratio) is performed for each data point in the NMR spectra. This ratio is related to the F-statistic or one-way ANOVA. The original paper, describing into detail the

CluPa workflow for alignment and quantification on NMR spectra can be found in [Vu *et al.* 2011].

■ *Implementation*

Speaq was subsequently applied on the four different datasets of brain, heart, liver and muscle. The default parameter settings of the package were used, as well as the user intervene allowance of the software to improve the alignment process by setting reference for regions and skipping unnecessary regions. In each dataset, a quantitative analysis was applied for 4 groups (controls, 1 day anoxia, 1 week anoxia and 1 week recovery) and each pair group.

5.3 Results

5.3.1 Polar (hydrophilic) tissue extracts

5.3.1.1 ^{1}H-NMR spectroscopy and statistical analyses of polar brain extracts

The ^{1}H-NMR spectra of polar brain extracts displayed a substantial amount of various metabolites. For example, the metabolites lactate, alanine, glucose, myo-inositol and ß-hydroxybutyric acid constituted some of the most intense resonances in those proton spectra. Consequently, the polar NMR spectra of all exposure groups provided a comprehensive insight in the metabolic composition of the crucian carp brain.

Univariate analysis

Table 5.3 represents the results of the ANOVA analyses with Benjamini-Hochberg correction test of brain, heart, muscle and liver extracts, which exposed the buckets (metabolites) that differed significantly ($p < 0.05$) between the normoxic controls and the three exposure groups (1 day and 1 week of anoxia and 1 week normoxic recovery). These significant buckets were identified as beta-hydroxybutyric acid, NAA, GABA, glutamate and glutamine, lactate and valine/(iso)leucine. Additionally, a student's t-test and Benjamini-Hochberg correction test ($p < 0.05$) were performed to find out whether these buckets also changed significantly between the various exposure groups. In order to have an idea about the dynamic behaviour of the metabolites among the different exposure groups, box plots of the brain metabolites (Fig. 5.3) were created. The box plot is characterized by the five-number summary: the sample minimum (the smallest observation), the first or lower quartile (Q1), the median (vertical black line, Q2), the third or upper quartile (Q3) and the sample maximum (the largest observation).

Table 5.3 – Overview of the identified metabolites, resulting from the two-way-ANOVA and Benjamini-Hochberg analysis ($p < 0.05$) in brain, heart, muscle and liver tissues.

Brain	**Heart**	**Muscle**	**Liver**
Valine/(Iso)Leu	Valine/(Iso)Leu	Valine/(Iso)Leu	Valine/(Iso)Leu
β-Hydroxybutyric acid	β-Hydroxybutyric acid	β-Hydroxybutyric acid	β-Hydroxybutyric acid
Lactate	Lactate	Lactate	Glutamate
Glutamate	Acetate	Acetate	Glutamine
Glutamine	Myo-inositol	Glutamate	(Phospho)Creatine
GABA	Glycine	Glutamine	Glucose
NAA	Glucose	Taurine	Glycogen
	Alanine	Glucose	Glycine
	Glutamate	Glycine	ATP/ADP
	ATP/ADP	ATP/ADP	
	Formate	Formate	

Compared to the normoxic controls, 24 h anoxia resulted in an increase in valine/(iso)leucine, lactate and GABA combined with a decrease in the concentrations of glutamate and glutamine. One week of anoxia resulted, compared to the normoxic controls, in an increase in valine/(iso)leucine, beta-hydroxybutyric acid, lactate and GABA; with beta-hydroxybutyric acid and GABA being higher than after 24 h of anoxia. Contrarily, 1 week of anoxia caused a decrease in glutamate, glutamine and NAA; with glutamate, glutamine and NAA being lower than after 24 h of anoxia. Furthermore, reoxygenation resulted in a recovery of valine/(iso)leucine, NAA, GABA, lactate, glutamine and glutamate. Lactate and glutamate even displayed significant elevated levels in the recovered group, compared to the controls. Contrary, one week of normoxic recovery was too short to recover completely for the levels of beta-hydroxybutyric acid, compared to the controls.

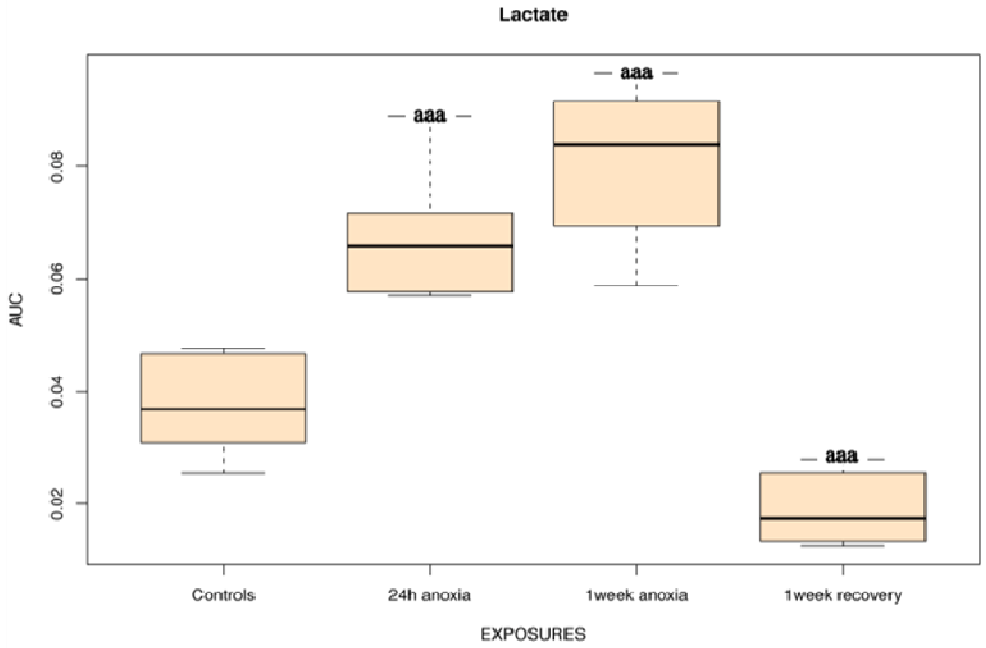
Lactate
AUC
0.02
0.04
0.06
0.08
aaa
aaa
aaa
Controls
24h anoxia
1week anoxia
1week recovery
EXPOSURES

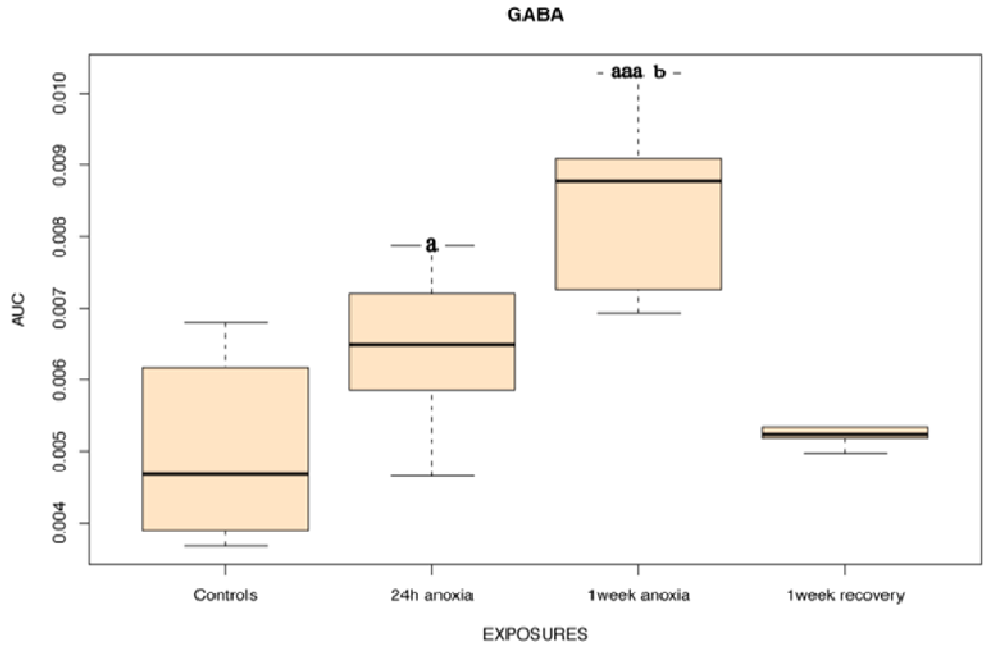
GABA
AUC
0.004
0.005
0.006
0.007
0.008
0.009
0.010
a
aaa b
Controls
24h anoxia
1week anoxia
1week recovery
EXPOSURES

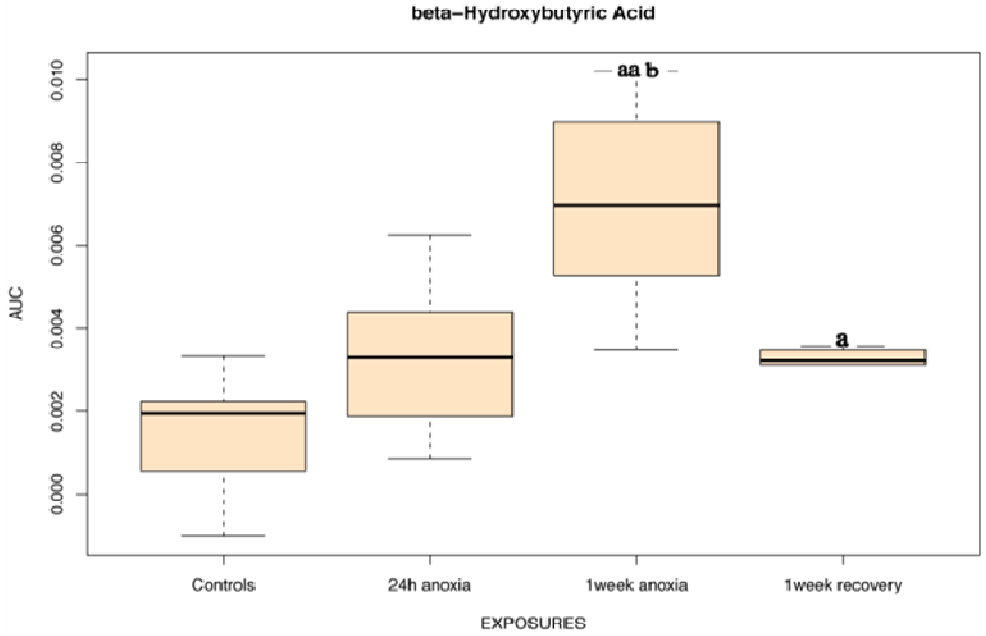
beta−Hydroxybutyric Acid
AUC
0.000
0.002
0.004
0.006
0.008
0.010
a
aa b
Controls
24h anoxia
1week anoxia
1week recovery
EXPOSURES

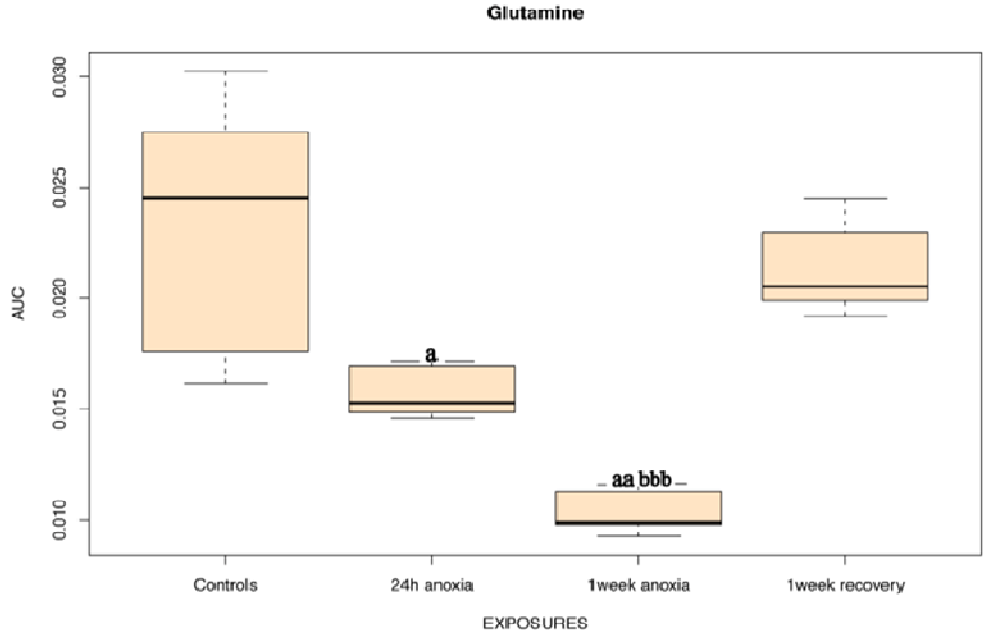
Glutamine
AUC
0.010
0.015
0.020
0.025
0.030
a
aa bbb
Controls
24h anoxia
1week anoxia
1week recovery
EXPOSURES

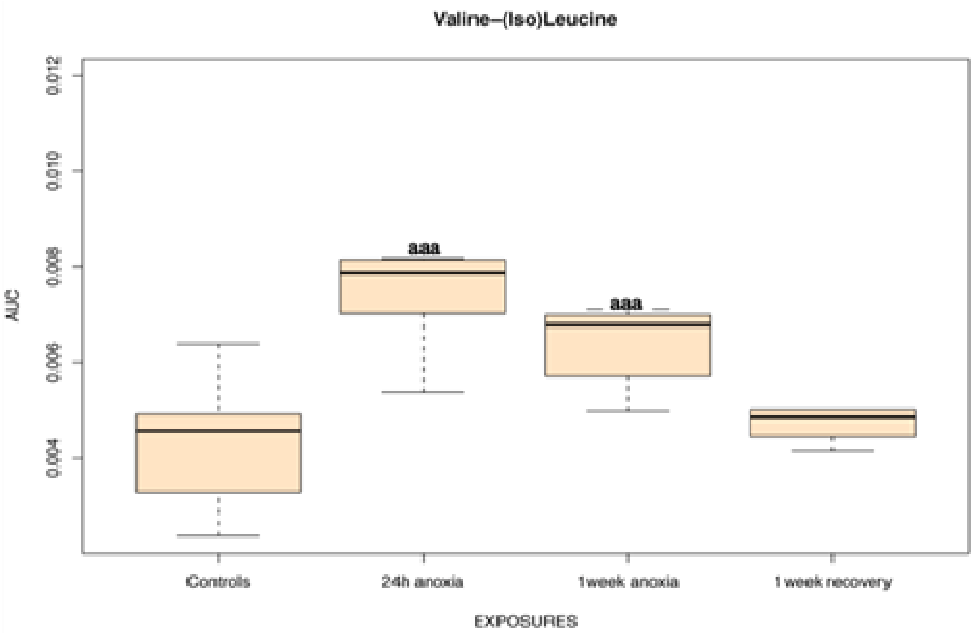
Valine−(Iso)Leucine
AUC
0.004
0.006
0.008
0.010
0.012
aaa
aaa
Controls
24h anoxia
1week anoxia
1week recovery
EXPOSURES

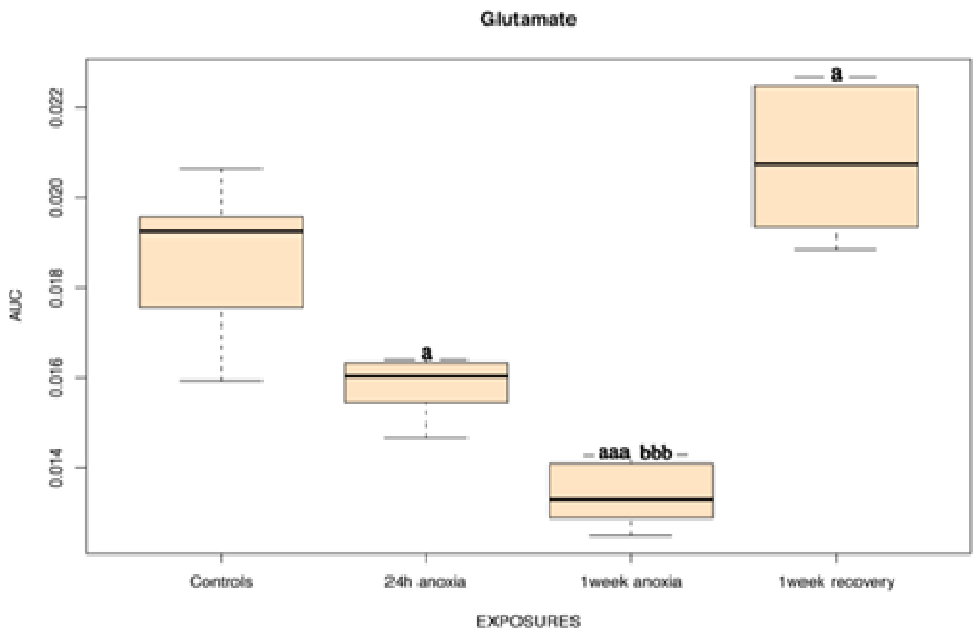
Glutamate
AUC
0.014
0.016
0.018
0.020
0.022
a
a
aaa bbb
a
Controls
24h anoxia
1week anoxia
1week recovery
EXPOSURES

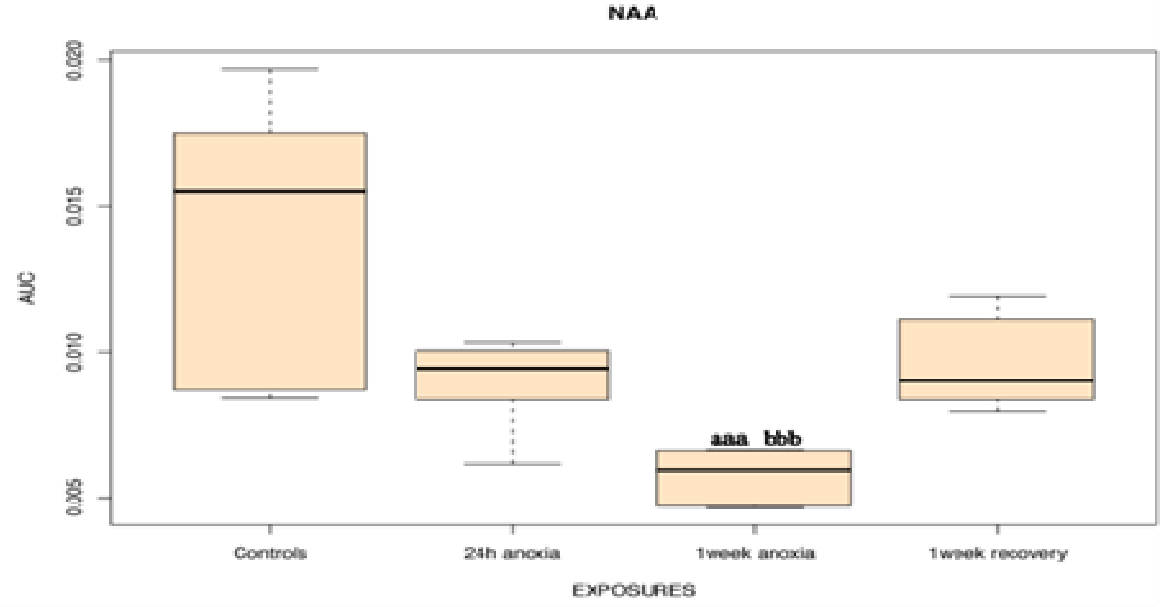

Figure 5.3 - Box plots of polar brain data to visualize the buckets/metabolites that differed significantly ($p < 0.05$) between the control and exposure groups and between the individual exposure groups, identified by student's t-tests and two-way ANOVA analysis followed by Benjamini-Hochberg correction tests. The vertical axis of each box plot represents the AUC or Area Under the Curve intensities. The horizontal axis displays the 4 experimental groups: normoxic controls, 24h anoxia, 1 week anoxia and one week recovery. An 'a' indicates a significant difference between exposed (N=19) and control fish (N=7) (a: $p < 0.05$; aa: $p < 0.01$; aaa: $p < 0.001$), 'b' indicates a significant difference between 24h (N=7) and 1 week anoxic fish (N=6) (b: $p < 0.05$; bb: $p < 0.01$; bbb: $p < 0.001$).

Figure 5.4 visualizes the metabolic changes in polar brain extracts of crucian carp exposed to 24 h or 1 week anoxia and subsequent to 1 week of normoxic recovery.

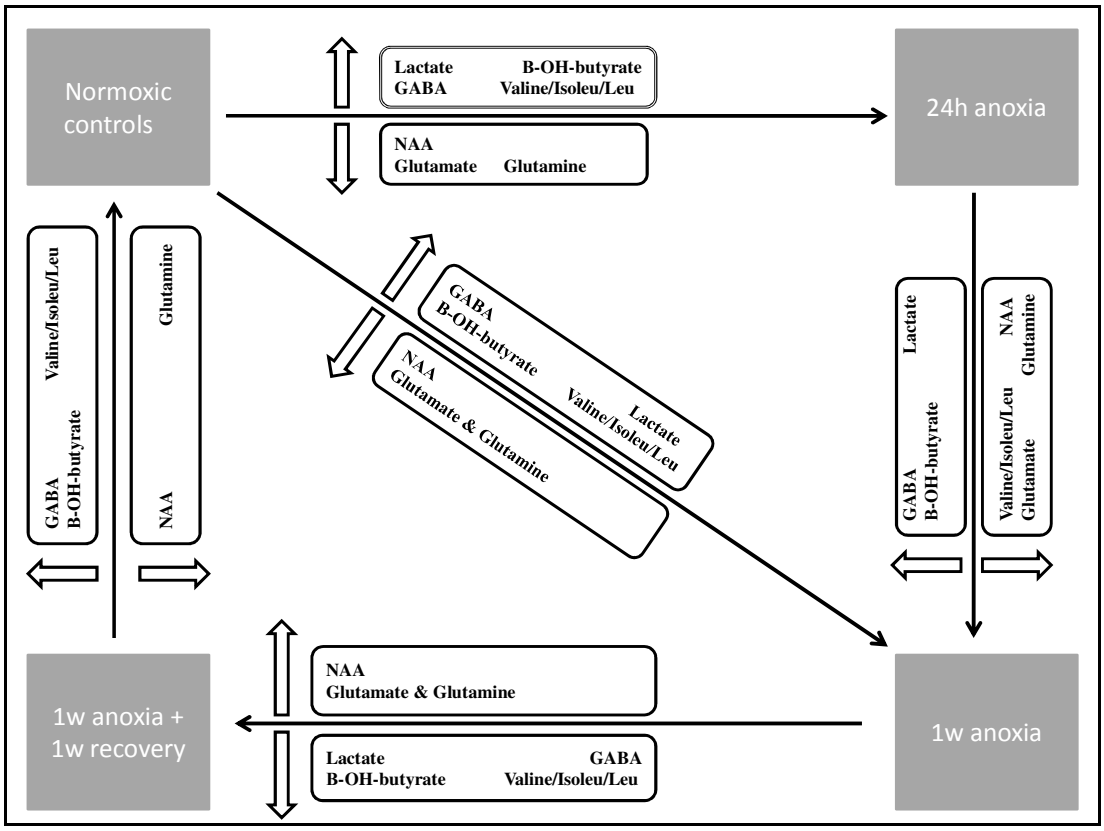

Figure 5.4 - Schematic overview of the metabolic changes in polar brain extracts of crucian carp exposed to anoxia (24 h or 1 week) and subsequent 1 week reoxygenation. Increased metabolites are indicated by the symbol ↑ and decreasing metabolites are indicated by the symbol ↓.

Key to metabolite abbreviations: Valine/Isoleu/Leu, valine/isoleucine/leucine; NAA, N-acetylaspartate, GABA, gamma-aminobutyric acid.

Multivariate analysis

In addition to the univariate statistical analysis, the 1D brain spectra of the four experimental groups were analyzed using unsupervised principal component analysis and no outliers were detected.

In addition, a PLS-DA model for all exposure groups was constructed and the corresponding scores plot (Fig. 5.5) illustrates the separation of the different treatment groups: normoxic controls can be distinguished from the 24 h and 1 week anoxia group, and the recovered class. Moreover, a clear separation of the anoxic groups (24 h and 1 week) and the normoxic groups

(controls and recovered) can be observed (along PLS 1). Secondly, the PLS-DA loadings plot revealed the significant metabolites, responsible for the observed separation of all exposure groups and these observations confirmed the results of the univariate analysis.

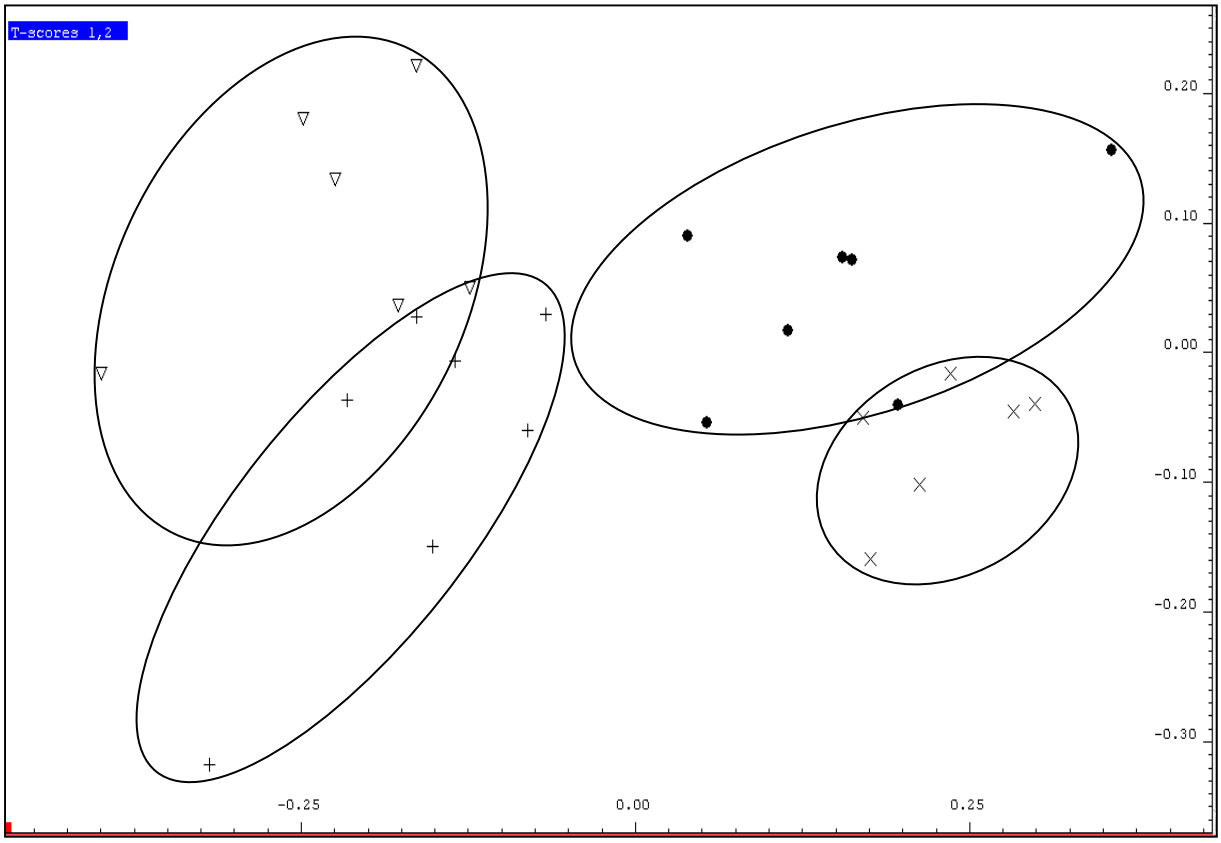

Figure 5.5 - PLS-DA scores plot of ^{1}H-NMR spectra from polar brain extracts to illustrate the separation of the normoxic control group (•), N=7, the 1 day anoxia group (+), N=7, the 1 week anoxia group (Δ), N=6 and the 1 week normoxic recovery group (x), N=6 according to the first PLS-component in the X-axis (PLS 1) and the second PLS-component (PLS2) in the Y-axis.

The subsequent table (Table 5.4) represents the average relative concentrations (mM) of the observed metabolites in polar brain extracts. The quantification of metabolites was performed through integration of the spectra, relative to the TMSP resonance at 0 ppm (0.1 mM).

Table 5.4 – Overview of the average relative concentrations (mM) and SEM of observed metabolites in polar brain extracts. * indicate the significant differences from the controls.

	Controls	**1 day anoxia**	**1 week anoxia**	**1 week recovery**
Acetate	0.92 ± 0.18	1.74 ± 0.44*	1.17 ± 0.19	0.88 ± 0.13
ATP/ADP	0.76 ± 0.11	1.21 ± 0.27*	0.81 ± 0.12	0.83 ± 0.11
GABA	0.58 ± 0.10	1.70 ± 0.42*	2.14 ± 0.31*	0.60 ± 0.09
Glutamate	2.18 ± 0.33	4.10 ± 1.01*	2.14 ± 0.36	2.42 ± 0.27
Glycine	0.20 ± 0.02	0.32 ± 0.06*	0.31 ± 0.03*	0.20 ± 0.02
Lactate	2.09 ± 0.24	7.58 ± 1.81*	6.51 ± 0.70*	1.05 ± 0.18
Phosphocreatine	2.39 ± 0.37	4.36 ± 0.93	3.16 ± 0.34	2.10 ± 0.34

Metabolic network modelling

A biological network is another way of visualizing changes in brain metabolites. Figure 5.6 depicts a superior biological network that links the observed differential compounds, according to the Cytoscape Metscape plugin. Specifically, the dynamic interactions of GABA, glutamate and glutamine in 1 week anoxic fish compared to normoxic controls, are summarized. In the model, the relative positioning of the three metabolites next to each other implies their metabolic relation during anoxic stress. Thus, the constructed network illustrates well some characteristic anoxia-induced features. For example, the inhibitory compounds (GABA, glycine) are upregulated after anoxia exposure combined with a downregulation of the excitatory metabolites glutamate and glutamine.

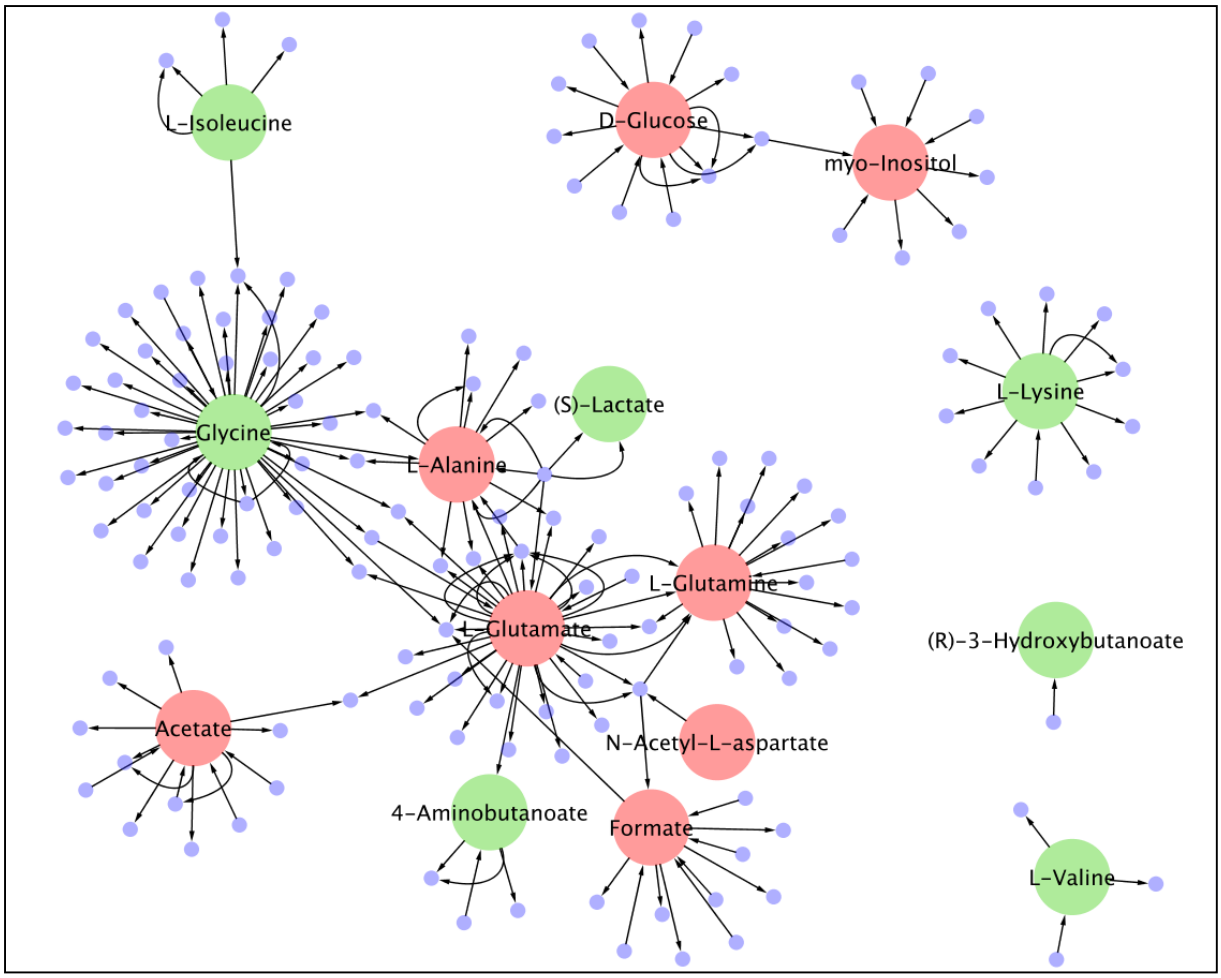

Figure 5.6 – Biological network of polar brain extracts, focusing on the dynamic interactions of metabolites GABA (4-aminobutanoate), glutamate and glutamine in 1 week anoxic fish compared to normoxic controls.

Heat map construction of brain data: clustering analyses of the exposure groups

Figure 5.7 demonstrates the constructed heat map of brain data which illustrates the highly efficient clustering of the different exposure groups, based on their resembling metabolic profiles. Concretely, two main clusters are visible: the first cluster includes the normoxic groups (i.e. the controls and recovered samples) which can be distinguished clearly from the the second cluster of anoxic groups (i.e. the 1d and 1w anoxic fish). This is illustrated by brace I that includes all anoxic samples from the 1d (D) and 1w anoxia groups (B) whereas brace II encompasses all normoxic samples from the controls (A) and the reoxygenated recovered group (C).

However, two exceptions occurred in the heat map and they are encircled in red (Fig. 5.7): one control sample was found in the anoxic groups while one sample of the 1d anoxia fish

was present in the normoxic groups. Nonetheless, the obtained clustering of the different treatment groups, based on their metabolic profiles is remarkably good and efficient.

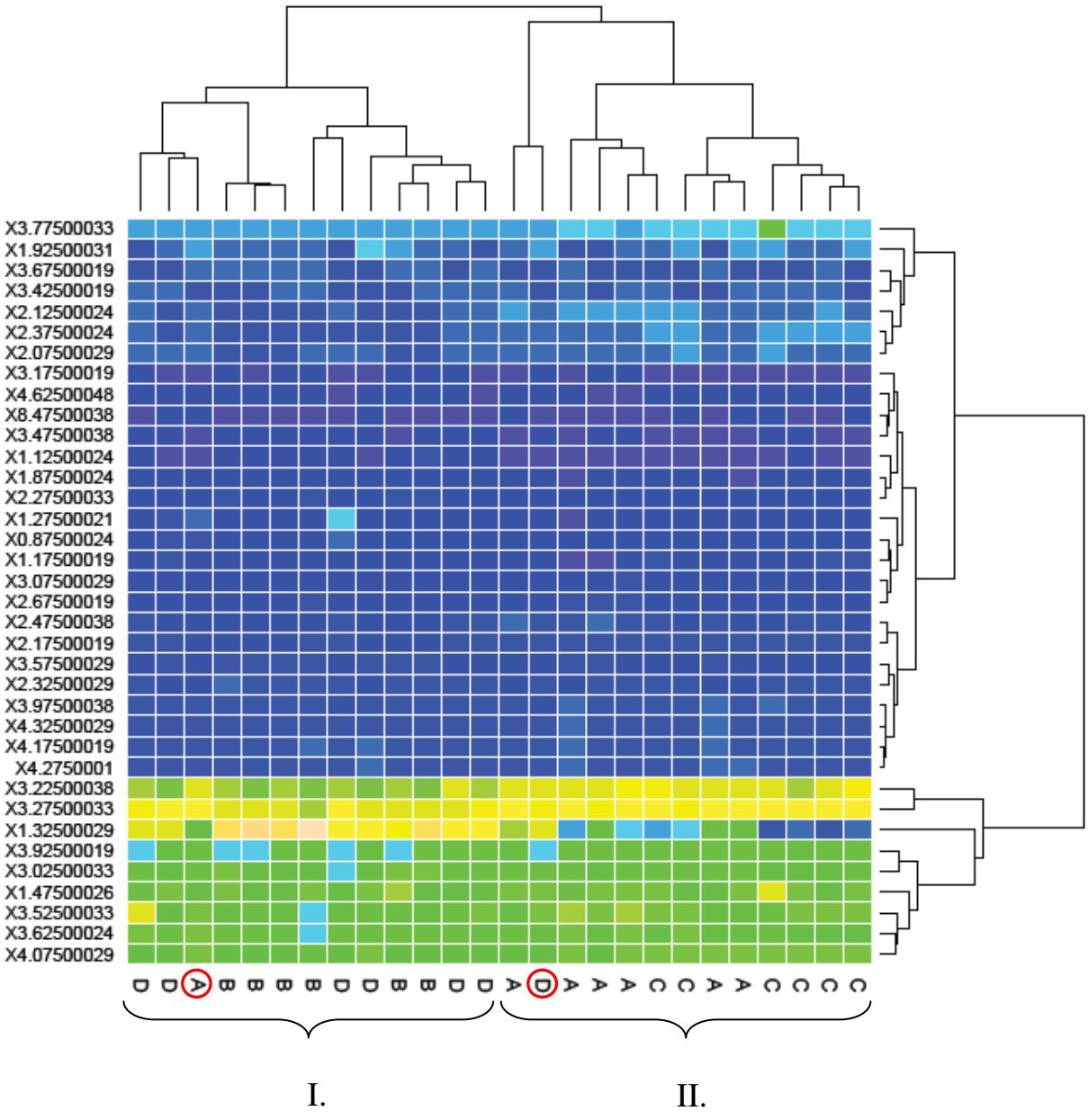

Figure 5.7 – Heat map of brain data: the vertical axis represents the significant features following hierarchal clustering i.e. the buckets (metabolites) that are found to be significant in the separation of the various exposure groups whereas the horizontal axis indicates the different exposure groups (A = controls, B = 1w anoxia, C = 1w recovery, D = 1d anoxia).

Brace I includes all anoxic samples whereas brace II involves the normoxic samples. Two exceptions occurred in the heat map and they are encircled in red.

5.3.1.2 ^{1}H-NMR spectroscopy and statistical analyses of polar heart extracts

Univariate analysis

Table 5.2 illustrates the results of the ANOVA analyses with Benjamini-Hochberg correction of polar heart extracts. The significant ($p < 0.05$) buckets resulting from these analysis were identified as acetate, ATP/ADP, beta-hydroxybutyric acid, formate, glucose, glycine, lactate, myo-inositol and valine/(iso)leucine. Figure 5.7 shows the box plots of the significant heart metabolites.

Compared to control normoxia, 24 h anoxia resulted in a significant increase in lactate, beta-hydroxybutyric acid and valine/(iso)leucine and a decrease in ATP/ADP. One week of anoxia resulted, compared to the normoxic controls, in an increase in lactate, beta-hydroxybutyric acid and valine/(iso)leucine. In contrast, compared to the normoxic controls, 1 week of anoxia caused a decrease in ATP/ADP, glucose, glycine, myo-inositol, formate, glutamate and acetate; with formate, glutamate, myo-inositol, and glycine being lower than after 24 h of anoxia.

Furthermore, reoxygenation resulted in a complete recovery to the control normoxic levels for valine/(iso)leucine , lactate, beta-hydroxybutyric acid, acetate, myo-inositol, glycine, glucose, ATP/ADP and formate.

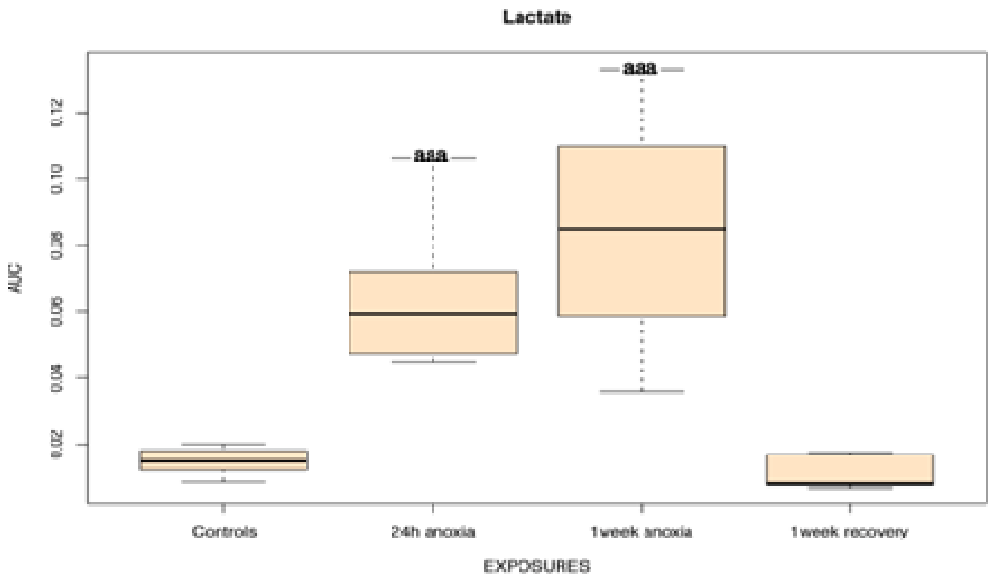
Lactate
AUC
aaa
aaa
Controls
24h anoxia
1week anoxia
1week recovery
EXPOSURES

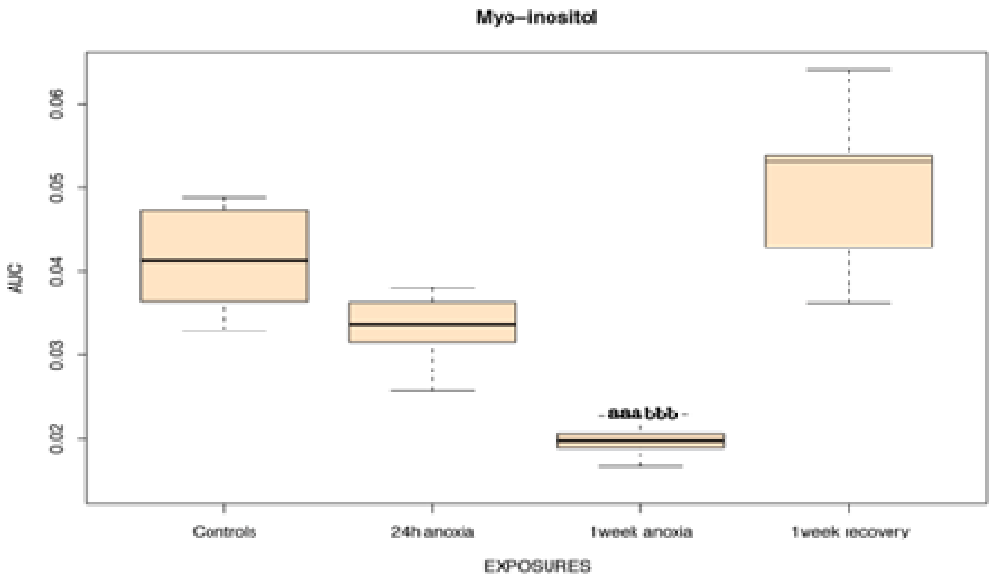
Myo−inositol
AUC
aaa bbb
Controls
24h anoxia
1week anoxia
1week recovery
EXPOSURES

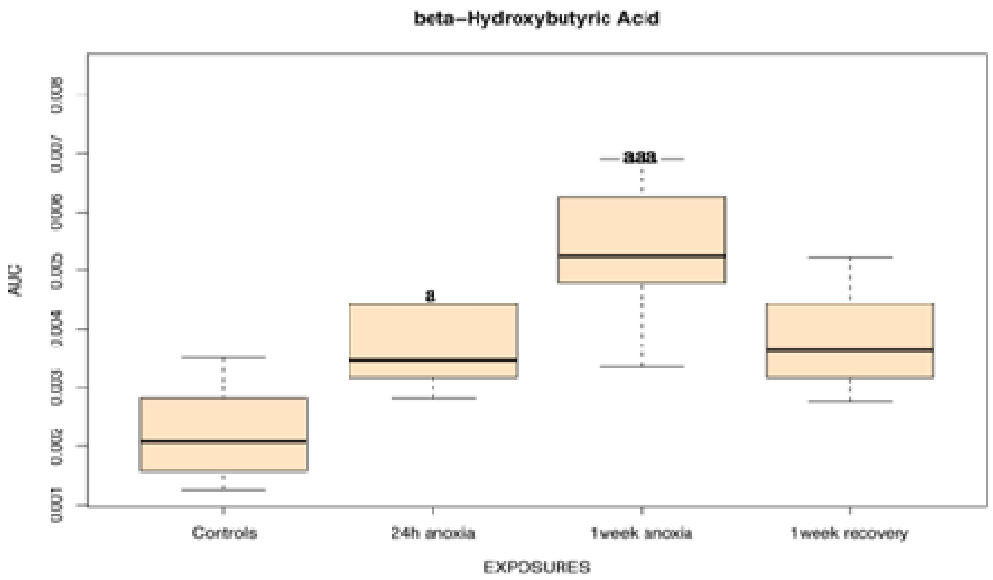
beta−Hydroxybutyric Acid
AUC
a
aaa
Controls
24h anoxia
1week anoxia
1week recovery
EXPOSURES

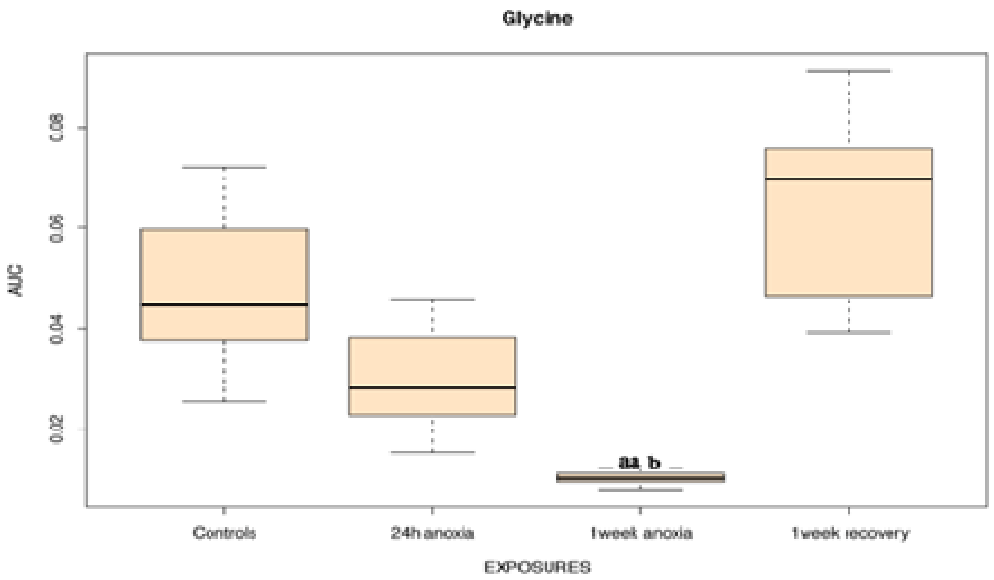
Glycine
AUC
aa b
Controls
24h anoxia
1week anoxia
1week recovery
EXPOSURES

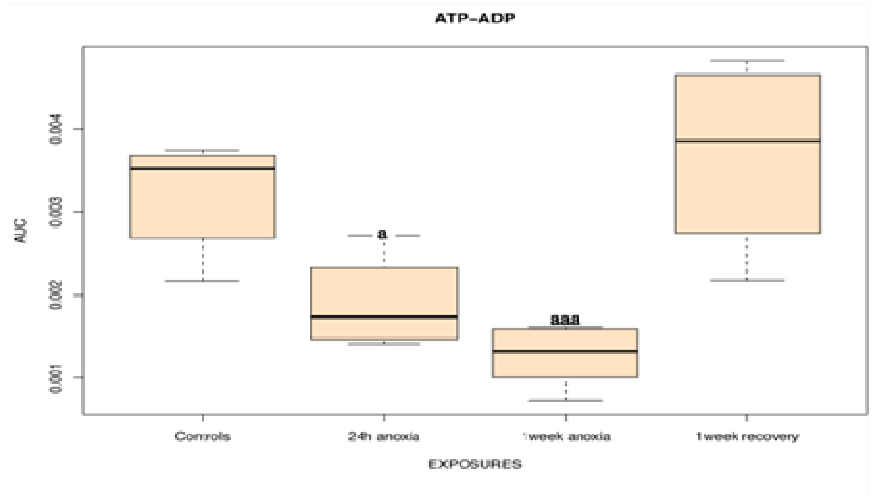
ATP-ADP
AUC
0.001
0.002
0.003
0.004
a
aaa
Controls
24h anoxia
1week anoxia
1week recovery
EXPOSURES

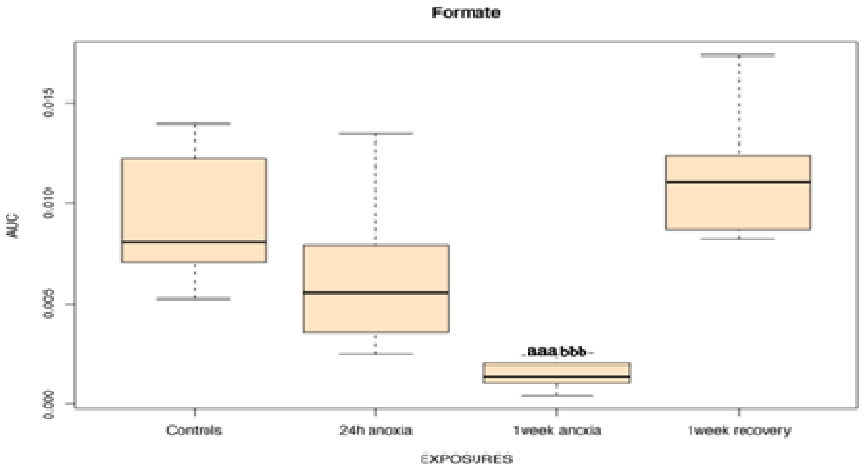
Formate
AUC
0.000
0.005
0.010
0.015
aaa bbb
Controls
24h anoxia
1week anoxia
1week recovery
EXPOSURES

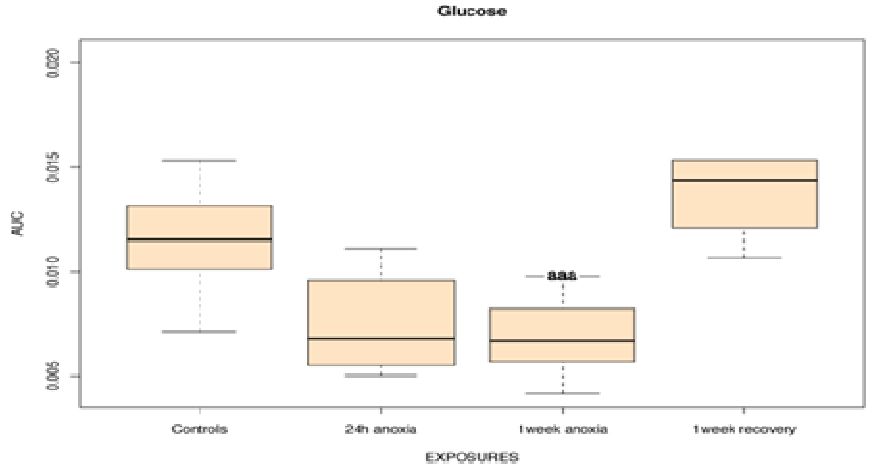
Glucose
AUC
0.005
0.010
0.015
0.020
aaa
Controls
24h anoxia
1week anoxia
1week recovery
EXPOSURES

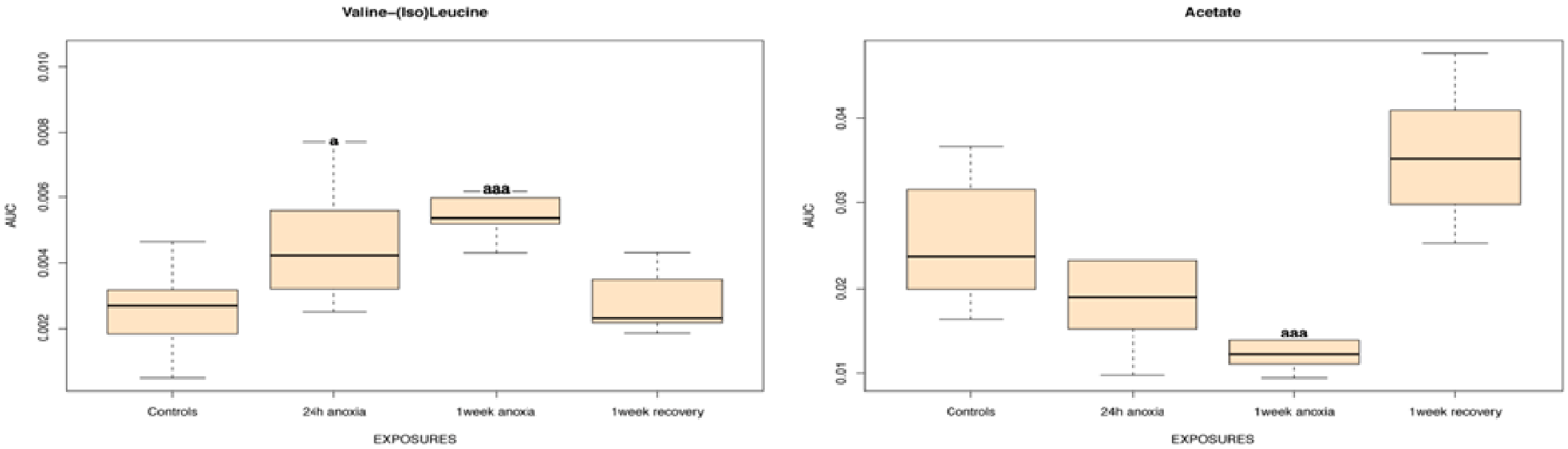

Figure 5.7 - Box plots of polar heart data to visualize the significant buckets/metabolites that differed significantly ($p < 0.05$) between the control and exposure groups and between the individual exposure groups, identified by student's t-tests and two-way ANOVA analysis followed by Benjamini-Hochberg correction tests. An 'a' indicates a significant difference between exposed (N=27) and control fish (N=7) (a: $p < 0.05$; aa: $p < 0.01$; aaa: $p < 0.001$), 'b' indicates a significant difference between 24h (N=8) and 1 week anoxic fish (N=13) (b: $p < 0.05$; bb: $p < 0.01$; bbb: $p < 0.001$).

Multivariate analysis

Principal Component Analysis was carried out to detect potential outliers in the polar heart data sets. Two data points were classified as outliers, more specifically two spectra of the one week anoxic group. When these spectra were reviewed, a distorted baseline was identified as the cause for this aberrant behaviour and these samples were not included for further analyses.

Secondly, PLS-DA was performed to detect which variables carry the class distinguishing information.

The separation of the different groups in the four-class PLS-DA model was adequate in the equivalent scores plot. Furthermore, the results of the corresponding loadings plot confirmed the identity of the metabolites which were detected by univariate analysis.

5.3.1.3 ^{1}H-NMR spectroscopy and statistical analyses of polar liver extracts

A typical 700 MHz ^{1}H-NMR spectrum of a normoxic polar liver extract using a standard water resonance presaturation pulse sequence is shown in Figure 5.8A. In order to demonstrate all metabolites, spectral enlargements are presented in Figures 5.8B (0-3 ppm), 5.8C (3-5 ppm) and 5.8D (5.2-8.6 ppm).

(A)

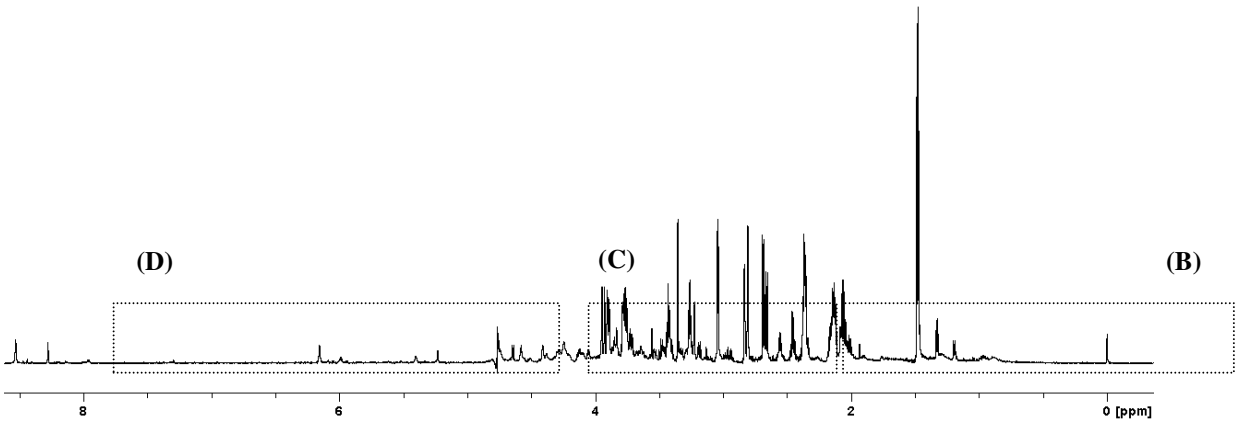

(B)

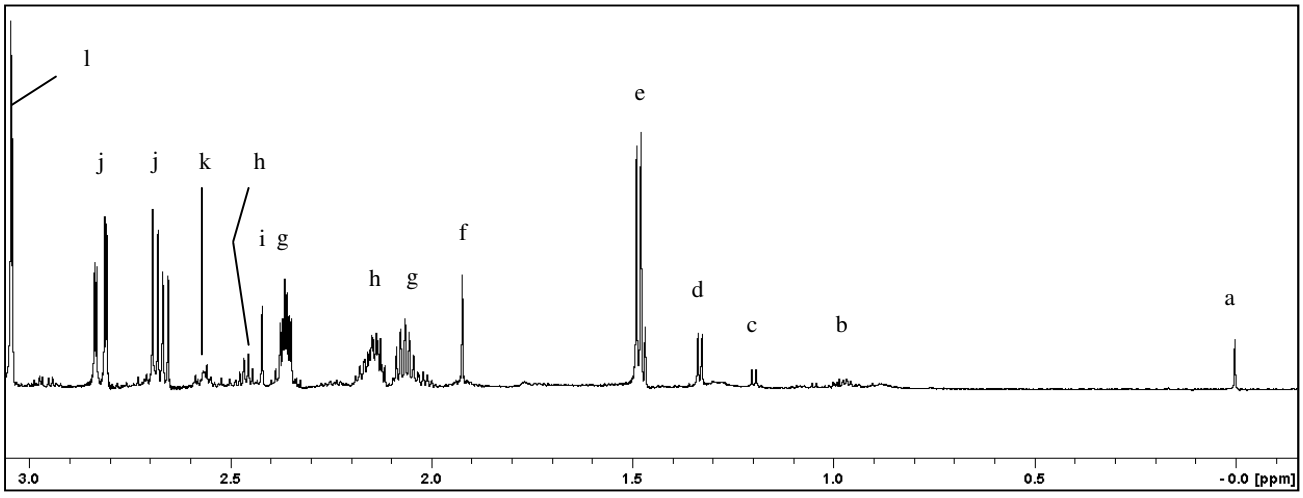

(C)

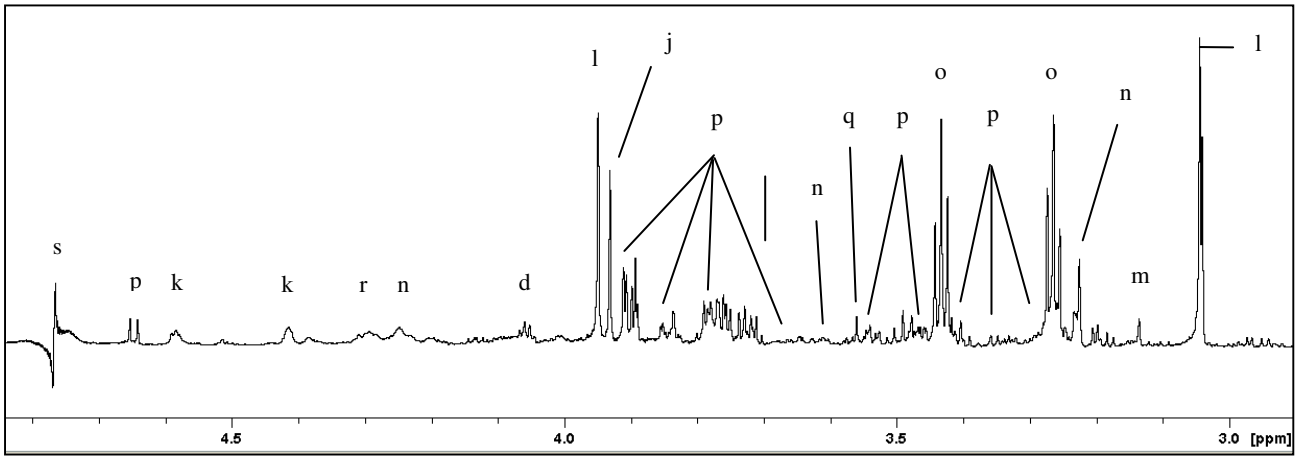

(D)

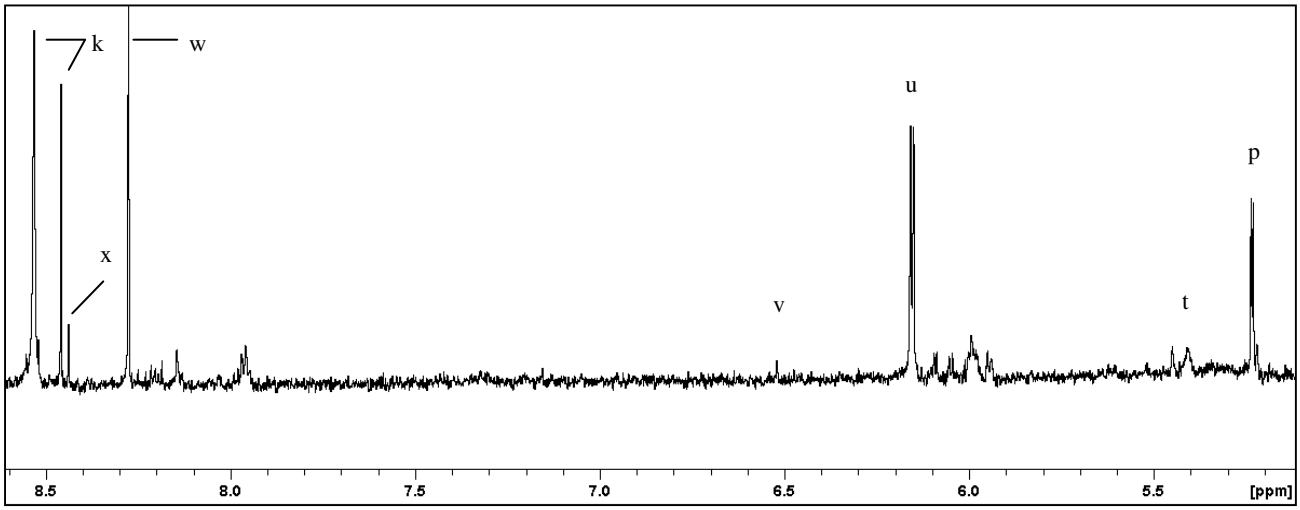

Figure 5.8A – 1D 700 MHz ^{1}H-NMR spectrum (0-8.6 ppm) representing a polar liver extract of a normoxic control fish, analyzed with a standard 90° pulse sequence. Low intensity regions are illustrated by inset spectral enlargements from 0-3 ppm (**Fig. 5.8B**), from 3-5 ppm (**Fig. 5.8C**) and from 5.2-8.6 ppm (**Fig. 5.8D**).

Key to peak assignments: a) TMSP (internal standard) – b) Valine(Iso)Leucine – c) beta-Hydroxybutyric acid – d) Lactate – e) Alanine – f) Acetate – g) Glutamate – h) Glutamine – i) Succinate – j) Aspartate – k) unknown – l) (Phospho)Creatine – m) Malonate – n) Phosphocholine – o) Taurine – p) Glucose - q) Glycine – r) Malate – s) residual suppressed water resonance – t) Glycogen – u) ATP/ADP – v) Fumarate – w) Oxypurinol – x) Formate

Univariate analysis

Table 5.3 and Figure 5.9 (Box plots of metabolites that differed significantly between all experimental groups) display the results of the univariate analysis in polar liver extracts ($p < 0.05$). The significant buckets include phosphocreatine, ATP/ADP, glutamine, glutamate, glycogen, glycine, glucose, beta-hydroxybutyric acid and valine/(iso)leucine.

In comparison to normoxic controls, 24 h anoxia resulted in a decrease in phosphocreatine, ATP/ADP, glutamine, glutamate and glycogen, combined with an increase in glycine, glucose, valine/(iso)leucine and beta-hydroxybutyric acid. Subsequently, 1 week anoxia led to a decrease in ATP/ADP, glycogen, phosphocreatine, glutamate and glutamine, compared to normoxic controls; with ATP/ADP and glucose being significantly lower than after 24 h of anoxia. In contrast, after 1 week anoxia, glycine, valine/(iso)leucine and beta-hydroxybutyric acid were increased compared to the controls; with glycine, valine/(iso)leucine and beta-hydroxybutyric acid being significantly higher than the 24 h anoxia group.

Reoxygenation resulted in a complete recovery of the levels of phosphocreatine, glycine, glutamate, glutamine, glucose, valine/(iso)leucine, ATP/ADP and glycogen to the control levels. On the other hand, beta-hydroxybutyric acid displayed a higher level compared to the normoxic controls.

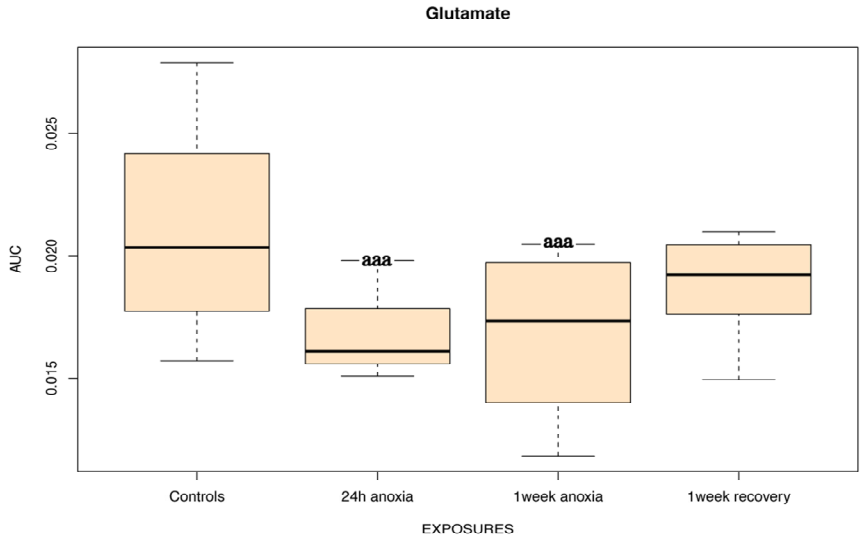
Glutamate
AUC
0.015
0.020
0.025
aaa
aaa
Controls
24h anoxia
1week anoxia
1week recovery
EXPOSURES

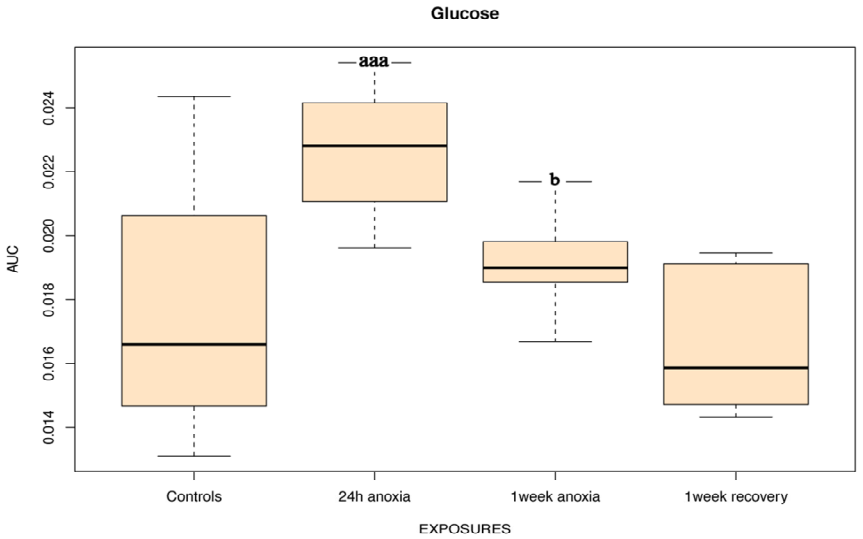
Glucose
AUC
0.014
0.016
0.018
0.020
0.022
0.024
aaa
b
Controls
24h anoxia
1week anoxia
1week recovery
EXPOSURES

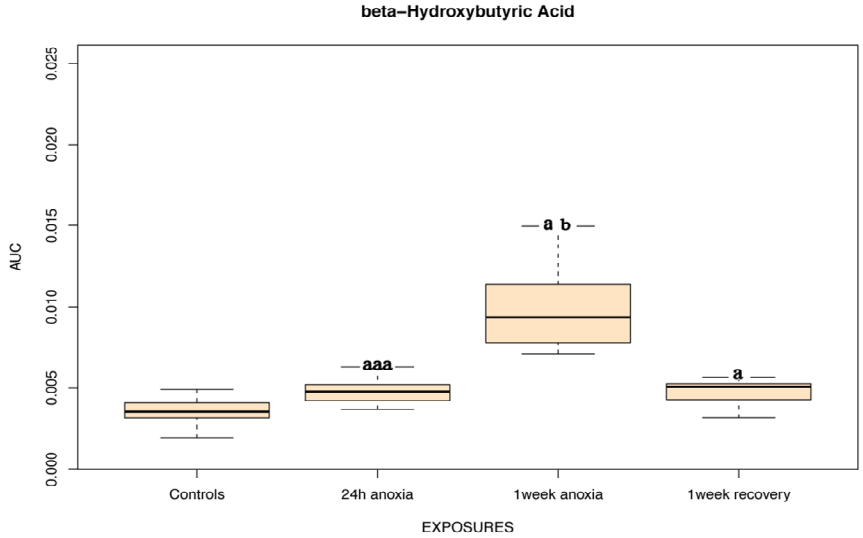
beta−Hydroxybutyric Acid
AUC
0.000
0.005
0.010
0.015
0.020
0.025
aaa
a b
a
Controls
24h anoxia
1week anoxia
1week recovery
EXPOSURES

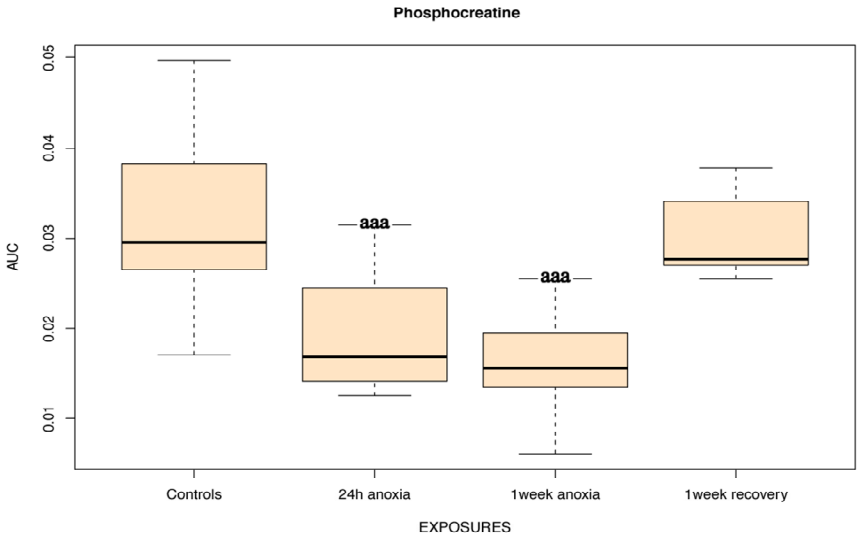
Phosphocreatine
AUC
0.01
0.02
0.03
0.04
0.05
aaa
aaa
Controls
24h anoxia
1week anoxia
1week recovery
EXPOSURES

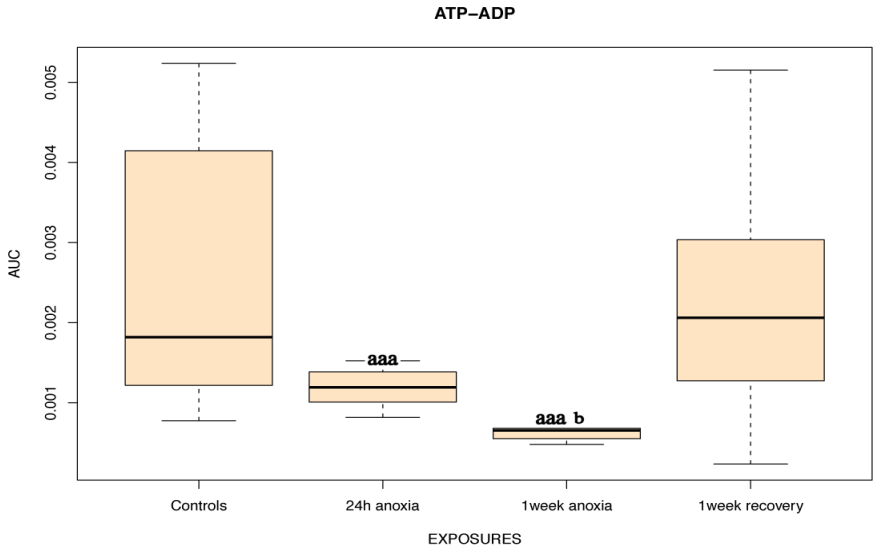
ATP–ADP
AUC
0.001
0.002
0.003
0.004
0.005
aaa
aaa b
Controls
24h anoxia
1week anoxia
1week recovery
EXPOSURES

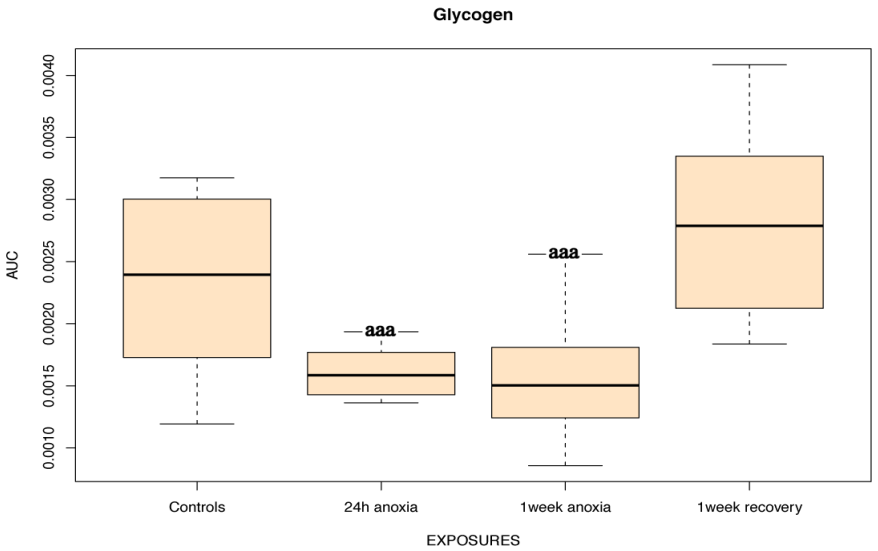
Glycogen
AUC
0.0010
0.0015
0.0020
0.0025
0.0030
0.0035
0.0040
aaa
aaa
Controls
24h anoxia
1week anoxia
1week recovery
EXPOSURES

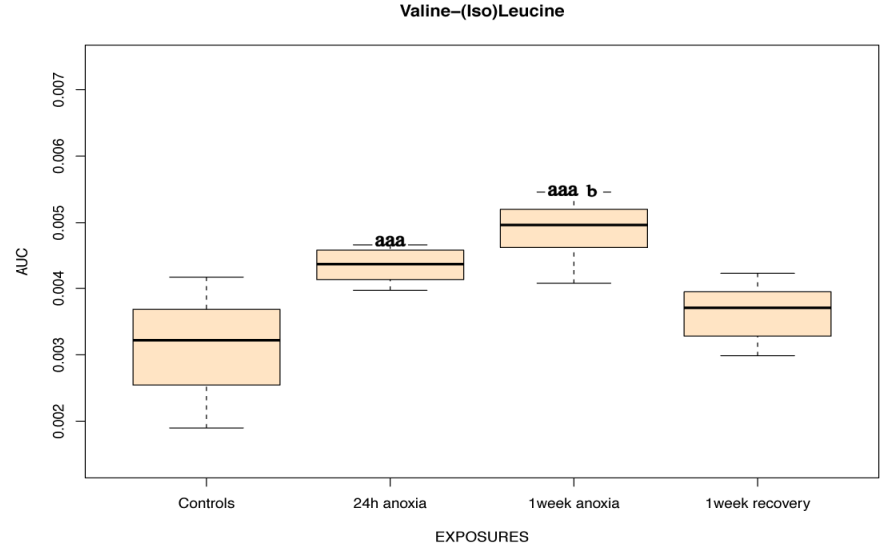
Valine–(Iso)Leucine
AUC
0.002
0.003
0.004
0.005
0.006
0.007
aaa
aaa b
Controls
24h anoxia
1week anoxia
1week recovery
EXPOSURES

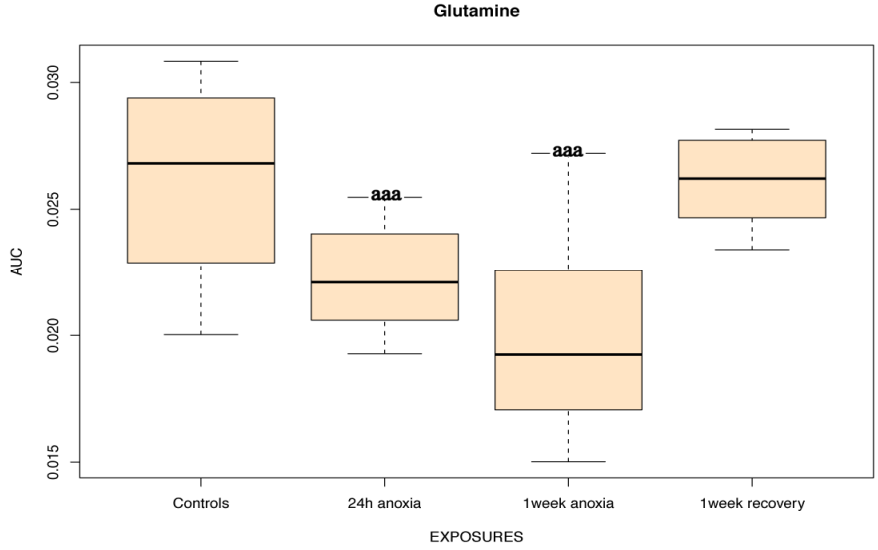
Glutamine
AUC
0.015
0.020
0.025
0.030
aaa
aaa
Controls
24h anoxia
1week anoxia
1week recovery
EXPOSURES

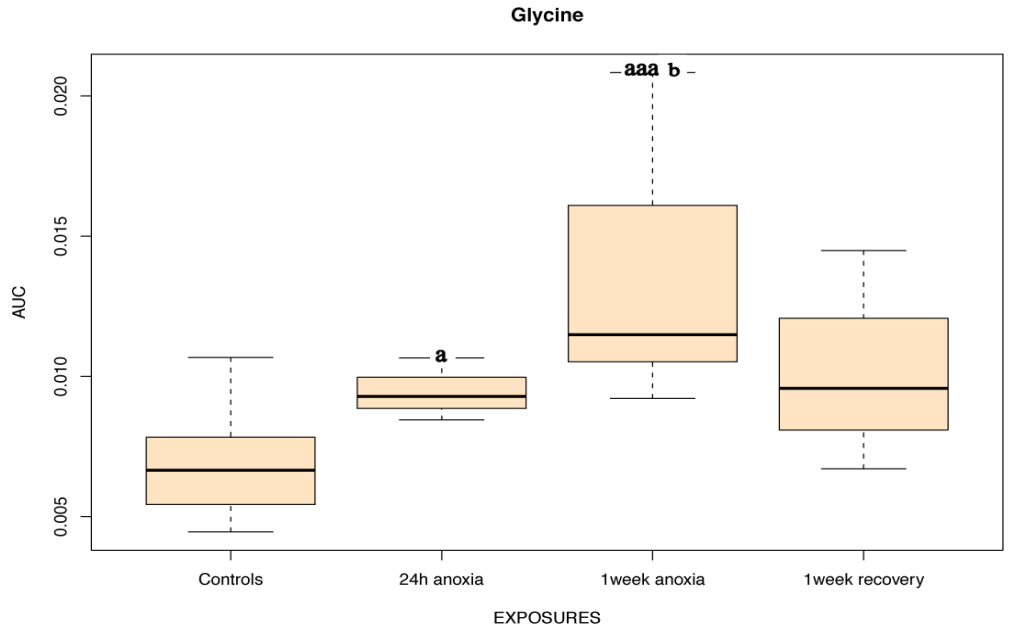

Figure 5.9 - Box plots of polar liver extracts to visualize the significant buckets/metabolites that differed significantly ($p < 0.05$) between the control and exposure groups and between the individual exposure groups, identified by student's t-tests and two-way ANOVA analysis followed by Benjamini-Hochberg correction tests. An 'a' indicates a significant difference between exposed (N=24) and control fish (N=10) (a: $p < 0.05$; aa: $p < 0.01$; aaa: $p < 0.001$), 'b' indicates a significant difference between 24h (N=8) and 1 week anoxic fish (N=9) (b: $p < 0.05$; bb: $p < 0.01$; bbb: $p < 0.001$).

Multivariate analysis

Principal component analysis was used to examine all liver data of the four exposure groups. In total, five samples were considered as outliers (due to technical variation in the measurement of the spectra) and removed from further analyses.

Subsequently, a four-class PLS-DA model was used to discriminate the samples according to their class membership as described above. The scores plot (Fig. 5.10) illustrates an adequate separation of all exposure groups. In particular, a clear separation of the normoxic groups (controls and recovered ones) and the anoxic groups (1 day and 1 week) can be observed along the first PLS-DA component (PLS 1).

Additionally, the metabolites that resulted from the PLS-DA loadings plot corresponded to the ones that were identified by univariate analysis.

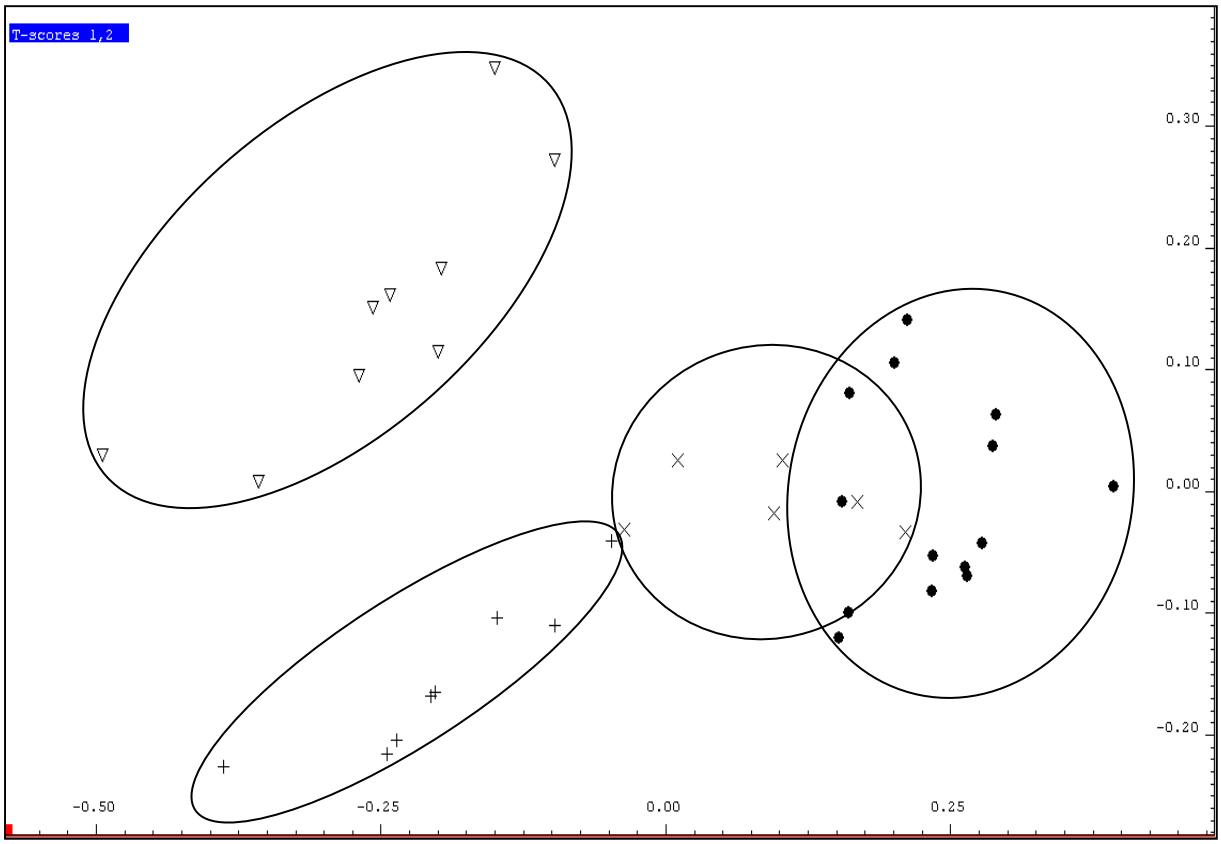

Figure 5.10 - PLS-DA scores plot of all groups in liver tissue, displaying the separation of the control group (•), N=14, the 1 day anoxia group (+), N=8, the 1 week anoxia group (Δ), N=9 and the 1 week normoxic recovery group (x), N=6 according to the first PLS-component in the X-axis (PLS 1) and the second PLS-component (PLS2) in the Y-axis.

5.3.1.4 ^{1}H-NMR spectroscopy and statistical analyses of polar white muscle extracts

The polar ^{1}H-NMR spectra of muscle extracts expose prominent resonances such as phosphocreatine/creatine, alanine, beta-hydroxybutyric acid, lactate and taurine as shown in Figure 5.11.

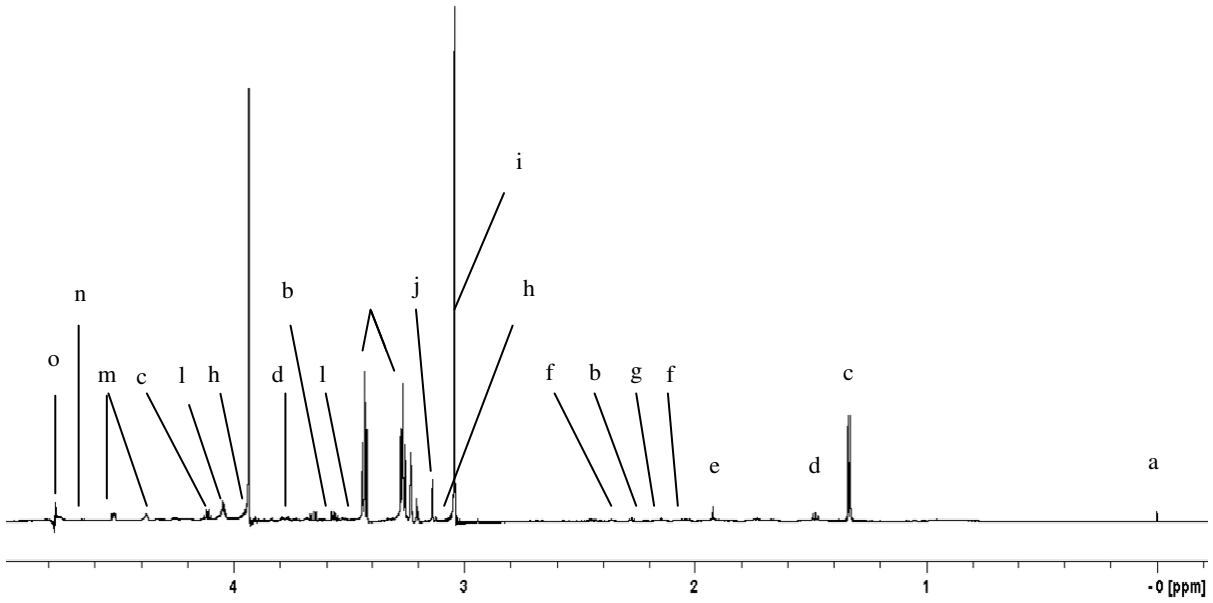

Figure 5.11 - Typical 700 MHz ^{1}H-NMR spectrum (0-5 ppm) representing a polar white muscle extract of a normoxic control fish, analyzed with a standard 90° pulse sequence.

Key to peak assignments: a) TMSP (internal standard) – b) Valine(Iso)Leucine – c) Lactate – d) Alanine – e) Acetate – f) Glutamate – g) Glutamine – h) Phosphocreatine – i) Creatine – j) Malonate – k) Taurine – l) Myo-inositol – m) ATP/ADP – n) Glucose – o) Residual suppressed water signal. The arrow indicates the carbohydrate region.

Univariate analysis

Table 5.3 and figure 5.12 show the results of the univariate analysis in muscle data. These tests identified the significant ($p < 0.05$) buckets that differed between the controls and the exposures. The metabolites were identified as beta-hydroxybutyric acid, lactate, glycine, acetate, valine/(iso)leucine, ATP/ADP, glucose, taurine, glutamate, glutamine and formate.

Compared to the normoxic status, 24 h anoxia resulted in a significant increase in the concentrations of beta-hydroxybutyric acid, lactate, glycine, acetate and valine/(iso)leucine,

combined with a decrease in ATP/ADP, glucose and taurine. After 1 week of anoxia, beta-hydroxybutyric acid, lactate, glutamate, glutamine and valine/(iso)leucine were significantly increased, compared to the controls; with beta-hydroxybutyric acid, glutamine, taurine and valine/(iso)leucine being higher than the 24 h anoxia group. In contrast, 1 week of anoxia caused a significant decrease in ATP/ADP, glucose, formate, glycine and taurine, compared to the controls; with glucose, formate, glycine, acetate being lower than the 24 h anoxia fish. A complete recovery was present for valine/(iso)leucine, ATP/ADP, formate, lactate, glucose, glycine, taurine, beta-hydroxybutyric acid, glutamate, glutamine and acetate.

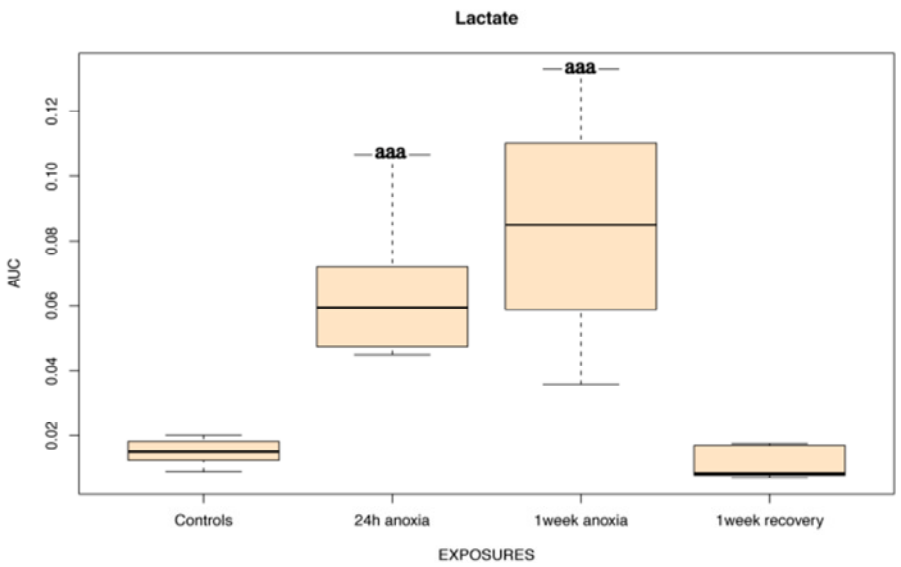
Lactate
AUC
0.02
0.04
0.06
0.08
0.10
0.12
aaa
aaa
Controls
24h anoxia
1week anoxia
1week recovery
EXPOSURES

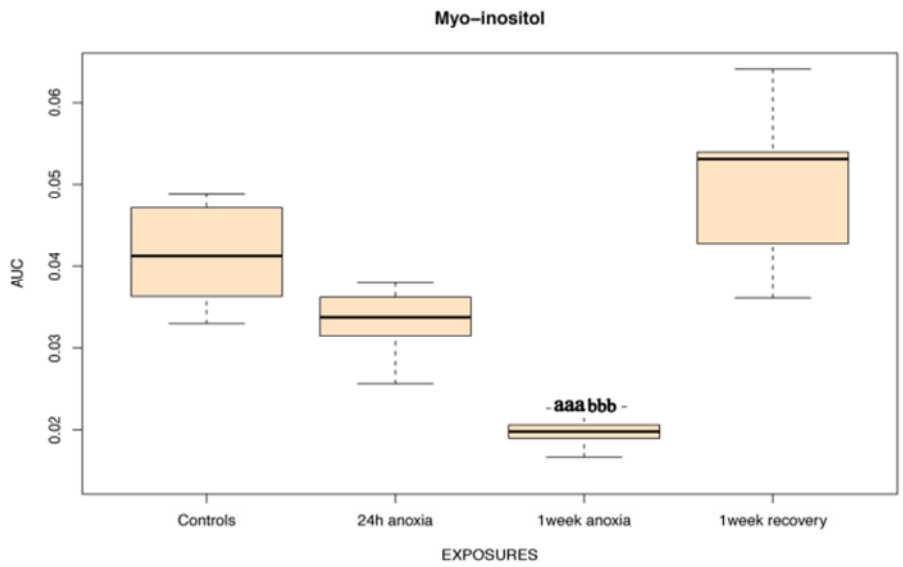
Myo−inositol
AUC
0.02
0.03
0.04
0.05
0.06
aaa bbb
Controls
24h anoxia
1week anoxia
1week recovery
EXPOSURES

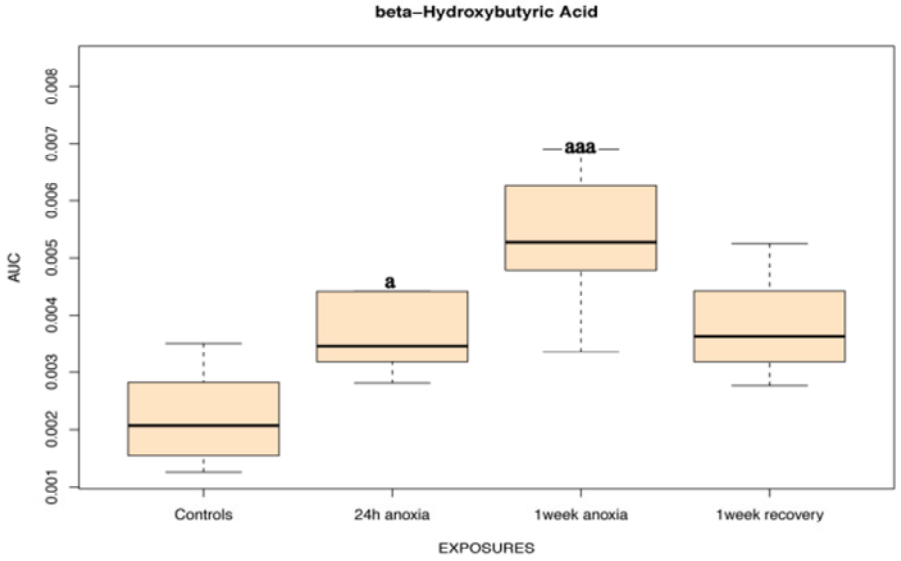
beta−Hydroxybutyric Acid
AUC
0.001
0.002
0.003
0.004
0.005
0.006
0.007
0.008
a
aaa
Controls
24h anoxia
1week anoxia
1week recovery
EXPOSURES

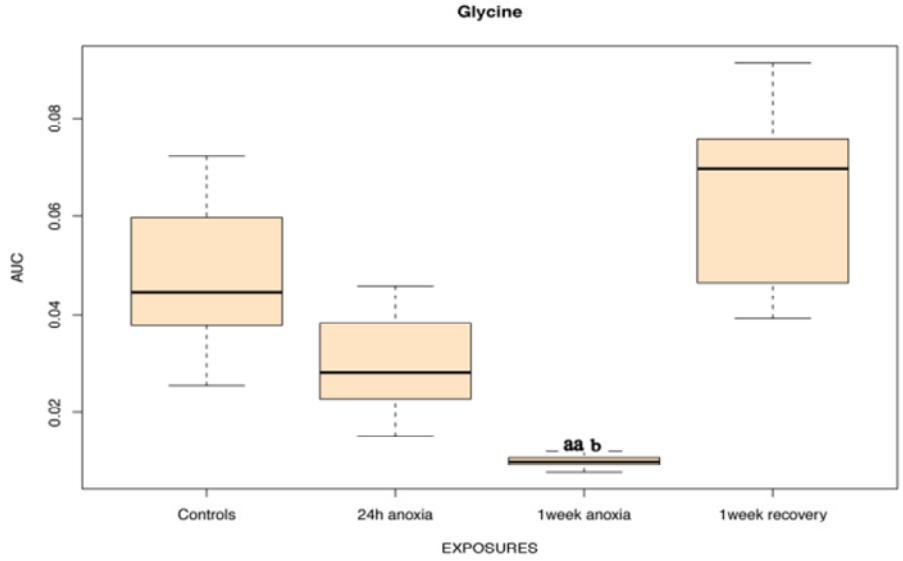
Glycine
AUC
0.02
0.04
0.06
0.08
aa b
Controls
24h anoxia
1week anoxia
1week recovery
EXPOSURES

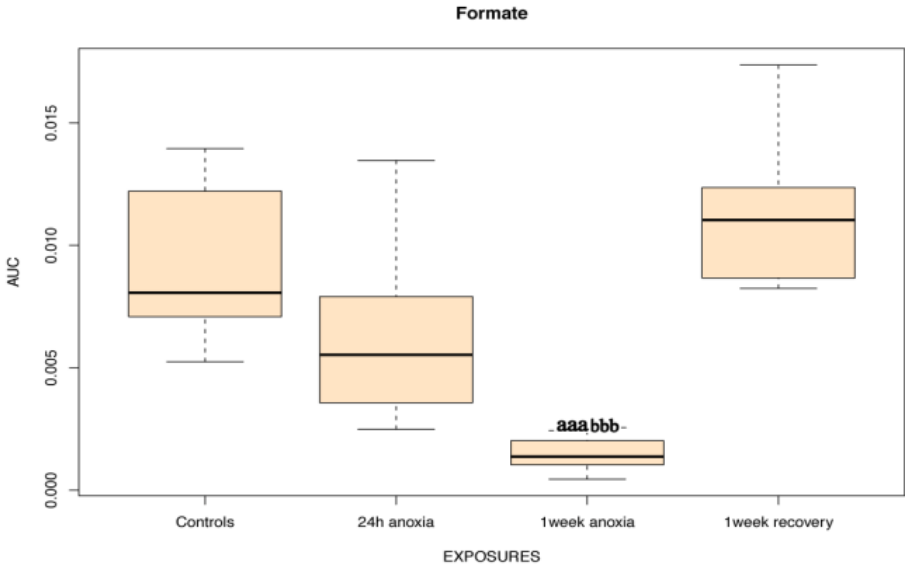
Formate
AUC
0.000
0.005
0.010
0.015
aaa
bbb
Controls
24h anoxia
1week anoxia
1week recovery
EXPOSURES

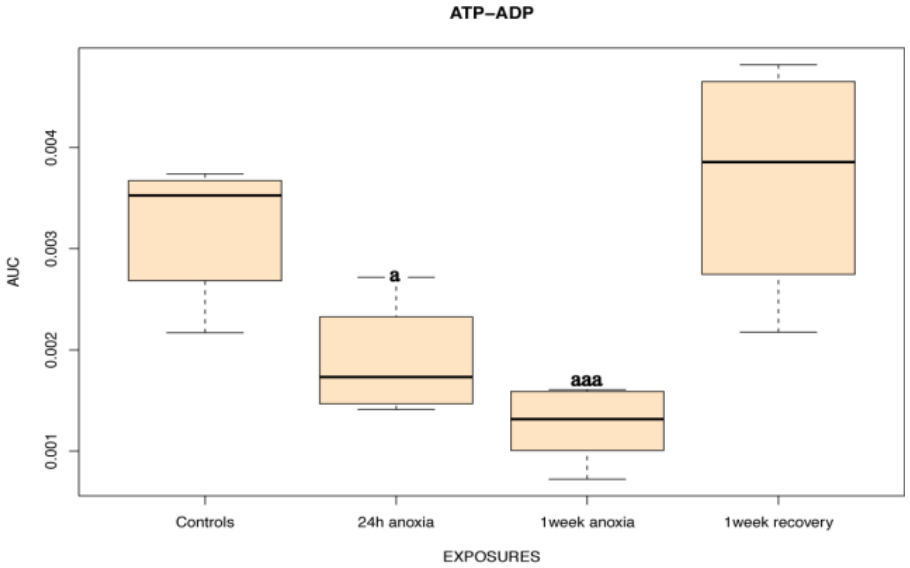
ATP−ADP
AUC
0.001
0.002
0.003
0.004
a
aaa
Controls
24h anoxia
1week anoxia
1week recovery
EXPOSURES

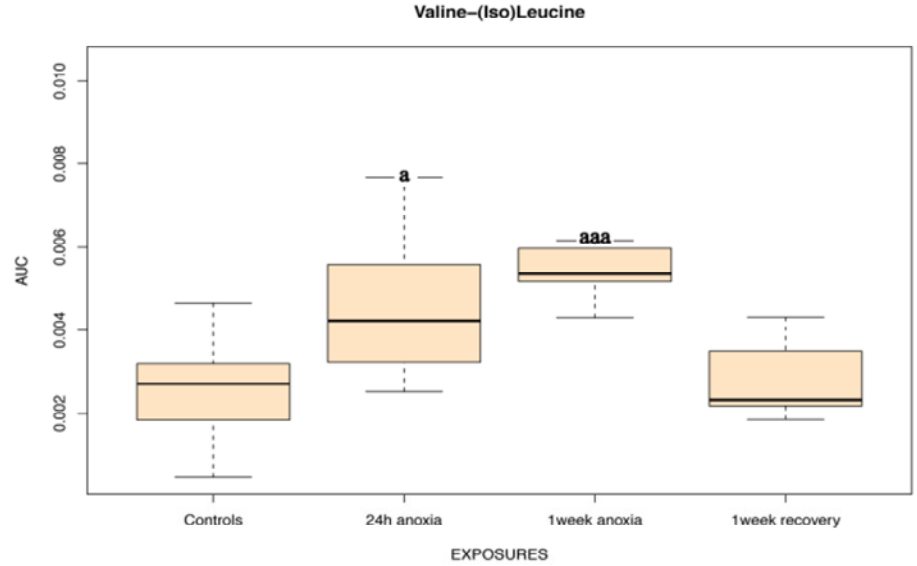
Valine−(Iso)Leucine
AUC
0.002
0.004
0.006
0.008
0.010
a
aaa
Controls
24h anoxia
1week anoxia
1week recovery
EXPOSURES

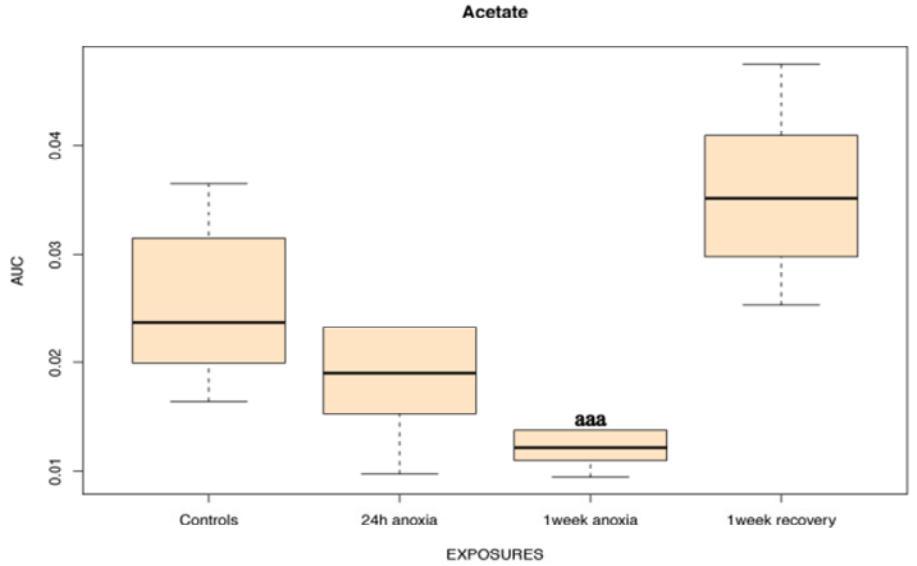
Acetate
AUC
0.01
0.02
0.03
0.04
aaa
Controls
24h anoxia
1week anoxia
1week recovery
EXPOSURES

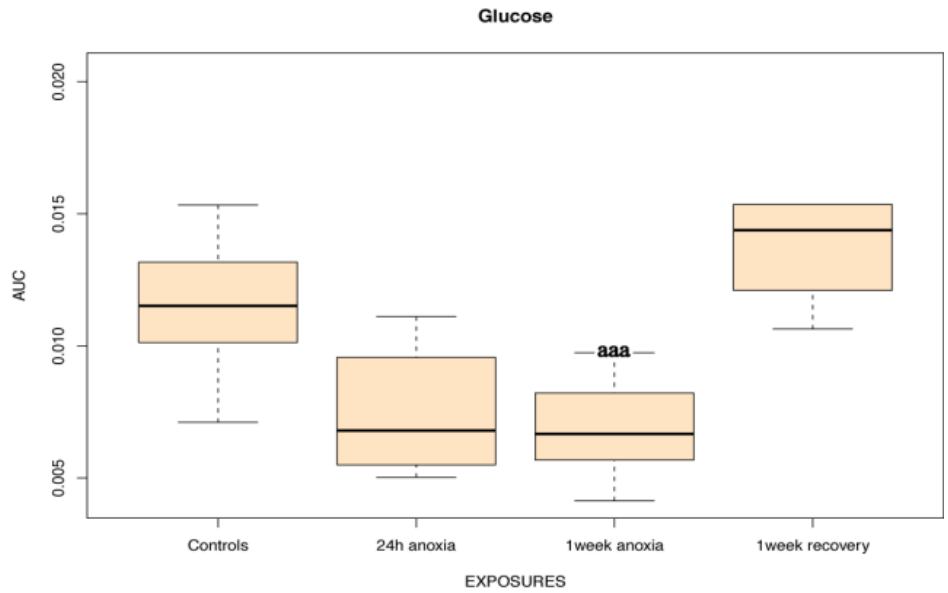

Figure 5.12 - Box plots of polar muscle extracts to visualize the significant buckets/metabolites that differed significantly ($p < 0.05$) between the control and exposure groups and between the individual exposure groups, identified by student's t-tests and two-way ANOVA analysis followed by Benjamini-Hochberg correction tests. An 'a' indicates a significant difference between exposed (N=26) and control fish (N=12) (a: $p < 0.05$; aa: $p < 0.01$; aaa: $p < 0.001$), 'b' indicates a significant difference between 24h (N=8) and 1 week anoxic fish (N=12) (b: $p < 0.05$; bb: $p < 0.01$; bbb: $p < 0.001$).

Multivariate analysis

The muscle spectra were subsequently analyzed by PCA and no outliers were detected in the different exposure groups. Following PCA, all datasets were submitted to the PLS-DA model in an attempt to discriminate the samples according to their class membership.

The PLS-DA scores plot of muscle extracts resulted in an adequate but less clear separation of the different exposure groups, compared to the scores plots of brain, heart and liver. Nevertheless, the corresponding loadings plot confirmed the metabolites identified by univariate analysis.

5.3.2 Apolar (hydrophobic) tissue extracts

The results of the applied CluPa alignment method on the four tissue types are shown by figures in the next sections. Only the quantitative analysis of brain, heart, liver and muscle are mentioned as the final results.

In any case, a region in the bottom panel is considered significant if its corresponding region in the top panel has the blue line higher than the black line.

Unfortunately, no significant regions were found in the NMR spectra of brain, heart, liver and muscle which indicate that there are no statistically significant differences in the apolar profiles of the different exposure groups within 1 tissue.

5.3.2.1 Apolar brain extracts

Figure 5.13 demonstrate the results of the CluPa alignment approach in the brain dataset.

Concretely, the results of the quantification are displayed, i.e. the determination of differential regions in the brain NMR spectra, based on the calculated BW-ratio. In any case, a region in the bottom panel (lower box) is considered significant if its corresponding region in the top panel has the blue line higher than the black line (upper box). As already mentioned and pointed out by Figure 2, no significant regions were found for brain extracts.

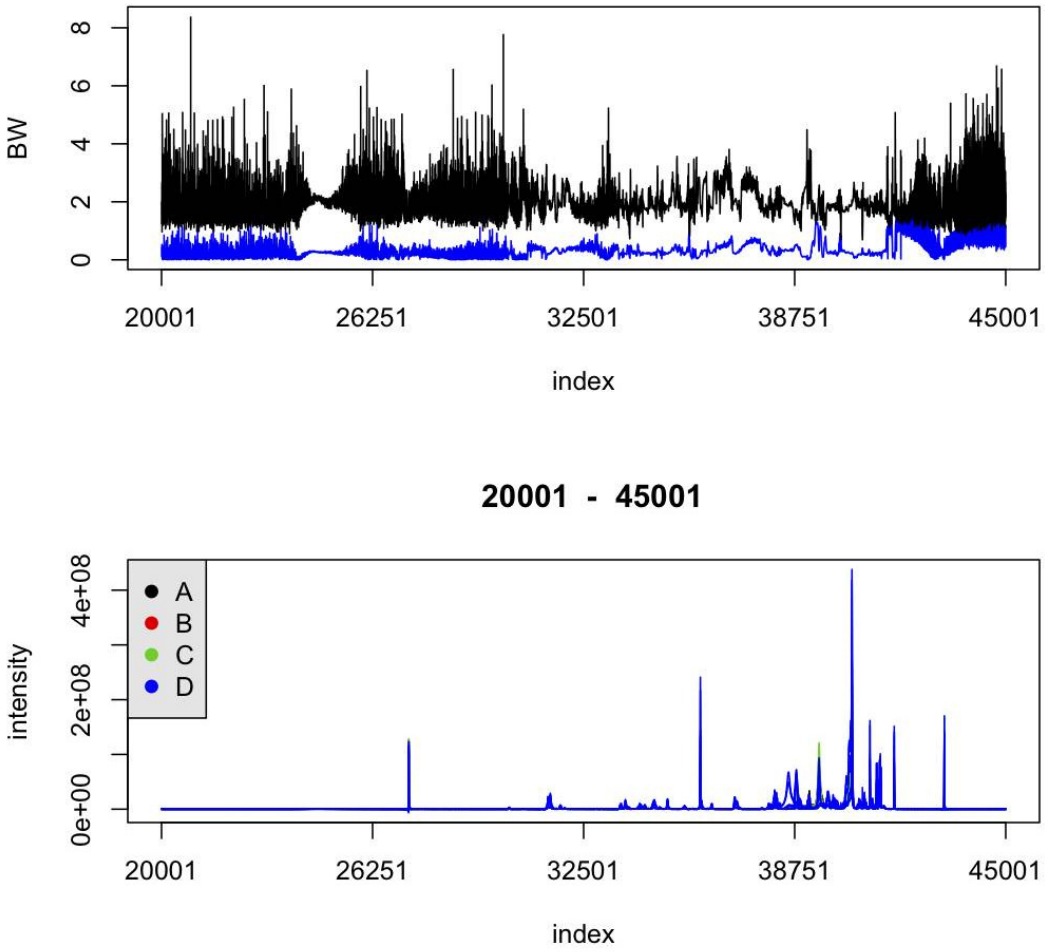

Figure 5.13 – CluPa analysis of apolar brain extracts.

5.3.2.2 Apolar heart extracts

Figure 5.14 presents the results of the CluPa alignment in heart datasets.

Similar to brain extracts, no significant regions were found here.

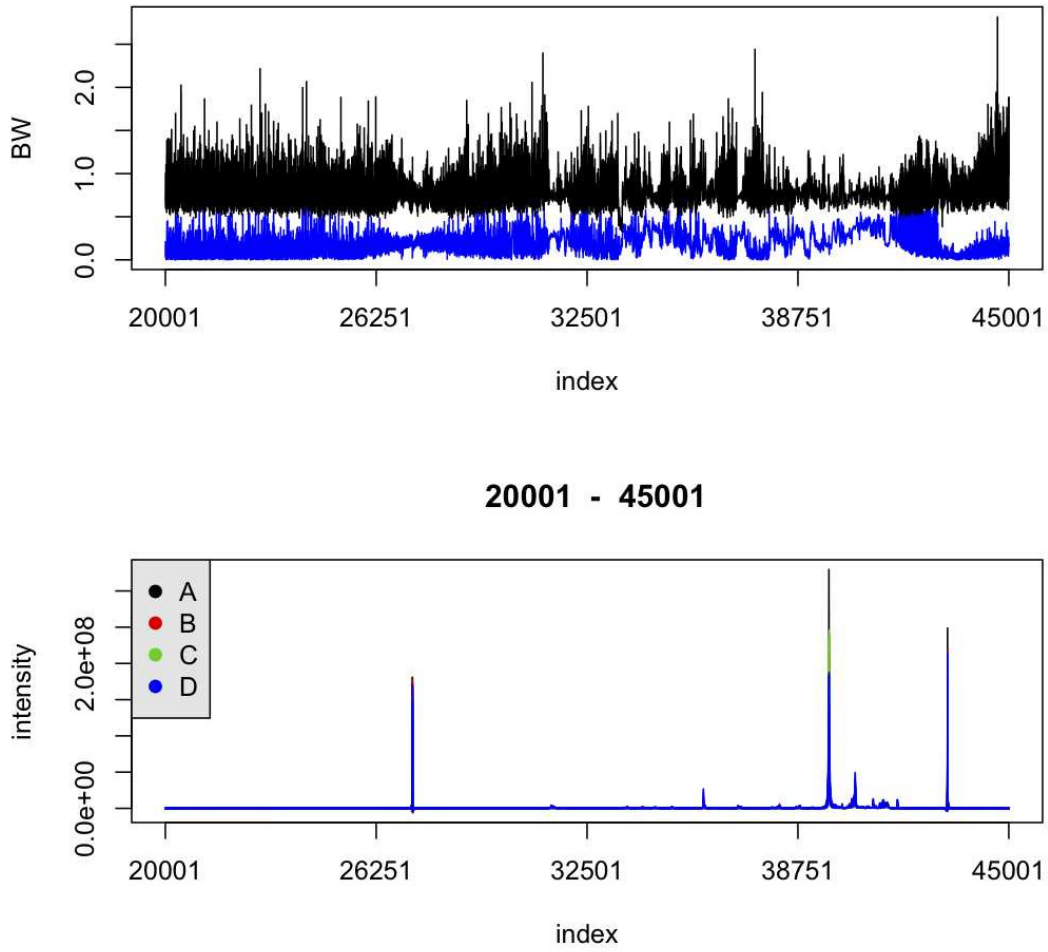

Figure 5.14 - CluPa analysis of apolar heart data.

5.3.2.3 Apolar liver extracts

The results of the applied CluPa method in liver extracts, i.e. no significant different regions, are illustrated by Figure 5.15.

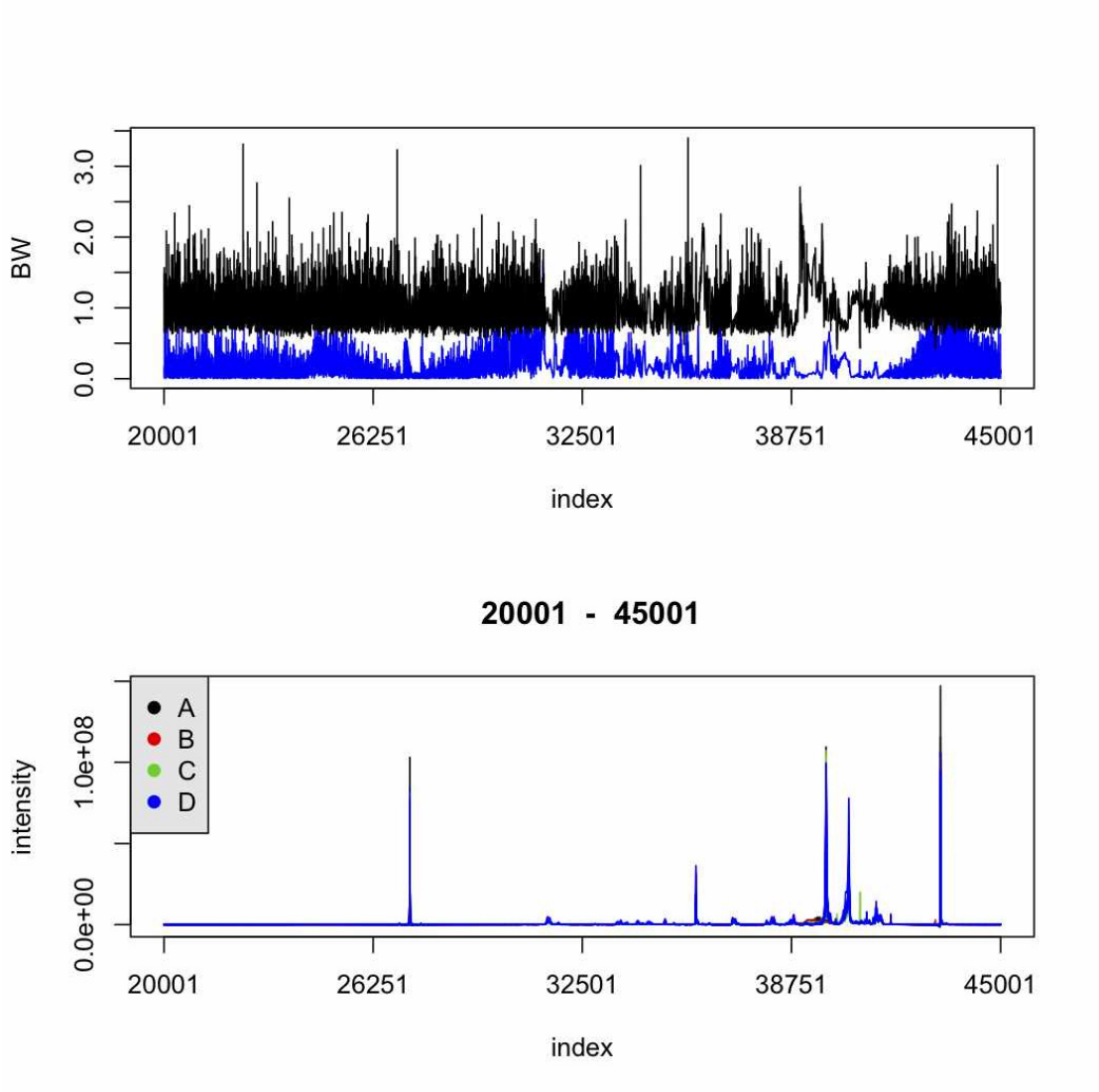

Figure 5.15 - CluPa analysis of apolar liver data.

5.3.2.4 Apolar white muscle extracts

No significant regions were found in the NMR spectra of muscle extracts, following CluPa analysis (Figure 5.16).

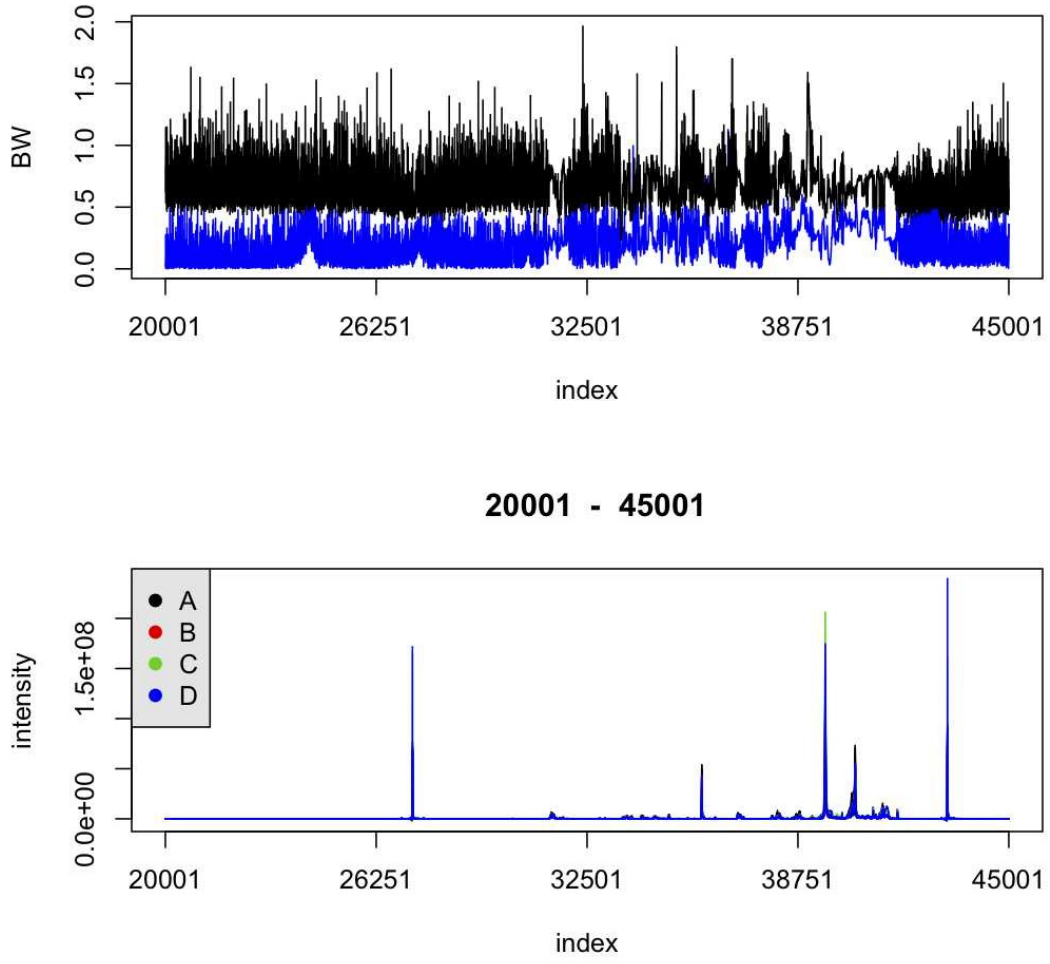

Figure 5.16 - CluPa analysis of apolar muscle data.

5.4 Discussion

In order to provide a transparent and comprehensive explanation for the achieved results for polar tissue extracts in this study, the discussion is divided into three sections that respectively examine the metabolites affiliated with the general energy metabolism (e.g. glucose, lactate, ATP/ADP, etc.), the amino acids and neurotransmitters (glutamate, NAA, GABA, etc.) and finally, the role of previously unrecognized changing metabolites in anoxia exposed fish.

5.4.1 General energy metabolism

Under normoxic conditions, greater than 95 % of ATP is produced aerobically in vertebrate cells, whereby each mole of glucose is oxidized by 6 moles of O_2 to yield 36 moles of ATP [Lutz, Nilsson and Prentice 2003]. In these aerobic conditions, most glucose is fully oxidized

to H_2O and CO_2. The net lactate production accounts for only a negligible (< 4 %) part of the total glucose metabolized. In contrast, anoxia causes a dramatic shift from aerobic to anaerobic metabolism where sufficient ATP can only be generated by up-regulating O_2-independent mechanisms, namely anaerobic glycolysis and other metabolic pathways that rely on substrate-level phosphorylation. Eventually, glucose/glycogen and/or high-energy phosphates (metabolic fuels) become exhausted and metabolic waste products such as lactate and H^+ accumulate.

Remarkably, crucian carp withstand lactate self-poisoning due to their unique ability to convert lactate into ethanol, which is then lost to the environment across the gills by diffusion [Nilsson 1988; Vornanen *et al.* 2009]. Ethanol was not detected in any tissues in this study. However, this might be due to the lyophilisation procedure, resulting in the evaporation of the volatile ethanol. An increase in lactate during anoxia was observed in the brain, heart and muscle. In the brain, the lactate increase was apparent already after 1 day of anoxic exposure and this was at least as high after 1week of anoxia. The lack of a major increase in lactate between 1 day and 7 days of anoxia shows that lactate was further metabolized to ethanol and was probably at a steady-state concentration.

A significantly increased lactate concentration was also present in the 1 week anoxic heart samples. Simultaneously, a decreased glucose concentration was observed when fish were exposed to 1 week of anoxia. However, we were not able to detect significantly changing lactate concentrations in anoxic livers but fluctuating glycogen and glucose concentrations were detected clearly during anoxia.

Short and long term anoxia caused a significant increase of glucose and a decrease of glycogen in liver extracts. Crucian carp has the largest glycogen store of all vertebrates [Vornanen *et al.* 2011] and the size of this carbohydrate deposits limits the hypoxia/anoxia tolerance of crucian carp. In contrast to liver tissue, no glycogen and thus no changes in the glycogen content of brain, heart and white muscle were observed in this study. In 2006, a study by Vornanen and co-workers [Vornanen and Paajanen 2006] investigated the glycogen concentrations in crucian carp brains. Apparently, clear seasonal cycling patterns were observed with glycogen values ranging from 203.7 µM/g in February to 12.9 µM/g in July. Furthermore, another study by this group analyzed the size of glycogen stores in different tissues of crucian carp [Vornanen *et al.* 2011]. Clearly, the highest mean glycogen content existed in the liver (18 % of wet weight) whereas lower glycogen levels were present in brain

(3 %), muscle (2 %) and heart (2 %). Possibly, we did not observe any glycogen resonances in brain, muscle and heart spectra due to the relatively low concentrations (µM range) of this metabolite in these tissues, in comparison to the detection limit of the NMR machine (mM range).

Furthermore, 1 and 7 days of anoxia exposure resulted in a decrease of liver phosphocreatine concentrations. Phosphocreatine stores are, in addition to tissue glycogen stores, important energy reserves (particularly in muscle) by giving off the phosphate group to ADP to form ATP [Mandic *et al.* 2008]. In this study, we did not detect any significant changes in the (phospho) creatine levels of muscle extracts. Possibly, this can be due to the way the spectra were bucketed in this study. Concretely, all ^{1}H-NMR spectra were automatically segmented into 0.05 ppm buckets between 0.5 and 10 ppm. In the case of phosphocreatine (PCr) and creatine (Crea), the resonances of both metabolites are situated almost next to each other in the muscle spectra, as demonstrated by Figure 5.17 A and B. By applying a bucket width of 0.05 ppm, both metabolites are located in the same bucket and thus, are considered as one for subsequent statistical analysis.

(A)

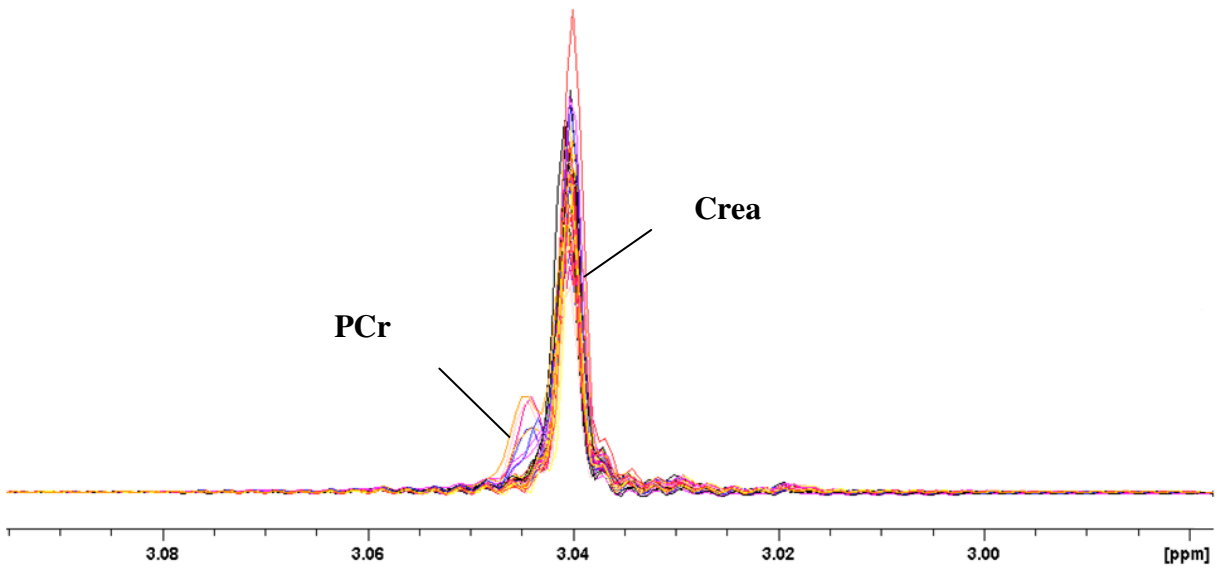

(B)

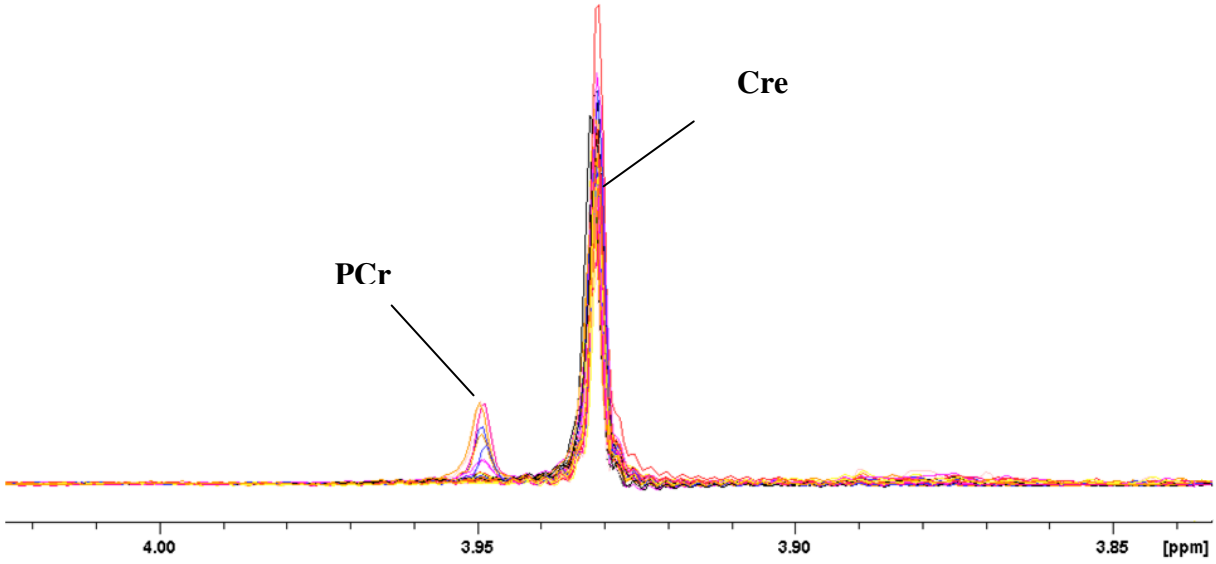

Figure 5.17 – **(A)** Enlargement of the spectral region from 3.02 - 3.04 ppm and **(B)** from 3.92 - 3.97 ppm, demonstrating the approximate locations of both phosphocreatine and creatine peaks in all overlapping ^{1}H-NMR spectra from muscle tissue.

In general, anoxia induces a decrease of phosphocreatine levels in muscle (to provide ATP) whereas the creatine levels increase correspondingly. Probably, this metabolic behaviour might have occurred in this study but due to the proximity of the phosphocreatine and creatine peaks in the spectra of the examined tissue extracts, statistical analysis likely did not reveal a straightforward, correct result concerning the significant changes in PCr and creatine.

All tissues, except for the brain, demonstrated a decrease in ATP in response to anoxia exposure but reoxygenation enabled a complete recovery. Compared to the normoxic controls, an increase of a keton body, beta-hydroxybutyric acid, was observed in all 1 week anoxic tissues. This probably reflects the stop in keton-body metabolism as the citric acid cycle is not functioning during anoxia.

5.4.2 Amino acids and neurotransmitters

Anoxia not only altered the cellular energy metabolism, it also influenced the amino acid and/or neurotransmitter patterns. Specifically, the characteristic anoxia-induced features, i.e. an increased concentration of inhibitory compounds (GABA, glycine) combined with a

decreased concentration of excitatory metabolites (glutamate, glutamine) were detected in the anoxic brain extracts [Nilsson *et al.* 1991].

GABA, a major inhibitory neurotransmitter in the adult vertebrate central nervous system and we observed an increase of brain GABA at 1 day of anoxia, and the increase was further noticed following 1 week of anoxia. Such an increase in GABA during periods of oxygen deficiency has previously been observed in crucian carp brain, both in tissue [Nilsson, 1990] and extracellulary [Hylland and Nilsson 1999] and the metabolic pathways supporting GABA production and degradation are well characterized in vertebrate nervous tissues. The elevation of brain GABA is thought to be a main mechanism for anoxic metabolic depression.

As a consequence of the activation of inhibitory GABA receptors, the synaptic and electrical activities in the brain decrease and hence, the overall energy consumption is reduced. Moreover, GABA is synthesized from glutamate and the continued production of GABA at the expense of glutamate during anoxia could provide further depression of brain activity, since glutamate is the major excitatory neurotransmitter in vertebrates. Indeed, the concentrations of glutamate and the intimately connected glutamine (precursor and storage form of glutamate in the brain) decreased when carp were exposed to 1 day and 1 week of anoxia.

Glutamate and glutamine are non-essential amino acids of the citric acid cycle superfamily and can be transaminated into citric acid cycle intermediates within most cells [Podrabsky *et al.* 2007]. Firstly, a decreased brain tissue glutamate level could be directly related to a decreased tricarboxylic acid cycle activity. However, studies are available, demonstrating an increase or a stabilization of glutamate in the liver and muscle of goldfish respectively [Van Waarde *et al.* 1982]. Secondly, a more straightforward explanation is related to the similar increase of brain GABA after anoxia. Glutamate is the immediate precursor of GABA and the glutamate decarboxylase reaction, which converts glutamate to GABA, proceeds during anoxia. Hence, an increased GABA concentration in the brains of anoxic carp can be related to a decreased glutamate (and glutamine) concentration. The created metabolic network (Fig. 5.6) demonstrates well the link between GABA, glutamate and glutamine. As illustrated, these three metabolites are positioned close to each other in the network, which implies that they are metabolically related during anoxic stress.

A significant decrease of N-acetylaspartate was present in the brain of 1 to 7 day anoxic fish. N-acetylaspartate is present almost exclusively in neurons/ neuronal processes

and is an important metabolite in brain. For instance, NAA is decreased in a variety of human neurodegenerative diseases associated with neuronal loss [Raman *et al.* 2005] and therefore, NAA can be considered as a marker of neuronal density or viability. The decreased brain NAA in this study can be due to a decreased production of NAA in neurons and a possible loss of NAA from damaged neurons. Although crucian carp obviously are masters of anoxic survival, it cannot be excluded that anoxia leads to some neuronal damage or loss that is effectively repaired or restored upon reoxygenation. Secondly, NAA can act as a source of acetate, enabling the lipid and myelin synthesis in oligodendrocytes. Therefore, the decreased NAA concentration in brain may reflect an attempt to diminish the extent of cell membrane damage during anoxia. Thirdly, the enzyme responsible for the synthesis of NAA, acetyl-CoA-l-aspartate-N-acetyltransferase, is localized exclusively in the mitochondria [Choi *et al.* 2007]. Accordingly, decreased NAA levels after anoxic periods may plausibly reflect an impaired mitochondrial energy production.

The branched-chain amino acids (BCAA) valine/isoleucine/leucine increased in all anoxic tissues. These essential amino acids are key molecules essential for regulating global growth and metabolism [Wang *et al.* 2011]. Particularly leucine is important for heart muscle health and can stimulate protein synthesis, cellular metabolism and cell growth (Wang *et al.* 2011). In addition, isoleucine is both glucogenic as well as ketogenic [Voet 1995]. In this study, the observed increase of the BCAA's can be due to the stop in oxidation by mitochondrial enzymes in anaerobic tissues. The increased concentration of BCAA can also be due to a reduced consumption of amino acids (protein synthesis suppression) or an increased catabolism in periods of anoxia [Podrabsky *et al.* 2007].

5.4.3 Novel metabolites

Lastly, the NMR study of anoxic tissue extracts introduced the appearance of compounds that are 'novel', i.e. previously unrecognized to play a role in the present context: myo-inositol in heart extracts and taurine in white muscle.

Myo-inositol decreased significantly in the heart of anoxic fish. So far, its exact function is not well understood, although it is believed to be an essential element for cell growth, an osmolite, a glial marker and a storage form for glucose [Govindaraju *et al.* 2000]. Maybe, the decrease of myo-inositol in the heart extracts could reflect a change in the heart phosphoinositide-energy metabolism.

Taurine decreased significantly in muscle tissue. A first decrease of taurine was noticed after 24 h of anoxia and the concentration continued to decrease after 1 week of anoxia. This sulfonic amino acid is highly concentrated in fish tissue (skeletal muscle, heart, brain and retina) and has many important metabolic functions. In the anoxic crucian carp brain, it may act as an inhibitory neuromodulator, counteracting brain damage [Hylland and Nilsson 1999]. Furthermore, taurine has antioxidative and membrane-stabilizing properties, is a natural calcium antagonist and osmoregulator and is essential for the development and function of skeletal muscle [Schaffer *et al.* 2010]. Additionally, it modulates the immune response, regulates the transport of ions, signal transduction, cell proliferation and DNA repair [Kuzmina *et al.* 2010]. In this study, a decrease of taurine was noticed following 24 h and 1 week of anoxic stress. This decrease might be due to the augmented consumption of this polyfunctional and beneficial amino acid in anoxic muscles.

5.5 Concluding remarks

To conclude, the present study provides an excellent example of the usefulness of NMR-based metabolomics to examine the biochemical responses of aquatic animals to environmental challenges. We used ^{1}H-NMR based metabolomics combined with chemometric tools, to explore the metabolic responses of crucian carp to anoxic stress.

Metabolic profiles of heart, brain, liver and muscle extracts confirmed previously observed changes in energy-related compounds, such as glucose and lactate, and in amino acid neuromodulators. Moreover and more importantly, the study also illustrates the potential of ^{1}H-NMR based metabolomics to discover changes in the levels of metabolites that previously not received attention in the present context. These “novel” metabolites included myo-inositol and taurine in this case.

Further research in this unique fish model will undoubtedly lead to the identification of other novel and key elements involved in the mechanism of anoxia resistance.

Chapter 6

The hypoxic common carp (Cyprinus carpio)

BASED ON:

"^{1}H-NMR study of the metabolome of a moderately hypoxia-tolerant fish, the common carp (*Cyprinus carpio*)"

Isabelle Lardon[*(1, 2)], Marleen Eyckmans [(2)], Trung Nghia Vu [(3,4)], Kris Laukens [(3,4)], Gudrun De Boeck [(2)], Roger Dommisse [(1)]

Submitted to ***Metabolomics***

[(1)] University of Antwerp - Department of Chemistry (Research Group for Applied NMR) - Groenenborgerlaan 171, B-2020 Antwerp, Belgium

[(2)] University of Antwerp – Department of Biology (Laboratory for Systemic Physiological and Ecotoxicological Research - SPHERE) - Groenenborgerlaan 171, B-2020 Antwerp, Belgium

[(3)] University of Antwerp - Department of Mathematics & Computer Science - Middelheimlaan 1, B-2020 Antwerp, Belgium - [(4)] Biomina - biomedical informatics research center Antwerp, Wilrijkstraat 10, 2650 Edegem (Antwerp), Belgium

Abstract

The common carp (*Cyprinus carpio)* is a worldwide distributed freshwater fish, able to survive low oxygen concentrations and tolerating a broad range of temperatures (4 up to 35 °C). The tolerance of common carp to limited oxygen concentrations is a shared ecological characteristic with its relative, the crucian carp (*Carassius carassius*).

In this paper, we studied the ^{1}H-NMR-based metabolomic responses of various tissue extracts (brain, heart, liver and white muscle) of common carp, subjected to anoxic and hypoxic exposure at 5 °C. Specifically, fish were exposed to normoxia (controls 24 h, 1 w and 2 w), acute hypoxia (24 h), chronic hypoxia (1 w) and chronic hypoxia (1 w) with normoxic reoxygenation (1 w). In addition, we also investigated the metabolic responses of fish to anoxic exposure for 2 h.

Both anoxia and hypoxia induced significant changes in the tissue levels of standard energy metabolites such as lactate, glycogen, ATP/ADP, phosphocreatine, etc. Remarkably, anoxic stress induced increased lactate levels in all tissues except for the heart whereas hypoxia resulted in decreased lactate concentrations in all examined tissues except for brains. Furthermore, hypoxia and anoxia also influenced the levels of amino acids (e.g. alanine, valine/(iso)leucine, etc.) and neurotransmitters (GABA, glutamate). Lastly, the ^{1}H-NMR study of tissue extracts enabled the detection of 'other' i.e. previously not reported compounds to play a role in the present context. Significant changes in the levels of scyllo-inositol in heart, liver and white muscle were observed, providing novel insights into the anoxia/hypoxic responses of the common carp.

Key words: common carp, metabolomics, ^{1}H-NMR, hypoxia, anoxia, tissue extracts

6.1 Introduction

Low dissolved oxygen concentrations are a common adverse environmental feature in aquatic systems worldwide and vary in temporal frequency, seasonality and persistence. Besides the naturally occurring hypoxic habitats, anthropogenic activities have contributed to an increase in hypoxic/anoxic habitats, both in fresh water and coastal systems [Zhou *et al.* 2000]. There are approximately 20.000 different fish species and they all vary greatly in their ability to tolerate and survive hypoxia i.e. when the content of oxygen in water decreases below a certain critical value [Bickler and Buck 2007]. The consequences for fish depend on their ability to withstand the hypoxia-related biochemical perturbations. Especially fish belonging to the genus *Carassius* are of particular interest due to their remarkable tolerance to limited oxygen concentrations, even to a complete lack of oxygen. The most extreme example is the crucian carp (*Carassius carassius*), able to survive anoxia for months, depending on the ambient temperature. Changes in its metabolome following anoxia have been studied recently (Lardon *et al.*, in press). Its cousin, the common goldfish (*Carassius auratus*) survives anoxia for 45 h (5 °C) and 22 h at 20 °C [Bickler and Buck 2007]. Both the crucian carp and the goldfish rely on the strategy of metabolic depression to conserve their glycogen stores. Also, they avoid lactate self-poisoning by converting lactate into ethanol and CO_2, a trait that is not shared with more distant relatives such as the common carp (*Cyprinus carpio*) used in this study.

The common carp is distributed worldwide and found commonly in a broad range of freshwater habitats with low oxygen levels. Therefore, it is assumed that this fish species developed adaptive mechanisms to cope with hypoxia. Although related to the crucian carp, the common carp is anoxia-intolerant and only able to survive 1-2 h of anoxia at room temperature or 1 h of hypoxia (0.8 mg $O_2\,l^{-1}$) at 23 °C. The most important challenge for fish in order to survive limited or absent oxygen levels is to match their energy supplies with the energy demands, allowing them to maintain an adequate level of ATP. Concerning the anoxia-tolerant crucian carp, different strategies in multiple organ systems have been described. For common carp, however, limited literature is available describing the mechanisms of hypoxia/anoxia tolerance. Consequently, till now, strategies that are applied to withstand the negative biochemical consequences of anoxia and/or hypoxia exposure in common carp are still not completely understood.

As indicated in the literature, high-resolution nuclear magnetic resonance (NMR) already proved to be a convenient tool to study the metabolomics of tissue extracts in fish [Kullgren *et al.* 2010; Segner *et al.* 1997; Karakach *et al.* 2009; Ekman *et al.* 2009]. Moreover, the exploratory approach of NMR-based metabolomics offers the possibility to extract simultaneously information on the type and on the concentration of different metabolites in a biological sample, without the requisite for prior knowledge on which metabolites are involved in the physiological response.

The objectives of the present study are to gain more insight in the metabolic pathways that allow common carp to withstand short term anoxia and/or long term hypoxia. To reach this goal, we (a) analyzed the biochemical profiles of various tissue extracts of the hypoxia-tolerant common carp by ^{1}H-NMR, and (b) compared these results to our previous results obtained with the related but anoxia-tolerant crucian carp [Lardon *et al.* 2012].

6.2 Materials and methods

6.2.1 Fish and fish maintenance

Young common carp (*Cyprinus carpio*), strain R8 F11 x R3 F11, three months old with a mean initial weight of 1 g and a mean body length of 1.5 cm were obtained from the fish hatchery at the University of Wageningen, The Netherlands. Fish were transported to the University of Antwerp where they were held and grown for one year at 25 °C and acclimated to a 12 L: 12 D photoperiod in softened city tap water. Common carp were fed daily with commercial fish pellets (food ratio of 3-5 %) but were not fed two days before the start of the experiment. Water quality and the general health status of the fish were checked daily. Subsequently, two months before the start of the experiment, the fish were transferred from their maintenance tanks into a climate chamber set at 25 °C and were allowed to further acclimatize by decreasing the temperature at a rate of 1 °C per day until the final exposure temperature of 5 °C was reached. The photoperiod was maintained at 12 L: 12 D and fish were able to acclimatize to 5 °C for an additional 4 weeks. This allows for a direct comparison with the earlier results on crucian carp tissue extracts (Lardon *et al.*, in press) which were obtained at 5 °C as well. Following this acclimatization period, fish were randomly distributed to 50 l glass aquaria, supplied with well oxygenated water (9 mg O_2 l^{-1}, 5 °C), with a density of 8 fish per tank/exposure. The experimental fish were still juvenile, and consisted of both sexes with a mean body length of 7.5 ± 0.6 cm (mean ± S.D.) and a mean body mass of 15.5 ± 3.7 g (mean ± S.D.).

6.2.2 Experimental setup anoxia- and hypoxia exposures

Levels of dissolved oxygen in the hypoxic/normoxic system were monitored and controlled continuously by the R362 Controller system for pH/mV/conductivity/oxygen (Consort, Turnhout, Belgium). A schematic overview of the experimental setup is provided in Figure 6.1.

In brief, the R362 system controls a predetermined oxygen level in test aquaria by opening or closing two types of valves (switches). The first valve is connected to an air supply and opens the flow of normoxic air to make the water more aerated whereas a second valve is attached to a nitrogen gas bottle and opens the flow of N_2 gas to make the water more hypoxic/anoxic. Prior to the start of the experiment, the level of hypoxia was set at 0.9 mg O_2 l^{-1}. In order to double check and to verify the results of the R362 oxygen electrodes, an additional oxygen meter electrode (WTW oxi 340i, Weilheim, Germany) was used throughout all experiments. The experiment started by gradually lowering the oxygen level in the experimental aquaria from the normoxic level (9 mg O_2 l^{-1}) to the hypoxic oxygen concentration of 0.9 mg O_2 l^{-1} within 3 h. Anoxia, on the other hand, was reached after 6 h of N_2 gas bubbling.

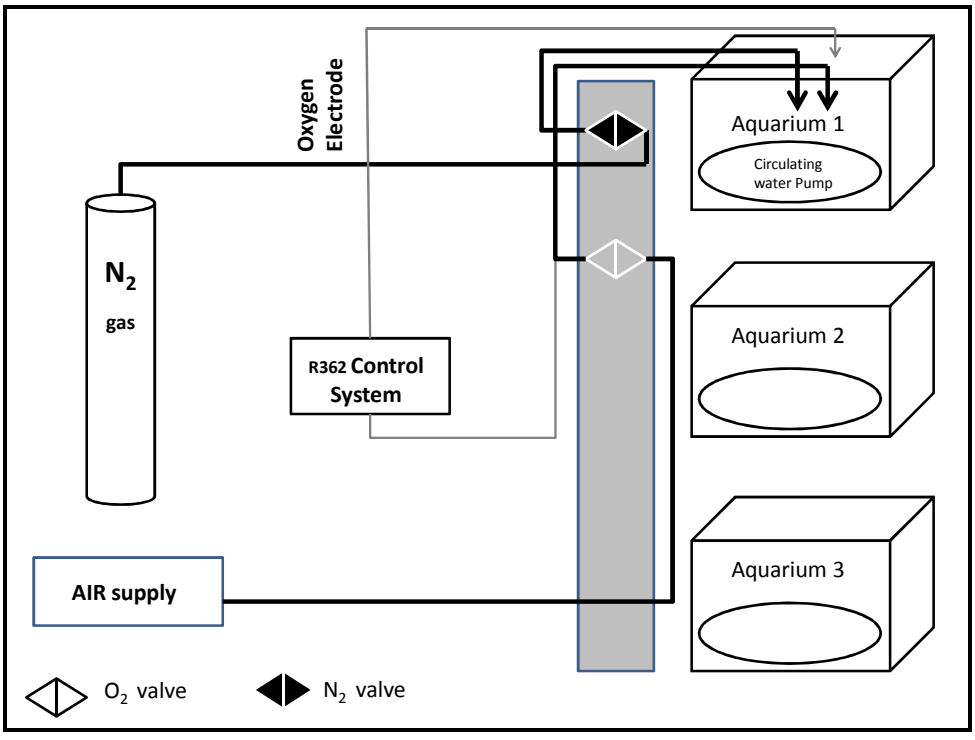

Fig. 6.1 - Schematic overview of the experimental set-up in anoxia/hypoxia experiments with common carp. The predetermined oxygen level of 0.9 mg O_2 l^{-1} (hypoxia) was controlled by opening/closing the respective valves of the R362 system for N_2 or air supply. Oxygen

concentrations were monitored continuously by two oxygen electrodes: one electrode of the R362 system and an additional WTW electrode.

In total, the experiment consisted of 7 different exposure groups with 8 fish per exposure group: a 24 h hypoxia group and a 1 week hypoxia group, combined with their respective control groups. Furthermore, we also exposed fish to 1 week of hypoxia and enabled them to recover from this hypoxic load by aerating the water gradually until normoxia was reached within 3 h, again with the corresponding control group. We also investigated the metabolic response of common carp to a complete lack of oxygen by exposing fish to 2 h of complete anoxia after anoxic conditions were reached at 5 °C. The 24 h control group was used as a reference for this anoxia group.

Each tank was sealed by a plastic lid, to avoid possible diffusion of oxygen from the air and oxygen levels were monitored every 10 minutes daily. The anoxic/hypoxic experiment started when the desired anoxic/hypoxic oxygen levels were reached.

At the end of the exposures, fish were quickly euthanized in an overdose of neutralised MS222 (1 g l^{-1}, pH 7.4, Sigma Chemical, St. Louis, MO, USA). Subsequently, brain, heart, liver and white muscle tissues were excised rapidly in this order on ice, immediately snap-frozen in liquid nitrogen and stored at -80 °C until further analysis. Additionally, water samples were collected from all exposure and control groups (except for the 2 h anoxia group) and Ca^{2+}, K^{+}, Mg^{2+} and Na^{+} concentrations were determined by ICP-MS.

6.2.3 Tissue extraction procedure: methanol/chloroform/water method (ratio 2/1/1.8)

Tissue extraction was carried out using the methanol/chloroform/water method based on the existing literature [Lin *et al.* 2007; Wu *et al.* 2008]. In the past, we tested and evaluated different extraction methods in order to select the most suited technique for ^{1}H-NMR-based metabolomics of fish extracts (paper submitted to the *Journal of Mediterranean Chemistry*). Eventually, we elected the methanol/chloroform/water extraction as a reliable and reproducible method, enabling the simultaneous detection of both the hydrophilic and the hydrophobic metabolites in a biological sample.

Frozen tissues were ground in a liquid nitrogen-cooled mortar and pestle and approximately 100 mg of homogeneous tissue powder was used for the extraction procedure [Nicholson *et*

al. 2007]. Ice cold methanol (4 ml/g of tissue; analaR normapur, min. 99.8 %, VWR, Pennsylvania, USA) and ice cold milliQ water (0.85 ml/g) were added to the powder and the homogenate was vortexed for 1 min. Polar organic solvents such as methanol were typically mixed with water to extract hydrophilic metabolites [Coen *et al.* 2003; Stentiford *et al.* 2005]. Subsequently, ice cold chloroform (4 ml/g; normapur, 99.3 %, VWR, Pennsylvania, USA) and milliQ water (2 ml/g) was added to extract the hydrophobic metabolites; the mixture was vortexed for 1 min and then incubated on ice for 10 min to partition. The supernatant was then centrifuged at 4 °C for 10 min at 2000 g, resulting in a biphasic solution. The upper polar and lower nonpolar layers were carefully removed and transferred to 15 ml sterile Falcon tubes. Subsequently, all samples were lyophilized overnight to avoid the presence of a dominant water signal in the ^{1}H-NMR spectra. Only the results of the aqueous fractions of brain, heart, liver and white muscle are discussed in the present study.

Prior to ^{1}H-NMR measurement, the polar tissue extracts were dissolved in 580 µl of sodium phosphate buffer prepared in D_2O to minimize variations in sample pH and to allow for deuterium locking, containing sodium-3-trimethylsilylpropionate (TMSP) as an internal standard (see following paragraph). Finally, the resulting samples were transferred to a 5 mm NMR tube (NE-HP5-7, Cortecnet, France) and analyzed immediately by ^{1}H-NMR.

The 50 mM sodium phosphate buffer in D_2O (99.9 atom % D) consisted of Na_2HPO_4, 33.5 mM (AnalaR Normapur); NaH_2PO_4, 16.45 mM (GPR rectapur) (all from Merck, Darmstadt, Germany); 0.1 mM TMSP (≥ 98 %, Cambridge Isotope Laboratories, MA, USA); 0.05 mM sodium azide (99 %, Acros Organics, NJ, USA). Deuterium chloride in D_2O (ClD, > 99 atom % D, 20 wt %) and sodium deuteroxide in D_2O (NaOD, > 99 atom % D, 40 wt %) (both from Acros Organics, NJ, USA) were added to achieve a pH of ~ 7.

6.2.4 ^{1}H-NMR based metabolomics of brain, heart, liver and white muscle extracts

All tissue extracts of common carp were analyzed on a Bruker Avance II-700 NMR spectrometer, operating at 700.13 MHz (Bruker Biospin, Europe), equipped with a 5 mm inverse TXI-Z probe and a BACS-60 automatic sample changer. Tuning, matching and shimming were performed automatically for each sample in order to minimize the variation due to sample manipulation.

One-dimensional ^{1}H-NMR spectra of brain, heart, liver and muscle extracts were acquired at 25 °C with a standard sequence using a 90° pulse (pulse sequence *zgpr*), a relaxation delay of

1.0 s with water presaturation, 64 scans collected into 16 k data points, a spectral width of 14 kHz and an acquisition time of 0.57 s per sample. Prior to Fourier transformation, all datasets were zerofilled to 32 k points and an exponential line broadenings of 0.3 Hz was applied as well. Finally, all spectra were phase and baseline corrected and chemical shifts were referenced to TMSP (0.0 ppm) using the Topspin software (version 2.1, Bruker Biospin).

In order to confirm the metabolite identities, the spectra were compared to in-house and public databases and, in addition, to the results of 2D NMR experiments.

Table 6.1 represents an overview of all metabolites (significant and non-significant), per tissue, that were discovered by ^{1}H-NMR in this study.

Table 6.1 - Overview of all the identified (significant and non-significant) metabolites in polar brain, heart, muscle and liver tissue extracts.

Brain	**Heart**	**Muscle**	**Liver**
Alanine	Acetate	Acetate	Lactate
(Phospho)Creatine	Alanine	Alanine	Alanine
Glucose	ATP/ADP	ATP/ADP	Aspartate
Glutamate	(Phospho)Creatine	(Phospho)Creatine	ATP/ADP
Glutamine	Glucose	Formate	Tyrosine
ATP/ADP	Lactate	Glucose	Formate
Lactate	Myo-inositol	Glutamate	Glucose
Scyllo-inositol	Scyllo-inositol	Glutamine	Glutamate
Myo-inositol	Succinate	Glycine	Glutamine
N-acetylaspartate (NAA)	Taurine	Lactate	Glycine
Phosphocholine	Valine/(Iso)Leu	Scyllo-inositol	Unidentified metabolite
Succinate	Malate	Taurine	Scyllo-inositol
Taurine		Valine/(Iso)Leu	Valine/(Iso)Leu
Valine/(Iso)Leu		Succinate	Choline
γ-amino butyric acid (GABA)			(Phospho)Creatine
			Scyllo-inositol
			Pyruvate
			Acetate
			Fumarate
			Taurine

6.2.5 Pre-processing of NMR data

The 1D spectra were converted to an appropriate format for statistical analysis by automatically segmenting each spectrum in 0.05 ppm integrated buckets between 0.5 and 10 ppm using AMIX (Analysis of Mixtures, version 3.8.5, Bruker Biospin). Buckets from 4.68 to 5.0 ppm, containing the residual water resonance, were excluded as well as the buckets from 0 to 0.5 ppm. All spectra were mean-centered and were normalized to total intensity in order to reduce the influence of concentration variability among the samples.

6.2.6 Statistical analyses

The generated bucket tables of all tissue extracts were exported as a spread sheet to Excel (Microsoft Office Excel 2007) and a two-way analysis of variance (ANOVA), followed by a Benjamini-Hochberg test [Benjamini and Hochberg 1995] to counter the effect of multiple testing, were applied in R (version 2.9.2) to identify the buckets/metabolites that differed significantly between the normoxic controls and the exposed fish. In all instances, $p < 0.05$ was used as the level of significance. Furthermore, in order to investigate whether these buckets also differed significantly between the different exposure groups, a student's t-test in Excel, followed by a Benjamini-Hochberg correction test in R were applied. In this case, $p < 0.05$ was applied as the level of statistical significance.

6.3 Results

Overall, the analyzed water quality parameters as $Ca^{2+}/K^{+}/Mg^{2+}/Na^{+}$ ions did not vary markedly between the exposed and control groups. The average values of $Ca^{2+}/K^{+}/Mg^{2+}/Na^{+}$ in the water samples were 63,047 – 3,612 – 7,259 and 30,412 mg/L respectively.

Table 6.2 represents the results of the two-way-ANOVA and Benjamini-Hochberg analysis ($p < 0.05$) in brain, heart, liver and muscle extracts following anoxic/hypoxic exposure and subsequent normoxic recovery. Metabolite concentrations that increased or decreased in comparison to their corresponding control groups are represented by '+' and '-' symbols respectively whereas the recovery capacity of common carp is presented by a '=' symbol.

One fish from the 1 week normoxic recovery group died at the end of the hypoxic exposure but no further mortality was observed throughout the complete experiment.

Table 6.2 - Dynamic behaviour of the significantly different metabolites among the various exposures (2h anoxia, 24 h and 1week hypoxia and 1 week normoxic recovery) in polar brain, heart, muscle and liver tissues, resulting from the two-way-ANOVA and Benjamini-Hochberg analysis ($p < 0.05$). Metabolite concentrations that increased, decreased or returned to control levels are indicated by '**+**', '**-**', '**=**' symbols respectively.

Metabolite	Tissue	2h A	24h H	1w H	Recov.	Metabolite	Tissue	2h A	24h H	1w H	Recov.
Acetate	Brain					**Glycine**	Brain				
	Heart		-		=		Heart				
	Liver						Liver		++	+	=
	Muscle	+		++	=		Muscle	-		(-)	=
Alanine	Brain				=	**Unidentified**	Brain				
	Heart						Heart				
	Liver	-		- -	=		Liver	+++	++++	++	=
	Muscle	+		-	=		Muscle				
Aspartate	Brain					**Lactate**	Brain	++			=
	Heart						Heart		- -		=
	Liver	++			=		Liver	+	-	- -	=
	Muscle						Muscle	++		- -	=
ATP/ADP	Brain					**NAA**	Brain				=
	Heart		-		=		Heart				
	Liver				=		Liver				
	Muscle	-		+	=		Muscle				
Glucose	Brain					**(P)Cr**	Brain				=
	Heart		- -		=		Heart				=
	Liver						Liver			(+)	=
	Muscle	-		+	=		Muscle	+		-	=
Glutamate	Brain				=	**Scyllo-inositol**	Brain				
	Heart						Heart		+++		=
	Liver						Liver		- - -		=
	Muscle	+		-	=		Muscle	-	- - - -	+	=
Glutamine	Brain				=	**Taurine**	Brain				
	Heart						Heart				
	Liver			+	=		Liver				
	Muscle			+	=		Muscle			(-)	=
Val/(Iso)Leu	Brain				=						
	Heart		-		=						
	Liver				=						
	Muscle			+	=						

6.3.1 ^{1}H-NMR spectroscopy and statistical analyses of polar brain extracts

Significantly different buckets ($p < 0.05$) between the normoxic controls and the treatment groups in brain were identified as N-acetylaspartate (NAA), lactate, myo-inositol, (phospho)creatine, glucose, alanine, phosphocholine, gamma-amino butyric acid (GABA), glutamate, glutamine, taurine, ATP and valine/(iso)leucine. The dynamic behaviour of the metabolites among the different exposure groups is shown in box plots in Figure 6.2.

The exposure of common carp to 2 h of anoxic challenge resulted in a strong increase of lactate in the anoxic group, compared to the 24 h controls.

Statistical analysis revealed no significantly changes ($p < 0.05$) in the levels of metabolites when the 24 h hypoxia group was compared to its control group. However, some trends were observed in the brain data set: glutamate ($p = 0.09$), glutamine ($p = 0.06$) and valine/(iso)leucine ($p = 0.06$) levels were lower as a consequence of 24 h hypoxia (compared to their controls). Furthermore, significant results were found when 24 h hypoxic fish were compared to 1w hypoxic samples: 1 week hypoxia induced higher levels of NAA, lactate, (phospho)creatine, glutamate, glutamine, alanine and valine/(iso)leucine in comparison to 24 h hypoxia. Statistical analysis of fish that recovered from 1 w hypoxia by 1 week normoxic reoxygenation, revealed no significantly different metabolites from either 1 w hypoxia or the 2 w controls. Again, when recovered fish were compared to the 2 w controls, no significant differences were found, indicating that common carp were able to restore metabolites that were altered during anoxia/hypoxia. Overall, very little changes were observed in common carp brain during hypoxia.

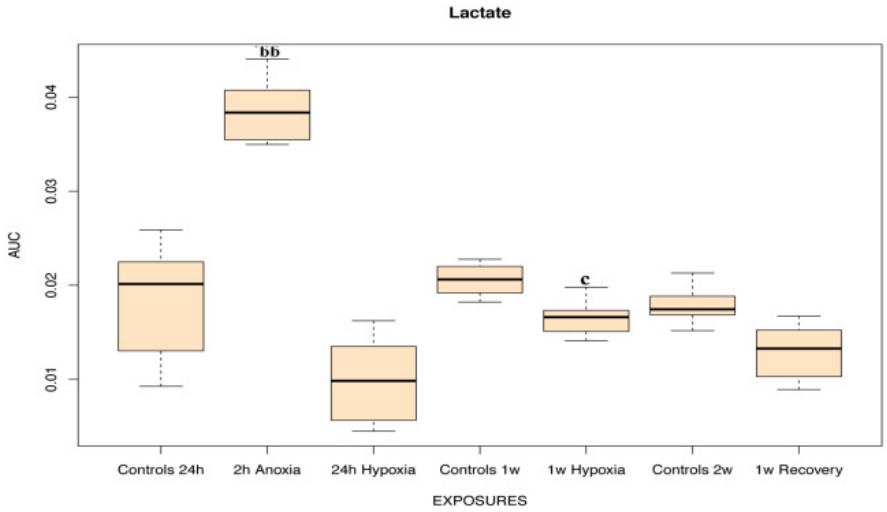
Lactate
AUC
0.01
0.02
0.03
0.04
bb
c
Controls 24h
2h Anoxia
24h Hypoxia
Controls 1w
1w Hypoxia
Controls 2w
1w Recovery
EXPOSURES

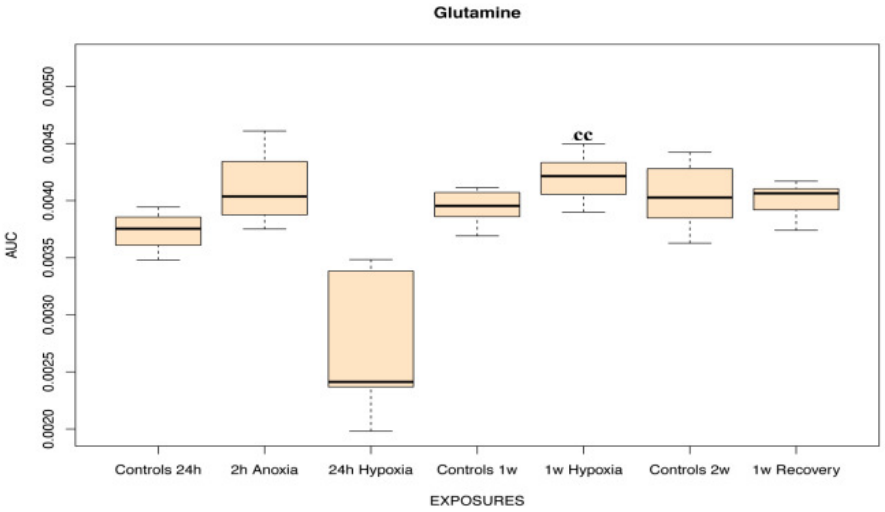
Glutamine
AUC
0.0020
0.0025
0.0030
0.0035
0.0040
0.0045
0.0050
cc
Controls 24h
2h Anoxia
24h Hypoxia
Controls 1w
1w Hypoxia
Controls 2w
1w Recovery
EXPOSURES

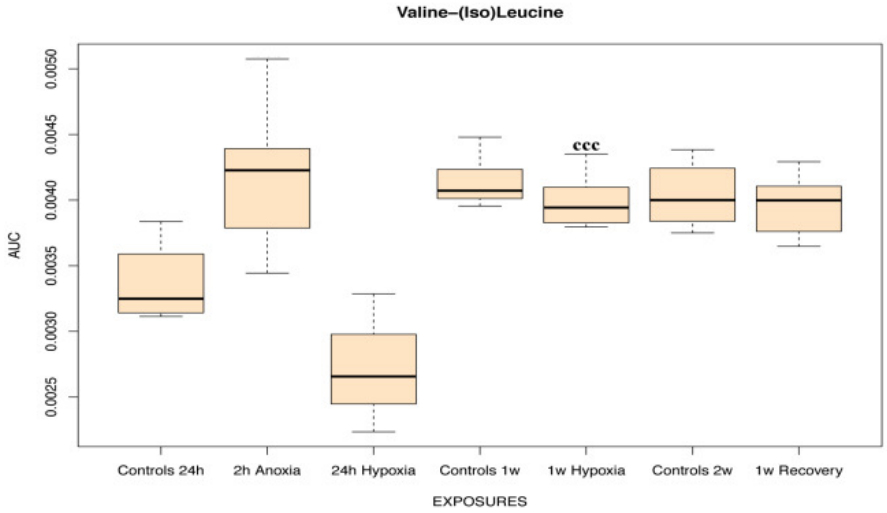
Valine–(Iso)Leucine
AUC
0.0025
0.0030
0.0035
0.0040
0.0045
0.0050
ccc
Controls 24h
2h Anoxia
24h Hypoxia
Controls 1w
1w Hypoxia
Controls 2w
1w Recovery
EXPOSURES

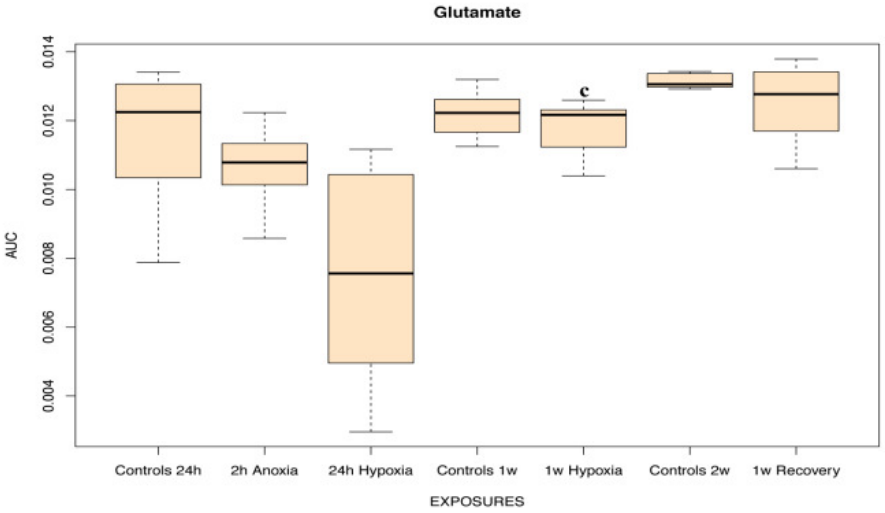
Glutamate
AUC
0.004
0.006
0.008
0.010
0.012
0.014
c
Controls 24h
2h Anoxia
24h Hypoxia
Controls 1w
1w Hypoxia
Controls 2w
1w Recovery
EXPOSURES

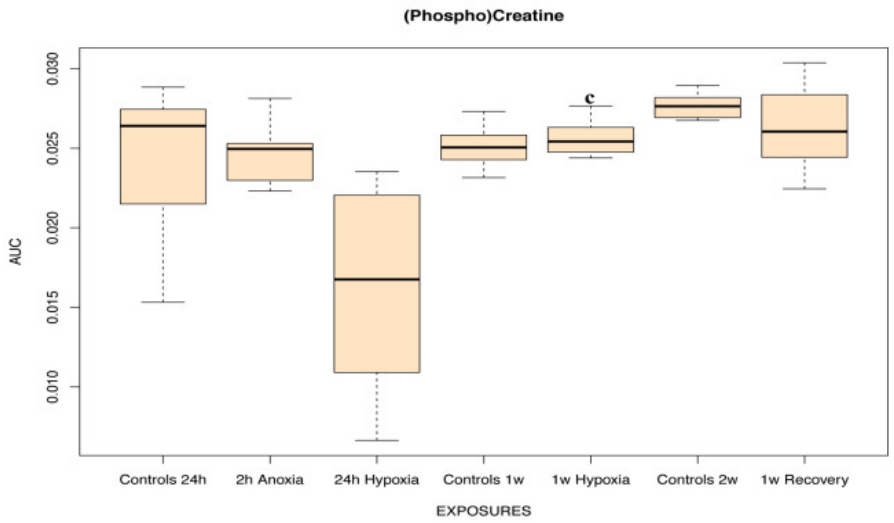

Figure 6.2 – Box plots of polar brain data to visualize the metabolites that differed significantly ($p < 0.05$) between the exposure groups and their corresponding controls (a: $p < 0.05$; aa: $p < 0.01$; aaa: $p < 0.001$), between the 2h anoxia group and the 24h controls (b: $p < 0.05$; bb: $p < 0.01$; bbb: $p < 0.001$) and between the 24h and the 1w hypoxic fish (c: $p < 0.05$; cc: $p < 0.01$; ccc: $p < 0.001$). The vertical axis of each box plot represents the Area Under the Curve (AUC) intensities. The horizontal axis displays the 7 experimental groups: 24h normoxic controls (N=8), 2h anoxia (N=8), 24h hypoxia (N7), 1w normoxic controls (N=8), 1w hypoxia (N=8), 2w normoxic controls (N=8) and 1w normoxic recovery following 1w hypoxia (N=7).

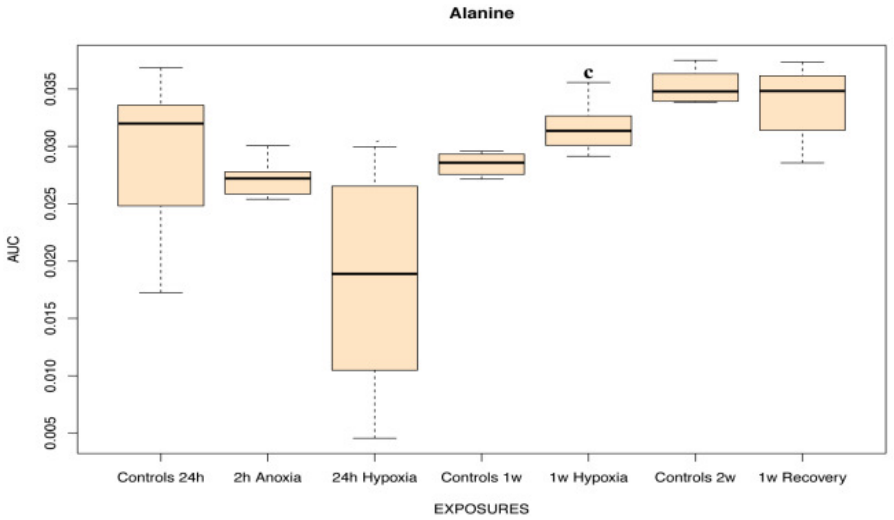

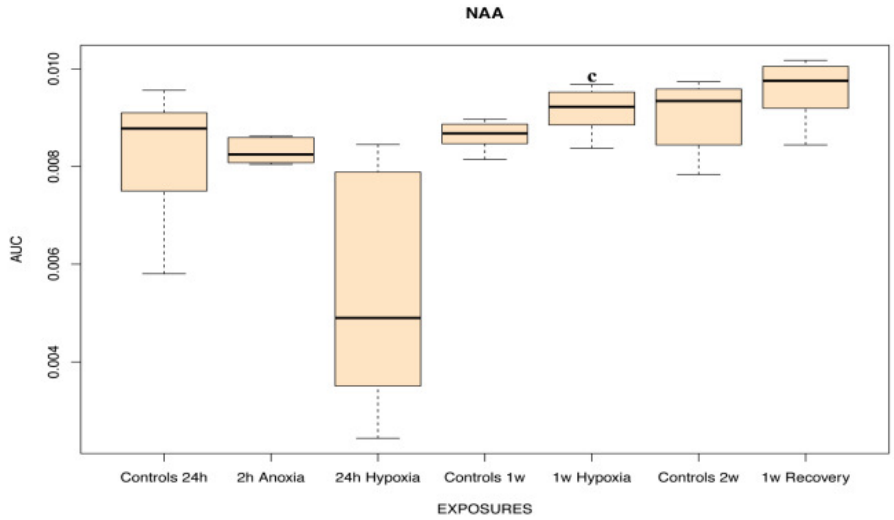

6.3.2 ^{1}H-NMR spectroscopy and statistical analyses of polar heart extracts

The ANOVA and Benjamini-Hochberg analysis identified the buckets, accounting for the significant differences between the controls and the exposed fish, as valine/(iso)leucine, acetate, scyllo-inositol, lactate, glucose, (phospho)creatine, myo-inositol, alanine and ATP/ADP. Figure 6.3 demonstrates the box plots of all significantly different metabolites in heart extracts.

In 2 h anoxic fish, no significantly different metabolites were detected when compared to their 24 h controls. In contrast, 24 h hypoxia induced a firm increase in the levels of scyllo-inositol (compared to the 24 h controls) and a decrease in acetate, lactate, glucose, ATP/ADP and valine/(iso)leucine concentrations. The levels of scyllo-inositol in 24 h hypoxic fish were notably higher in comparison to the 1 w hypoxia group whereas the levels of acetate, glucose, (phospho)creatine, ATP/ADP and valine/(iso)leucine were lower. No significantly different metabolites were observed in the spectra of 1 week hypoxic fish, compared to the spectral data of their controls, although there was a trend observed for scyllo-inositol to increase following 1w of hypoxia ($p = 0.09$).

The statistical comparative analysis of 1 week hypoxic fish and fish that were allowed to recover during 1 week of normoxia, demonstrated no significantly changing metabolites. Also, when the recovered group was then compared to their 2 w controls, no significantly metabolite changes were found. All these results suggest that common carp hearts are able to fully acclimatize to 1 w hypoxia, with or without recovery.

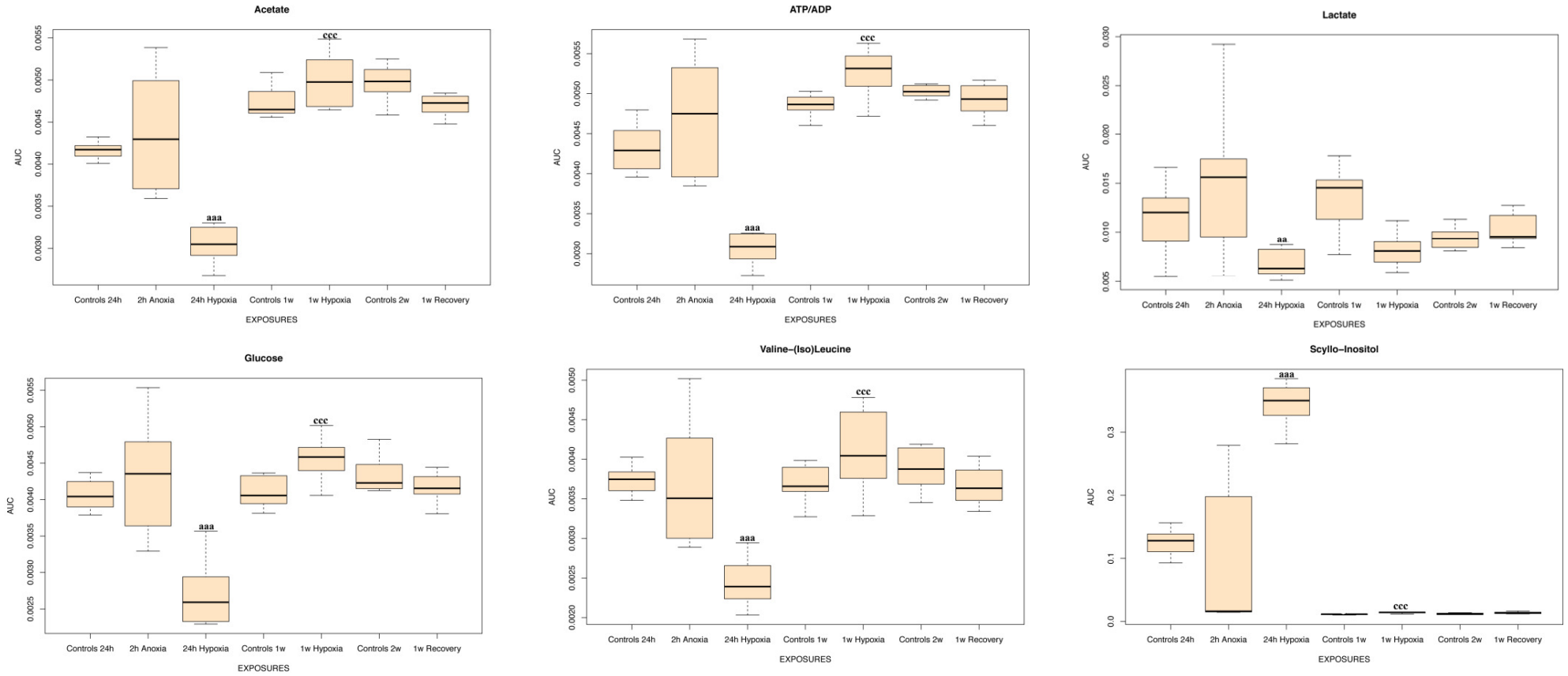

Figure 6.3 - Box plots of polar heart data to visualize the metabolites that differed significantly ($p < 0.05$) between the exposure groups and their corresponding controls (a: $p < 0.05$; aa: $p < 0.01$; aaa: $p < 0.001$), between the 2h anoxia group and the 24h controls (b: $p < 0.05$; bb: $p < 0.01$; bbb: $p < 0.001$) and between the 24h and 1w hypoxic fish (c: $p < 0.05$; cc: $p < 0.01$; ccc: $p < 0.001$). The vertical axis of each box plot represents the Area Under the Curve (AUC) intensities. The horizontal axis displays the 7 experimental groups: 24h normoxic controls (N=8), 2h anoxia (N=8), 24h hypoxia (N=8), 1w normoxic controls (N=7), 1 week hypoxia (N=8), 2w normoxic controls (N=8) and 1w normoxic recovery following 1w hypoxia (N=7).

6.3.3 ^{1}H-NMR spectroscopy and statistical analyses of polar liver extracts

In liver extracts, ATP/ADP, an unidentified metabolite, glucose, valine/(iso)leucine, alanine, scyllo-inositol, (phospho)creatine, glutamate, glutamine, glycine, aspartate and lactate were identified as being significant for the difference between controls and exposed fish. Figure 6.4 shows an overview of the box plots of all significantly different metabolites.

Anoxia resulted (compared to the 24 h controls) in a decrease of alanine and a notably increase of an unidentified metabolite, aspartate and lactate. Furthermore, a trend for ATP/ADP (p = 0.09) was seen by its decreased concentration after anoxia treatment (compared to the 24 h controls).

A significantly decrease in scyllo-inositol was noticed in the 24 h hypoxic fish in relation to the 24 h controls while a strong increase in an unidentified compound and glycine was present. In addition, a trend was noticed for valine/(iso)leucine (p = 0.09), (phospho)creatine (p = 0.07), glutamate (p = 0.08) and lactate (p = 0.09) which displayed lower levels in 24 h hypoxic fish, compared to the controls.

Compared to the controls, one week hypoxia resulted in an increase of the unidentified metabolite, glycine, (phospho)creatine and glutamine; with the unknown metabolite, alanine, glycine and lactate being lower than after 24 h of hypoxia. For aspartate, a trend was observed (p = 0.09), showing increased levels after 1w of hypoxia (in relation to the 1w controls). Oppositely, alanine and lactate decreased in the 1 w hypoxic group (compared to the 1 w controls) with ATP/ADP, (phospho)creatine, valine/(iso)leucine, glutamine and aspartate being higher than after 24 h of hypoxia.

Likewise to the observations in brain and heart extracts, no significantly different metabolite concentrations were found for the 1 w hypoxic group when compared to the 2 w controls. This might again indicate that 1 week normoxic recovery enabled common carp to reassure the (levels of the) metabolites that changed as a consequence of anoxic and/or hypoxic perturbation.

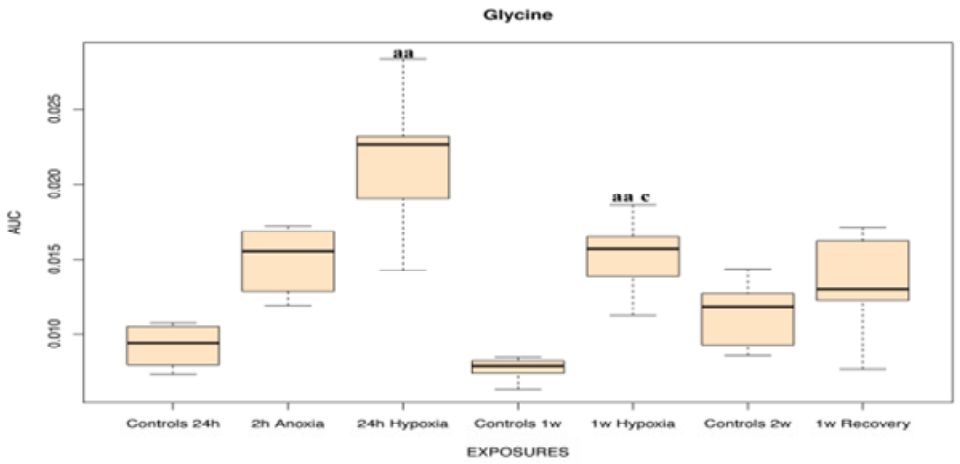
Glycine
AUC
0.010
0.015
0.020
0.025
aa
aa c
Controls 24h
2h Anoxia
24h Hypoxia
Controls 1w
1w Hypoxia
Controls 2w
1w Recovery
EXPOSURES

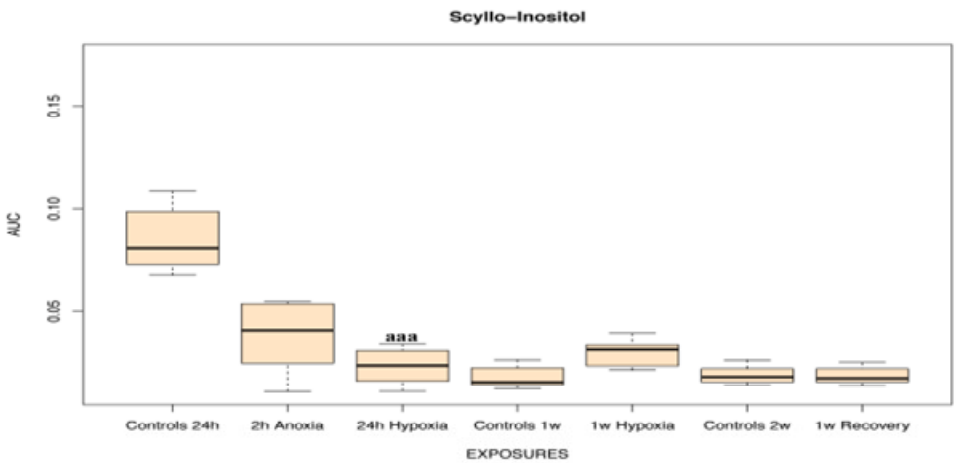
Scyllo-Inositol
AUC
0.05
0.10
0.15
aaa
Controls 24h
2h Anoxia
24h Hypoxia
Controls 1w
1w Hypoxia
Controls 2w
1w Recovery
EXPOSURES

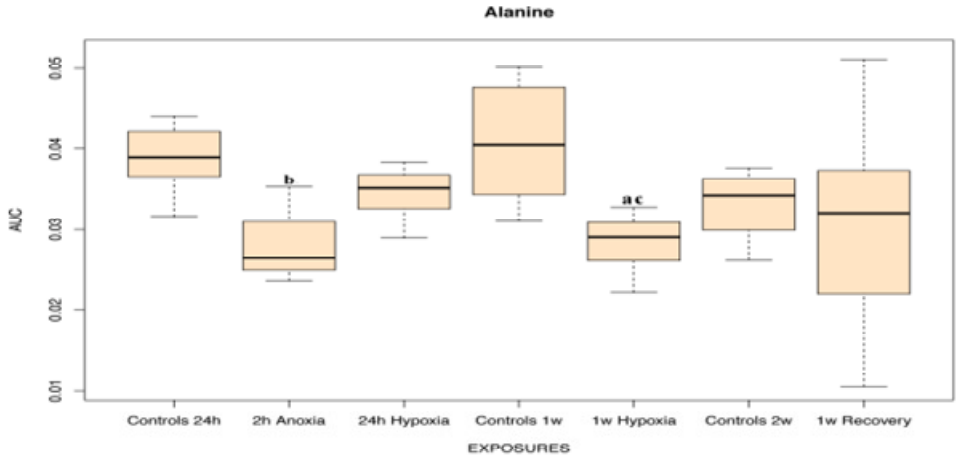
Alanine
AUC
0.01
0.02
0.03
0.04
0.05
b
ac
Controls 24h
2h Anoxia
24h Hypoxia
Controls 1w
1w Hypoxia
Controls 2w
1w Recovery
EXPOSURES

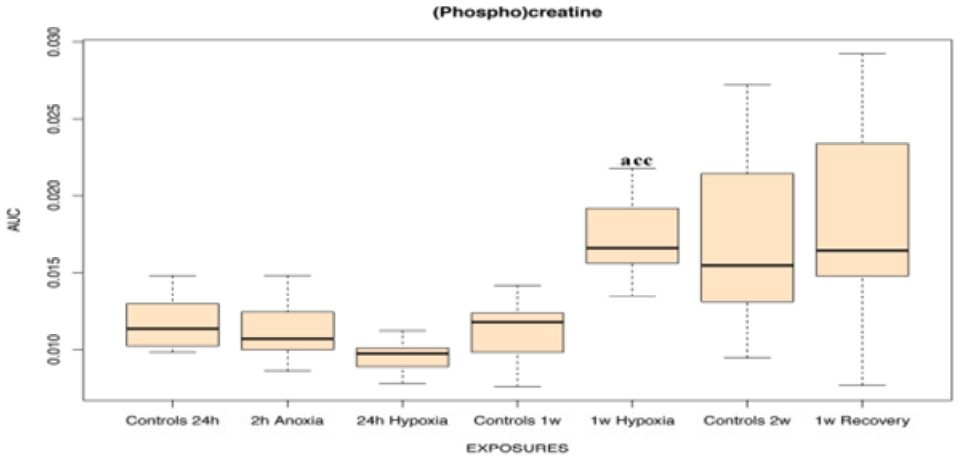
(Phospho)creatine
AUC
0.010
0.015
0.020
0.025
0.030
acc
Controls 24h
2h Anoxia
24h Hypoxia
Controls 1w
1w Hypoxia
Controls 2w
1w Recovery
EXPOSURES

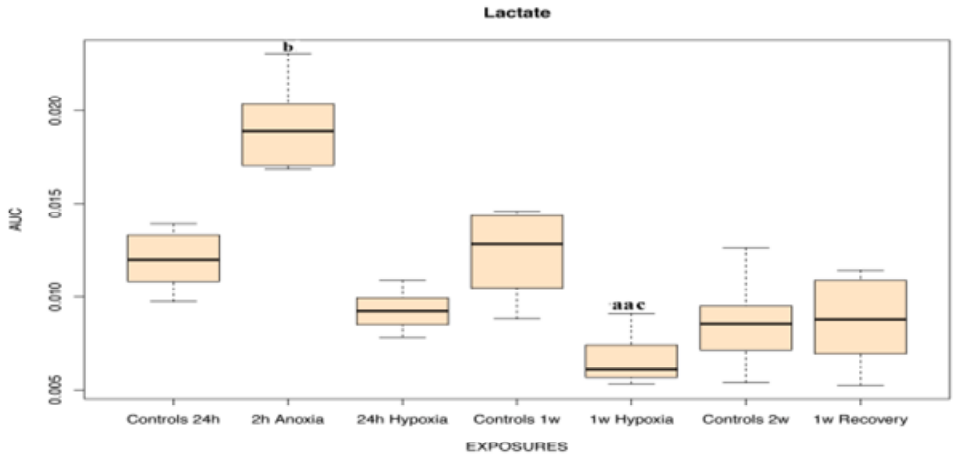
Lactate
AUC
0.005
0.010
0.015
0.020
b
a a c
Controls 24h
2h Anoxia
24h Hypoxia
Controls 1w
1w Hypoxia
Controls 2w
1w Recovery
EXPOSURES

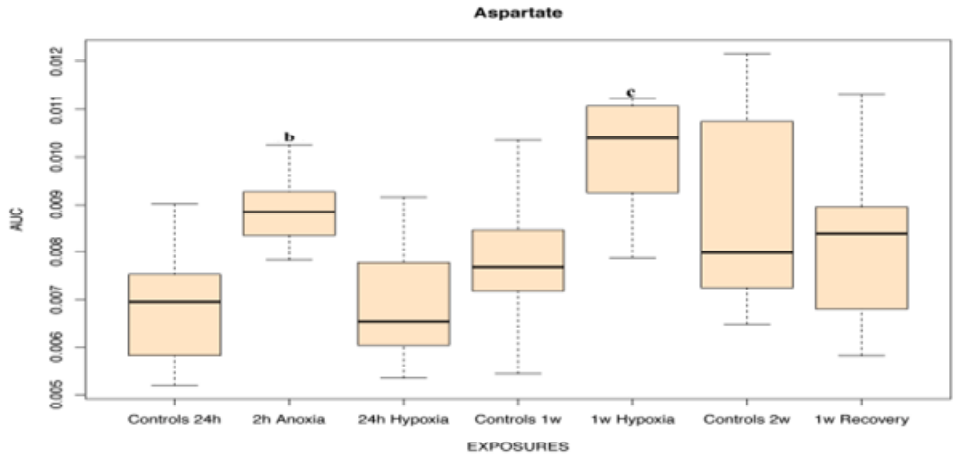
Aspartate
AUC
0.005
0.006
0.007
0.008
0.009
0.010
0.011
0.012
b
c
Controls 24h
2h Anoxia
24h Hypoxia
Controls 1w
1w Hypoxia
Controls 2w
1w Recovery
EXPOSURES

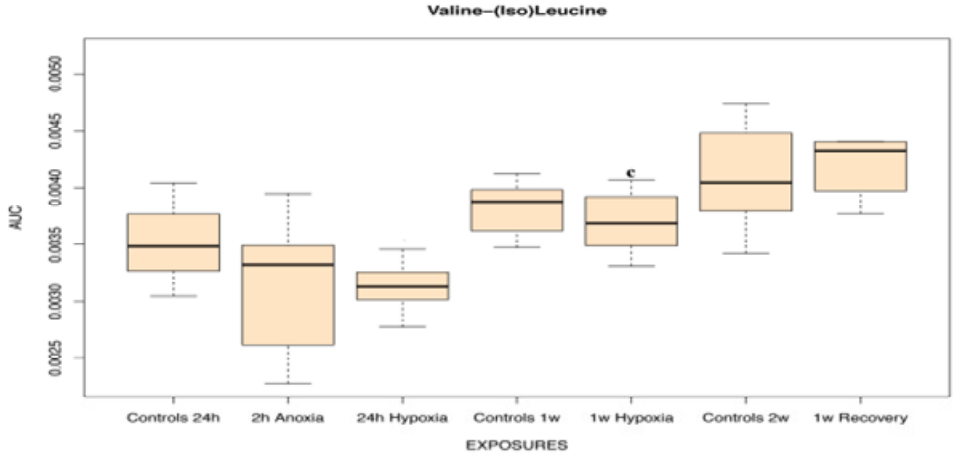
Valine−(Iso)Leucine
AUC
0.0025
0.0030
0.0035
0.0040
0.0045
0.0050
c
Controls 24h
2h Anoxia
24h Hypoxia
Controls 1w
1w Hypoxia
Controls 2w
1w Recovery
EXPOSURES

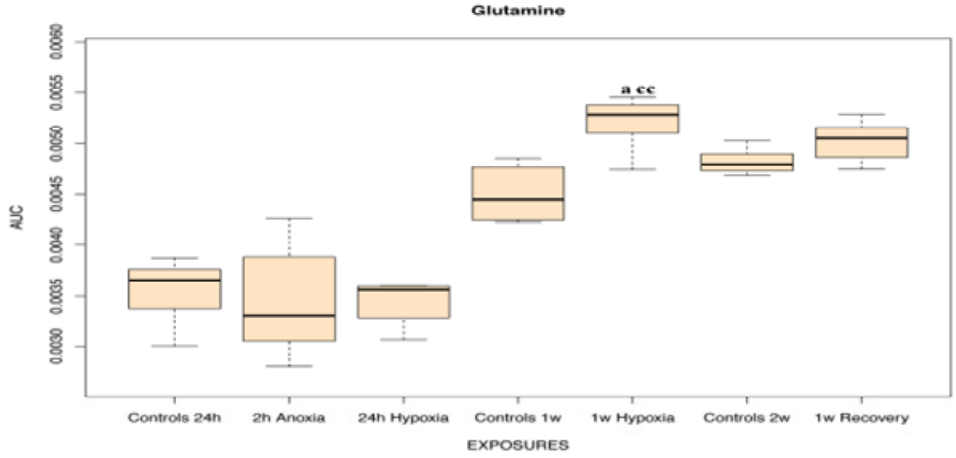
Glutamine
AUC
0.0030
0.0035
0.0040
0.0045
0.0050
0.0055
0.0060
a c c
Controls 24h
2h Anoxia
24h Hypoxia
Controls 1w
1w Hypoxia
Controls 2w
1w Recovery
EXPOSURES

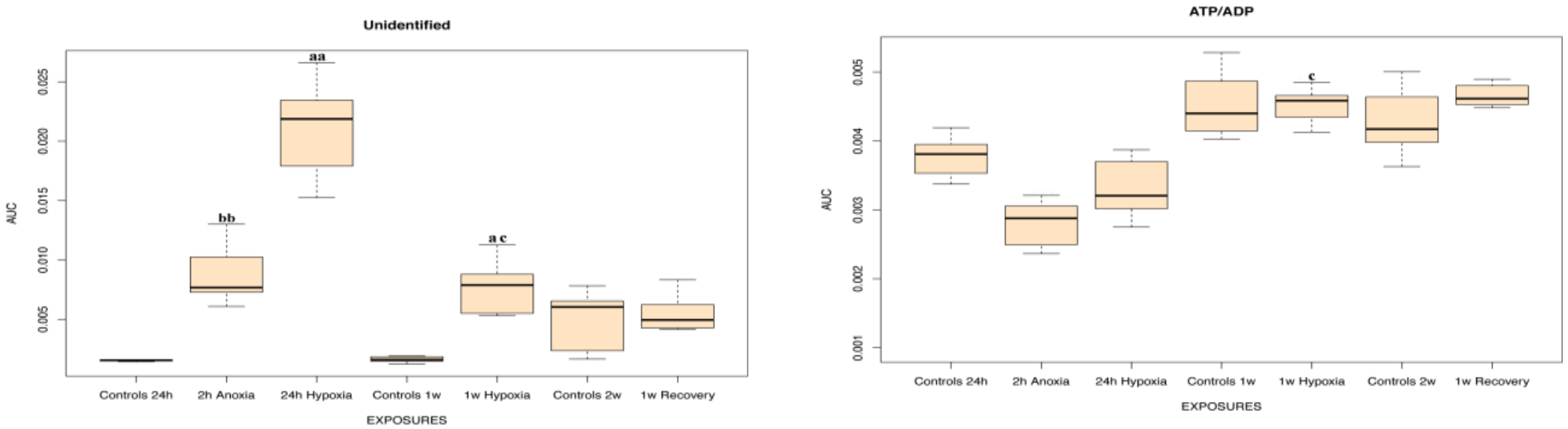

Figure 6.4 - Box plots of polar liver data to visualize the metabolites that differed significantly ($p < 0.05$) between the exposure groups and respective controls (a: $p < 0.05$; aa: $p < 0.01$; aaa: $p < 0.001$), between the 2h anoxia group and the 24h controls (b: $p < 0.05$; bb: $p < 0.01$; bbb: $p < 0.001$), between the 24h and 1w hypoxic fish (c: $p < 0.05$; cc: $p < 0.01$; ccc: $p < 0.001$). The vertical axis of each box plot represents the Area Under the Curve (AUC) intensities. The horizontal axis displays the 7 experimental groups: 24h normoxic controls (N=8), 2h anoxia (N=8), 24h hypoxia (N=7), 1w normoxic controls (N=8), 1 week hypoxia (N=7), 2w normoxic controls (N=7) and 1w normoxic recovery following 1w hypoxia (N=7).

6.3.4 ^{1}H-NMR spectroscopy and statistical analyses of polar white muscle extracts

ANOVA and Benjamini-Hochberg analysis revealed the subsequent significant differences in metabolites: acetate, glutamine, glutamate, (phospho)creatine, lactate, ATP/ADP, glucose, alanine, valine/(iso)leucine, scyllo-inositol, taurine and glycine. Figure 6.5 shows the significant metabolites by their box plots.

In contrast to heart muscle, where no effects of 2 h anoxia were observed, anoxia exposure of white muscle resulted in a decrease in ATP/ADP, glucose, scyllo-inositol and glycine when compared to its control group. Additionally, anoxia caused an increase in acetate, glutamate, glutamine, (phospho)creatine, alanine and a strong increase in lactate.

A 24 h hypoxic load markedly decreased the levels of scyllo-inositol in white muscle tissue, compared to the 24 h controls. Additionally, a trend was observed for acetate (p = 0.08), glucose (p = 0.09) which increased after 24 h of hypoxia while valine/(iso)leucine (p = 0.06) decreased (compared to the 24 h controls).

Compared to the controls, one week hypoxia resulted in an increase of acetate, glutamine, ATP/ADP, glucose, valine/(iso)leucine and scyllo-inositol; with valine/(iso)leucine being higher than after 24 h of hypoxia. Oppositely, the concentrations of glutamate, (phospho)creatine, lactate, alanine, taurine and glycine decreased in the 1 w hypoxic group, compared to the controls.

The comparison of 1 week recovered fish with the 2 w controls and the 1 w hypoxia group resulted in no significantly different metabolites which may suggest again that common carp were able to recover completely from a long-term hypoxic exposure within 1 week.

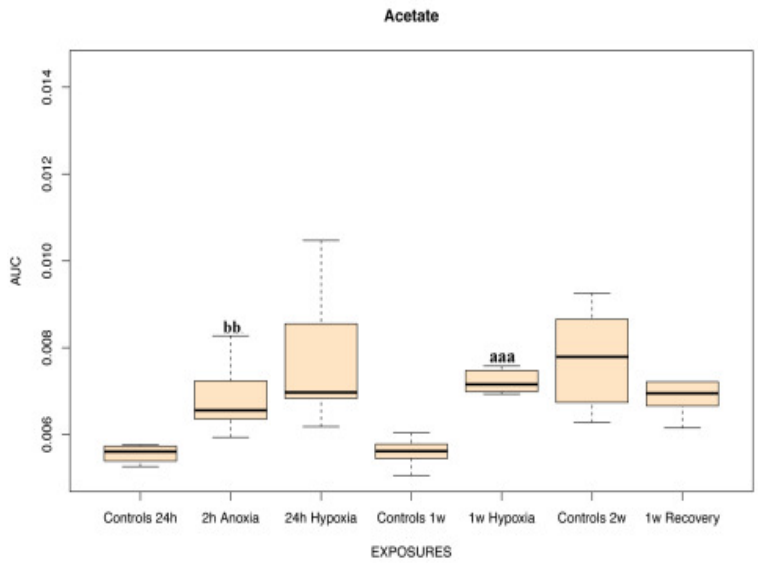
Acetate
AUC
0.006
0.008
0.010
0.012
0.014
bb
aaa
Controls 24h
2h Anoxia
24h Hypoxia
Controls 1w
1w Hypoxia
Controls 2w
1w Recovery
EXPOSURES

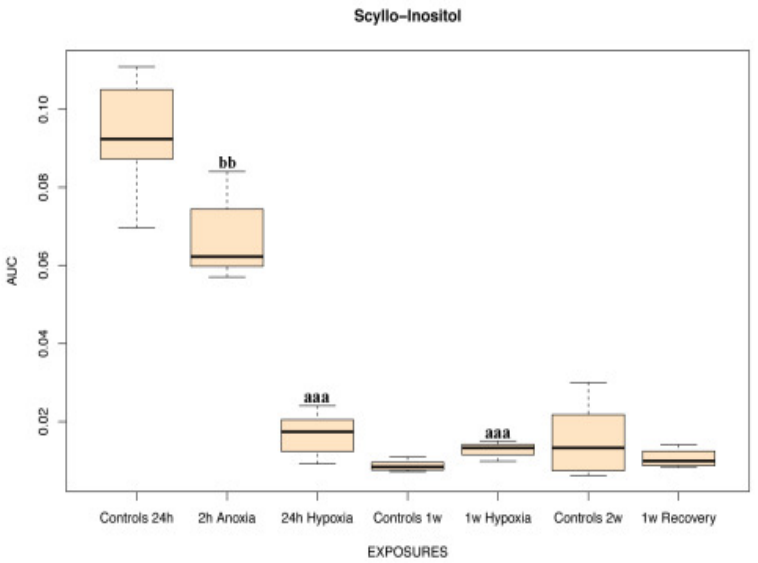
Scyllo-Inositol
AUC
0.02
0.04
0.06
0.08
0.10
bb
aaa
aaa
Controls 24h
2h Anoxia
24h Hypoxia
Controls 1w
1w Hypoxia
Controls 2w
1w Recovery
EXPOSURES

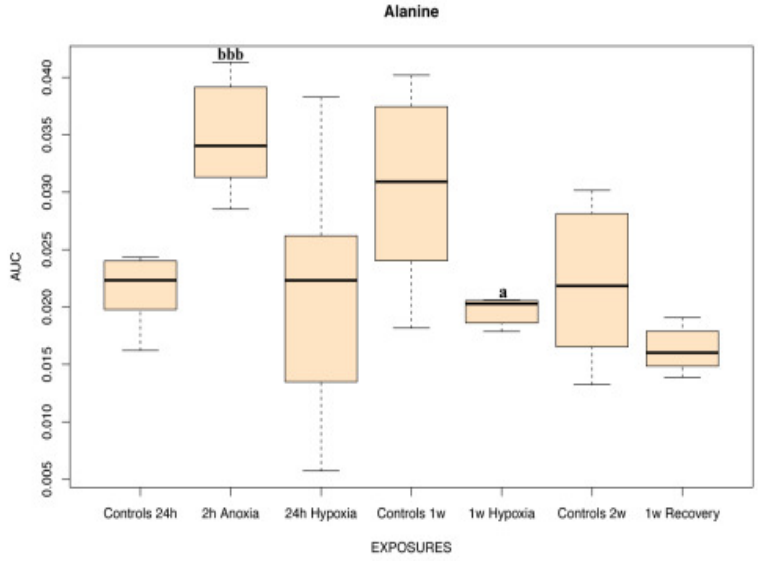
Alanine
AUC
0.005
0.010
0.015
0.020
0.025
0.030
0.035
0.040
bbb
a
Controls 24h
2h Anoxia
24h Hypoxia
Controls 1w
1w Hypoxia
Controls 2w
1w Recovery
EXPOSURES

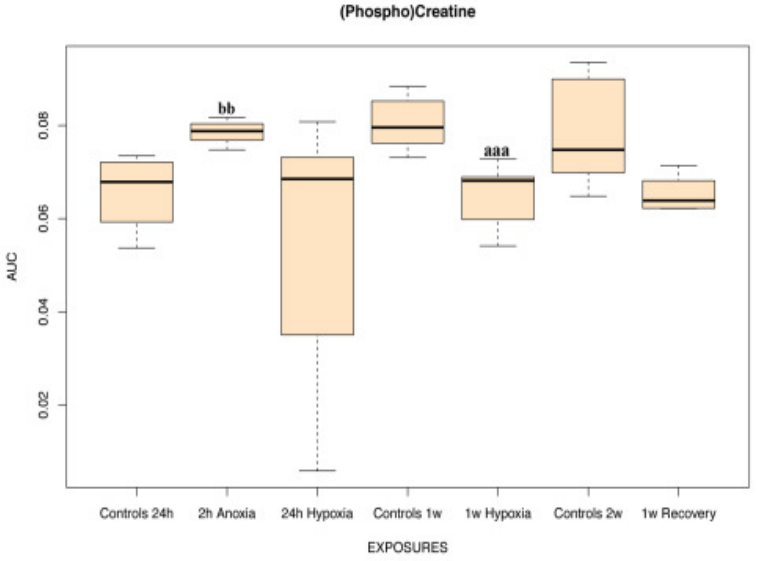
(Phospho)Creatine
AUC
0.02
0.04
0.06
0.08
bb
aaa
Controls 24h
2h Anoxia
24h Hypoxia
Controls 1w
1w Hypoxia
Controls 2w
1w Recovery
EXPOSURES

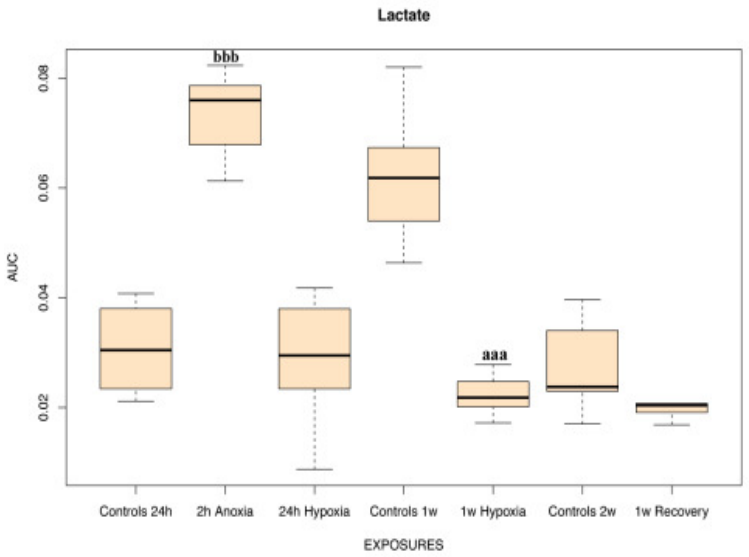
Lactate
AUC
0.02
0.04
0.06
0.08
bbb
aaa
Controls 24h
2h Anoxia
24h Hypoxia
Controls 1w
1w Hypoxia
Controls 2w
1w Recovery
EXPOSURES

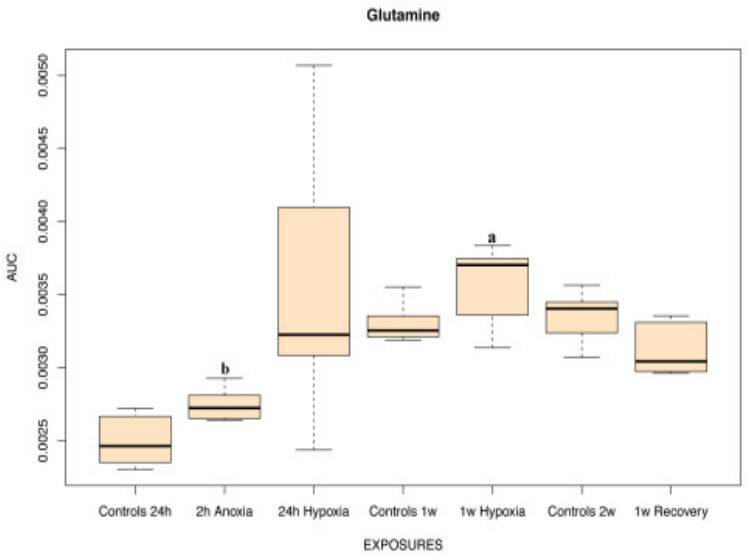
Glutamine
AUC
0.0025
0.0030
0.0035
0.0040
0.0045
0.0050
b
a
Controls 24h
2h Anoxia
24h Hypoxia
Controls 1w
1w Hypoxia
Controls 2w
1w Recovery
EXPOSURES

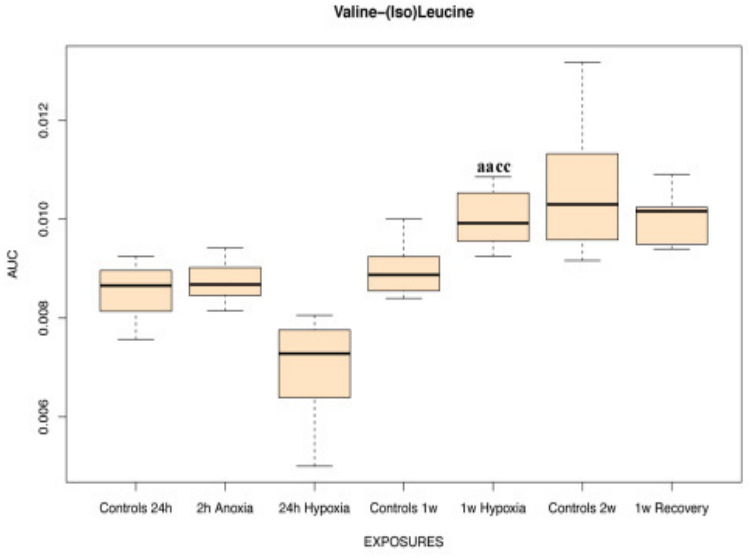
Valine–(Iso)Leucine
AUC
0.006
0.008
0.010
0.012
aacc
Controls 24h
2h Anoxia
24h Hypoxia
Controls 1w
1w Hypoxia
Controls 2w
1w Recovery
EXPOSURES

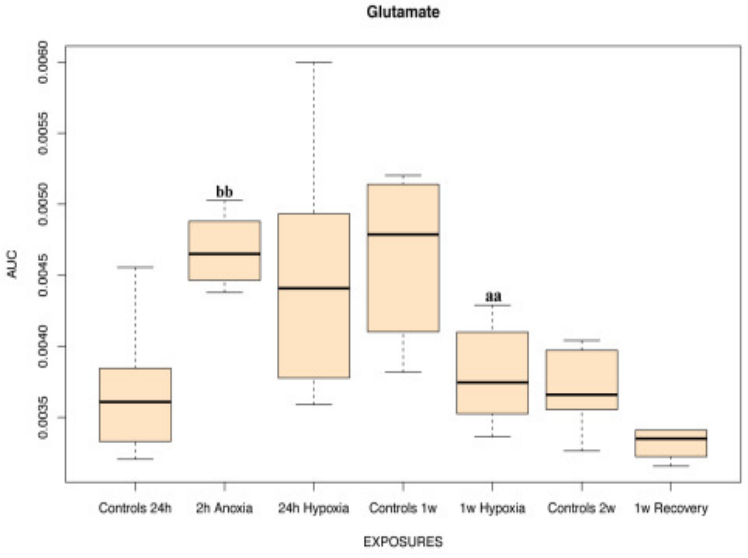
Glutamate
AUC
0.0035
0.0040
0.0045
0.0050
0.0055
0.0060
bb
aa
Controls 24h
2h Anoxia
24h Hypoxia
Controls 1w
1w Hypoxia
Controls 2w
1w Recovery
EXPOSURES

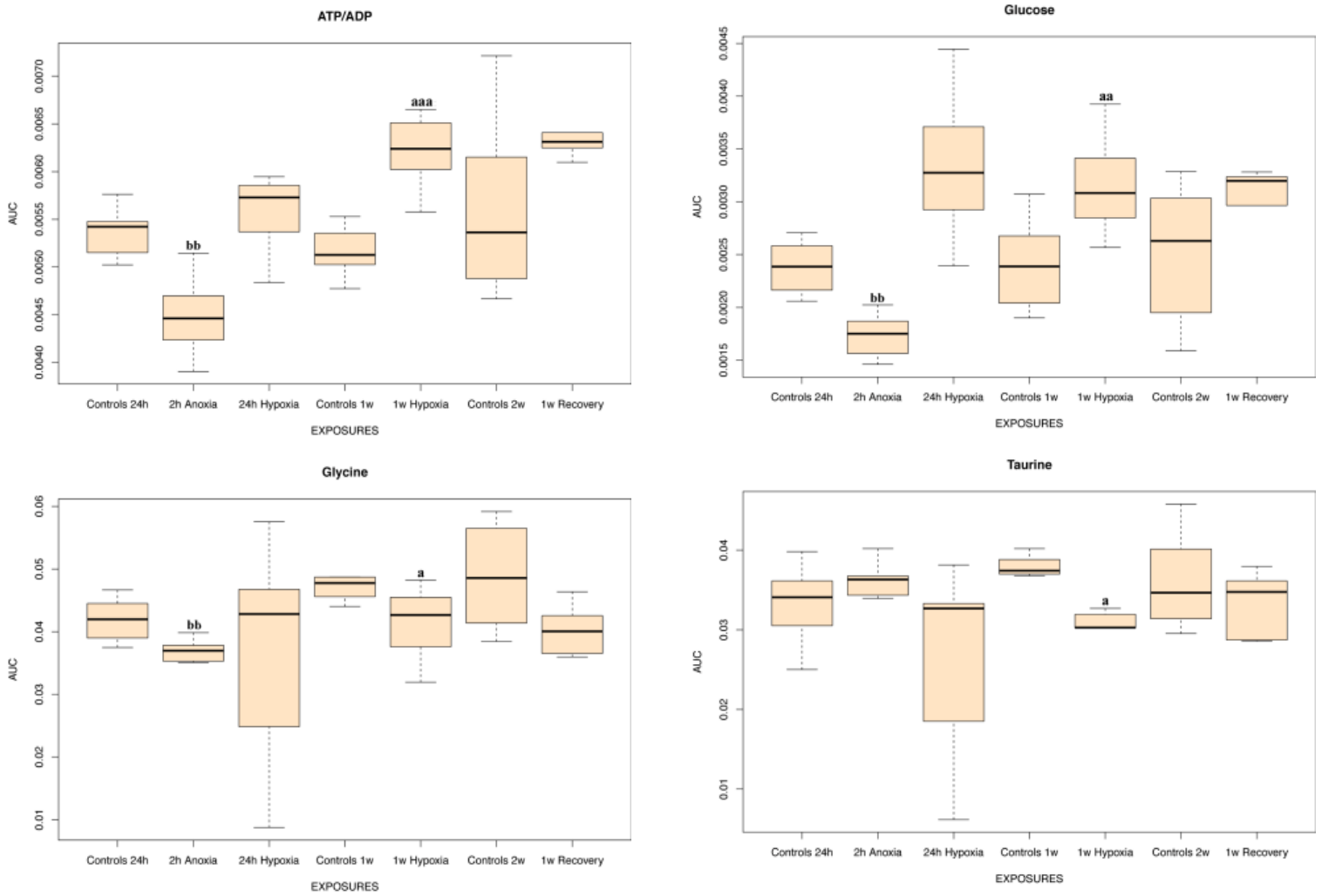

Figure 6.5 - Box plots of polar white muscle data to visualize the metabolites that differed significantly ($p < 0.05$) between the exposure groups and their corresponding controls (a: $p < 0.05$; aa: $p < 0.01$; aaa: $p < 0.001$), between the 2h anoxia group and the 24h controls (b: $p < 0.05$; bb: $p < 0.01$; bbb: $p < 0.001$) and between the 24h and 1w hypoxic fish (c: $p < 0.05$; cc: $p < 0.01$; ccc: $p < 0.001$). Exposure groups: 24h normoxic controls (N=8), 2h anoxia (N=7), 24h hypoxia (N=8), 1w normoxic controls (N=8), 1 week hypoxia (N=7), 2w normoxic controls (N=8) and 1w normoxic recovery following 1w hypoxia (N=6).

6.4 Discussion

6.4.1 General energy metabolites

In all tissues except for the heart, anoxic exposure during 2 h resulted in a strong increase in lactate levels. This firm lactate increase is not surprising since the absence of oxygen forces common carp to switch to anaerobic glycolysis, resulting in an accumulation of lactate. Strikingly, there was no significant increase in cardiac lactate levels following anoxia. As indicated by a previous study [Tota *et al.* 2011], the common carp significantly depresses its cardiac activity when exposed to anoxia and/or hypoxia whereas its relative, the crucian carp, maintains normal cardiac performance and autonomic cardiovascular control for at least 5 days of anoxia at 8 °C [Steyck *et al.* 2004]. The depressed cardiac activity in anoxic common carp sustains the reduction of the whole-animal metabolic rate, ensuring a low myocardial ATP demand apparently below the cardiac glycolytic capacity to provide ATP [Tota *et al.* 2011]. Secondly, the absence of increased lactate levels in the heart extracts can be explained by its role in cardiac energy metabolism. In contrast to the brain, which relies almost exclusively on glucose for oxidative ATP supply, the heart uses a wide range of substrates for energy production [Chatham 2002]. Particularly in cardiac tissue, where energy demand is high and continuous, it is of essential importance to maintain a balance between energy demand and supply. Concretely, the substrates that are used for cardiac energy production include glucose, fatty acids, ketone bodies, lactate and pyruvate. As generally stated, the predominant fuels for energy production *in vivo* are long chain fatty acids and glucose [Neely and Morgan 1974]. Despite the evidence that lactate may be an important fuel in myocardial energy metabolism, there is remarkably little information about the interactions between lactate and glucose utilization or lactate and fatty acid oxidation. Chatham and co-workers investigated the cardiac glucose uptake and phosphorylation in humans at rest and at three different exercise intensities. They concluded that following a high intensity exercise, other substrates than glucose, e.g. lactate, can contribute significantly to the cardiac energy production [Chatham 2002]. The results were supported by a negative correlation between serum lactate levels and glucose uptake at moderate exercise intensity. In addition, Kemppainen et al. illustrated that the regulation of substrate selection by the myocardium is a dynamic process: the contributing role of various substrates to energy supply changes according to the physiological environment [Kemppainen *et al.* 2002]. In this study, cardiac lactate levels might have contributed to myocardial energy production following anoxia, restoring the balance between energy supply and demand.

Contrastingly, short-and long term hypoxia induced a decrease in lactate concentrations in all tissues except for the brain. The reduced extent to which lactate is accumulated after 1 day and 1 week hypoxia might be explained by the strategy of metabolic depression. By suppressing the ATP consumption/turnover, a more economized use of energy is applied in periods of limited oxygen availabilities, thereby minimizing the accumulation of lactate and hence, metabolic acidosis [Zhou 2000]. Another explanation for the hypoxia-induced decreased lactate levels may be found in the Cori cycle. Although it is generally stated that the Cori cycle is of little importance in certain fish species [Milligan and Pagnotta 1991; Tang and Boutilier 1991; Jobling 1994], the observed decreased lactate levels in hypoxic common carp tissues can be due to its conversion into glycogen. The metabolic Cori cycle starts with the reconversion of lactate into pyruvate in liver tissue and pyruvate is then converted to glucose and stored as glycogen in liver and/or muscle (gluconeogenesis) [Voet 1995]. This might clarify the decreased lactate levels in the examined tissues.

Besides the depletion of glycogen stores, vertebrates can generally respond to fluctuating oxygen levels by adjusting their phosphocreatine stores in different tissues, particularly in white muscle and liver. That way, the synthesis of cellular ATP is guaranteed by the process of phosphocreatine hydrolysis [Hallman *et al.* 2008]. In this study, the presence of very fluctuating tissue responses of liver and muscle (phospho)creatine to anoxia/hypoxia exposure can be explained by the way the spectra were bucketed. Briefly, each spectrum was automatically segmented in 0.05 ppm integrated spectral regions (bins or buckets) between 0.5 and 10 ppm. Concerning phosphocreatine and creatine, both resonances are positioned approximately next to each other and are often considered as one for subsequent statistical analysis. In this case, a decrease of phosphocreatine possibly occurred associated with an increase in creatine but do to the shared location of the peaks of both metabolites, statistical analysis was unable to reveal the commonly expected results. It might be suggested that anoxia/hypoxia probably induce a decrease in phosphocreatine levels by donating the phosphate group to ADP to provide ATP energy whereas creatine levels will rise accordingly. In this study, anoxia exposure only influenced the (phospho)creatine levels in muscle: an increased concentration was noticed in comparison to the 24h controls. Furthermore, 1 week hypoxia decreased the (phospho)creatine levels in muscle in contrast to the observed increase in liver, compared to the 1w controls.

The levels of ATP/ADP following anoxic and hypoxic treatment differed throughout the four examined tissues. In brain, neither anoxia nor hypoxia changed the concentrations of

ATP/ADP levels significantly. This might illustrate the capacity of common carp to conserve a relatively constant level of these brain energy compounds throughout periods of oxygen stress. Possibly, if hypoxic or anoxic stresses do not alter ATP levels, it can be assumed that metabolic suppression is occurring in the brain of common carp [Hallman *et al.* 2008]. In muscle, anoxia induced a decrease of ATP/ADP stores as a consequence of the inhibited oxidative phosphorylation to provide energy. One week hypoxia, on the other hand, increased the levels of ATP/ADP in comparison to the controls. However, a complete recovery of ATP/ADP was observed in this tissue, suggesting that recovered fish re-established their energy stores by synthezing ATP through oxidative phosphorylation.

6.4.2 Amino acids and neurotransmitters

In brain, significant changes in the levels of N-acetylaspartate (NAA) were solely detected when 24 h hypoxic fish were compared to 1w hypoxic samples whereby the highest NAA-concentrations were observed in the 1w hypoxic group. Since no significantly differences were found in the NAA-levels of 24 h and 1 w hypoxic samples (in comparison to their controls), no straightforward explanation can be provided for the higher concentrations of NAA in 1 w hypoxic fish (compared to the 24 h hypoxia group).

Remarkably, 2 h anoxia did not change the levels of brain NAA in common carp. This is in contrast to the related, anoxia-tolerant crucian carp which demonstrates decreased brain NAA levels following 1 d and 1 w anoxia [Lardon *et al.* 2012].

Furthermore, although GABA resonances were observed in the brain spectra of common carp, no statistically significant differences were found in the GABA levels in the various exposure groups. This observation is in sharp contrast to the anoxia-tolerant crucian carp, which displays increased GABA concentrations following anoxic stress. As being the major inhibitory neurotransmitter in the adult vertebrate central nervous system, GABA increases contribute to a reduced ATP consumption in anoxia and to protect crucian carp brains against the detrimental effects of brain anoxia [Prentice 2009]. Specifically, the elevation of brain GABA is thought to be a main mechanism for anoxic metabolic depression to restore ATP levels [Nilsson 1990; Hylland and Nilsson 1999] and the metabolic pathways supporting GABA production and degradation are well characterized in vertebrate nervous tissues. Contrastingly, no significant changes in the levels of brain GABA were found in the anoxic/hypoxic common carp. Assuming that GABA concentrations remained unaffected by brain anoxia and/or hypoxia, these observations suggest that the common carp may not

suppress brain activity or utilize a changed balance between GABA and other transmitter systems in the brain to withstand oxygen limitations.

The branched-chain amino acids (BCAA) valine/isoleucine/leucine decreased in all 1 d hypoxic tissues (related to the normoxic controls) but a complete recovery was present in all tissues. These essential amino acids are assumed to be key molecules that contribute to a global regulation of growth and metabolism [Wang *et al.* 2011]. Only in muscle, hypoxia exposure for 1 week increased the BCAA levels (compared to the controls). In comparison to 24 h of hypoxia, 1 w hypoxic exposure resulted in higher BCAA-levels for brain, liver and muscle whereas the opposite occurred in heart tissue.

Anoxia, on the other hand, did not change the BCAA-levels significantly in common carp and this is contradictory to the results of the anoxic crucian carp. The latter is characterized by increased brain BCAA levels which can be explained by a possible oxidation stop by mitochondrial enzymes in anaerobic tissues, a reduced consumption of amino acids (protein synthesis suppression) or an increased catabolism in periods of anoxia [Podrabsky *et al.* 2007].

6.4.3 Other metabolites

Finally, 'other' i.e. previously not reported compounds in the present context, were identified in hypoxic tissues of common carp. More specifically, scyllo-inositol displayed different tissue responses following anoxia/hypoxia.

Little is known about the exact function of scyllo-inositol, also called 'scyllitol'. In brain, elevated scyllo-inositol levels are found in vertebrates with Alzheimer's disease or amnestic mild cognitive impairment. This compound is believed to reverse memory deficits in Alzheimer disease as well as to reduce the amount of Aβ-plaques in the brain of Alzheimer patients [Griffith *et al.* 2007]. In this study, significant changes in the levels of scyllo-inositol were only apparent in heart, liver and muscle tissue. Anoxia resulted in a decrease in muscle scyllo-inositol levels whereas no changes were detected in the anoxic heart tissue. One day hypoxia reduced the levels of scyllo-inositol notably in liver and muscle whereas one week hypoxia increased scyllo-inositol concentrations in muscle (compared to their controls). All tissues showed a complete recovery of scyllo-inositol following normoxic reoxygenation. Strangely and in contrast to liver and muscle tissue, heart extracts demonstrated an increase in scyllo-inositol after 1 d of hypoxia and additionally, a trend was observed of increased scyllo-inositol levels following 1 w of hypoxia (related to the controls).

Definitely, more studies are necessary to explore the exact role of scyllo-inositol the anoxia/hypoxia survival mechanisms of common carp.

6.5 Conclusions

Despite the wealth of information available on the metabolic and molecular responses of a broad variety of fish species to anoxia/hypoxia, we are still far from a universal concept of the most important adaptations underlying anoxia/hypoxia tolerance.

In this study, we focused on the metabolic responses of common carp, both at the cellular and tissue level which were subjected to anoxic, hypoxic and normoxic regimes. Significant changes in the levels of metabolites associated with the general energy pathways were observed (e.g. lactate, phosphocreatine, ATP/ADP) as well as changes in the levels of specific amino acids and neurotransmitters (e.g. glutamate, valine/(iso)leucine, etc.). However, in contrast with crucian carp, no changes in brain NAA or GABA were noticed. Finally, this paper also describes a newly reported metabolite i.e. scyllo-inositol in tissues of anoxic and hypoxic common carp.

Further research is anyhow needed to elucidate the multi-phase physiological mechanisms of common carp to withstand anoxia and/or hypoxia.

Chapter 7

The hypoxic dogfish shark (Squalus acanthias)

BASED ON:

"^{1}H-NMR study of the metabolome of the hypoxic spiny dogfish shark (*Squalus acanthias*)"

Isabelle Lardon [*(1, 2)], Marleen Eyckmans [(2)], Trung Nghia Vu [(3,4)], Kris Laukens [(3,4)], Roger Dommisse [(1)], Gudrun De Boeck [(2)]

Submitted soon to ***Metabolomics***

[(1)] University of Antwerp - Department of Chemistry (Research Group for Applied NMR) - Groenenborgerlaan 171, B-2020 Antwerp, Belgium

[(2)] University of Antwerp – Department of Biology (Laboratory for Systemic Physiological and Ecotoxicological Research - SPHERE) - Groenenborgerlaan 171, B-2020 Antwerp, Belgium

[(3)] University of Antwerp - Department of Mathematics & Computer Science - Middelheimlaan 1, B-2020 Antwerp, Belgium - [(4)] Biomina - biomedical informatics research center Antwerp, Wilrijkstraat 10, 2650 Edegem (Antwerp), Belgium

Abstract

Oxygen availability appears to be a major ambient selection pressure in aquatic vertebrates and many diverse physiological responses contributing to hypoxia tolerance are identified in fresh water, euryhaline and marine fish. In this study, the metabolic consequences of acute (2 h) and extended exposure to hypoxia (6 h) in different tissues of the pacific spiny dogfish shark (*Squalus acanthias*) were investigated as well as its capacity to recover from this 6 h hypoxic insult by exposing the same fish to 6 h of normoxic reoxygenation. The highest number of significant metabolite changes was observed in white muscle extracts, followed by gills-rectal gland and liver tissue. Concretely, oxygen restriction in dogfish resulted in an up-regulation of anaerobic glycolysis, as evidenced by the increased lactate levels in all tissues except for the rectal gland. Additionally, the increased reliance on ketone bodies as oxidative substrates, typically displayed by elasmobranchs and in contrast to teleost fish, is demonstrated in this study by the decreased concentrations of acetoacetate in hypoxic white muscle tissue. Possibly, these results might illustrate a potentially important role of acetoacetate as a fuel source in dogfish muscles during periods of constrained aerobic metabolism. Furthermore, ^{1}H-NMR spectroscopy of tissue extracts enabled the detection of significant changes in the concentrations of amino acids such as valine and isoleucine as well as taurine and carnitine. The levels of all these amino acids decreased in hypoxic muscle while increased levels of taurine were observed in the rectal gland (compared to their controls). Finally, a number of miscellaneous metabolites were found to change as a consequence of hypoxia: trimethylamine oxide (TMAO) and oxypurinol levels increased and decreased respectively in hypoxic muscles whereas myo-inositol displayed opposite tissue-specific responses in gills and rectal gland.

Keywords: hypoxia, spiny dogfish, ^{1}H-NMR based metabolomics, tissue extracts

7.1 Introduction

Environmental hypoxia also occurs in marine ecosystems (although to a lesser extent than in fresh water) and varies both spatially and temporally, affecting the survival and distribution of marine fish species worldwide. Hypoxic areas are commonly observed in shallow and open ocean areas and thus, due to this variable marine environment, fish may regularly encounter hypoxic stress. Oxygen concentrations are influenced by depth, salinity, time of the day, temperature, season, and level of productivity [Carlson and Parsons 2001]. The ability to tolerate aquatic hypoxia varies greatly among and within fish species, as demonstrated previously by the divergent tolerance mechanisms of fresh water cyprinid fish as the common- and crucian carp.

Elasmobranchs are a subclass of Chondrichthyes or cartilaginous fish and include sharks, rays and skates. These ancient vertebrates have high potential as model species and therefore, are used extensively to study evolutionary physiology, genomics and other relevant biological and biomedical-related topics. As being the oldest extant group of jawed vertebrates, elasmobranchs offer a number of advantages in experimental design and interpretation [Rytkönen *et al.* 2010]. Concretely, they exhibit the major functions of all subsequently appearing animals but in a more simple organized way [Barnes 2012]. The most common elasmobranch used for experimental purposes, is the spiny dogfish shark *Squalus acanthias*. The distribution of these sharks range from the mid to north Atlantic Ocean, depending on season and temperature. Due to their migratory behaviour, they might encounter hypoxic conditions on a regular basis [Barnes 2012].

To date, studies are available that investigated responses to oxygen limitation in the subsequent shark species: the dogfish [Metcalfe and Butler 1984; Perry and Gilmour 1996], the grey carpet shark (*Chiloscyllium punctatum*) [Renshaw and Chapman 2009], the bonnethead shark (*Sphyrna tiburo*) [Parsons and Carlson 2003], the blacknose shark (*Carcharhinus acronotus*) [Carlson 1998], the Florida smoothound shark (*Mustelus norrisi*) [Carlson 1998] and the epaulette shark (*Hemiscyllium ocellatum*) [Speers-Roesch I & II *et al.* 2012; Nilsson and Renshaw 2004; Renshaw and Chapman 2009]. Especially the latter shark is of particular interest due to its extreme hypoxia as well as anoxia tolerance at tropical temperatures (close to 30 °C). The epaulette shark inhabits the reef platform surrounding Heron Island – a small and low coral cay situated close to the southern end of the Great Barrier Reef. At nocturnal low tides, the water of the reef platform becomes cut off from the

surrounding ocean, forming a very large tide pool. At that time, the respiration of coral and the associated organisms in that tide pool still proceeds and hence, the water can become severely hypoxic (e.g. a fall below 18 % of air saturation) [Nilsson and Renshaw 2004]. The increasing scientific interest in this shark species can thus be explained by its remarkable hypoxia tolerance at tropical temperatures but also by its ability to perform hypoxic preconditioning. Accordingly, the identification of physiological responses which contribute to hypoxia tolerance in fish and their additional ability to avoid detrimental perfusion injuries are an area of major biomedical research interest [Speers-Roesch *et al.* 2012b].

In this study, we investigated the tissue metabolic responses of spiny dogfish sharks (*S. acanthias*) subjected to hypoxia exposure and consequent normoxic recovery. High-resolution ^{1}H-NMR spectra were obtained from brain, liver, muscle, gill, white muscle and rectal gland tissue extracts. At first, we aimed at identifying the significantly different metabolites in the tissues of controls, hypoxia-exposed and normoxic recovered fish. Consequently, the results of this study offer a comprehensive picture of the hypoxia tolerance mechanisms in ancient elasmobranchs but it also provides comparative insights in the metabolic responses associated with hypoxia tolerance of between teleosts and sharks.

Even though the physiological attributes underlying these variations/differences in hypoxia tolerance remain incompletely understood, such comparative studies in different fish species will undoubtedly contribute to a better understanding of the miscellaneous physiological responses to oxygen depletion among fishes.

7.2 Materials and methods

7.2.1 Animal collection

The experiments were conducted at the Bamfield Marine Sciences Centre, British Columbia, Canada. Male spiny dogfish, *S. acanthias* (n = 21), weighing 1.84 ± 0.41 kg were caught by angling in the proximity of the Bamfield inlet during the summer of 2009 (July). All sharks were subsequently kept in a large concrete indoor tank (151.000 l) continuously supplied with running aerated Bamfield Marine Station seawater (14 °C, salinity 30 ‰) and were able to acclimatize for minimum 1 week before the start of the experiments. Fish were fed twice a week with commercially purchased frozen hake (*Merluccius productus*) but fasted prior to and for the duration of the experimental period.

7.2.2 Hypoxia experiments

In this study, four experimental groups of dogfish sharks were examined: controls (N = 6), a 2 h (N=5) and a 6 h hypoxic group (N=5), and a group that was allowed to recover (6h) from the 6 h hypoxia exposure (recovered group, N=5).

Prior to the start of the hypoxia exposures, all dogfish were placed in metal boxes (volume of 75 l) to acclimatize overnight in fresh aerated seawater at 14.6 °C. The control animals were maintained at normal seawater oxygenation (8.9 mg O_2 /l). Hypoxia was induced gradually by bubbling nitrogen gas through the water to displace dissolved oxygen and by sealing the test box with a rubber sheet to avoid oxygen diffusion from the air. Experimental animals were exposed to hypoxic conditions of 1 mg O_2/l during 2 h and 6 h. The recovered group includes fish that were exposed to 6 h of hypoxia and allowed to recover for 6 h in normoxic seawater. The dissolved O_2 levels were monitored every 15 min using a WTW oxygen electrode (WTW oxi 3400i, Weilheim, Germany).

At the completion of the experiments, dogfish were euthanized in an overdose of neutralised MS222 (1 g/l, pH 7.4, Sigma Chemical, St. Louis, MO, USA). Brain, liver, gills, white muscle and rectal gland tissue samples were subsequently excised rapidly on ice in this order, immediately snap-frozen in liquid nitrogen and stored at -80 °C until further analysis at the University of Antwerp (Departments of Chemistry and Biology), Belgium. During tissue-harvesting, the water in the hypoxic tank was continuously nitrogen-gassed to ensure hypoxic conditions for the remaining dogfish in the tank.

7.2.3 Tissue extraction: methanol/chloroform/water protocol (ratio 2/1/1.8)

Tissue extraction was carried out using the methanol/chloroform/water method based on the protocols described by Lin and Wu [Lin *et al.* 2007; Wu *et al.* 2008].

Frozen tissue samples were ground in a liquid nitrogen-cooled mortar and pestle and approximately 100 mg of homogeneous tissue powder was used for the extraction. Ice cold methanol (4 ml/g of tissue; analaR normapur, min. 99.8 %, VWR, Pennsylvania, USA) and ice cold milliQ water (0.85 ml/g) were added to the powder to extract the aqueous metabolites and the homogenate was vortexed for 1 min. Subsequently, ice cold chloroform (4 ml/g; normapur, 99.3 %, VWR, Pennsylvania, USA) and milliQ water (2 ml/g) were added to extract the hydrophobic metabolites; the mixture was vortexed for 1 min and then incubated on ice for 10 min to partition. The supernatant was then centrifuged at 4 °C for 10 min at

2000 g, resulting in a biphasic solution. The upper polar and lower non-polar layers were carefully removed and transferred to 15 ml sterile Falcon tubes. Subsequently, all samples were lyophilized overnight to avoid the presence of a dominant water signal in the ^{1}H-NMR spectra. Only the results of the aqueous fractions of brain, liver, gills, white muscle and rectal gland are discussed in the present study.

Prior to ^{1}H-NMR measurement, the polar tissue extracts were dissolved in 580 µl of sodium phosphate buffer prepared in D_2O to minimize variations in sample pH and to allow for deuterium locking, containing sodium-3-trimethylsilylpropionate (TMSP) as an internal standard (see subsequent paragraph). Finally, the resulting samples were transferred to a 5 mm NMR tube (NE-HP5-7, Cortecnet, France) and analyzed immediately by ^{1}H-NMR.

The 50 mM sodium phosphate buffer in D_2O (99.9 atom % D) consisted of Na_2HPO_4, 33.5 mM (AnalaR Normapur); NaH_2PO_4, 16.45 mM (GPR rectapur) (all from Merck, Darmstadt, Germany); 0.1 mM TMSP (≥ 98 %, Cambridge Isotope Laboratories, MA, USA); 0.05 mM sodium azide (99 %, Acros Organics, NJ, USA). Deuterium chloride in D_2O (ClD, > 99 atom % D, 20 wt %) and sodium deuteroxide in D_2O (NaOD, > 99 atom % D, 40 wt %) (Both from Acros Organics, NJ, USA) were added to achieve a pH of ~ 7.

7.2.4 ^{1}H-NMR based metabolomics of aqueous brain, liver, gills, white muscle and rectal gland extracts

Tissue extracts of spiny dogfish were analyzed on a Bruker Avance II-700 NMR spectrometer, operating at 700.13 MHz (Bruker Biospin, Europe), equipped with a 5 mm inverse TXI-Z probe and a BACS-60 automatic sample changer. Tuning, matching and shimming were performed automatically for each sample in order to minimize the variation due to sample manipulation.

One-dimensional ^{1}H-NMR spectra of brain, liver, gills, white muscle and rectal gland extracts were measured at 25 °C with a standard sequence using a 90° pulse (pulse sequence *zgpr*), a relaxation delay of 1.0 s with water presaturation, 64 scans collected into 16 k data points, a spectral width of 14 kHz and an acquisition time of 2.33 min per sample. Prior to Fourier transformation, all datasets were zero-filled to 32 k points and exponential line broadenings of 0.3 Hz were applied as well. Finally, all spectra were phase and baseline corrected and chemical shifts were referenced to TMSP (0.0 ppm) using the Topspin software (version 2.1, Bruker Biospin).

The identity of significant metabolites was assigned by comparison to tabulated chemical shifts in literature (Fan 1996) and confirmed by comparison to in-house and public databases (e.g. The Human Metabolome Database - HMDB, Chenomx).

7.2.5 *Spectral pre-processing*

The 1D spectra were converted to an appropriate format for subsequent statistical analysis by automatically segmenting each NMR spectrum in 0.05 ppm integrated spectral regions (bins or buckets) between 0.5 and 10 ppm using AMIX (Analysis of Mixtures, version 3.8.5, Bruker Biospin). Buckets from 4.70 to 5.0 ppm, containing the residual water resonance, were excluded. All spectra were mean-centered and were normalized to total intensity in order to reduce the influence of concentration variability among the samples.

7.2.6 Statistical analyses

Multivariate analysis

The pre-processed NMR spectra were first subjected to principal component analysis (PCA) using AMIX, to reduce the dimensionality of the data and to obtain an overview by showing trends, clusters and potential outliers within the data sets. Data points were identified as outliers when they were not situated within the 95 % confidence ellipse (Hotelling T^2 multivariate profiling) [Lindon *et al.* 2007] and outliers were subsequently removed from the data sets.

Univariate analysis

Following PCA analysis and outlier detection and elimination, the created bucket tables of the different tissue types were exported as a spread sheet to Excel (Microsoft Office Excel 2007). A two-way analysis of variance (ANOVA), followed by a Benjamini-Hochberg test [Benjamini & Hochberg 1995] to counter the effect of multiple testing, were applied in R (version 2.9.2) to identify the buckets/metabolites that differed significantly between the control and the exposed fish. In all instances, $p < 0.05$ was used as the level of significance. Furthermore, in order to investigate whether these buckets also differed significantly between the different exposure groups, a student's t-test in excel followed by a Benjamini-Hochberg correction test in R were applied. In this case, $p < 0.05$ was applied as the level of statistical significance.

7.3 Results

7.3.1 ^{1}H-NMR metabolomics and statistical analyses of polar brain extracts

Brain data sets were examined by PCA analysis and no outliers were detected. Remarkably, the ANOVA analyses with Benjamini-Hochberg correction test of polar brain extracts revealed no significantly different metabolites, so it seems that brains were well protected from this short-term hypoxic event.

7.3.2 ^{1}H-NMR metabolomics and statistical analyses of polar liver extracts

The PCA analysis of liver spectral data resulted in the detection and the subsequent removal of two outliers. Subsequently, univariate statistics only revealed significantly increased lactate concentrations in extracts of 2 h hypoxic fish, in comparison to its control group. Figure 7.1 shows the box plot of lactate.

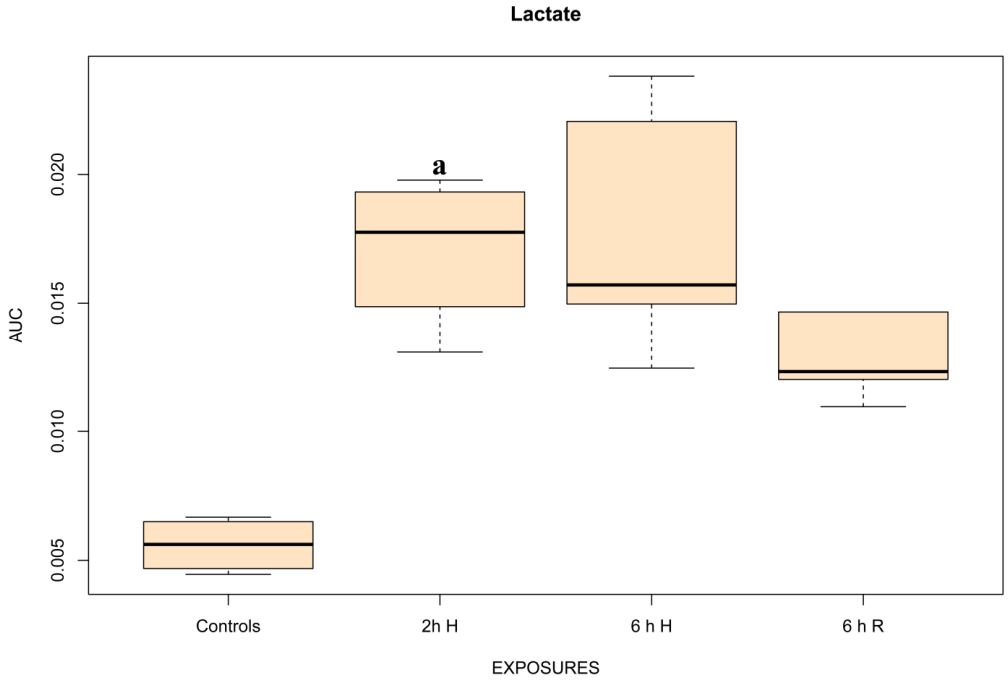

Figure 7.1 – Box plot of liver data, demonstrating a significant difference in lactate levels between the normoxic controls and the 2h hypoxia group: a ($p<0,05$) - aa ($p<0,01$) - aaa ($p<0,001$). The vertical axis expresses the metabolite levels as Area Under the Curve (AUC) intensities. The horizontal axis represents the four experimental groups: the normoxic controls (N=4), 2h hypoxia (N=5), 6h hypoxia (N=5) and the 6h reoxygenated group (N=5).

7.3.3 ^{1}H-NMR metabolomics and statistical analyses of polar gill extracts

Three outliers were identified by PCA analysis and hence, removed from the data set. The subsequent buckets/metabolites were assigned by univariate study as being significantly different between controls and exposed groups: valine, lactate, glutamate, trimethylamine-oxide (TMAO), myo-inositol, (phospho)creatine, phosphocholine, glucose and formate. Box plots of the significant changing metabolites in gills are displayed in Figure 7.2.

Both 2 h and 6 h of hypoxic treatment decreased the concentrations of valine, glutamate, myo-inositol, (phospho)creatine, glucose and formate (compared to their respective controls) whereas this was accompanied by increases in the levels of lactate, TMAO and phosphocholine. When recovered fish (animals exposed to 6 h of hypoxia and allowed to recover during 6 h of normoxia) were compared to their controls, higher concentrations of lactate, TMAO, phosphocholine were found in the recovered group associated with lower

levels of glutamate, myo-inositol, (phospho)creatine, glucose and formate were observed. Apparently, dogfish did not manage to recover completely from the hypoxic insult (2 h and 6 h) during reoxygenation since metabolites, which decreased after hypoxia, were still lower in recovered animals (compared to the controls) and vice versa. Only a recovery for valine levels was obtained in dogfish gill extracts.

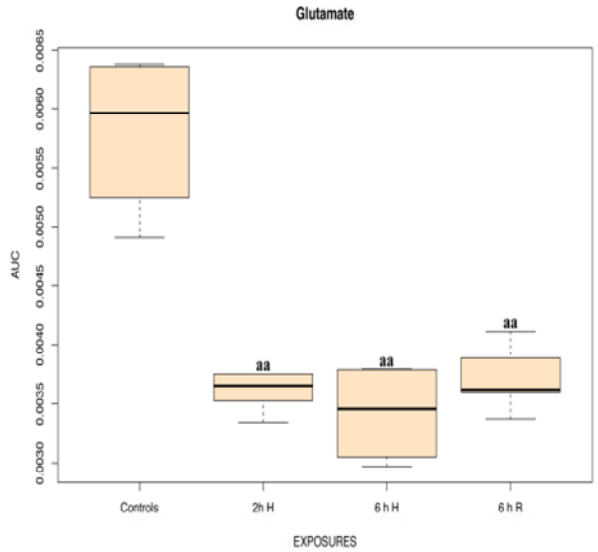
Glutamate
AUC
0.0030
0.0035
0.0040
0.0045
0.0050
0.0055
0.0060
0.0065
aa
aa
aa
Controls
2h H
6 h H
6 h R
EXPOSURES

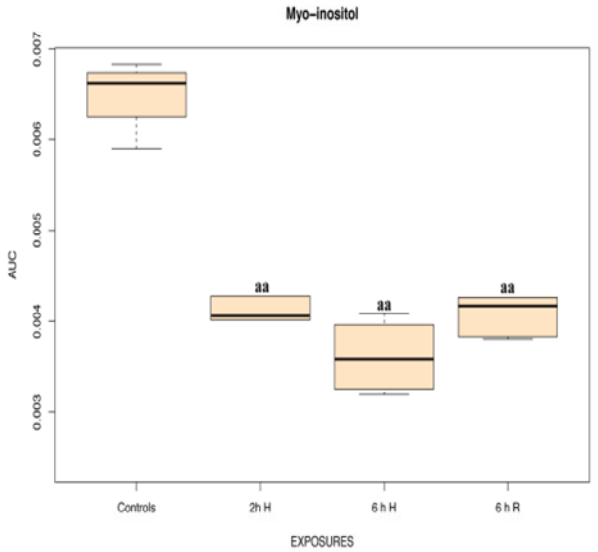
Myo–inositol
AUC
0.003
0.004
0.005
0.006
0.007
aa
aa
aa
Controls
2h H
6 h H
6 h R
EXPOSURES

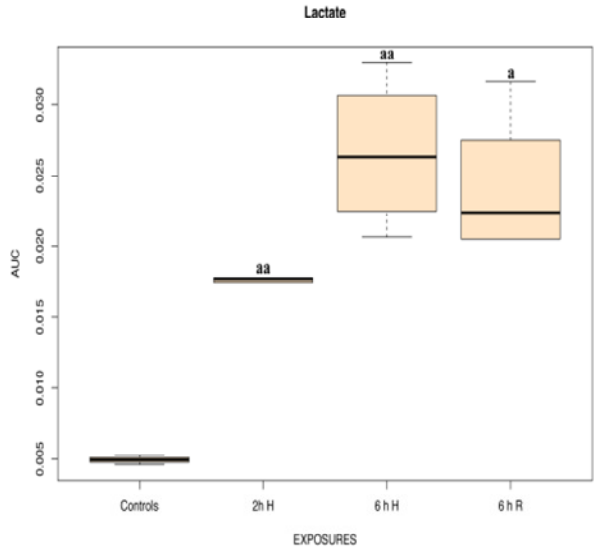
Lactate
AUC
0.005
0.010
0.015
0.020
0.025
0.030
aa
aa
a
Controls
2h H
6 h H
6 h R
EXPOSURES

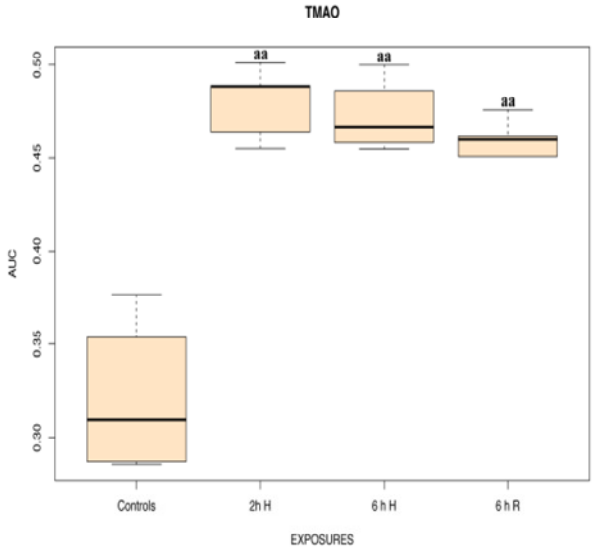
TMAO
AUC
0.30
0.35
0.40
0.45
0.50
aa
aa
aa
Controls
2h H
6 h H
6 h R
EXPOSURES

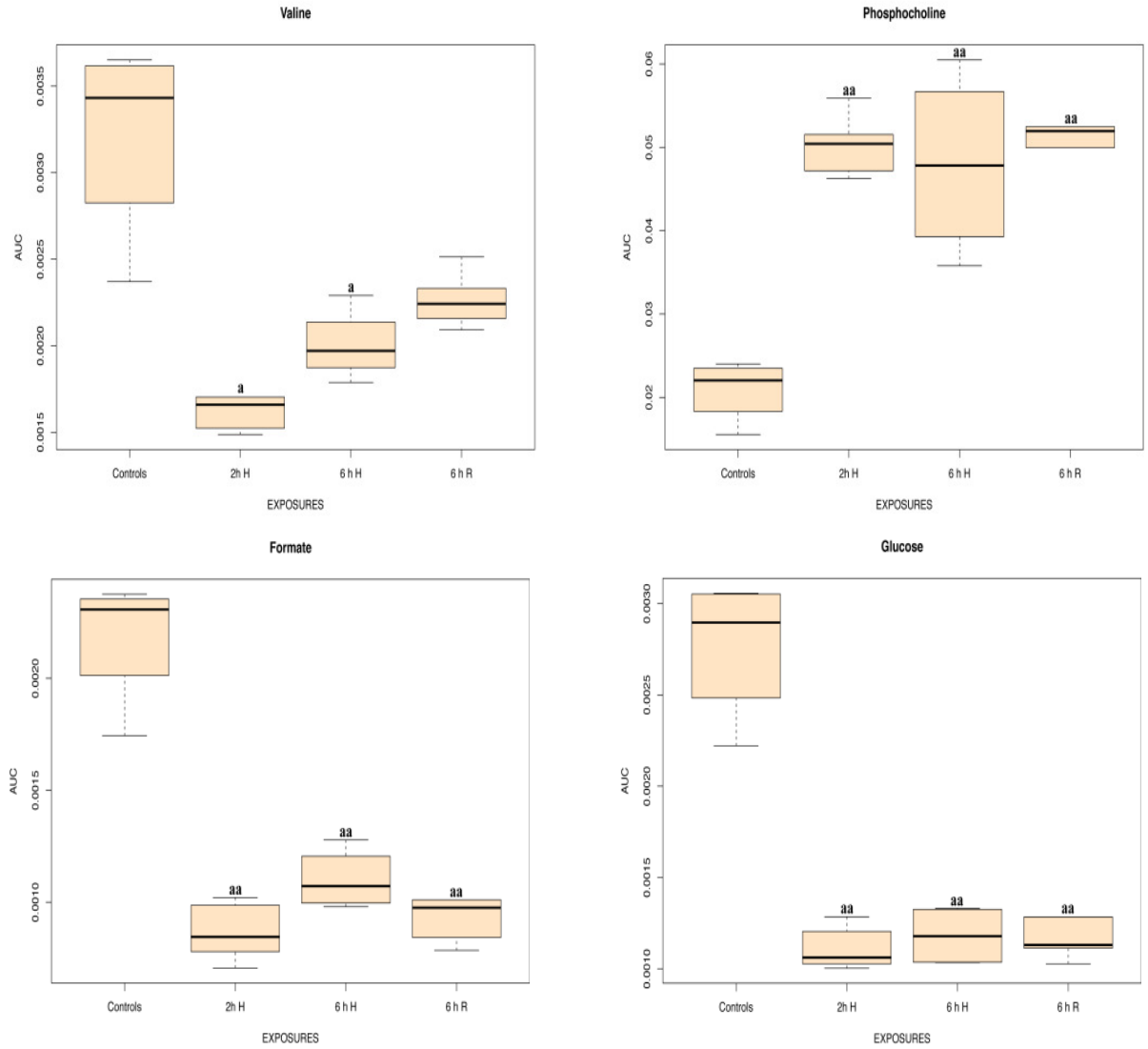
Valine
AUC
0.0015
0.0020
0.0025
0.0030
0.0035
a
a
Controls
2h H
6 h H
6 h R
EXPOSURES
Phosphocholine
AUC
0.02
0.03
0.04
0.05
0.06
aa
aa
aa
Controls
2h H
6 h H
6 h R
EXPOSURES
Formate
AUC
0.0010
0.0015
0.0020
aa
aa
aa
Controls
2h H
6 h H
6 h R
EXPOSURES
Glucose
AUC
0.0010
0.0015
0.0020
0.0025
0.0030
aa
aa
aa
Controls
2h H
6 h H
6 h R
EXPOSURES

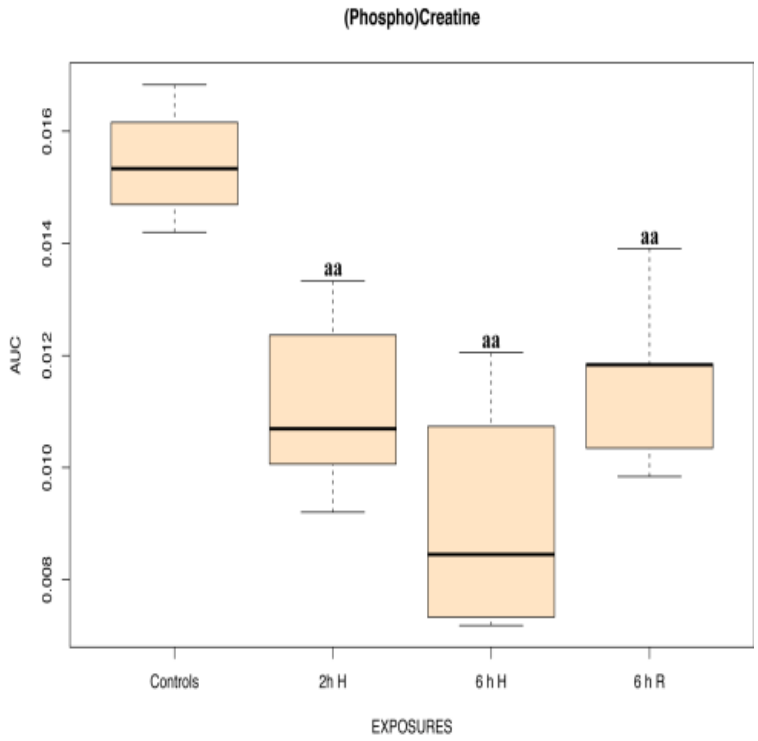

Figure 7.2 – Box plot of gill data set, demonstrating the significant differences in various metabolites between the normoxic controls and the exposed groups (a: $p < 0,05$) – aa: $p < 0,01$) – aaa: $p < 0,001$). The vertical axis displays the metabolite levels as Area Under the Curve (AUC) intensities.

The horizontal axis represents the four experimental groups: the normoxic controls (N=4), 2h hypoxia (N=5), 6h hypoxia (N=4) and the 6h reoxygenated group (N=5).

7.3.4 ^{1}H-NMR metabolomics and statistical analyses of polar white muscle extracts

The PCA study of muscle samples revealed three outliers in the data sets which were subsequently removed from further statistical analysis. A substantial amount of metabolites were observed in the ^{1}H-NMR muscle spectra: isoleucine, valine, 3-hydroxybutyrate, lactate, alanine, acetate, glutamate, glutamine, aceto-acetate, succinate, carnitine, TMAO/betaine, (phospho)creatine, malonate, taurine, glycine, sarcosine, tartrate, oxypurinol, ATP/ADP/AMP. Hence, Figure 7.3 illustrates the box plots of the metabolites in white muscle, resulting from the statistical analysis.

Hypoxia exposure in general (2 h and 6 h) induced decreases in the levels of isoleucine, valine, glutamine, aceto-acetate, taurine, glycine, oxypurinol and carnitine (compared to the controls) while the concentrations of lactate, acetate and TMAO increased accordingly. Furthermore, a recovery was observed for the levels of lactate and acetate but contrastingly, recovered fish still displayed lower levels of 3-hydroxybutyrate, isoleucine, valine, glutamine, aceto-acetate, taurine, glycine, oxypurinol and carnitine (which previously decreased as a consequence of hypoxia), compared to their controls. Similarly, the levels of TMAO were still higher in the recovered group, in comparison to the controls.

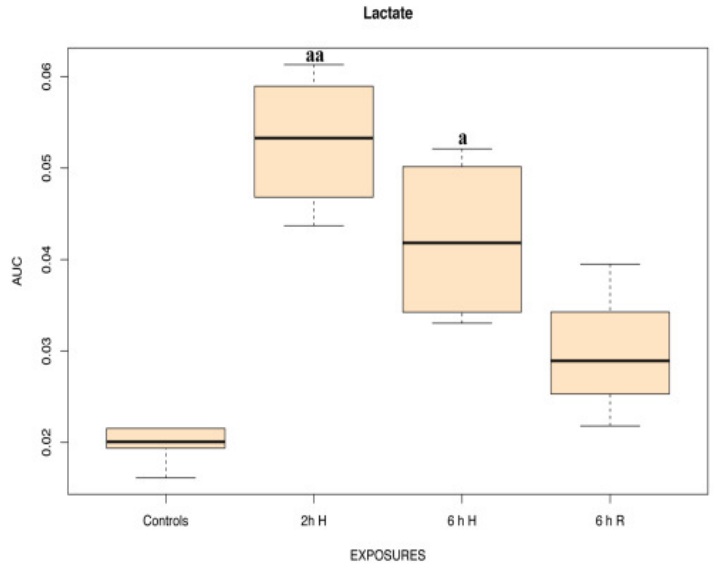
Lactate
AUC
0.02
0.03
0.04
0.05
0.06
aa
a
Controls
2h H
6 h H
6 h R
EXPOSURES

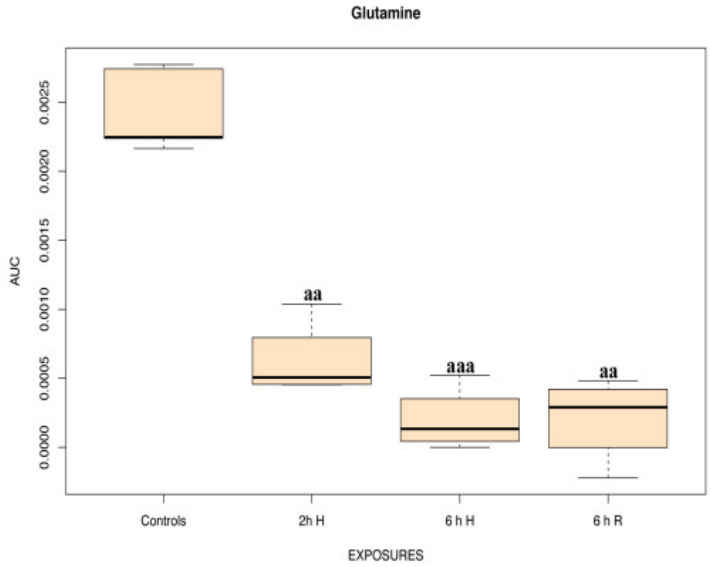
Glutamine
AUC
0.0000
0.0005
0.0010
0.0015
0.0020
0.0025
aa
aaa
aa
Controls
2h H
6 h H
6 h R
EXPOSURES

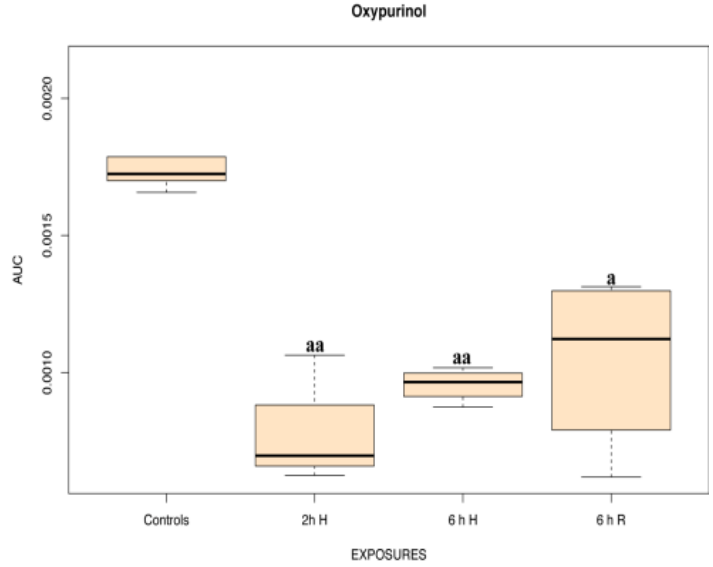
Oxypurinol
AUC
0.0010
0.0015
0.0020
aa
aa
a
Controls
2h H
6 h H
6 h R
EXPOSURES

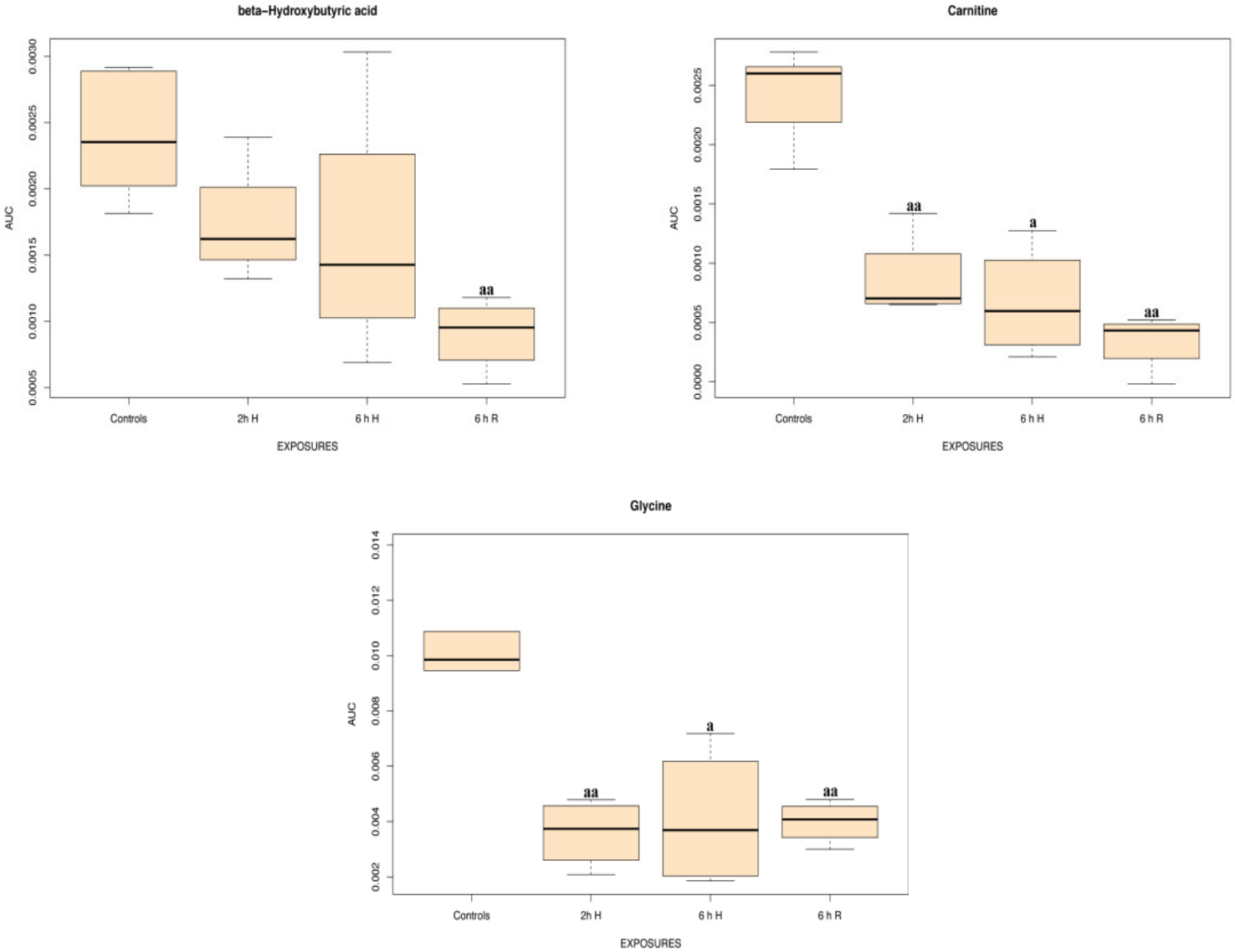
beta−Hydroxybutyric acid
AUC
0.0005
0.0010
0.0015
0.0020
0.0025
0.0030
aa
Controls
2h H
6 h H
6 h R
EXPOSURES
Carnitine
AUC
0.0000
0.0005
0.0010
0.0015
0.0020
0.0025
aa
a
aa
Controls
2h H
6 h H
6 h R
EXPOSURES
Glycine
AUC
0.002
0.004
0.006
0.008
0.010
0.012
0.014
aa
a
aa
Controls
2h H
6 h H
6 h R
EXPOSURES

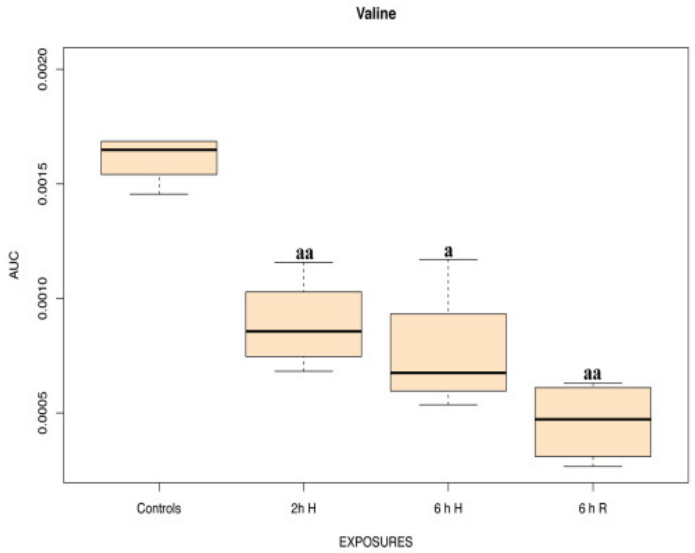
Valine
AUC
0.0005
0.0010
0.0015
0.0020
aa
a
aa
Controls
2h H
6 h H
6 h R
EXPOSURES

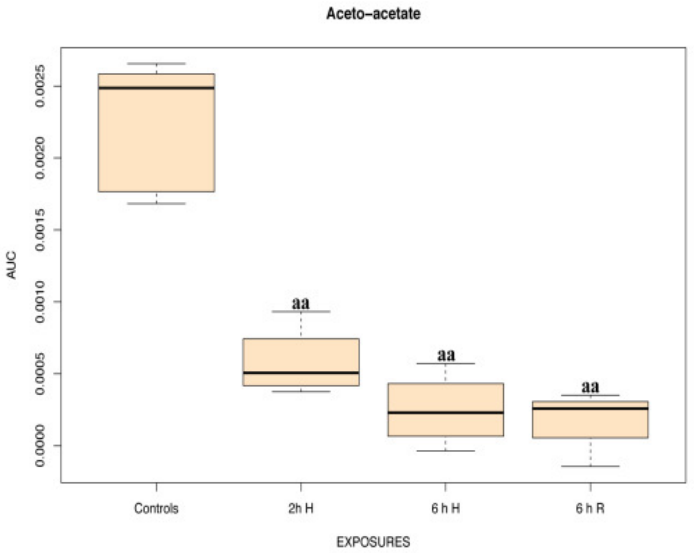
Aceto–acetate
AUC
0.0000
0.0005
0.0010
0.0015
0.0020
0.0025
aa
aa
aa
Controls
2h H
6 h H
6 h R
EXPOSURES

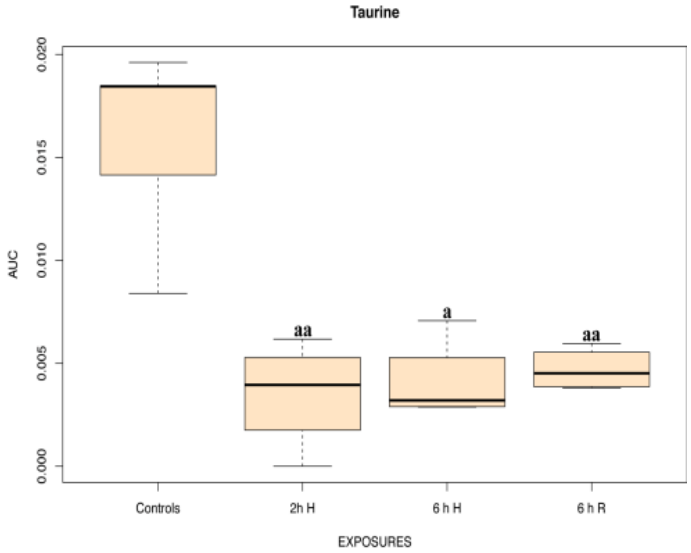
Taurine
AUC
0.000
0.005
0.010
0.015
0.020
aa
a
aa
Controls
2h H
6 h H
6 h R
EXPOSURES

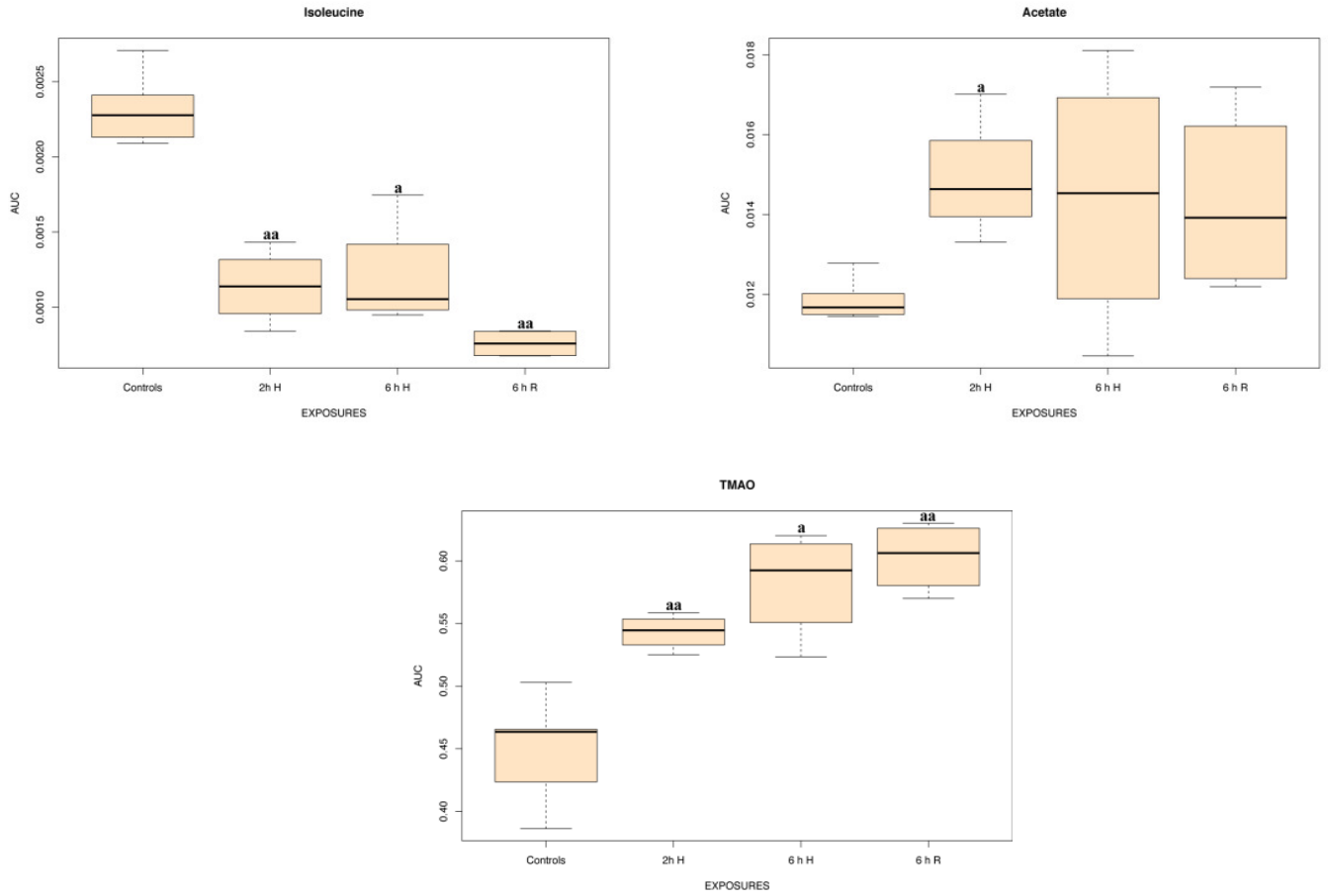

Figure 7.3 – Box plot of muscle extracts, demonstrating the significant differences in various metabolites between the normoxic controls and the exposed groups (a: $p < 0,05$ – aa: $p < 0,01$ – aaa: $p < 0,001$). The vertical axis displays the metabolite levels as Area Under the Curve (AUC) intensities. The horizontal axis represents the four experimental groups: the normoxic controls (N=5), 2h hypoxia (N=4), 6h hypoxia (N=4) and the 6h reoxygenated group (N=4).

7.3.5 ^{1}H-NMR metabolomics and statistical analyses of polar rectal gland extracts

Rectal gland spectra were investigated by PCA analysis and one outlier was detected and removed from the data set. The polar rectal gland spectra showed resonances of isoleucine, valine, ethanol, lactate, alanine, acetate, glutamate, glutamine, succinate, pyruvate, (phospho)creatine, malonate, phosphocholine, TMA(O), taurine, myo-inositol, glycine, NAD^{+}, oxypurinol, ATP/ADP/AMP and hypoxanthine. Figure 7.4 shows the box plots of the significant metabolites in rectal gland tissue.

Remarkably, all significantly different metabolites were found in the 2 h hypoxic group and the recovered group. Specifically, 2 h hypoxia resulted in increased levels of lactate, taurine, myo-inositol and glycine combined with a decrease in acetate, glutamate and succinate (compared to the controls). Additionally, recovered fish displayed higher levels of malonate, taurine and myo-inositol whereas decreases in isoleucine, acetate and were observed (compared to the controls).

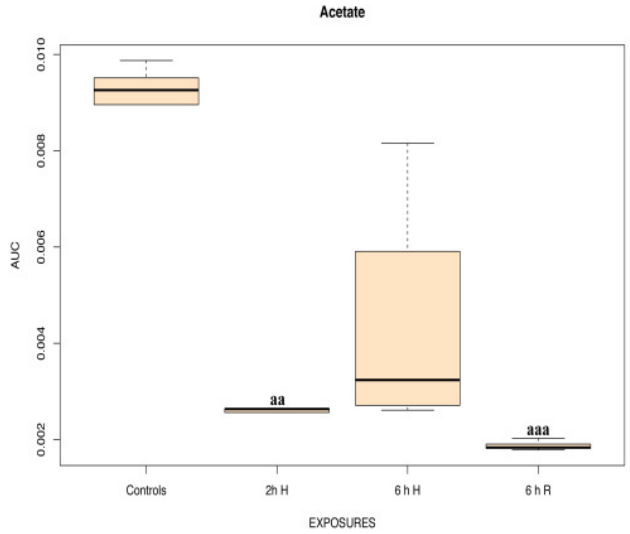
Acetate
AUC
0.002
0.004
0.006
0.008
0.010
aa
aaa
Controls
2h H
6 h H
6 h R
EXPOSURES

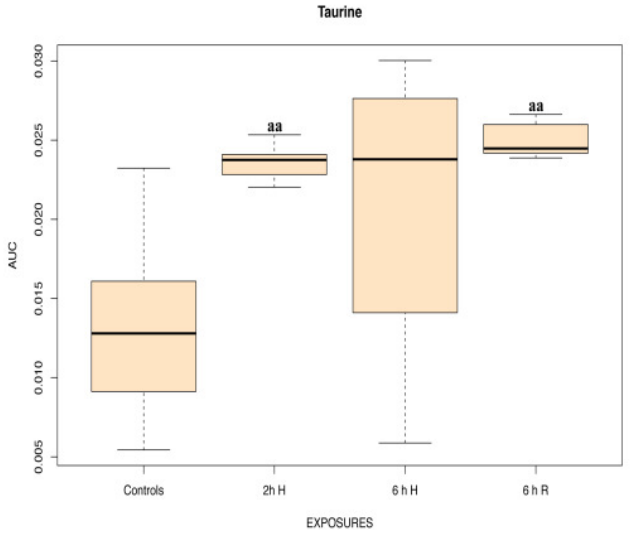
Taurine
AUC
0.005
0.010
0.015
0.020
0.025
0.030
aa
aa
Controls
2h H
6 h H
6 h R
EXPOSURES

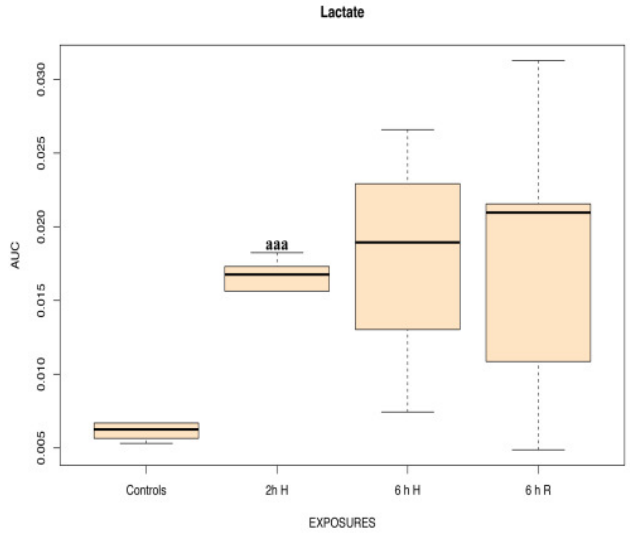
Lactate
AUC
0.005
0.010
0.015
0.020
0.025
0.030
aaa
Controls
2h H
6 h H
6 h R
EXPOSURES

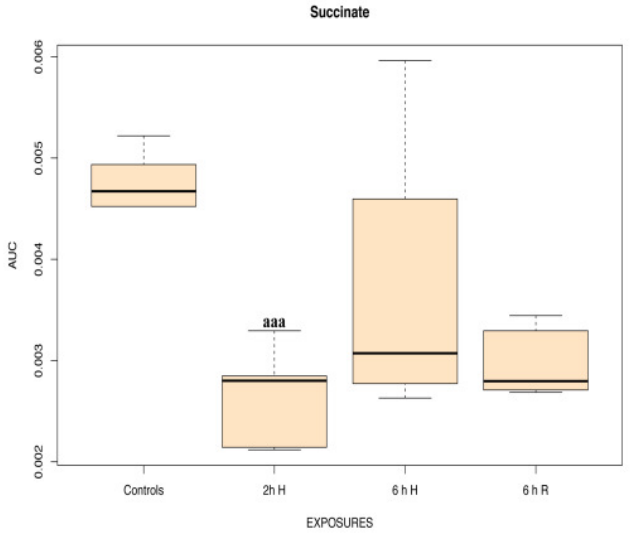
Succinate
AUC
0.002
0.003
0.004
0.005
0.006
aaa
Controls
2h H
6 h H
6 h R
EXPOSURES

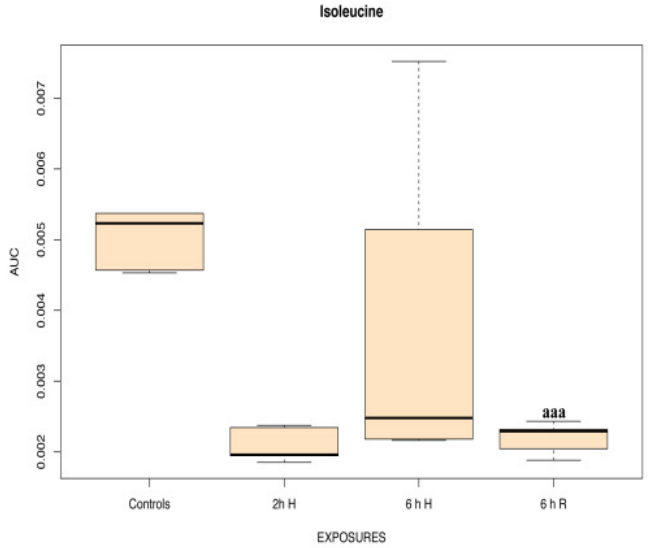
Isoleucine
AUC
0.002
0.003
0.004
0.005
0.006
0.007
aaa
Controls
2h H
6 h H
6 h R
EXPOSURES

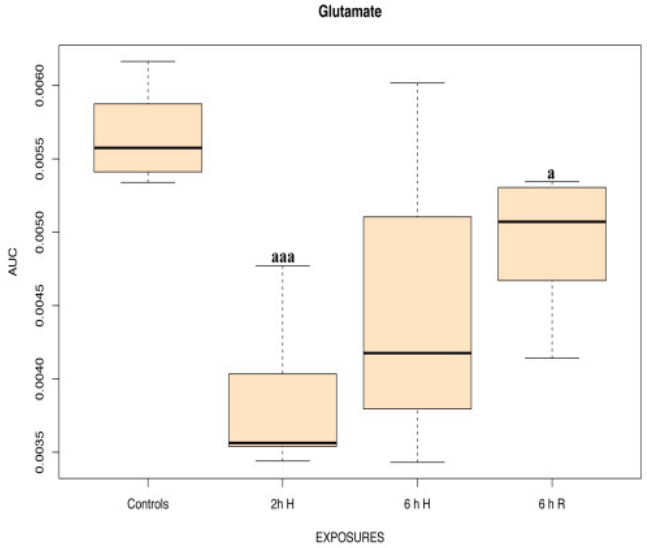
Glutamate
AUC
0.0035
0.0040
0.0045
0.0050
0.0055
0.0060
aaa
a
Controls
2h H
6 h H
6 h R
EXPOSURES

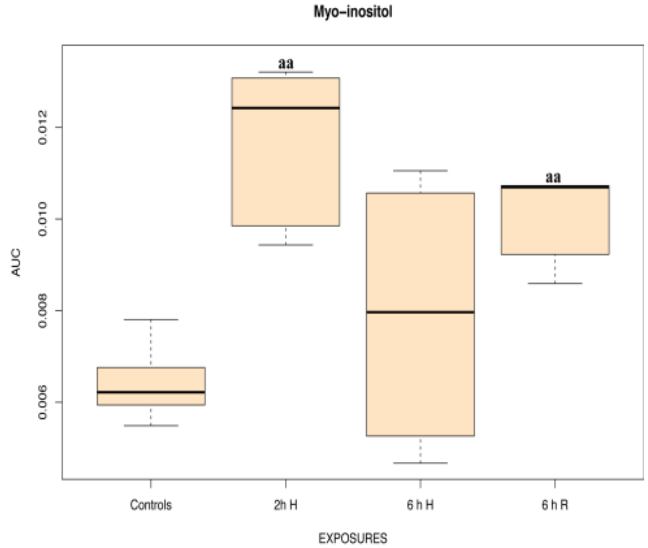
Myo–inositol
AUC
0.006
0.008
0.010
0.012
aa
aa
Controls
2h H
6 h H
6 h R
EXPOSURES

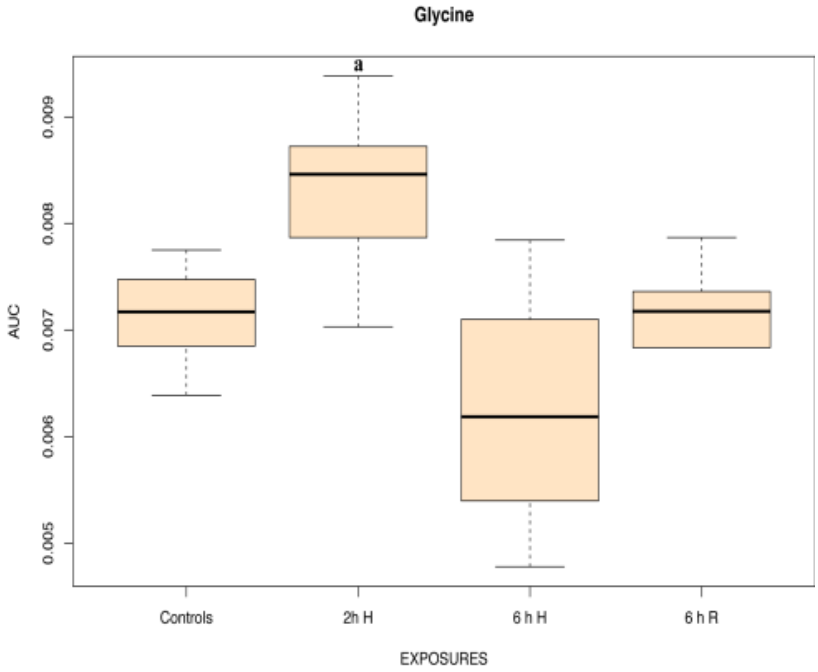

Figure 7.4 – Box plot of rectal gland data, illustrating the significant differences in various significant metabolites between the normoxic controls and the exposed groups (a: $p < 0,05$ – aa: $p < 0,01$ – aaa: $p < 0,001$). The vertical axis displays the metabolite levels as Area Under the Curve (AUC) intensities. The horizontal axis represents the four experimental groups: the normoxic controls (N=6), 2h hypoxia (N=5), 6h hypoxia (N=4) and the 6h reoxygenated group (N=5).

7.4 Discussion

In general, hypoxic treatment resulted in significant changes in the levels of miscellaneous metabolites of the spiny dogfish but overall, most changes were found in white muscle tissue.

When dogfish were exposed to hypoxia (2 h and 6 h) and allowed to recover upon normoxic reoxygenation, no significant changes were found in brain metabolite levels. These results may therefore indicate that the severity and/or the length of hypoxic exposure used in this study might be too low and/or too short to elicit significant changes in the brain metabolism of these elasmobranchs. At this point, it is difficult to tell whether the absence of significant brain metabolite changes following hypoxia is due to a sufficient energy supply from other tissues, possibly metabolic depression in brain activity, or due to other strategies applied in dogfish brains. More studies are therefore required to clarify the influence of oxygen limitation on the central nervous system of spiny dogfish.

7.4.1 Significant metabolite changes associated with the general energy metabolism

As mentioned, most significant metabolite changes resulting from the hypoxic and subsequent reoxygenation regimes are observed in white muscle extracts, followed by gills - rectal gland and liver tissue.

Acute hypoxia exposure (i.e. 2 h of hypoxia) induced increased lactate levels in liver, muscle and gill extracts (compared to its control group). The more extended exposure to hypoxia of 6 h, on the contrary, induced increased lactate concentrations in white muscle while no significant changes in lactate concentrations were observed at all in rectal gland. In elasmobranchs, lactate concentrations are known to rise quickly when they are exposed to acute stress such as diminished oxygen levels [Renshaw and Chapman 2009]. The higher tissue lactate levels in spiny dogfish reveal that there was a significant up-regulation of anaerobic energy metabolism, consistent with a continued need for cellular energy supply in the presence of limited oxygen, aiming at prolonged survival.

Additionally, glucose levels were unaffected by 2 h and 6 h of hypoxia (except for the gills which showed decreased glucose concentrations after 2 h of hypoxia in relation to the controls), similar to the results of previous studies on other elasmobranchs exposed to hypoxia [Routley *et al.* 2002; Speers-Roesch and Treberg 2010; Speers-Roesch *et al.* 2012b]. These observations might indicate that blood and tissue glucose homeostasis is maintained sensitively in hypoxic spiny dogfish.

In general, the metabolism of marine elasmobranchs differs from teleosts and virtually all other vertebrates in a number of ways. First, marine elasmobranchs exhibit a low capacity for extrahepatic lipid oxidation and secondly, they display an increased reliance on ketone body metabolism as oxidative substrates [Ballantyne and Speers-Roesch 2006]. The results of this study demonstrated decreased concentrations of acetoacetate in white muscle. Concretely, both 2 h and 6 h of hypoxia decreased the levels of this ketone body (compared to their controls). Furthermore, when recovered fish (i.e. sharks exposed to 6 h of hypoxia and allowed to recover during 6 h of normoxia) were compared to the corresponding control group, lower levels of acetoacetate were still found which might suggest that 6 h of normoxic reoxygenation was insufficient (i.e. too short) to restore the tissue levels back to control concentrations. We did not observe significant changes in the levels of this ketone body in other tissues and therefore, this might illustrate a potentially important role of acetoacetate as a fuel source in dogfish muscles. Additionally, there was a trend (p = 0.09) observed for another ketone body i.e. 3-hydroxybutyrate which decreased after 2h of hypoxia (compared to the controls) in muscle.

As a consequence of oxygen deprivation and to assure a sufficient metabolic fuel supply, dogfish muscles might increase the consumption of ketone bodies to provide energy. The results of this study correspond well with other studies showing that elasmobranch muscles do not rely on lipid oxidation but, instead, prefer to use ketone bodies as major oxidative fuels [Zammit & Newsholme 1979; Moyes *et al.* 1990; Ballantyne *et al.* 1992; Ballantyne and Speers-Roesch 2006]. The latter is in sharp contrast to the situation in teleosts where red muscle and heart heavily rely on fatty acid oxidation [Ballantyne and Speers-Roesch 2006].

7.4.2 Amino acids and neurotransmitters

Similar to the results for the general energy metabolites, the majority of significant changes in the levels of neurotransmitters and amino acids were found in white muscle, followed by rectal gland and gills. In contrast, the statistical analysis of liver extracts did not reveal any changes in the levels of amino acids or neurotransmitters.

Generally, the majority of anoxia-tolerant fish (e.g. the crucian carp) rely on neurotransmitters and neuromodulators to suppress the consumption of valuable energy reserves. One well-examined neuroprotective mechanism in hypoxia- and anoxia-tolerant animals is to alter the balance of excitatory (i.e. glutamate) and inhibitory (e.g. GABA)

neurotransmitters such that a significant increase in GABA release is accompanied by a decreased glutamate release (e.g. in crucian carp) [Renshaw *et al.* 2010].

In this study, we detected significant changes in the levels of glutamate in ^{1}H-NMR spectra of gills and rectal gland extracts and statistical analysis pointed out that 2 h of hypoxia induced decreased glutamate concentrations in both tissues (compared to the controls). In contrast, the glutamate levels observed in dogfish brain extracts did not significantly change as a consequence of the hypoxic treatment. Therefore, one might hypothesize that the severity and length of the hypoxic exposure in this experiment was unsufficient to cause any significant changes in the glutamate levels in shark brain.

In rectal gland and gills, decreased glutamate levels were observed after subjecting dogfish to 2 h of hypoxia (compared to the controls). Glutamate demonstrates two contrasting roles in elasmobranchs metabolism: one in hepatic energy production and one in the ureogenesis. The first role implies that glutamate is deaminated into α-ketoglutarate by glutamate dehydrogenase (GDH) for energy production [Ballantyne 1997]. Secondly, glutamate can also be converted to glutamine by glutamine synthetase (GS) in order to shuttle nitrogen to the ornithine-urea cycle [Anderson 1991]. In this study, we focussed on the metabolism of a marine elasmobranchs (i.e. the spiny dogfish) which typically display high levels of urea and therefore, we postulate that emphasis in this shark will be on the role of glutamate in ureogenesis. Furthermore, the observation that significant decreases in the concentrations of glutamate were demonstrated in gills and rectal gland of hypoxic dogfish, two major osmoregulatory organs in elasmobranchs, further supports this hypothesis. In contrast to marine sharks, fresh water elasmobranchs possess lessened or no urea synthesis (Tam *et al.* 2003) and therefore, available glutamate is then preferably deaminated for energy production.

Conjointly, decreased glutamine levels were discovered in white muscle. Both 2 h and 6 h of hypoxia resulted in a notably decrease of glutamine concentrations in muscle (compared to their controls) and recovered sharks still displayed lower levels of glutamine in comparison to their respective controls. In marine elasmobranchs such as the spiny dogfish, glutamine can be used as substrate to fuel urea production in the liver and thus, to maintain internal urea-N levels, which is extremely important to marine elasmobranchs for osmoregulation purposes [Wood *et al.* 1995].

Both valine and isoleucine, two branched chain amino acids (BCAA's) and key regulators in many metabolic functions, decreased in white muscle as a result of 2 h and 6 h of

hypoxia. In addition, recovered fish demonstrated lower levels of both essential amino acids (compared to the 2 w controls) suggesting that 6 h of normoxic recovery was too short to restore their control levels. The decreased levels of BCAA's in hypoxic muscle tissue can reflect an increased reliance on amino acids when anaerobic energy is up-regulated (also demonstrated by the increased lactate concentrations in hypoxic muscle). In contrast, valine concentrations increased in gills and rectal gland of dogfish subjected to 2 h of hypoxia. The role of increased valine concentrations in these organs remains unclear and should be further clarified by additional studies.

Taurine decreased significantly in muscle tissue, particularly when dogfish were exposed to 2 h and the decrease of taurine was also observed after 6 h of hypoxia (in comparison to their control groups). An opposite response in taurine levels, however, was observed for rectal gland, which displayed significant increased taurine concentrations after 2 h of hypoxia. This sulfonic amino acid is present in high concentrations in fish tissues as the heart, brain, retina and skeletal muscle and exerts many important metabolic functions. For example, taurine acts as an osmoregulator and regulates the transport of ions which might explain the observed increased taurine levels in the rectal gland after 2 h of hypoxia. Furthermore, taurine is essential for the development and function of skeletal muscle [Schaffer *et al.* 2010] and the decreased taurine levels in muscle after 2 h and 6 h of hypoxia may suggest that this polyvalent amino acid was catabolized increasingly to ensure a proper functioning of white muscle under hypoxic conditions.

In addition to the noticed changes of taurine and valine/isoleucine concentrations, white muscle also demonstrated decreased levels of carnitine after 2 h and 6 h of hypoxia (in relation to their controls). In elasmobranchs tissues, carnitine is involved in fatty acid metabolism, facilitating the transport of fatty acids into the mitochondria.

7.4.3 Other metabolites

In this study, hypoxia exposure of dogfish not only altered the concentrations of energy metabolites and amino acids but also it also induced significant changes in the levels of other metabolites such as trimethylamine oxide (TMAO), myo-inositol and oxypurinol.

Elasmobranchs typically possess substantial concentrations of methylamines in their tissues, particularly trimethylamine oxide (TMAO) and glycine betaine. It has been postulated by several authors that intracellular methylamines may serve as counteracting solutes in order to encounter the potentially denaturalizing consequences of characteristically high urea

concentrations in the blood and tissues of these animals [Yancey and Somero 1979; Seibel and Walsh 2002]. In this study, increased TMAO levels as a result of 2 h and 6 h of hypoxia were noticed in gills and muscle tissues (compared to their controls).

Myo-inositol levels decreased in gills following 2 h of hypoxia (compared to its control group) while significant increases in its levels were noticed in rectal gland tissue exposed to 2 h of hypoxia. To date, the precise function of this metabolite is not completely understood, although it is considered to be an essential element for cell growth, an osmolite and a storage form for glucose [Govindaraju *et al.* 2000]. Especially the role as osmolyte might suggest that the observed increased levels of myo-inositol in rectal gland may function as an attempt to restore the osmolarity in dogfish tissues, exposed to acute hypoxia.

Finally, the exposure of dogfish to 2 h of hypoxia markedly decreased the levels of oxypurinol in muscle and this decrease was also notices in 6 h hypoxic fish (compared to their corresponding controls). When recovered sharks were compared to the controls, a lower concentration of this metabolite was still apparent in their muscles, indicating that they did not recover completely from the 6 h hypoxic insult. Oxypurinol is the active metabolite of allopurinol and a xanthine oxidase inhibitor, hereby inhibiting the enzymatic generation of reactive oxygen species (ROS) by xanthine oxidase. Although allopurinol is perfectly suited to scavenge highly reactive hydroxyl radicals, oxypurinol performs this important task more effectively than is allopurinol. Moreover, in the present context of tissue hypoxia and possibly reoxygenation injury, oxypurinol plays an important role in protecting tissues and cells against the detrimental effects of reperfusion damage after hypoxic insults [Halliwell *et al.* 1987]. Additionally, oxypurinol is nowadays used in the therapy of congestive heart failure. The application of this compound in animal and human medicine is based on the possibility that xanthine oxidase inhibitors may improve myocardial work efficiency by sensitising cardiac muscle cells to calcium ions, which are a key determinant of cardiac muscle function. Eventually, this results in a more efficient contraction of cardiac muscle cells, without the same increase in oxygen demand [Naumova *et al.* 2006]. In this study, decreased concentrations of oxypurinol in white muscle of hypoxia-exposed dogfish were observed which might suggest that oxypurinol is used increasingly in muscle to combat the negative effects of ROS formation following hypoxia and normoxic reoxygenation. Furthermore, it can also indicate that more oxypurinol was consumed in muscle to maintain proper contraction efficiency in periods of limited oxygen supply and thus, to combat the consequences of disturbed aerobic energy production.

7.5 Conclusions

In conclusion, the present study outlines some of the common, treatment-specific and more importantly, tissue-specific mechanisms involved in the spiny dogfish's response to hypoxia and to subsequent normoxic reoxygenation. We observed 'general' metabolite changes, i.e. compounds involved in energy metabolism such as lactate, as well as changes in the levels of essential and non-essential amino acids (e.g. valine, isoleucine, etc.). Additionally, the importance of ketone bodies in elasmobranchs metabolism was confirmed in this study by observing significant changes in the concentrations of acetoacetate in hypoxic white muscle. Furthermore, ^{1}H-NMR spectroscopy also enabled the detection of metabolites which were typically associated with elasmobranchs metabolism (e.g. TMAO) and other miscellaneous compounds as myo-inositol and oxypurinol.

Chapter 8

Final discussion & Conclusions

Oxygen (O_2) is an essential gas for most life forms on earth and it is generally known that fluctuating oxygen concentrations can influence key cellular functions of organisms.

At present, hypoxia or temporal depletion of oxygen in aquatic environments is considered to be one of the most pressing and critical problems in the world which will continue to be an ever increasing threat to aquatic systems. Fish have often encountered hypoxia and therefore, O_2 availability has been a potent evolutionary force driving the natural selection of many unique adaptive traits. As such, fish represent the ideal model system to understand the selection of traits underlying hypoxia tolerance due to their extremely O_2-diverse habitats.

In general, fish respond to hypoxia with a suite of physiological, behavioural, biochemical and molecular responses to prolong anoxic/hypoxic survivorship and to limit the devastating consequences of an O_2 restriction at the tissue level. Although there is a generally accepted picture of how fish respond to oxygen restrictions, less is known about the interspecies and intraspecies or even tissue-specific responses to anoxia/hypoxia. It can be clear that the dynamic aquatic ecosystem with its complex biodiversity will undoubtedly reveal a wealth of information about the diverse adaptive responses in vertebrates to anoxia/hypoxia.

From a biomedical point of view, the results of this thesis might provide interesting insights in the mechanisms of oxygen depletion on a tissue to cellular level in vertebrates. This could be very relevant to the future therapy of hypoxia-induced diseases in humans such as stroke, asphyxia, ischemia, etc. as well as to the subsequent reoxygenation/reperfusion injury understanding.

The aim of this doctoral thesis was to investigate the metabolomics of the main tissues of the anoxic crucian carp (*Carassius carassius*) and those of the related, but anoxia-sensitive common carp (*Cyprinus carpio*). Although the crucian carp and the common carp are closely related species, they demonstrate different ecophysiological adaptations that may prolong their survivorship during severe limitations in oxygen availability.

High-resolution ^{1}H-NMR spectra were obtained from the main organs, representing accurate biochemical profiles of the metabolite dynamics following anoxia and/or hypoxia exposure and subsequent normoxic reoxygenation. By studying the aqueous tissue extracts of both fish, we confirmed the extensively reported metabolite changes in the anoxic crucian carp and the hypoxic common carp but we also detected previously unrecognized metabolite changes.

Besides the study of anoxia/hypoxia tolerance mechanisms in fresh water fish (carp species), this manuscript also describes the metabolomics of the marine spiny dogfish shark (*Squalus acanthias*). The first sharks appeared in the oceans 350 to 400 million years ago and are considered as one of the most conserved vertebrates, which make them excellent study models to investigate conservative traits in oxygen limitation. In addition, sharks and bony fish have had separate evolutionary trajectories from the Ordovician (500 million years before the present) so this study might offer an enormous potential to provide an understanding of the underlying mechanisms, involved in the diverse array of strategies, that specialize fish to cope with oxygen deprivation.

The subsequent paragraphs provide a general overview of the most important metabolite changes found in anoxic and/or hypoxic fresh water cyprinid fish as well as in hypoxia-exposed marine elasmobranchs. Similarities and differences in the tolerance mechanisms to environmental oxygen depletion will be highlighted and discussed briefly.

This final discussion is divided into three chapters corresponding to the observed changes in the metabolites following anoxia and/or hypoxia exposure: (a) general energy metabolites, (b) amino acids and neurotransmitters patterns and (c) novel i.e. previously unreported metabolites.

8.1 Metabolites associated with general energy metabolism

Anoxia exposure of both crucian carp and common carp induced an increase in lactate concentrations in brain, heart and muscle tissues (crucian carp) and in all tissues from the common carp except for the heart. This is somehow an ‘expected’ observation since the complete absence of molecular oxygen eventually stops the aerobic ATP production from mitochondrial oxidative phosphorylation. A consequent fall in [ATP] rapidly becomes life threatening to fish, as seen in the majority of animals such as mammals, due to the inhibited activity of ATP-dependent ion pumps, leaving the cell in a depolarized state. A continued ATP supply can then only be guaranteed by up-regulating anaerobic ATP-producing pathways such as the anaerobic glycolysis. In this study, anoxic exposure of crucian- and common carp clearly induced a switch from aerobic to activated anaerobic metabolism as evidenced by the increased tissue concentrations in lactate.

Additionally, a far more efficient strategy is applied by extremely anoxia-tolerant fish species of the *Carassius* species (crucian carp and goldfish) that avoid a possible tissue acidification

as a consequence of anoxia by producing ethanol as the major metabolic end product. Ethanol readily penetrates membranes, is released to the blood circulation and prevents a build-up of anaerobic waste products by excretion into the water via the gills. Since alcohol dehydrogenase (ADH) activities are only high in skeletal muscle (white and red), ethanol production occurs solely in this tissue. Other *Carassius* tissues such as the brain lack ADH enzymes so lactate and not ethanol will be the major anaerobic end product in that tissue. Some of this lactate may be transported to the muscles for conversion into ethanol, which explains why fewer tissues are affected by increased lactate levels in crucian carp.

Although closely related to crucian carp, common carp completely lack the ability to produce ethanol and, therefore are more sensitive to the negative effects of tissue acidosis. Instead, they probably evolved other mechanisms (e.g. metabolic depression, lactate as potential substrate for cardiac energy supply) to minimize the extent to which potential harmful anaerobic end products are stored. As such, these findings demonstrate the heterogeneity in adaptive mechanisms among closely related fish species such as the crucian- and common carp.

Remarkably, in contrast to the increased lactate levels in the anoxic crucian carp heart, no significant lactate increase was found in anoxic heart tissue of common carp. Possibly, common carp depress their cardiac activity under anoxia and/or hypoxia regimes in order to reduce the ATP consumption and to ensure a low myocardial ATP demand below the glycolytic capacity to synthesize ATP. This is in sharp contrast to the heart performance of anoxic crucian carp which possess the incredible ability to maintain normal cardiac functioning and autonomic cardiovascular control under anoxic stress. Secondly, the absent increased lactate levels in common carp hearts might be explained by its role in cardiac energy production. Unlike the brain, which mainly consumes glucose to generate aerobic ATP, the heart can apply to a broad range of substrates to provide cardiac energy. Specifically, glucose, fatty acids, ketone bodies, lactate and pyruvate can be utilized to ensure adequate myocardial energy supplies. Therefore, in this study, the cardiac lactate levels might have contributed to the myocardial energy production in anoxic common carp to restore the impaired ATP balance.

Contrastingly, acute (1 day) and long term (1 week) hypoxia induced decreased concentrations of lactate in all common carp tissues except for brains. This is in sharp contrast to the increased lactate levels in common carp tissues following anoxia exposure. The reduced

extent to which lactate is build up after short- and long term hypoxia might be explained by the strategy of metabolic depression. To date, mechanisms by which hypoxia-tolerant organisms reduce their metabolic rate to minimal levels during oxygen deprivation are still not fully understood. Concretely, it is uncertain whether the regulation of ATP-producing (glycolysis, oxidative phosphorylation) or ATP-reducing (protein synthesis, ion pumping) pathways or both contribute to the mechanism of metabolic suppression. The common carp seems to handle the hypoxic challenge well enough to induce the appropriate metabolic changes in time and depresses its energy turnover by applying a more economized use of energy during periods of restricted oxygen concentrations, hereby minimizing the accumulation of lactate or tissue acidosis.

When we examined the metabolic responses of the marine spiny dogfish shark (*Squalus acanthias*) to 2 h of hypoxia, increased lactate levels were observed in all tissues, except for the rectal gland. Similar to teleosts (common- and crucian carp), lactate concentrations are known to rise quickly in elasmobranchs tissues during periods of limited oxygen availability. Since dogfish showed increased lactate levels during the hypoxic phase of the experiments, anaerobic glycolytic ATP production was thus stimulated, probably to ensure a sufficient level of energy supply and hence, to increase the fish's survival capacity. Strikingly, we did not observe any significant lactate changes in hypoxic rectal glands and this is quite surprising since this gland exerts an important ionoregulatory function in sharks. More specifically, the rectal gland is an extrarenal organ in dogfish that excretes hypertonic sodium chloride into the water, throughout a coordination of ion transport processes which typically consume significant amounts of aerobically derived ATP (i.e. from ketone bodies) to fuel the high Na^+/K^+ ATPase activity but it may also have substantial anaerobic activity. As such, it is remarkable that we did not notice any significant changes in the levels of lactate and/or ATP/ADP/AMP concentrations when dogfish sharks were exposed to acute (2 h) and to longer periods of hypoxia (6 h). Are these results therefore likely indicative of an increased resistance of rectal glands to hypoxia, or was the level of hypoxia used in this study (i.e. 1 mg O_2/l) too low to induce significant changes in rectal gland metabolites? Accordingly, future studies are warranted to answer these questions.

Intimately associated with lactate metabolism, glucose and glycogen changes (glycolytic adaptations) are extensively described by many authors that investigated the anoxia/hypoxia responses in fish. Under normoxic conditions, 36 moles of ATP are produced aerobically in vertebrate cells by the oxidation of 1 mole of glucose (oxidative

phosphorylation). Anoxia, on the other hand, forces vertebrates to switch from aerobic to anaerobic energy metabolism i.e. up-regulation of anaerobic glycolysis (Pasteur effect) or other pathways relying on substrate phosphorylation. In that case, the only factor that eventually limits the anoxic survival time of an organism is the total exhaustion of its tissue glycogen/glucose store.

The major glycogen stores in mammalian vertebrates exist in liver and muscle, and to a lesser extent, in kidney, intestine and several other tissues. Recent studies, however, reported that the role of muscle glycogen, in contrast to liver glycogen, is limited (although not excluded) in the blood glucose regulation under anoxia. Therefore, future studies are needed to elucidate the significance of muscle glycogen dynamics in the anoxia tolerance of fish.

Glycogen is a vital energy storage for fish because it can be degraded for ATP production under reduced oxygen availability (hypoxia) or in complete absence of molecular oxygen (anoxia). For that reason, crucian carp exhibit an exceptionally enormous glycogen store in the liver which is the largest of any vertebrate studied. The combination of the seasonally-influenced and massive glycogen reserves in the liver as well as the unique ability to avoid a detrimental self-poisoning with waste end products is clearly one of the most effective strategies that crucian carp apply when facing anoxia. Common carp, however, do not produce ethanol after lethal anoxia exposure which significantly shortens their survival time to any exposure of oxygen concentrations below their aerobic capacity. It must also be noted that fish and other animals are limited in the capacity to store fermentable fuels (e.g. glucose and glycogen) because, unlike aerobic fuels as fat, these fuels are stored intracellularly, are hydrated and thus, occupy a larger space. Therefore, if metabolic depression is not induced to save the precious fermentable stores, a rapid depletion of the stored metabolic fuels occurs. Available data report that the glycogen content of the whole fish (a sum of muscle and liver glycogen) varies between 0.0 % and 0.67 %, and this is in the range of glycogen contents of humans (e.g. 0.7 % and 6-8 % for whole body glycogen stores and liver glycogen respectively). Strikingly, crucian carp deviate from this typical vertebrate pattern and can store glycogen reserves from 2 to 6.1 %, depending on the size of the fish, and up to 25-30 % of the liver wet mass is glycogen. In this study, anoxia exposure of crucian carp resulted in decreases of liver glycogen as a consequence of boosted glycolysis in anaerobic energy production.

In contrast to teleosts, which typically elevate their blood glucose levels following hypoxia (hyperglycaemia), the spiny dogfish (and epaulette shark) are unable to do this. Likewise, we noticed no significant changes in the tissue glucose levels of dogfish exposed to 2 h and 6 h of

hypoxia (except for the gills which showed decreased glucose concentrations after 2 h of hypoxia in relation to the controls). These data confirm that elasmobranchs have a rather limited ability to elevate the release of glucose to the blood during hypoxia.

Furthermore, ATP turnover during exposure to low or absent oxygen concentrations is, besides glycolysis, supported by phosphocreatine hydrolysis. Phosphocreatine (PCr) stores serve as highly mobilizable reserves of high-energy phosphates in muscle tissue. By donating its phosphate group to ADP to form ATP, it plays a major role in tissues that are metabolically active and highly energy-consuming such as the brain and muscle. In anoxia-tolerant vertebrates for instance, a depletion of phosphocreatine concentrations and an accompanied increase in creatine levels is described.

The results of the (phospho)creatine level measurements in crucian carp and common carp that were exposed to anoxia/hypoxia and to subsequent normoxic recovery were contradictory. As an example, we reported decreased phosphocreatine levels in the liver of anoxic crucian carp whereas common carp displayed increased muscle PCr levels under anoxia and decreased muscle PCr concentrations following hypoxia. An explanation for these confounding results might be found in the way the spectra were bucketed in this doctoral thesis. Concretely, spectra were automatically segmented into 0.05 ppm buckets between 0.5 and 10 ppm, a bucketing technique which is commonly applied in metabolomics studies of biological samples. Phosphocreatine and creatine resonances are situated next to each other in the muscle spectra and thus, are considered together (i.e. in one bucket) for subsequent statistical analysis. Possibly, decreased phosphocreatine levels and increased creatine levels were present in the tissues of both common- and crucian carp but due to their proximate NMR peaks in the spectra, statistical analysis was unable to reveal the significant changes in the levels of these individual metabolites.

Finally, anoxia exposure of common- and crucian carp resulted in decreased ATP levels in heart, muscle and liver (crucian carp) and in muscle (common carp). Remarkably, no significantly different changes were found in brain ATP levels when both fishes were subjected to anoxia. Previous studies on the brain metabolism of anoxic crucian carp already indicated that these fish are capable of surviving anoxia with the brain turned on. Especially in brain, the rate of ATP consumption is high and it is of vital importance to maintain its ATP levels for the proper functioning of neurons. Unlike turtles, which enter a comatose state during anoxia, crucian carp maintain brain ATP levels during anoxia, partially by reducing the ATP consumption. This strategy of metabolic depression provides benefits to crucian carp survival: brain ATP consumption is down-regulated to save energy but fish still remain

physically active under anoxia, although at a reduced level. This enables them to move to cooler or more aerated water when facing anoxia.

Similar to the crucian carp's brain, the common carp possibly employs metabolic depression to prevent any drastic fall in brain ATP levels. In this study, neither anoxia nor hypoxia changed the concentrations of ATP significantly in common carp brain extracts.

In addition to the earlier described differences in responses to hypoxia between teleost fishes and elasmobranches, a divergent role of ketone bodies is apparent during periods of stress (e.g. hypoxia). Generally, the metabolism of marine elasmobranchs such as the spiny dogfish is characterized by an increased reliance on ketone bodies as oxidative substrates (as alternative delivery source of acetyl CoA to extrahepatic tissues) and a low capacity for extrahepatic lipid oxidation. In this manuscript, this was evidenced by the observed decreases in acetoacetate concentrations of dogfish white muscles, exposed to 2 h- and to 6 h of hypoxia. Additionally, there was a trend observed for another ketone body i.e. 3-hydroxybutyrate which decreased after 2h of hypoxia (compared to the controls) in muscle. These results correspond well with other studies showing that elasmobranch muscles do not rely on lipid oxidation but, instead, they prefer to use ketone bodies as major oxidative fuels. The latter is in sharp contrast to the situation in teleosts where red muscle and heart heavily rely on fatty acid oxidation.

8.2 Amino acids and neurotransmitters

Anoxia-tolerant fish such as the crucian carp also rely on neurotransmitters and neuromodulators to suppress their energy use. As an important example, levels of GABA, the most abundant inhibitory transmitter in the vertebrate brain, increase when crucian carp encounter anoxia. The release of this inhibitory transmitter is accompanied by a decrease in (potentially harmful) excitatory transmitters such as glutamate. The antagonistic functioning of both compounds causes a neuronal depression, large enough to restore their brain ATP levels and to promote survival.

Here, we also observed an increase of GABA levels as well as a decrease in glutamate and glutamine levels in the brain extracts of anoxic crucian carp. Common carp, however, displayed different responses in these compound levels. GABA resonances were observed in the ^{1}H-NMR spectra of brain but statistical analysis revealed no significant changes. However, hypoxia resulted in significant changes in the levels of glutamate and glutamine: 1

week hypoxia induced higher glutamate and glutamine concentrations (when compared to the 24 h hypoxic group) in common carp brain. Additionally, we also observed a trend for decreases in glutamate and glutamine levels following 24 h of hypoxia (related to their controls). From these observations, we can conclude that, unlike crucian carp, common carp do not employ GABA-induced neuronal metabolism. Possibly, they apply another changed balance between GABA and other transmitter systems in the brain to withstand oxygen limitations.

The role of N-acetylaspartate (NAA) in anoxic/hypoxic fish brains is unclear. In this study, we found decreased NAA levels in the brain of crucian carp exposed to anoxia. N-acetylaspartate is synthesized and stored primarily in neurons and is considered to be an important marker of neuronal viability. In humans, for instance, decreased NAA levels are reported as a consequence of neurodegenerative diseases associated with neuronal loss (Alzheimer, etc.) or other brain pathology (e.g. schizophrenia). In the case of crucian carp, we suggest that the decreases in NAA might be the result of a decreased production of neuronal NAA and a possible loss of NAA from damaged neurons. Although crucian carp obviously are masters of anoxic survival, it cannot be excluded that anoxia leads to some neuronal damage or loss that is effectively repaired or restored upon reoxygenation. Moreover, we previously (Chapter 5) described that less important sensory functions are downregulated in the anoxic crucian carp brain (e.g. vision and hearing) so a temporally depression of certain brain centres functioning effectively occurs in these fish, potentially resulting in loss or damage of neurons. Secondly, NAA can act as a source of acetate, enabling the lipid and myelin synthesis in oligodendrocytes. Decreased NAA concentrations in brain may then reflect an attempt to diminish the extent of cell membrane damage during anoxia [Lardon *et al.* 2012].

In contrast to crucian carp, anoxia did not influence the NAA levels significantly in common carp brain. Significant changes in the levels of NAA were solely detected when 24 h hypoxic fish were compared to 1week hypoxic samples whereby the highest NAA-concentrations were observed in the 1 week hypoxic group. Since no significantly differences were found in the NAA-levels of 24 h and 1 week hypoxic samples (in comparison to their controls), no straightforward explanation can be provided for the higher concentrations of NAA in 1 week hypoxic fish (compared to the 24 h hypoxia group).

Contrary to the results of common- and crucian carp, no significant changes in brain metabolites were found when dogfish shark were subjected to hypoxia.

Furthermore, anoxia significantly increased the levels of branched-chain amino acids (BCAA) in all tissues of crucian carp. In contrast to these results, anoxic treatment of common carp did not change the BCAA-levels significantly in any of the studied tissue extracts.

These essential amino acids are key regulators in a number of essential processes such as growth and general metabolism. Of particular interest is leucine, playing an important role in heart muscle health and stimulating protein synthesis, cellular metabolism and cell growth. Likewise, isoleucine appears to be both glucogenic as well as ketogenic. The observed increase of the BCAA's in anoxic crucian carp tissues might therefore reflect a possible stop in oxidation by mitochondrial enzymes under anaerobic tissue conditions. Alternatively, increased BCAA's can also be the result of a reduced consumption, i.e. protein synthesis suppression (which is commonly employed in anoxia-tolerant animals).

Hypoxia exposure of common carp, however, decreased the BCAA concentrations in all tissues. In contrast to anoxia, hypoxia still allows some aerobic processes to function. Therefore, it might be postulated that common carp rather suppress any energy-consuming processes such as protein synthesis during anoxic periods while hypoxia on its turn will stimulate them to use BCAA's as metabolic fuels for oxidative metabolism (indicated by the decreased levels of BCAA's in all tissues).

Similar to the results of hypoxic common carp, hypoxia also induced decreased levels of BCAA's valine and isoleucine in the white muscle tissue of marine dogfish. In tissues where lipids are not oxidized and this is indeed the case for elasmobranchs red and white muscle, the possibility exists that other fuels such as amino acids (i.e. BCAA's) could substitute for oxidative substrates when aerobic metabolism is constrained.

8.3 Other metabolites

In this thesis, ^{1}H-NMR spectroscopy offered a unique insight in the biochemical profiles of various tissue responses of different fish species, coping with oxygen-diverse habitats. Besides the confirmation of previously reported metabolic changes in carp species following diverse oxygen regimes, we also found novel metabolites, i.e. compounds that were unrecognized to play a role in vertebrate anoxia/hypoxia tolerance mechanisms.

These include myo-inositol (crucian carp, spiny dogfish), taurine (crucian carp, spiny dogfish), scyllo-inositol (common carp), trimethylamine oxide (TMAO) and oxypurinol (spiny dogfish).

As a consequence of oxygen depletion, myo-inositol levels decreased in the heart of crucian carp. The exact function of this metabolite is not well understood, although it is believed to be an essential element for cell growth, an osmolite, a glial marker and a storage form for glucose. Indeed, if the latter is the case, myo-inositol reserves might act as extra glucose stores, providing energy in times of energy deficits (i.e. anoxia). Remarkably, myo-inositol decreased in heart, a metabolically active and highly energy-consuming tissue. Especially in this central organ, it is extremely important to maintain an ATP balance and glucose is hereby the most important metabolic fuel in brain. Also in marine dogfish sharks, significant changes in the myo-inositol levels were noticed for gills (decreased concentrations) and rectal gland (increased concentrations) when they were exposed to hypoxia. Bearing in mind that osmoregulation is even more important in dogfish due to their marine environment and their inherent high blood urea concentrations, a potential role for myo-inositol in restoring osmolarity (particularly in two important osmoregulatory organs as gills and rectal gland) can be present under hypoxic conditions.

Furthermore, taurine was significantly reduced in the liver of anoxic crucian carp. A first decrease of taurine was noticed after 24 h of anoxia and the concentration continued to decrease after 1 week of anoxia. Similar to BCAA's, taurine is an amino acid with important metabolic functions: it has antioxidative and membrane-stabilizing properties, is a natural calcium antagonist and osmoregulator and is essential for the development and function of skeletal muscle. It also modulates the immune response, regulates the transport of ions, signal transduction, cell proliferation and DNA repair. The decrease of taurine observed in this study might be due to the augmented consumption of this polyfunctional and beneficial amino acid in anoxic muscles. Additionally, decreased taurine levels were also observed in muscle extracts of hypoxic dogfish whereas increases in taurine were noticed in their rectal glands.

However, less information is known about the exact function of scyllo-inositol, also called 'scyllitol'. In common carp, different responses of various tissues were observed as a result of anoxia/hypoxia exposure. In muscle, anoxia and acute hypoxia both induced decreased scyllo-inositol levels while chronic hypoxia resulted in elevated concentrations. In heart, on the other hand, acute and chronic hypoxia resulted in higher scyllo-inositol concentrations. Elevated scyllo-inositol levels are commonly found in brains of Alzheimer's

patients or in case of amnestic mild cognitive impairment. The exact function of scyllo-inositol in other tissues than brain remains unclear and more studies are needed to explore its role in fish metabolism.

Lastly, ^{1}H-NMR spectroscopy of spiny dogfish tissues displayed some characteristic elasmobranchs features such as the presence of TMAO, a methylamine which is commonly present in these fish. In this study, increased TMAO levels were observed in 2 h hypoxic gills as well as in 2 h and 6 h hypoxic muscles and it has been hypothesized that methylamines may serve as counteracting solutes to combat the potentially destabilizing effects of typically high urea concentrations in the blood and tissues of these animals.
Furthermore, we also reported decreased levels of oxypurinol in white muscle following hypoxia in dogfish. Oxypurinol is a xanthine oxidase inhibitor, hereby inhibiting the enzymatic generation of reactive oxygen species (ROS) by xanthine oxidase. In the present context of tissue hypoxia, we suggested that oxypurinol was used increasingly in muscle to combat the negative effects of ROS formation following hypoxia and normoxic reoxygenation and/or to allow for maintained, proper contraction efficiency in periods of limited oxygen supply.

We can conclude this doctoral thesis by stating that, despite the wealth of information available on the metabolic and molecular responses of a variety of fish species, we are still far from a unified concept of the major adaptations underlying anoxia/hypoxia tolerance. Fish are ideal model systems to understand the selection of traits that enable the tolerance to anoxia/hypoxia due to the extremely O_2-diverse environments they inhabit. Experimental results of comparative studies in different fish species, however, should be interpreted rigorously, being aware of complex influences of tissue-specific and species-specific differences, and other interfering factors as temperature, the magnitude and length of hypoxia exposure, seasonal and pH fluctuations, etc.

Nevertheless, due to the inherent complex biodiversity of the aquatic world and its inhabitants, future comparative studies of hypoxia- and anoxia tolerant animals will undoubtedly offer more insights in the underlying mechanisms that enable vertebrates to deal with oxygen deprivation.

Chapter 9
Future perspectives

As mentioned before, aquatic hypoxia constitutes one of the most critical problems in the world and the occurrence of this threat will likely increase as a consequence of continuing anthropological activities. Therefore, the study of fish and their strategies to survive depleted oxygen environments is needed to understand the potential effects of reduced oxygen concentrations on different levels of an organism.

In this doctoral thesis, we focussed on the anoxia/hypoxia tolerance mechanisms of two fresh water fish species (crucian- and common carp) and one marine fish (the spiny dogfish shark) and the obtained results offer some interesting insights in the heterogeneous strategies of different fish and the inter- and intraspecies specific responses. In addition, the subsequent topics are recommended for future research to complete and thus, to improve our understanding of how vertebrates survive fluctuations of aquatic oxygen levels.

In this thesis, we mainly studied the aqueous (hydrophilic, polar) tissue extracts of fish by ^{1}H-NMR, except for the crucian carp where we examined both hydrophilic and lipophylic tissue extracts. It might be interesting to explore the lipidomic profiles of the common carp and the dogfish shark as well since these results can offer more information on the differential role of lipids in both fishes e.g. as source of energy supply. In order to do so, a further optimization of the statistical techniques will be required since shifts in the apolar spectra of fish occurred in this work. Furthermore and accompanying, of special interest in sharks is the ketone metabolism. Marine elasmobranchs hereby differ from teleosts due to their increased reliance on ketones as sources of energy and by studying ketone metabolic pathways following oxygen deprivation and subsequent reoxygenation, a more integral picture of their hypoxia adaptations can be provided.

Another interesting topic for future research involves the phylogenetic relationships of hypoxia adaptations in different fish lineages. In this thesis, we briefly discussed this subject in Chapter 1 but prospective studies on the evolutionary analysis of hypoxia defense mechanisms in different fishes are urgently needed and researchers in the field are waiting for this work with high interest. Additional animal model species might then be discovered in the near future that provide a better knowledge about the catastrophically hypoxia-related diseases in humans as stroke, myocardial and cerebral ischemia, chronic obstructive pulmonary disease, etc.

Lastly, some papers already described the effects of dual tolerances to several stressors in fish. For example, the combined effects of hyperammonemia and hypoxia/anoxia were

studied in fish and future studies may examine the effects of e.g. temperature and anoxia/hypoxia in fish as well. In reality, fish are likely to encounter several ambient stressors simultaneously so this research is very ecologically relevant.

Chapter 10
Nederlandstalige samenvatting

Zuurstof (O_2) is een ogenschijnlijk simpel element vanuit chemisch perspectief maar ontontbeerlijk voor elke vorm van biologisch leven op deze aarde. Door de grote inherente zuurstoffluctuaties in het aquatische milieu zijn vissen in het bijzonder, één van de belangrijkste modelorganismen om effecten van verminderde zuurstofconcentraties (hypoxie) en/of zelfs de totale afwezigheid van zuurstof (anoxie) te kunnen onderzoeken. Er zijn ongeveer 20.000 verschillende vissoorten en allen varieren ze sterk in hun capaciteit en strategie om anoxie/hypoxie te tolereren en te overleven. Vooral in het zoetwater milieu, dat gekenmerkt wordt door grote verschillen in zuurstofconcentraties, is zuurstof een van de meest potente evolutionaire drijfkrachten geweest voor het ontwikkelen van unieke adaptieve tolerantiemechanismen in vissen.

Bovendien is het probleem van anoxie/hypoxie ook bijzonder actueel: door de toenemende milieuvervuiling als een gevolg van menselijke activiteiten en de daarmee onlosmakelijk verbonden 'global climate change' problematiek zal hypoxie alleen maar toenemen in frequentie, verspreding en magnitude. Bijgevolg is het uiterst ecologisch relevant om de strategieën, die vissen toelaten anoxie en hypoxie te overleven, van naderbij te bestuderen. Vanuit medisch standpunt geldt hier zelfs nog een grotere relevantie: mensen kunnen immers slechts enkele luttele minuten zonder zuurstof overleven omdat onze vitaalste organen zoals hersenen en hart slechts optimaal functioneren bij een voldoende hoge zuurstofconcentratie. Wanneer hypoxie dan effectief gebeurt, bijvoorbeeld bij beroertes of verstikking, resulteert dit vaak in desastreuse gevolgen zoals irreversiebele hersenschade of kan dit zelfs leiden tot de dood.

Ondanks het feit dat intolerantie voor anoxie en hypoxie een algemene regel blijkt te zijn voor de meerderheid der vertebraten, blijken er toch een aantal uitzonderingen te bestaan in het dierenrijk. Meer specifiek bestaan er een aantal Noord-Amerikaanse zoetwater schildpadden (Genera *Trachemys* and *Chrysemys*) alsook enkele vissoorten die moeiteloos kunnen overleven in extreme, zuurstofarme tot anoxische wateren. De best gekende vissoorten zijn hierbij de kroeskarper (*Carassius carassius*), de goudvis (*Carassius auratus*) en een tropische rifhaai (*Hemiscyllium ocellatum*).

Wanneer vissen daadwerkelijk geconfronteerd worden met anoxie/hypoxie, zullen zij hierop anticiperen door middel van fysiologische, ethologische, biochemische en moleculaire responses die enerzijds de zuurstofopname uit hun omgeving zullen bevorderen en/of anderzijds de potentieel negatieve effecten van zuurstofgebreken kunnen minimaliseren.

Tijdens dit doctoraat werden de metabolome weefselresponsen (*Metabolomics*) van zoetwater- en zoutwater vissen bestudeerd door middel van ^{1}H-NMR.

De techniek van 'Metabolomics' is relatief nieuw en werd voor het eerst gedefinieerd in 1998 als de kwantitatieve meting van alle laagmoleculaire moleculen (metabolieten) die voorkomen in cellen. Door het bestuderen van de aanwezige metabolieten in cellen, weefsels, organen, lichaamsvloeistoffen (het metaboloom) van een organisme kan op die manier een gedetailleerd inzicht beeld verkregen worden in het biochemisch profiel en bijgevolg in fysiologische toestand van dat organisme op dat bepaalde moment.

In deze doctorale thesis werden metabolieten bekomen van verscheidene weefsels aan de hand van extracties waarbij verschillende extractieprocedures eerst nauwkeurig werden getest en geëvalueerd tijdens het eerste jaar van het onderzoek. Immers, elk weefsel is uniek en verschilt structureel als functioneel van andere weefsels. Vandaar is het van uiterst belang om een gepaste extractiemethode te gebruiken die toelaat om een zo hoog mogelijke kwantititeit alsook kwaliteit van de bekomen metabolieten te bereiken. Voor de detectie van weefselmetabolieten werd hier gebruik gemaakt van NMR of nucleaire magnetische resonantie spectroscopie. Meer informatie omtrent deze analysetechniek kan gevonden worden in Hoofdstuk 2 van dit manuscript.

In dit onderzoek werden de metabolome anoxie/hypoxie strategieën van 3 vissen bestudeerd: de extreem anoxie-tolerante kroeskarper (*Carassius carassius*), de middelmatig hypoxie-tolerante gewone karper (*Cyprinus carpio*) en de doornhaai (*Squalus acanthias*). Beide karpersoorten leven in zoetwater en zijn nauw verwant aan elkaar. Toch verschillen zij sterk in hun mechanismen om lage tot afwezige zuurstofconcentraties in het water te overleven. Doornhaaien leven zowel in zeewater als in brakwater en komen, door hun migratie patroon, frequent in contact met hypoxie. In vergelijking met de veelvuldig beschreven adaptatiemechanismen van de kroes-en gewone karper, is relatief weinig informatie is voorhanden omtrent de anoxie/hypoxie strategieën in doornhaaien (en haaien in het algemeen).

Door het vergelijken van de metabolomics van zoetwatervissen onderling en met deze van mariene haaien, werd getracht een globaal beeld te verkrijgen over de gelijkenissen en verschillen in hun tolerantie t.o.v. beperkte zuurstofconcentraties. Het bestuderen van primitieve vertebraten zoals haaien, die sinds eeuwen in onze oceanen zwemmen, biedt bovendien de mogelijkheid om de conservatieve karakteristieken van hun evolutionaire

fysiologie te bestuderen van waaruit verdere adaptieve mechanismen zijn geëvolueerd in daarna ontwikkelde vissoorten.

Hoofdstuk 1 van dit manuscript omschrijft het hedendaags en wereldwijd probleem van anoxie/hypoxie en aansluitend worden onze vooropgestelde onderzoeksdoelen besproken.

Hoofdstuk 2 omvat een algemene introductie en omschrijft de 3 bestudeerde vissoorten die gedetailleerd werden onderzocht in dit doctoraat. Een overzicht wordt hier gegeven van hun diverse strategieën t.o.v. gelimiteerde zuurstofconcentraties. Vervolgens wordt de techniek van Metabolomics uitvoerig aangehaald alsook het gebruik van NMR voor de detectie van het metaboloom van vissen.

Hoofdstuk 3 beschrijft de nauwkeurige evaluatie en selectie van een efficiënte extractiemethode die toelaat om zoveel mogelijk verschillende soorten metabolieten te kunnen opsporen in de weefsels van de onderzochte vissen. Op basis van de huidige litaratuurgegevens werd geopteerd om de perchloorzuurextractie alsook de methanol/chloroform/water extracties te testen.

Hoofdstuk 4 verschaft een inzicht in de ontwikkeling en opbouw van een NMR database die een correcte identificatie van de gevonden metabolieten in dit onderzoek kan vereenvoudigen en verifiëren.

Hoofdstuk 5 handelt over het anoxie-experiment in kroeskarpers (*Carassius carassius*) dat werd uitgevoerd aan de Universiteit van Oslo. Een uitgebreide spectroscopische analyse van hydrofiele als lipofiele biochemische profielen van vier verschillende weefsels (hersenen, hart, lever en spier) wordt hier besproken alsook de diverse statistische analysemethoden (univariate en multivariate statistiek, netwerkmodellen, etc.) van deze complexe datasets. Er werd onder meer aangetoond dat anoxie een duidelijk invloed heeft gehad op de metabolieten die geassocieerd zijn met het algemene energiemetabolisme (vb. Glucose, melkzuur, fosfocreatine, etc.) alsook op de concentraties van bepaalde aminozuren en neuromodulatoren zoals glycine, GABA, glutamaat en glutamine. Bovendien en belangrijker, bood ^{1}H-NMR de mogelijkheid om nieuwe (voordien nog niet beschreven) metabolieten te detecteren die een rol spelen tijdens periodes van anoxie zoals myo-inositol in hart en taurine in spierweefsel.

Aansluitend werd een anoxie/hypoxie-experiment uitgevoerd in de nauw verwante, gewone karper (*Cyprinus carpio*) aan de Universiteit van Antwerpen (**Hoofdstuk 6**). Om vervolgens een correcte vergelijking met het metaboloom van de anoxie-tolerante kroeskarper mogelijk te

maken, werden de ^{1}H-NMR experimenten van identieke weefsels (hersenen, hart, lever en spier) alsook de statistische analyses op dezelfde manier uitgevoerd voor datasets van de gewone karper. Ook hier werden veranderingen in het energiemetabolisme vastgesteld alsook fluctuaties in de concentraties van aminozuren en transmitters tengevolge van een afwezige (anoxie) of lage zuurstofconcentraties (hypoxie). Bovendien werd, met ^{1}H-NMR, twee nieuwe metabolieten aangetoond in weefsels van de gewone karper, meer bepaald scyllo-inositol en myo-inositol. Finaal wordt in dit hoofdstuk een eerste vergelijking gemaakt van de belangrijkste gelijkenissen en verschillen in de anoxie/hypoxie tolerantiemechanismen van beide zoetwater karpersoorten.

Hoofdstuk 7 beschrijft het metaboloom van een mariene doornhaai die werd blootgesteld aan hypoxie aan het Bamfield Marine Sciences Centre in Canada. Opnieuw werden weefselextracten (hersenen, kieuwen, lever, spier en rectale klier) onderzocht d.m.v. ^{1}H-NMR en onderworpen aan univariate en multivariate statistiek. Dit resulteerde in een aantal algemene bevindingen zoals de veranderingen in metabolieten van het energie- en eiwitmetabolisme maar bovendien werden resultaten bekomen die specifiek gelinkt zijn aan het metabolisme van haaien. Zo werden metabolieten gedetecteerd die van specifiek belang zijn in de ionhomeostase van deze dieren zoals TMAO. Andere metabolieten blijken dan weer een mogelijks positieve rol te spelen als anti-oxidanten die haaien kunnen beschermen tijdens periodes van stress (hypoxie).

Tenslotte wordt in **Hoofdstuk 8** een uitgebreid overzicht weergegeven van de bekomen bevindingen in de 3 bestudeerde vissen van waaruit voorzichtige conclusies worden getrokken omtrent hun tolerantiemechanismen. Hieruit blijkt dat waakzaamheid is geboden bij het interpreteren van deze resultaten, mede door de complexiteit van de inter- en intraspecies verschillen die heersen in vissen.

Tenslotte komen enkele aanbevelingen voor toekomstig onderzoek in aanmerking (**Hoofdstuk 9**).

We besluiten deze doctorale thesis met de conclusie dat ^{1}H-NMR doeltreffend was om het metaboloom van zoetwater- en mariene vissen te exploreren teneinde significante metabolieten te vinden die een rol spelen in hun anoxie/hypoxie adaptaties. Bovendien werden, in dit onderzoek, een aantal nieuwe metabolieten gedetecteerd die een nieuw licht kunnen werpen op de tolerantiemechanismen van vissen tov beperkte zuurstofconcentraties in hun ecosystemen. Finaal kunnen deze resultaten bijdragen tot een uitbreiding van de huidige

kennis omtrent de oorzaken van humane hypoxie-gerelateerde ziekten die mogelijks kunnen leiden tot efficiëntere therapieën.

De resultaten van dit werk werden ingediend in diverse vaktijdschriften en gepresenteerd op (inter)nationale congressen. De ingezonden manuscripten maken integraal deel uit van de Engelstalige tekst van dit doctoraatsproefschrift.

Supplementary Information

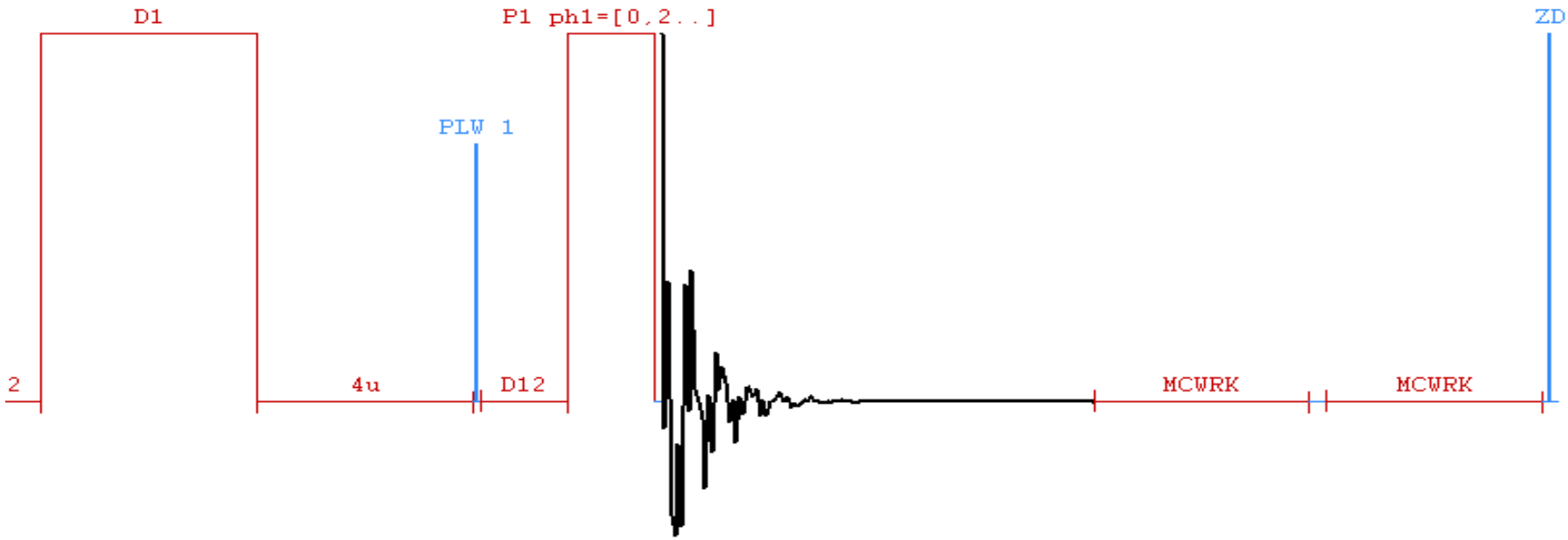

Graphical representation of the **ZGPR** pulse program

D_n: recycling delay (sec) – PLW: power level (Watt) – P_n: pulse (µsec)

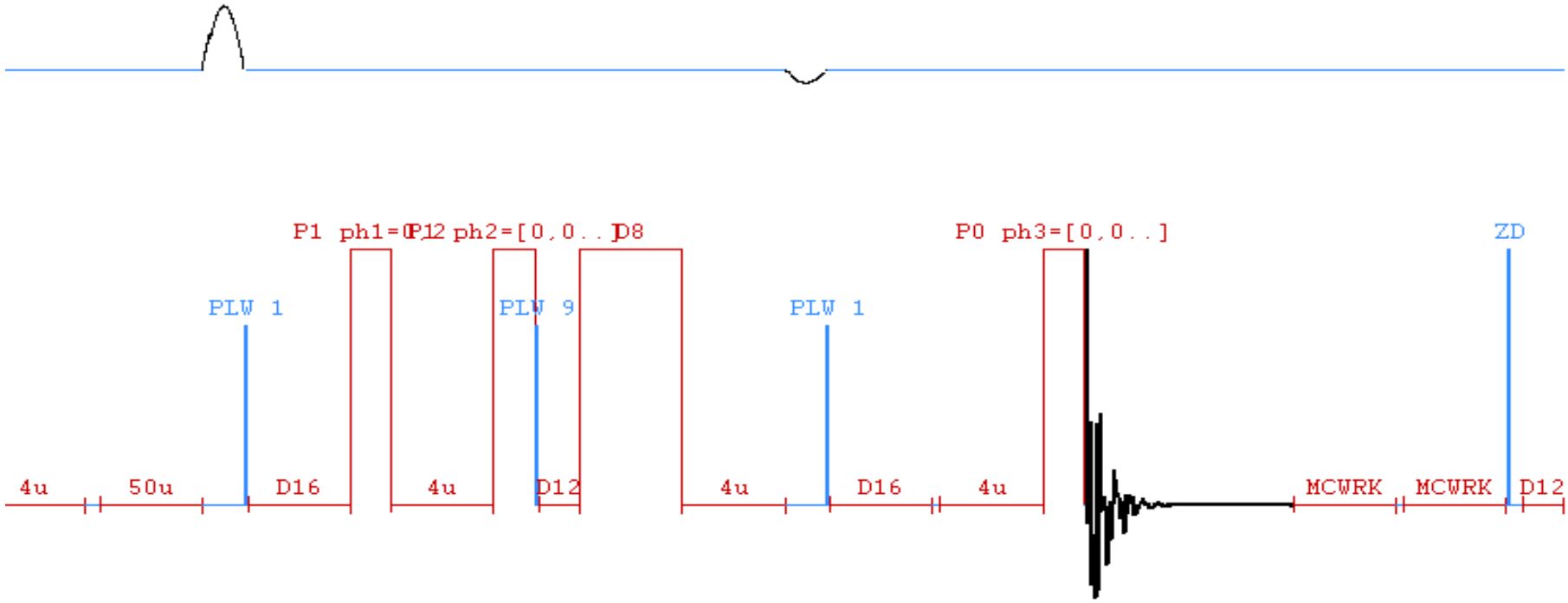

Graphical representation of the **1D NOESY** pulse program

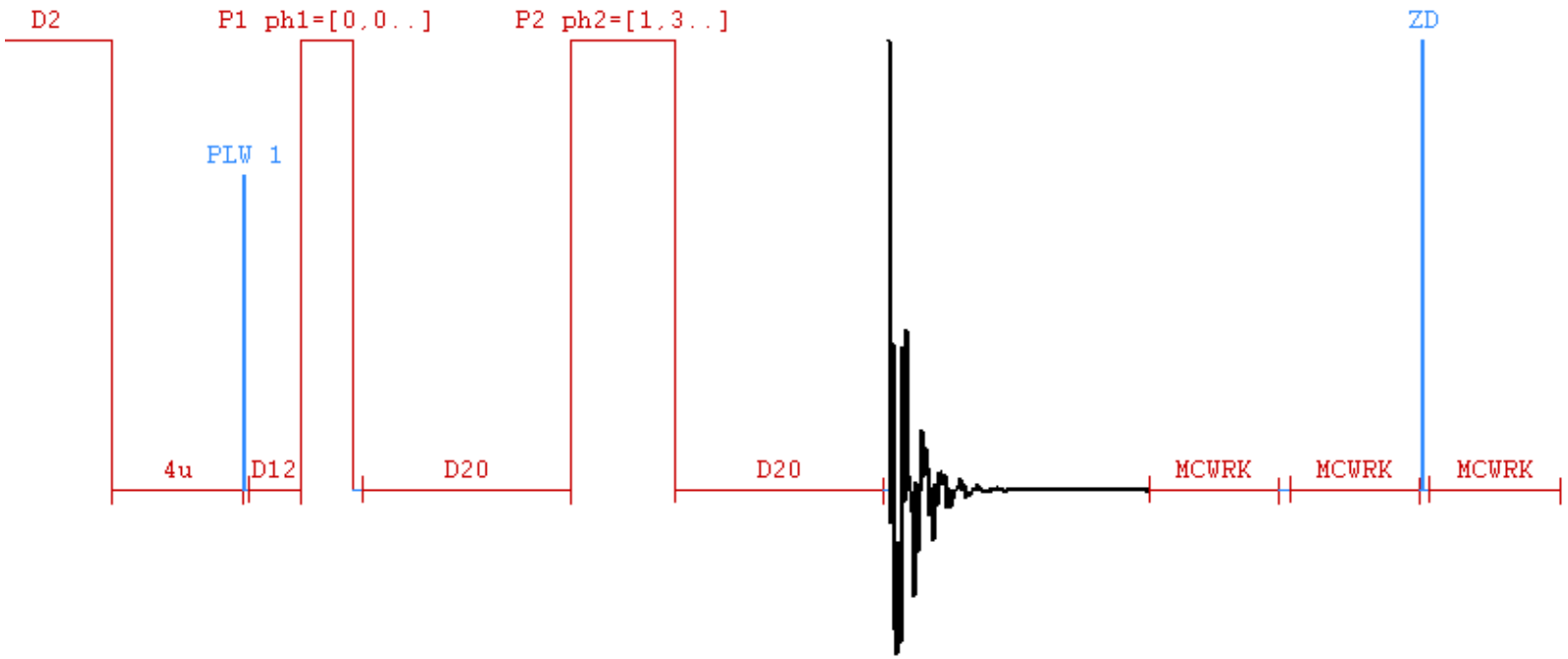

Graphical representation of the **CPMG** pulse program

Presentations, Publications & Research Stays

1. (Poster) Presentations & Conferences

National

- 7th Young Belgian Magnetic Resonance Scientists Congres (YBMRS), Brussel, Belgium, 21-11-2008
- Statistics at Antwerp III: multivariate statistical analysis, UA, Belgium, 26-01-2009
- First Belgian Symposium on Metabolomics and Metabonomics, Mons, Belgium, 30-01-2009
- StatUA, Statistical methods in (pre)clinical trials, UA, Belgium, 10-11-2009
- Bruker NMR workshop: Small molecule characterization with complete molecular confidence, Brussel, Belgium, 12-11-2009
- StatUA 2010: Statua day for users of statistical methods, UA, Belgium, 01-02-2010
- 10th Flemish Youth Conference of Chemistry, Blankenberge, Belgium, 01 & 02-03-2010
- Workshop 'How to write a world class paper', organized by Elseviers, UA, Belgium, 08-10-2010
- 9th YBMRS Congres, Brussel, Belgium, 26-11-2010

International

- NMR Bruker workshop, Lyon, France, 27-04-2008
- Metabomeeting 2008, Lyon, France, 28 & 29-04-2008: Poster presentation
- EU-NMR workshop: NMR-based Metabolomics, European Centre Lyon, 30-04-2008
- Seminar Multivariate Analysis, Amsterdam, The Netherlands, 08 & 09-05-2008
- SEB annual Congres, Marseille, France, 6 till 10-07-2008: Poster presentation
- BeNeLux NMR User Meeting, Eindhoven, The Netherlands, 14-11-2008
- SEB annual Congres, Prague, Czech Republic, 30-06 till 03-07-2010: Poster presentation

2. Publications

- **^{1}H-NMR study of the metabolome of an exceptionally anoxia tolerant vertebrate, the crucian carp (*Carassius carassius*)** (I. Lardon, G. Nilsson, J. A.W. Stecyk, T.N. Vu, K. Laukens, R. Dommisse, G. De Boeck).

  Metabolomics, DOI 10.1007/s11306-012-0448-y.

- **Metal accumulation and metallothionein induction in the spotted dogfish *Scyliorhinus canicula*** (G. De Boeck, M. Eyckmans, I. Lardon, R. Bobbaers, A.K. Sinha, R. Blust).

  Journal of Comparative Biochemistry and Physiology, Part A 155, 503-508.

- **Physiological effects of waterborne lead exposure in spiny dogfish (*Squalus acanthias*)** (M. Eyckmans, I. Lardon, C. Wood, G. De Boeck).

  Accepted for publication in ***Aquatic Toxicology***.

- **Methanol/Chloroform/Water extraction to be preferred over Perchloric acid extraction for the ^{1}H-NMR-based metabolomic analysis of white muscle and liver extracts in fish** (I. Lardon, G. De Boeck, R. Dommisse).

  Under review in the ***Journal of Mediterranean Chemistry***.

- **^{1}H-NMR study of the metabolome of a moderately hypoxia-tolerant fish, the common carp (*Cyprinus carpio*)** (I. Lardon, M. Eyckmans, T. N. Vu, K. Laukens, G. De Boeck, R. Dommisse).

  Submitted to ***Metabolomics***.

- **^{1}H-NMR based Metabolomics of tissue extracts of the hypoxic spiny dogfish (*Squalus acanthias)***. (I. Lardon, M. Eyckmans, R. Dommisse, G. De Boeck).

  In preparation for ***Metabolomics***.

3. International Research Stays

- **Bruker Biospin, Switzerland - Avance 1D/2D Training on High Resolution NMR**

  High resolution 1D and 2D NMR experiments: theoretical background and practical sessions.

  From 02-03 till 06-03-2009

- **University of Oslo, Norway - Department of Molecular Biosciences**
  Anoxia experiments in crucian carp (*Carassius carassius*) in cooperation with Prof. dr. Göran Nilsson.

  Resulting publication: "^{1}H-NMR study of the metabolome of an exceptionally anoxia tolerant vertebrate, the crucian carp (*Carassius carassius*)"

  From 06-04 till 15-04-2009

- **Bamfield Marine Sciences Centre, British Colombia, Canada**

  Hypoxia experiments in Pacific spiny dogfish sharks (*Squalus acanthias*) in cooperation with Prof. dr. Chris Wood.

  Resulting publication: "^{1}H-NMR based Metabolomics of tissue extracts of the hypoxic spiny dogfish (*Squalus acanthias)*"

  From 05-07 till 03-08-2009

Bibliography

Åberg K.M., Alm E., Torgrip R.J.O. (2009). The correspondence problem for metabonomics datasets. *Journal of Analytical and Bioanalytical Chemistry* 394, 151–162.

Akiyama K., Chikayama E., Yuasa H., Shimada Y., Tohge T., Shinozaki K., Yokota Hirai M., Sakurai T., Kikuchi J., Saito K. (2008). PRIMe: a Web site that assembles tools for metabolomics and transcriptomics. *Silico Biology* 8, 339–345.

Anderson P. M. (1991). Glutamine-dependent urea synthesis in elasmobranch fishes. *Biochem. Cell Biol.* 69, 317-319.

Ballantyne J. S., Chamberlin M. E., Singer T. D. (1992). Oxidative metabolism in thermogenic tissues of the swordfish and mako shark. *Journal of Experimental Zoology* 261, 110-114.

Ballantyne J. S. (1997). Jaws: the inside story. The metabolism of elasmobranch fishes. *Comp. Biochem. Physiol.* 118B, 703-742.

Ballantyne J.S., Speers-Roesch B. (2006). Metabolic organization of freshwater, euryhaline, and marine elasmobranchs: implications for the evolution of energy metabolism in sharks and rays. *Journal of Experimental Biology* 209, 2495-2508.

Barnes D.W. (2012). Cell and molecular biology of the spiny dogfish *Squalus acanthias* and little skate *Leucoraja erinacea*: insights from *in vitro* cultured cells. *Journal of Fish Biology* 80, 2089-2111.

Bedford J. J., Harper J. P. L., Smith R.A.J. (1998). Identification and measurement of methylamines in elasmobranch tissues using proton nuclear magnetic resonance (^{1}H-NMR) spectroscopy. *Journal of Comparative Physiology B* 168, 123-131.

Bellamy D., Petersen J.A. (1968). Anaerobiosis and the toxicity of cyanide in turtles. *Comp. Biochem. Physiol.* 24, 543-548.

Benjamini Y, Hochberg Y. (1995) Controlling the false discovery rate: a practical and powerful approach to multiple testing. *Journal of the Royal Statistical Society* - Series B 57 (1):289–300.

Bickler P.E., Buck L.T. (2007). Hypoxia tolerance in reptiles, amphibians, and fishes: life with variable oxygen availability. *Annu. Rev. Physiol*. 69, 145-70.

Blow N. (2008). Biochemistry's new look. *Nature* 455(2).

Bouchereau A, Guenot P, Lather F (2000). Analysis of amines in plant materials. *Journal of Chromatography* B (747), 49-67.

Bruice P.Y. (2004). Organic Chemistry. Fourth edition, Pearson Education Inc., NJ.

Bundy J.G., Papp B., Harmston R., Browne R.A., Clayson E.M., Burton N., Reece R.J., Oliver S.G., Brindle K.M. (2007). Evaluation of predicted network modules in yeast metabolism using NMR-based metabolite profiling. *Genome Res* 17, 510-519.

Canelas A.B., ten Pierick A., Ras C., Seifar R.M., van Dam J.C., van Gulik W.M., Heijnen J.J. (2009). Quantitative evaluation of intracellular metabolite extraction techniques for yeast metabolomics. *Anal Chem* 81(17), 7379-89.

Carlson J.K. (1998). The physiological ecology of the bonnethead shark, *Sphyrna tiburo*, blacknose shark, *Carcharhinus acronotus*, and Florida smoothhound shark, *Mustelus norrisi*:effects of dissolved oxygen and temperature. Ph.D. Thesis, University of Mississippi, Oxford. 106 pp.

Carlson J.K., Parsons G.R. (2001). The effects of hypoxia on three sympatric shark species: physiological and behavioural responses. *Environmental Biology of Fishes* 61, 427-433.

Cascante M., Boros L.G., Comin-Anduix B., de Atauri P., Centelles J.J., Lee P.W.N. (2002). Metabolic control analysis in drug discovery and disease. *Nature Biotechnology* 20, 243 – 249.

Cascante M., Marin S. (2008). Metabolomics and fluxomics approaches. *Essays Biochem.* 45, 67–82.

Chatham J.C. (2002). Lactate – The forgotten fuel! *Journal of Physiology* 542 (2), 333.

Cheng L.L., Ma M.J., Becerra L. (1997). Quantitative neuropathology by high resolution magic angle spinning proton magnetic resonance spectroscopy. *Proceedings of the national academy of sciences of the United States of America*, 94 (12), 6408-6413.

Chih C.P., Rosenthal M., Sick T.J. (1989). Ion leakage is reduced during anoxia in turtle brain: a potential survival strategy. *Am. J. Physiol*. 255, R338-R343.

Choi J.K., Dedeoglu A., Jenkins B.G. (2007). Application of MRS to mouse models of neurodegenerative illness. *NMR in biomedicine*, 20, 216-237.

Claireaux G., Chabot D. (2005). A review of the impact of environmental hypoxia on fish: the case of Atlantic cod. *Comparative Biochemistry and Physiology* A – Molecular & Integrative Physiology 141 (3), S177-S177.

Coen M., Lenz E.M., Nicholson J.K., Wilson I.D., Pognan F., Lindon J.C. (2003). An integrated metabonomic investigation of acetaminophen toxicity in the mouse using NMR spectroscopy. *Chemical Research in Toxicology*, 16 (3), 295-303.

Connett R.J., Honig C.R., Gayeski T.E.J., Brooks G.A. (1990). Defining hypoxia: a systems view of V_{O2}, glycolysis, energetic, and intracellular P_{O2}. *J. Appl. Physiol*. 68, 833-842.

Crocker C.E., Ultsch G.R., Jackson D.C. (1999). The physiology of diving in a north-temperate and three tropical turtle species. *Comp. Biochem. Physiol*. B169, 249-255.

De Boeck G., Vlaeminck A., Van der Linden A., Blust R. (2000). Salt stress and resistance to hypoxic challenges in the common carp (*Cyprinus carpio* L.). *Journal of Fish Biology* 57 (3), 761-776.

Diaz R.J., Breitburg D.L. (2009). The hypoxic environment. In *Hypoxia* (Ed. Richards J.G., Farrell A.P., Brauner C.J.), 1-23. San Diego: Elsevier.

Dowd W.W., Renshaw G.M.C., Cech J.J., Kültz D. (2010). Compensatory proteome adjustments imply tissue-specific structural and metabolic reorganization following episodic hypoxia or anoxia in the epaulette shark (*Hemiscyllium ocellatum*). *Physiological Genomics* 42, 93-114.

Du P., Kibbe W.A., Lin S.M. (2006). Improved peak detection in mass spectrum by incorporating continuous wavelet transform-based pattern matching. *Bioinformatics* 22 (17), 2059-2065.

Dunn W.B., Bailey N.J.C., Johnson H.E. (2005). Measuring the metabolome: current analytical technologies. *Analyst* 130, 606-625.

Ekman D.R., Teng Q., Villeneuve D.L., Kahl M.D., Jensen K.M., Durhan E.J., Ankley G.T., Collette T.W. (2008). Investigating compensation and recovery of fathead minnow (Pimephales promelas) exposed to 17α-ethynylestradiol with metabolite profiling. *Environmental Science & Technology* 42 (11), 4188-419.

Ekman D.R., Teng Q.N., Villeneuve D.L., Kahl M.D., Jensen K.M., Durhan E.J., Ankley G.T., Collette T.W. (2009). Profiling lipid metabolites yields unique information on sex- and time-dependent responses of fathead minnows (*Pimephales promelas*) exposed to 17 alpha-ethynylestradiol. *Metabolomics* 5 (1), 22-32.

Fan T.W.M. (1996). Metabolite profiling by one- and two-dimensional NMR analysis of complex mixtures. *Progress in Nuclear Magnetic Resonance Spectroscopy* 28, 161-219.

Fan T.W.M., Higashi R.M., Lane A.N. (2006). Integrating metabolomics and transcriptomics for probing Se anticancer mechanisms. *Drug Metab Rev* 38, 707-732.

Fernandez X, Rammouz RE, Létisse F, Durand S, Portais JC, Moussa ZW. (2010).

Analysis of skeletal muscle metabolome: Evaluation of extraction methods for targeted metabolite quantification using liquid chromatography tandem mass spectrometry.

Anal Biochem, 398(2), 169-177.

Fiehn O. (2001). Combining genomics, metabolome analysis, and biochemical modelling to understand metabolic networks. *Comp Funct Genom* 2, 155-168.

Fiehn O., Weckwerth W. (2002). Can we discover novel pathways using metabolomic analysis? *Biotechnology* 13, 156-160.

Gao J., Tarcea V.G., Karnovsky A. (2010). Metscape: a Cytoscape plug-in for visualizing and interpreting metabolomic data in the context of human metabolic networks. *Bioinformatics*, 26 (7), 971-973.

Gilmour K.M., Perry S.F. (2007). Branchial chemoreceptor regulation of cardiorespiratory function. *Fish Physiology* 25, *Sensory Systems Neuroscience* (ed. Zielinski B., Hara T.J.), 97-151. San Diego: Academic Press.

Gomase V. S., Changbhale S. S., Patil S. A., Kale K. V. (2008). Metabolomics. *Current Drug Metabolism* 9 (1), 89-98.

Goodacre R., Vaidyanathan S., Dunn W.B., Harrigan G.G., Kell D.B. (2004). Metabolomics by numbers: acquiring and understanding global metabolite data. *Trends Biotechn.* 22 (5), 245-255.

Govindaraju V., Young K., Maudsley A.A. (2000). Proton NMR chemical shifts and coupling constants for brain metabolites. *NMR In Biomedicine*, 13 (3), 129-153.

Graham J.B. (1997). Air-breathing fishes: Evolution, Diversity and Adaptation. Academic Press, San Diego, CA, 1-299.

Griffith H.R., den Hollander J.A., Stewart C.C., Evanochko W.T., Buchthal S.D., Harrell L.E. Zamrini E.Y., Brockington J.C., Marson D.C. (2007). Elevated brain scyllo-inositol concentrations in patients with Alzheimer's disease. *NMR IN BIOMEDICINE* 20 (8), 709-716.

Günther H. (1994). NMR Spectroscopy: Basic Principles, concepts, and applications in chemistry. Second edition, John Wiley & Sons, England.

Hall J.R., Short C.E., Petersen L.H., Stacey J., Gamperl J.K., Driedzic W.R. (2009). Expression levels of genes associated with oxygen utilization, glucose transport and glucose phosphorylation in hypoxia exposed Atlantic cod (*Gadus morhua*). *Comparative Biochemistry and Physiology*, Part D 4, 128–138.

Halliwell B., Moorhouse P.C., Grootveld M., Quinlan J.G., Gutteridge J.M.C (1987). Allopurinol and oxypurinol are hydroxyl radical scavengers. *Federation of European Biochemical Societies* 213 (1), 23-28.

Hallman T.M., Rojas-Vargas A.C., Jones D.R., Richards J.G. (2008). Differential recovery from exercise and hypoxia exposure measured using (31)P- and (1)H-NMR in white muscle of the common carp *Cyprinus carpio*. *Journal of Experimental Biology* 211 (20), 3237-3248.

Hansen J.L.S., Bendtsen J. (2009). Effects of climate change on hypoxia in the North Sea-Baltic Sea transition zone. *Earth and Environmental Science* 6 302016.

Hashemi S.S., Blust R., De Boeck G. (2008). Combined effects of different food rations and sublethal copper exposure on growth and energy metabolism in common carp. *Archives of Environmental Contamination and Toxicology* 54 (2), 318-324.

Hassell K.I., Coutin P.C., Nugegoda D. (2009). A novel approach to controlling dissolved oxygen levels in laboratory experiments. *Journal of Experimental Marine Biology and Ecology* 371, 147-154.

Hochachka P.W., Lutz P.L. (2001). Mechanism, origin, and evolution of anoxia tolerance in animals. *Comp. Biochem. Physiol. B* 130, 435-459.

Hochachka P.W., Somero G.N. (2002). Biochemical adaptation – Mechanism and process in physiological Evolution. First edition, Oxford University Press, New York.

Hylland P., Nilsson G. E., Lutz P. L. (1994). Time course of anoxia induced increase in cerebral blood flow rate in turtles: evidence for a role of adenosine. *J. Cereb. Blood Flow Metab.* 14, 877-881.

Hylland, P., Nilsson, G.E. (1999). Extracellular levels of amino acid neurotransmitters during anoxia and forced energy deficiency in crucian carp brain. *Brain Research*, 823, 49-58.

Jeng S.S., Lin T.Y., Wang M.S., Chang Y.Y., Chen C.Y., Chang C.C. (2008). Anoxia survival in common carp and crucian carp is related to high zinc concentrations in tissues. *Fisheries Science* 74, 627-634.

Jian-Fei X., Qiong-Lin L., Ping H.U., Yi-Ming W., Guo-An L. (2009). Recent trends in strategies and methodologies for metabonomics. *Chinese Journal of Analytical Chemistry* 37 (1), 136-143.

Jobling M. (1994). Book of Fish Bioenergetics- Fish and Fisheries Series 13. First edition. Kluwer Academic Publishers, Chapman & Hall, London.

Johansson D., Nilsson G.E. (1995). Roles of energy status, K_{ATP} channels, and channel arrest in fish brain K^+ gradient dissipation during anoxia. *Journal of Experimental Biology* 198, 2575-2580.

Johansson D., Nilsson G.E., Doving K.B. (1997). Anoxic depression of light-evoked potentials in retina and optic tectum of crucian carp. *Neuroscience Letters*, 237 (2-3), 73-76.

Jones M.J., Stuart I.G. (2009). Lateral movement of common carp (*Cyprinus carpio* L.) in a large lowland river and floodplain. *Ecology of Freshwater Fish* 18 (1), 72-82.

Kaddurah-Daoul R., Kristal B.S., Weinshilboum R.M. (2008). Metabolomics: a global biochemical approach to drug response and disease. *Annu. Rev. Pharmacol. Toxicol*. 48, 653-83.

Kaiser K.A., Barding G.A., Larive C.K. (2009). A comparison of metabolite extraction strategies for ^{1}H-NMR-based metabolic profiling using mature leaf tissue from the model plant Arabidopsis thaliana. *Magn Reson Chem* 47 (1), 147-156.

Karakach T.K., Huenupi E.C., Soo E.C., Walter J.A., Afonso L.O.B. (2009). (1)H-NMR and mass spectrometric characterization of the metabolic response of juvenile Atlantic salmon (*Salmo salar*) to long-term handling stress. *Metabolomics* 5 (1), 123-137.

Kemppainen J., Fujimoto T., Kalliokoski K.K., Viljanen T., Nuutila P., Knuuti J. (2002). Myocardial and skeletal muscle glucose uptake during exercise in humans. *Journal of Physiology* 542 (2), 403–412.

Kohavi R. (1995). A study of cross-validation and bootstrap for accuracy estimation and model selection. *Proceedings of the Fourteenth International Joint Conference on Artificial Intelligence*, 2, 1137-1143.

Krivoruchko A., Storey K.B. (2010). Forever young: Mechanisms of natural anoxia tolerance and potential links to longevity. *Oxidative Medicine and Cellular Longevity* 3 (3), 186–198.

Kullgren A., Samuelsson L.M., Forlin L. (2010). A metabolomics approach to elucidate effects of food deprivation in juvenile rainbow trout (*Oncorhynchus mykiss*). *American Journal of Physiology- Regulatory Integrative and Comparative Physiology*, 299 (6), R1440-R1448.

Kuzmina V.V., Gavrovskaya L.K., Ryzhova O.V. (2010). Taurine. Effect on Exotrophia and Metabolism in Mammals and Fish. *Journal of Evolutionary Biochemistry and Physiology*, 46 (1), 19-27.

Lamers R.J.A.N., Wessels E.C.H.H., van der Sandt J.J.M., Venema K., Schaafsma G., van der Greef J., van Nesselrooij J.H.J. (2003). A pilot study to investigate effects of inulin on Caco-2 cells through in vitro metabolic fingerprinting. *J. Nutrition* 133, 1080-3084.

Lardon I., Nilsson G.E., Stecyk J.A.W., Vu T.N., Laukens K., Dommisse R., De Boeck G. (2012). ^{1}H-NMR study of the metabolome of an exceptionally anoxia tolerant vertebrate, the crucian carp (*Carassius carassius*). *Metabolomics* DOI 10.1007/s11306-012-0448-y.

Le Belle J.E., Harris N.G., Williams S.R. (2002). A comparison of cell and tissue extraction techniques using high-resolution ^{1}H-NMR spectroscopy. *NMR Biomed* 15, 37-44.

Lee C.H., Hong Y.S., Son H.S., Kim K.M., Van den Berg F., Hwang G.S., Park W.M. (2008). H-1 nuclear magnetic resonance-based metabolomic characterization of wines by grape varieties and production areas. *Journal of Agricultural and Food Chemistry* 56 (17), 8007-8016.

Lin C.Y., Viant M.R., Tjeerdema R.S. (2006). Metabolomics: Methodologies and applications in the environmental sciences. *J.Pestic.Sci* 31 (3), 245-251.

Lin C.Y., Wu H.F., Tjeerdema R.S., Viant M.R. (2007). Evaluation of metabolite extraction strategies from tissue samples using NMR metabolomics. *Metabolomics*, 3 (1), 55-67.

Lin T-Y., Chen Y-H., Liu C-L., Jeng S.S. (2011). Role of high zinc levels in the stress defense of common carp. *The Japanese Society of Fisheries Science* 77, 557–574.

Lindon J.C., Nicholson J.K., Everett J.R. (1999). NMR spectroscopy of biofluids. *Annual Reports on NMR spectroscopy*, 38, 1-88.

Lindon J.C., Nicholson J.K., Holmes E. (2007). The Handbook of Metabonomics and Metabolomics. First edition, Elsevier, Amsterdam.

Lindon J.C., Nicholson J.K. (2008). Analytical technologies for metabonomics and metabolomics, and multi-omic information recovery. *Trends in Analytical Chemistry*, 27 (3).

Ludwig C., Viant M.R. (2010). Two-dimensional *J*-resolved NMR spectroscopy: review of a key methodology in the Metabolomics toolbox. *Phytochemical Analysis* 21, 22-32.

Lushchak V.I., Bagnyukova T.V., Lushchak O.V., Storey J.M., storey K.B. (2005). Hypoxia and recovery perturb free radical processes and antioxidant potential in common carp (*Cyprinus carpio*) tissues. *The International Journal of Biochemistry & Cell Biology* 37, 1319–1330.

Lutz P.L., Mcmahon P., Rosenthal M., Sick T.J. (1984). Relationships between aerobic and anaerobic energy production in turtle brain in situ. *American Journal of Physiology*, 247 (4), R740-R744.

Lutz P.L., Nilsson G.E. (1997). Contrasting strategies for anoxic brain survival-glycolysis up or down. *Journal of Experimental Biology* 200, 411-419.

Lutz P.L., Nilsson G.E., Prentice H.M. (2003). The Brain Without Oxygen Causes of Failure-Physiological and Molecular Mechanisms for Survival. Mechanisms of Brain Anoxia Tolerance. Third edition. Kluwer Academic Publishers, The Netherlands, pp. 131-189.

Lutz P.L., Prentice H.M., Milton S.L. (2003). Is turtle longevity linked to enhanced mechanisms for surviving brain anoxia and reoxygenation? *Experimental Gerontology*, 38 (7), 797-800.

Maharjan RP, Ferenci T. (2003). Global metabolite analysis: the influence of extraction methodology on metabolome profiles of Escherichia coli. *Analytical Biochemistry* 313 (1), 145-154.

Mandic M., Lau G.Y., Nijjar M.M.S., Richards J.G. (2008). Metabolic recovery in goldfish: A comparison of recovery from severe hypoxia exposure and exhaustive exercise. *Comparative Biochemistry and Physiology, Part C* 148, 332–338.

Marban E., Stull L.B., Leppo M.K., Szweda L., Gao W.D. (2004). Chronic Treatment With Allopurinol Boosts Survival and Cardiac Contractility in Murine Postischemic Cardiomyopathy. *Circulation Research* 95, 1005-1011.

Martineau E., Tea I, Loaëc G, Giraudeau P, Akoka S. (2011)

Strategy for choosing extraction procedures for NMR-based metabolomic analysis of mammalian cells. *Anal Bioanal Chem* 401, 2133-2142.

McDougal D.B., Holowach J., Howe M.C., Jones E.M., Thomas C.A. (1968). The effects of anoxia upon energy sources and selected metabolic intermediates in the brains of fish, frog and turtle. *Journal of Neurochemistry* 15, 577-588.

McKay R.T. (2011). How the 1D-NOESY suppresses solvent signal in Metabonomics NMR spectroscopy: An examination of the pulse sequence components and evolution. *Concepts in Magnetic Resonance* Part A, 38A (5), 197–220.

Metcalfe J.D., Butler P.J. (1984). Changes in activity and ventilation response to hypoxia in unrestrained, unoperated dogfish, *Scyliorhinus canicula*. *Journal of Experimental Biology* 108, 411–418.

Milligan L.C., Pagnotta A. (1991). The role of blood glucose in the restoration of muscle glycogen during recovery from exhaustive exercise in rainbow trout (*Oncorhynchus mykiss*) and winter flounder (*Pseudopleuronectes americanus*). *Journal of Experimental Biology* 161, 489-508.

Moco S., Bino R.J.B., De Vos R.C.H., Vervoort J. (2007). Metabolomics technologies and metabolite identification. *Trends in Analytical Chemistry* 26 (9).

Moyes C. D., Buck L. T., Hochachka P. W. (1990). Mitochondrial and peroxisomal fatty acid oxidation in elasmobranchs. *Am. J. Physiol.* 258, R756-R762.

Mulvey J.M., Renshaw G.M.C. (2009). GABA is not elevated during neuroprotective neuronal depression in the hypoxic epaulette shark (*Hemiscyllium ocellatum*). *Comparative Biochemistry and Physiology*, Part A 152, 273-277.

Mustafa S.A., Al-Subiai S.N., Davies S.J., Jha A.N. (2011). Hypoxia-induced oxidative DNA damage links with higher level biological effects including specific growth rate in common carp, *Cyprinus carpio* L. *Ecotoxicology* 20, 1455-1466.

Naumova A.V., Chacko V.P., Ouwerkerk R., Stull L., Marban E., Weiss R.G. (2006). Xanthine oxidase inhibitors improve energetics and function following infarction in the failing mouse heart. *Am J Physiol Heart Circ Physiol.* 290, 837–843.

Neely J.R., Morgan H.E. (1974). Relationship between carbohydrate and lipid metabolism and the energy balance of heart muscle. *Annual Review of Physiology* 36, 413–459.

Nelson J.S. (1994). Fishes of the World, 3rd Edition. Wiley, NY, 1-600.

Nelson D.L., Cox M.M. (2008). Lehninger Principles of Biochemistry. Students' educational figures. Fifth edition, Freeman W.H. and Company, New York, U.S.A.

Nicholson J.K., Wilson I.D. (1989). High-resolution proton magnetic resonance spectroscopy of biological fluids. *Progress in NMR Spectroscopy* 21, part 4-5, 444-501.

Nicholson J.K., Lindon J.C., Holmes E. (1999). 'Metabonomics': understanding the metabolic responses of living systems to pathophysiological stimuli via multivariate statistical analysis of biological NMR spectroscopic data. *Xenobiotica* 29, 1181-1189.

Nicholson J.K., Beckonert O., Keun H.C., Ebbels T.M.D., Bundy J., Holmes E., Lindon J.C. (2007). Metabolic profiling, metabolomic and metabonomic procedures for NMR spectroscopy of urine, plasma, serum and tissue extracts. *Nature Protocols* 2 (11), 2692-2703

Nilsson G. E. (1988). A comparative study of aldehyde dehydrogenase and alcohol dehydrogenase activity in crucian carp and three other vertebrates: apparent adaptations to ethanol production. *Journal of Comparative Physiology B* (158), 479-485.

Nilsson, G.E. (1990). Long term anoxia in crucian carp: changes in the levels of amino acid and monoamine neurotransmitters in the brain, catecholamines in chromaffin tissue, and liver glycogen. *Journal of Experimental Biology*, 150, 295-320.

Nilsson G.E. (1991). The adenosine receptor blocker aminophylline increases anoxic ethanol production in crucian carp. *Am J Physiol* 261, 1057-1060.

Nilsson G. E., Lutz, P. L. (1991). Release of inhibitory neurotransmitters

in response to anoxia in turtle brain, *Am. J. Physiol. Reg. Integ. Comp. Physiol.* 261, R32-R37.

Nilsson, G.E., Lutz, P.L., Jackson, T.L. (1991). Neurotransmittors and anoxic survival of the brain: a comparison between anoxia-tolerant and anoxia-intolerant vertebrates. *Journal of Physiological Zoology* 64, 638-652.

Nilsson G.E. (1993). Neurotransmitters and anoxia resistance – comparative physiological and evolutionary perspectives. In: Surviving hypoxia: Mechanisms of ontrol and Adaptation. Hochachka P.W., Lutz P.L., Sick T., Rosenthal M., Van den Thillart G. (Eds). Boca Raton, FL: CRC press, 1993, 401-413.

Nilsson G.E., Rosén P., Johansson D. (1993). Anoxic depression of spontaneous locomotor activity in crucian carp quantified by a computerized imaging technique. *Journal of Experimental Biology* 180, 153-163.

Nilsson G.E., Hylland P., Löfman C. O. (1994). Anoxia and adenosine induce increased cerebral blood flow in crucian carp. *Am. J. Physiol. Integ. Reg. Comp. Physiol.* 267, R590-R595.

Nilsson G.E., Lutz P.L. (2004). Anoxia tolerant brains. *Journal of Cerebral Blood Flow & Metabolism* 24, 475-486.

Nilsson G.E., Renshaw G.M.C. (2004). Review: Hypoxic survival strategies in two fishes: extreme anoxia tolerance in the North European crucian carp and natural hypoxic preconditioning in a coral-reef shark. *The Journal of Experimental Biology* 207, 3131-3139.

Oliver S.G. (1998). Systematic functional analysis of the yeast genome. *Trends Biotechn.* 16, 373-378.

Parsons G.R., Carlson J.K. (1998). Physiological and behavioural responses to hypoxia in the bonnethead shark, *Sphyrna tiburo*: routine swimming and respiratory regulation. *Fish Phys. Biochem.* 19, 189–196.

Peréz-Pinzon M., Rosenthal M., Sick T., Lutz P.L., Pablo P., Marsh D. (1992). Down-regulation of sodium channels during anoxia: a putative survival strategy of turtle brain. *Am. J. Physiol*. 262, R712-R715.

Perry S.F., Gilmour K.M. (1996). Consequences of catecholamine release on ventilation and blood oxygen transport during hypoxia and hypercapnia in an elasmobranchs (*Squalus acanthias*) and a teleost (*Oncorhynchus mykiss*). *The Journal of Experimental Biology* 199, 2105–2118.

Pollock M.S., Clarke L.M.J., Dube M.G. (2007). The effects of hypoxia on fishes: from ecological relevance to physiological effects. *Environmental Reviews* 15, 1-14.

Podrabsky J.E., Lopez J.P., Fan T.W.M., Higashi R., Somero G.N. (2007). Extreme anoxia tolerance in embryos of the annual killifish Austrofundulus limnaeus: insights from a metabolomics analysis. *Journal of Experimental Biology*, 210 (13), 2253-2266.

Prentice H.M. (2009). The major contribution of brain GABAergic function to anoxic survival. *Physiol Genomics* 36, 59-60.

Raman L., Tkac I., Ennis K. (2005). In vivo effect of chronic hypoxia on the neurochemical profile of the developing rat hippocampus. *Developmental Brain Research*, 156 (2), 202-209.

Renshaw G.M.C., Kerrisk C.B., Nilsson G.E. (2002). The role of adenosine in the anoxic survival of the epaulette shark, *Hemiscyllium ocellatum*. *Comparative Biochemistry and Physiology* Part B, 133-141.

Renshaw G.M.C., Chapman C.A. (2009). Hematological responses of the grey carpet shark (*Chiloscyllium punctatum*) and the epaulette shark (*Hemiscyllium ocellatum*) to anoxia and re-oxygenation. *Journal of Experimental Zoology* 311A, 422-438.

Renshaw G.M.C., Wise G., Dodd P.R. (2010). Ecophysiology of neuronal metabolism in transiently oxygen-depleted environments: Evidence that GABA is accumulated pre-synaptically in the cerebellum. *Journal of Comparative Biochemistry and Physiology A,* 155, 486-492.

Richards J.G. (2011). Physiological, behavioural and biochemical adaptations of intertidal fishes to hypoxia. *Journal of Experimental Biology* 214, 191-199.

Rosati A.M., Traversa U., Lucchi R., Poli A. (1995). Biochemical and Pharmacological evidence for the presence of A1 but not A2 (A) adenosine receptors in the brain of the low vertebrate teleost *Carassius auratus* (goldfish). *Neurochemistry International* 26 (4), 411-423.

Routley M.H., Nilsson G.E., Renshaw G.M.C. (2002). Exposure to hypoxia primes the respiratory and metabolic responses of the epaulette shark to progressive hypoxia. *Journal of Comparative Biochemistry and Physiology* 131A, 313-321.

Rytkönen K.T., Renshaw G.M.C., Ashton K.J., Williams-Pritchard G., Leder E.H., Nikinmaa M. (2010). Elasmobranch qPCR reference genes: a case study of hypoxic preconditioned epaulette sharks. *BMC Molecular Biology* 11 (27), 1471-2199.

Salaman J.R. (1991). Monitoring of rejection in renal transplantation. *Immunol Lett* 29, 139-142.

Samuelsson L.M., Förlin L., Karlsson G., Adolfsson-Erici M., Larsson J. (2006). Using NMR metabolomics to identify responses of an environmental estrogen in blood plasma of fish. *Aquatic Toxicology* 78, 341-349.

Segner H., Dolle A., Bohm R. (1997). Ketone body metabolism in the carp *Cyprinus carpio*: Biochemical and H-1 NMR spectroscopical analysis. *Comparative Biochemistry and Physiology B-Biochemistry & Molecular Biology* 116 (2), 257-262.

Seibel B.A., Walsh P.J. (2002). Trimethylamine oxide accumulation in marine animals: relationship to acylglycerol storage. *The Journal of Experimental Biology* 205, 297–306.

Sekiyama Y., Chikayama E., Kikuchi J. (2011). Evaluation of a semipolar solvent system as a step toward heteronuclear multidimensional NMR-based metabolomics for 13C-labeled bacteria, plants, and animals. *Anal Chem* 83 (3), 719-26.

Serkova N.J., Reisdorph N.A., Tissot van Patot M.C. (2008). Metabolic markers of hypoxia: systems biology application in biomedicine. *Toxicology Mechanisms and Methods* 18, 81-95.

Shaffer H.B., Meylan P., McKnight M.L. (1997). Tests of turtle phylogeny: molecular, morphological, and paleontological approaches. *Syst. Biol.* 46, 235-268.

Schaffer S.W., Jong, C.J., Ramila, K.C., Azuma, J. (2010). Physiological roles of taurine in heart and muscle. *Journal of Biomedical Science*, 17 (1), 1-8.

Shannon P., Markiel A., Ozier O. (2003). Cytoscape: A Software Environment for Integrated Models of Biomolecular Interaction Networks. *Genome Research*, 13 (11), 2498-2504.

Shin M.H., Lee D.Y., Wohlgemuth G., Choi I-G., Fiehn O., Kim K.H. (2010). Global metabolite profiling of agarose degradation by Saccharophagus degradans 2-40. *New Biotechnology* 27 (2).

Shoubridge E.A., Hochachka P.W. (1980). Ethanol: novel end-product in vertebrate anaerobic metabolism. *Science* 209, 308-309.

Smith R.W., Houlihan D.F., Nilsson G.E., Brechin J.G. (1996). Tissue-specific changes in protein synthesis rates in vivo during anoxia in crucian carp. *Am. J. Physiol., Regul. Integr. Comp. Physiol*. 271, 897-904.

Sobolev A.P., Mannina L., Capitani D., Iaffaldano N., Rosato M.P., Ragni P., Reale A., Sorrentino E., D'Amico I., Coppola R. (2008). NMR metabolic profiling of organic and aqueous sea bass extracts: Implications in the discrimination of wild and cultured sea bass. *Talanta* 77, 433-444.

Söderström V., Renshaw G.M.C., Nilsson G.E. (1999). Brain blood flow and blood pressure during hypoxia in the epaulette shark *Hemiscyllium ocellatum*, a hypoxia-tolerant elasmobranchs. *The Journal of Experimental Biology* 202, 829-835.

Soengas J.L., Aldegunde M. (2002). Energy metabolism of fish brain. *Comparative Biochemistry and Physiology B – Biochemistry & Molecular Biology*, 131 (3), 271-296.

Sollid J., De Angelis P., Gundersen K., Nilsson G. E. (2003). Hypoxia induces adaptive and reversible gross morphological changes in crucian carp gills. *J. Exp. Biol.* 206, 3667-3673.

Sollid J., Nilsson G. E. (2006). Plasticity of respiratory structures-adaptive remodelling of fish gills induced by ambient oxygen and temperature. *Respir. Physiol. Neurobiol*. 154, 241-251.

Speers-Roesch B., Treberg J.R. (2010). The unusual energy metabolism of elasmobranch fishes. *Journal of Comparative Biochemistry and Physiology* 155A, 417-434.

Speers-Roesch B., Richards J.G., Brauner C.J., Farrell A.P., Hickey A.J.R., Wang Y.S., Renshaw G.M.C. (2012**a**). Hypoxia tolerance in elasmobranchs. I. Critical oxygen tension as a measure of blood oxygen transport during hypoxia exposure. *The Journal of Experimental Biology* 215, 93-102.

Speers-Roesch B., Brauner C.J., Farrell A.P., Hickey A.J.R., Renshaw G.M.C., Wang Y.S., Richards J.G. (2012**b**). Hypoxia tolerance in elasmobranchs. II. Cardiovascular function and tissue metabolic responses during progressive and relative hypoxia exposures. *The Journal of Experimental Biology* 215, 103-114.

Stecyk J.A.W., Farrell A.P. (2002). Cardiorespiratory responses of the common carp (*Cyprinus carpio*) to severe hypoxia at three acclimation temperatures. *Journal of Experimental Biology* 205 (6), 759-768.

Stecyk J.A.W., Stensløkken K.-O., Farrell A.P., Nilsson G.E. (2004). Maintained cardiac pumping in anoxic crucian carp. *Science* 306, 77-77.

Stecyk J. A.W., Farrell A.P. (2006). Regulation of the cardiorespiratory system of common carp (*Cyprinus carpio*) during severe hypoxia at three seasonal acclimation temperatures. *Physiological and Biochemical Zoology* 79 (3), 614-627.

Stecyk J.A.W., Stensløkken K-O., Nilsson G.E., Farrell A.P. (2007). Adenosine does not save the heart of anoxia-tolerant vertebrates during prolonged oxygen deprivation. *Comparative Biochemistry and Physiology*, Part A 147, 961–973.

Stecyk J. A.W., Larsen B. C., Nilsson G. E. (2011). Intrinsic contractile properties of the crucian carp (*Carassius carassius*) heart during anoxic and acidotic stress. *American Journal of Physiology – Regulatory Integrative and Comparative Physiology* 301 (4), R1132-R1142.

Stentiford G.D., Viant M.R., Ward D.G., Johnson P.J., Martin A., Wenbin W., Cooper H.J., Lyons B.P., Feist S.W. (2005). Liver tumors in wild flatfish: A histopathological, proteomic, and metabolomic study. *Omics – A Journal of Integrative Biology* 9 (3), 281-299.

Stoyanova R., Nicholls A.W., Nicholson J.K., Lindon J.C., Brown T.R. (2004). Automatic alignment of individual peaks in large high-resolution spectral data sets. *Journal of Magnetic Resonance* 170, 329-335.

Swenson K.E., Eveland R.L., Gladwin M.T., Swenson E.R. (2005). Nitric oxide (NO) in normal and hypoxic vascular regulation of the Spiny Dogfish, *Squalus acanthias*. *Journal of Experimental Zoology* 303A, 154-160.

Tam W. L., Wong W. P., Loong A. M., Hiong K. C., Chew S. F., Ballantyne J. S., Ip Y. K. (2003). The osmotic response of the Asian freshwater stingray (*Himantura signifer*) to increased salinity: a comparison with marine (*Taeniura lymma*) and Amazonian freshwater (*Potamotrygon motoro*) stingrays. *The Journal of Experimental Biology* 206, 2931-2940.

Tang Y., Boutilier R.G. (1991). White muscle intracellular acid-base and lactate status following exhaustive exercise: a comparison between freshwater- and seawater-adapted rainbow trout. *Journal of Experimental Biology* 156, 153-171.

Tian C., Chikayama E., Tsuboi Y. Kuromori T., Shinozaki K., Kikuchi J., Hirayama T. (2007). Top-down phenomics of Arabidopsis thaliana-metabolic profiling by one- and two-dimensional nuclear magnetic resonance spectroscopy and transcriptome analysis of albino mutans. *J Biol Chem* 282, 18532-18541.

Tota B., Angelone T., Mancardi D., Cerra M.C. (2011). Hypoxia and anoxia tolerance of vertebrate hearts: an evolutionary perspective. *Antioxidants & Redox Signaling* 14 (5), 851-862.

Ultsch G.R. (1989). Ecology and physiology of hibernation and overwintering among freshwater fishes, turtles, and snakes. *Biol. Rev.* 64, 435-516.

Ultsch G.R., Carwile M.E., Crocker C.E., Jackson D.C. (1999). The physiology of hibernation among painted turtles: the eastern painted turtle, *Chrysemys picta picta*. *Physiol. Zool.* 72, 493-501.

Urbanczyk-Wochniak E., Luedemann A., Kopka J., Selbig J., Roessner-Tunali U., Willmitzer L., Fernie A.R. (2003). Parallel analysis of transcript and metabolic profiles: a new approach in systems biology. *EMBO Reports* 4 (10), 989-993.

Val A.L., de Almeida Val V.M.F. (1996). Fishes of the Amazon and Their environment. Springer-Verlag, Berlin, 1-224.

Van der Linden A., Verhoye M., Nilsson G.E. (2001). Does Anoxia Induce Cell Swelling in Carp Brains? In Vivo MRI Measurements in Crucian Carp and Common Carp. *J Neurophysiol* 85, 125-133.

Van Ginneken V., Nieveen M., Van Eersel R., Van den Thillart G., Addink A. (1996). Neurotransmitter levels and energy status in brain of fish species with and without the survival strategy of metabolic depression. *CompBiochem Physiol A Physiol* 114, 189–196.

Van Ginneken V.J.T., Van Caubergh P., Nieveen M., Balm P., Van den Thillart G., Addink A. (1998). Influence of hypoxia exposure on the energy metabolism of common carp (*Cyprinus carpio* L.). *Netherlands Journal of Zoology* 48 (1), 65-82.

Van Waarde A., Van den Thillart G., Dobbe F. (1982). Anaerobic metabolism of goldfish,*Carassius auratus* (L.). Influence of anoxia on mass-action ratios of transaminase reactions and levels of ammonia and succinate. *Journal of Comparative Physiology B – Biochemical, Systemic, and Environmental Physiology*, 147 (1), 53-59.

Van Waarde A., Van den Thillart G., Erkelens C., Addink A., Lugtenburg J. (1990). Functional coupling of glycolysis and phosphocreatine utilization in anoxic fish muscle. *Journal of Biological Chemistry*, 265 (2), 914-923.

Van Waversveld J., Addink A.D.F., Van Den Thillart G. (1989). Simultaneous direct and indirect calorimetry on normoxic and anoxic goldfish. *Journal of Experimental Biology* 142, 325-335.

Verpoorte R, Kim HK, Choi YH. (2011). NMR-based plant metabolomics: where do we stand, where do we go? *Trends in Biotechnology* 29 (6), 267-275.

Viant M.R., Rosenblum E.S., Tjeerdema R.S. (2003). NMR-based metabolomics: A powerful approach for characterizing the effects of environmental stressors on organism health. *Environmental Science & Technology* 37 (21), 4982-4989.

Viant M.R., Werner I., Rosenblum E.S., Gantner A.S., Tjeerdema R.S., Johnson M.L. (2003). Correlation between heat-shock protein induction and reduced metabolic condition in juvenile steelhead trout (*Oncorhynchus mykiss*) chronically exposed to elevated temperature. *Fish Physiology and Biochemistry* 29 (2), 159-171.

Viant M.R., Wu H., Southam A.D., Hines A. (2008). High-throughput tissue extraction protocol for NMR- and MS- based metabolomics. *Anal. Biochem. 372*, 204-212.

Villas-Boas S.G., Hojer-Pedersen J, Akesson M, Smedsgaard J, Nielsen J. (2005). Global metabolite analysis of yeast: evaluation of sample preparation methods. *Yeast* 22 (14), 1155-1169.

Voet D., Voet J.G. (1995). Biochemistry. United States of America, John Wiley & Sons Inc., second edition.

Vornanen M., Paajanen V. (2006). Seasonal changes in glycogen content and Na^+-K^+-ATPase activity in the brain of crucian carp. *Am J Physiol Regul Integr Comp Physiol* 291, 1482–1489.

Vornanen M., Stecyk J. A. W., Nilsson G. E. (2009). The anoxia-tolerant crucian carp (*Carassius carassius* L.). *Fish Physiology*, 27, 397-441.

Vornanen M., Asikainen J., Haverinen J. (2011). Body mass dependence of glycogen stores in the anoxia-tolerant crucian carp (*Carassius carassius L.). Naturwissenschaften* 98, 225–232.

Vu T.N., Valkenborg D., Smets K., Verwaest K., Dommisse R., Lemiere F., Verschoren A., Goethals B., Laukens K. (2011). An integrated workflow for robust alignment and simplified quantitative analysis of NMR spectrometry data. *BMC Bioinformatics* 12 (405).

Walker R.M., Johanson P.H. (1977). Anaerobic metabolism in goldfish *Carassius auratus*. *Canadian Journal of Zoology* 55 (8), 1304-1311.

Wang Y., Haipeng S., Lu G., Ren S., Chen J. (2011). Catabolism of branched-chain amino acids in heart failure: insights from genetic models. *Pediatr Cardiol* 32, 305-310.

Walsh P.J., Veauvy C.M., McDonald M.D., Pamenter M.E., Buck L.T., Wilkie M.P. (2007). Piscine insights into comparisons of anoxia tolerance, amoonia toxicity, stroke and hepatic encephalopathy. *Comparative Biochemistry and Physiology A* 147, 332-343.

Weckwerth W. (2003). Metabolomics in systems biology. *Annu. Rev. Plant Biol*. 54, 669-89.

Westerhuis J.A., Hoefsloot H.C.J., Smit S. (2008). Assessment of PLSDA cross validation. *Metabolomics*, 4 (1), 81-89.

Wilson I.D., Lenz E.M. (2007). Analytical strategies in metabonomics. *Journal of Proteome Research* 6, 443-458.

Winder C.L., Dunn W.B., Schuler S., Broadhurst D., Jarvis R., Stephens G.M., Goodacre R. (2008). Global metabolic profiling of Escherichia coli cultures: an evaluation of methods for quenching and extraction of intracellular metabolites. *Anal Chem* 80 (8), 2939-48.

Wishart D.S. (2005). Metabolomics: The principles and potential applications to transplantation. *American Journal of Transplantation* 5, 2814-2820.

Wood C.M., Pärt P., Wright P.A. (1995). Ammonia and urea metabolism in relation to gill function and acid-base balance in a marine elasmobranch, the spiny dogfish (*Squalus acanthias*). *The Journal of Experimental Biology* 198, 1545–1558.

Wu H.F., Southam A.D., Hines A., Viant M.R. (2008). High-throughput tissue extraction protocol for NMR and MS-based metabolomics. *Journal of Analytical Biochemistry*, 372 (2), 204-212.

Xia J., Psychogios N., Young N., Wishart D. S. (2009). MetaboAnalyst: a web server for metabolomic data analysis and interpretation. *Nucleic Acids Res* 37, W652–660.

Yancey P.H., Somero G.N. (1979). Counteraction of urea destabilisation of protein structure by methylamine osmoregulatory compounds of elasmobranchs fishes. *Journal of Biochemistry* 183, 317-323.

Yang C., He Z., Yu W. (2009). Comparison of public peak detection algorithms for MALDI mass spectrometry data analysis. *BMC Bioinformatics* 10 (4).

Yoshikawa H., Ishida Y., Kawata K., Kawai F., Kanamori M. (1995). Electroencephalograms and cerebral blood flow in carp, *Cyprinus carpio*, subjected to acute hypoxia. Jo*urnal of Fish Biology* 46, 114–122.

Zammit V. A., Newsholme E. A. (1979). Activities of enzymes of fat and ketone-body metabolism and effects of starvation on blood concentrations of glucose and fat fuels in teleost and elasmobranch fish. *Journal of Biochemistry* 184, 313-322.

Zhou B.S., Wu R.S.S., Randall D.J., Lam P.K.S., Ip Y.K., Chew S.F. (2000). Metabolic adjustments in the common carp during prolonged hypoxia. *Journal of Fish Biology* 57, 1160-1171.